UPPER JURASSIC (OXFORDIAN) DINOFLAGELLATE CYST TAXONOMY, PALYNOSTRATIGRAPHY AND BIOSEQUENCE STRATIGRAPHY OF THE JANSZ-IO GAS FIELD, NORTH WEST SHELF, AUSTRALIA.

A thesis submitted for the degree of
Doctor of Philosophy
of The Australian National University

Natalie G. Sinclair

October, 2012

Research School of Earth Sciences
The Australian National University

STATEMENT

The work presented in this thesis is the author's own, except where otherwise acknowledged, and has not been submitted for a degree at any other university.

Natalie G. Sinclair

ACKNOWLEDGMENTS

My sincerest thanks go to:

- My supervisors, Patrick De Deckker and Eric Monteil, and advisors, Elizabeth Truswell and Clinton Foster, for the assistance and advice you provided throughout my PhD. In particular: Eric, thank you for sharing with me your knowledge and expertise and for helping me ride the storm associated with project changes; and Liz, thanks for your feedback and generous gift of references.
- Daniel Mantle for stepping in as an unofficial advisor since your arrival at GA. Thanks for your advice, assistance and encouragement.
- ExxonMobil and Chevron Texaco for providing me with access to the materials, samples raw data and reports with which to conduct this project.
- Geoscience Australia (GA) Petroleum and Marine Division (Timescales project and the Palaeontology and Sedimentology Laboratory) for the use of office and laboratory facilities, and funding for courses and sample processing.
- GA present and past staff: Stuart McEwen, Richard Brown, Christian Thun, Tony Watson, Alex McLachlan, Billie Poignand and other current and former PalSed Lab staff for sample processing assistance and training, technical support, and always good company; previous staff member Richard Howe for sampling and photographing the Io-1 core in Perth; John Laurie for CPP slide access and helpful discussions; previous staff member Justin Parker for discussions on foraminifera; Karen Earl for map preparation assistance; and Andrew Kelman for Stratabugs training.
- ANU's Electron Microscopy Unit for access to SEM facilities at the ANU.
- Numerous palynologists, especially: Roger Morgan and Nigel Hooker for invaluable assistance initiating this project, individual training, advice and providing access to samples and important references; Robin Helby for extremely useful taxonomic feedback and advice; John Backhouse for the provision of important reference material; and Barrie Dale, Kenneth Mertens, Paul Milner, Henrik Nøhr-Hansen, Jim Riding and Gwyd Williams for stimulating taxonomic and morphological discussions and/or access to international samples for comparison purposes.
- ANU for an Endowment for Excellence PhD Scholarship and conference travel grants (Vice Chancellors Travel Grant and RSES travel grant).
- VCEMP, PESA, AASP, IGC 2004 and Dino8 for greatly appreciated scholarships, course funding or conference travel grants.
- All my family and friends, too many to name individually, thanks for your kindness, support and encouragement throughout my PhD.
- Mum and Dad – I did it!
- And always to my loving husband, Nathan Sinclair, for your ongoing support, relieving humour, and enormous supply of strength, patience and encouragement.

It is finished.

UPPER JURASSIC (OXFORDIAN) DINOFLAGELLATE CYST TAXONOMY, PALYNOSTRATIGRAPHY AND BIOSEQUENCE STRATIGRAPHY OF THE JANSZ-IO GAS FIELD, NORTH WEST SHELF, AUSTRALIA.

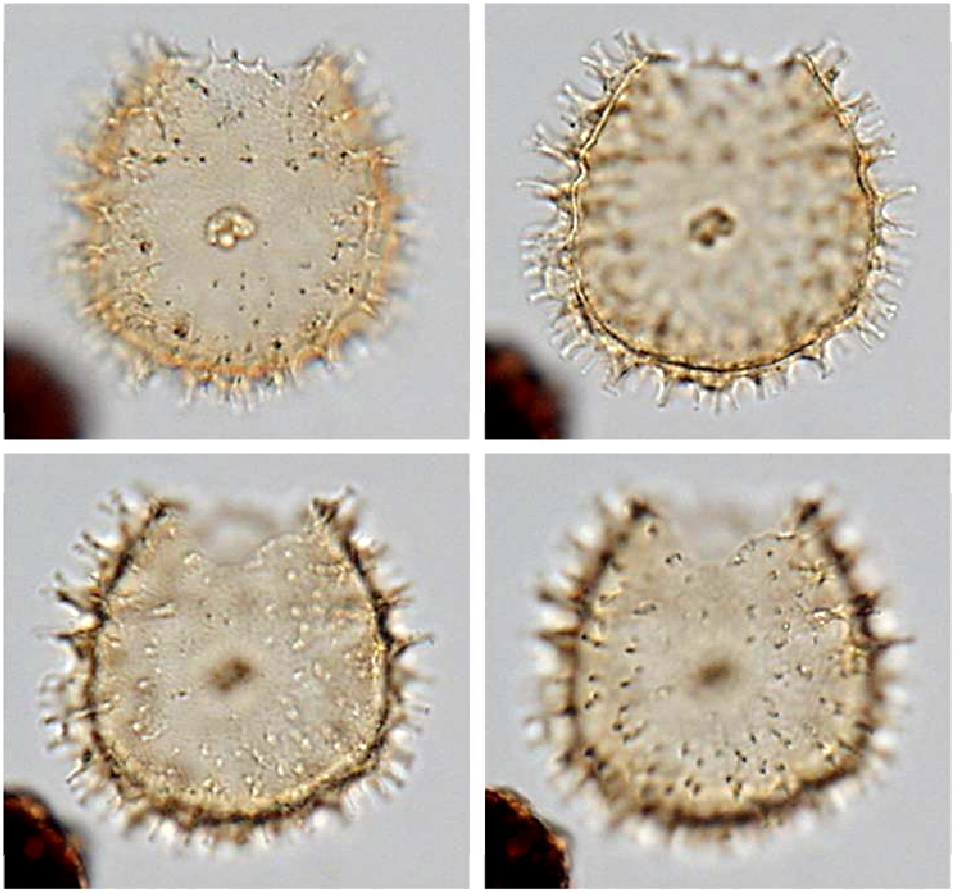

Frontispiece: *Tenua monteilii* sp. nov. – A new Oxfordian *Wanaea spectabilis* microplankton zone species described herein.

"To see clearly something that no one has ever examined before, whether one is using a hand lens or an electron microscope, is a creative intellectual act; and to realize how a new observation is related to previous knowledge is an act of insight of the kind on which all advance in scientific knowledge is based."

R. E. Holttum, 1961

Holttum, R. E., 1961. Plant taxonomy as a scientific discipline. *Advanc. Sci., v.18(73).* p.1-9.

ABSTRACT

High-resolution palynological analysis was conducted from four wells of the Jansz-Io Gas Field (Exmouth Plateau, Northern Carnarvon Basin) to refine the Australian Oxfordian *Wanaea spectabilis* microplankton biozone. The refined biozonation scheme was then utilised to produce integrated biostratigraphic, sequence stratigraphic and palaeoenvironmental interpretations of the Jansz Sandstone reservoir sequence.

Palynological preparations from 155 conventional core samples yielded a highly diverse assemblage of dinoflagellate cysts and acritarchs of good to excellent preservation. The assemblage comprises 112 genera with 194 microplankton species and varieties. Of these, 2 new genera and 26 new species are formally described, 2 species are emended with 1 species generically reattributed, and an additional 11 genera and 37 species are informally described.[1] For future reference of this well preserved material, each species is illustrated in a large catalogue of plates. Examination of a complex continuum of dinoflagellate cyst morphotypes with intratabular processes, the "*Contracysta* complex", revealed new insights into the process and trabeculum development of dinoflagellate cysts and is discussed in detail.

Key taxa identified through quantitative analysis are utilised to refine the intersected portion of the *Wanaea spectabilis* microplankton zone. Three *Wanaea spectabilis* Zone subzones, WS1-3, are proposed for the analysed sequence. WS2 and WS3 are divided into 3 (WS2A-C) and 7 (WS3A-G) zonules respectively. Proposed zonal subdivisions are defined on first and last stratigraphic occurrences, first and last common occurrences and species acmes which can be correlated across the Jansz-Io Field. The subzones are tentatively correlated to the Poulsen & Riding, 2003 Northern Hemisphere Dinoflagellate Cyst Zones; Bown & Cooper, 1998 Nannofossil Zones; the Groupe Français d'Étude du Jurassique, 1997 Tethyan, Sub-Boreal and Boreal Ammonoid Zones; and the ICS 2008 Geologic Time Scale.

Lithofacies and qualitative palynofacies analyses are integrated with petrophysical wireline logs to produce bio-sequence stratigraphic and palaeoenvironmental interpretations for the Jansz Sandstone reservoir sequence. Bioevent-derived zonule boundaries are identified to reflect 'biostratigraphic parasequences' arranged in transgressive/regressive couplets as indicated by an inversely oscillating AOM/wood ratio. These biostratigraphic parasequences provide valuable information regarding sequence and reservoir architecture in the absence of lithostratigraphic controls.

[1] Note: Newly identified taxa recorded herein as "gen. nov." or "sp. nov." are pending formal publication.

The application of selected dinoflagellate cyst species as palaeoenvironmental proxies is examined. Extreme intraspecific variability of some dinoflagellate cyst taxa may reflect salinity and/or temperature changes caused by a high-frequency, cyclical climatic regime, such as a seasonal monsoonal climate.

TABLE OF CONTENTS

LIST OF FIGURES

LIST OF TABLES

PLATES

LIST OF APPENDICES

LIST OF ENCLOSURES

Chapter 1
INTRODUCTION

The Northern Carnarvon Basin is the southernmost basin of Australia's North West Shelf petroleum province. Since petroleum exploration began in this region in the mid-1960's, dinoflagellate cysts have become an essential tool for dating and correlating Australia's Mesozoic marine sequences. Until the late 1980's many Australian petroleum companies employed groups of palynologists to produce in-house biozonation schemes for use in their exploration and development programs. These schemes were considered highly proprietary, therefore multiple independent schemes were developed simultaneously. The resulting informal schemes were typically restricted to specific geographic areas and/or time intervals, and frequently based on key taxa that were identified only by informal alphanumeric codes. Use of the different schemes and codes impeded communication, and resulted in confusion and difficulty in dating and correlating lithostratigraphic units and basin events (Helby *et. al.*, 1987; Foster, 2001).

A palynological zonation of the Australian Mesozoic by Helby, Morgan & Partridge (Helby *et. al.*, 1987; commonly referred to as the HMP biozonation scheme) was the first Australian publication of a single, unified and integrated palynological biozonation scheme. The parallel Spore-Pollen and Microplankton zonal schemes introduced in this landmark publication have since been widely accepted and extensively utilised by petroleum companies and geological institutions as the Mesozoic palynological biozonation standard for Australia and the neighbouring regions.

The aim of Helby *et. al.* (1987) was to present a "preliminary rather than comprehensive" zonal outline, with future revisions anticipated by the authors at the time of publication (Helby *et. al.*, 1987). Since Helby *et. al.* (1987) was published, advances in petroleum development and production techniques have increased demand for high resolution biostratigraphy, resulting in further development of independent and informal schemes (Foster, 2001). In response, Riding & Helby (2001a-h) and Helby & Partridge (2001) published a series of papers describing additional key Jurassic and Cretaceous microplankton taxa with the intention of providing the taxonomic foundation upon which to formalise zonal subdivisions of Helby *et. al.*, 1987. However, while the framework of the Helby *et. al.* (1987) microplankton (dinoflagellate cyst) scheme was updated by Helby *et. al.* (2004), tied to the 2004 Geologic Time Scale by Partridge (2006a-d), and revised and tied to the 2008 Geologic Time Scale by Riding *et. al.* (2010), a complete scheme with formal zonal subdivisions remains unpublished.

In April 2000, Australia's largest gas field (at that time) was discovered at Jansz-1 on the Exmouth Plateau of the Northern Carnarvon Basin. The Jansz reservoir revealed a new Oxfordian petroleum play for the North West Shelf petroleum province. The discovery of the Jansz Sandstone highlighted the need for increased resolution of the Oxfordian *Wanaea spectabilis* dinoflagellate cyst zone – the longest duration dinoflagellate cyst zone in the Middle to Late Jurassic. The high yield, great diversity and often excellent preservation of the microplankton recovered from the Jansz reservoir provided ideal material with which to refine the *Wanaea spectabilis* Zone.

This project aims to produce a practical subdivision of the *Wanaea spectabilis* Zone intersected by the Jansz reservoir. Palynological samples were collected while logging conventional core from the reservoir sequence of four wells across the Jansz-Io field. To ensure the accuracy of the zonal subdivision, samples were collected at high resolution and evenly spaced throughout the cored sequence. Detailed taxonomic analysis of the diverse microplankton assemblage has identified key dinoflagellate cyst marker species to form a solid foundation for *Wanaea spectabilis* zonal subdivision. Quantitative and qualitative analyses of the microplankton and palynodebris content enabled the development of a biostratigraphic framework for high resolution reservoir correlation. Integration of this biostratigraphic framework with lithofacies and downhole petrophysical data results in biostratigraphic and bio-sequence stratigraphic interpretations of the Jansz Sandstone reservoir sequence. Palaeoenvironmental and palaeoecological conclusions drawn from the biostratigraphic and palynofacies analyses are presented.

Chapter 2
GEOLOGY

2.1 REGIONAL GEOLOGICAL SETTING

2.1.1 North West Shelf

The Jansz-Io Gas Field is located on the Exmouth Plateau of the Northern Carnarvon Basin, in the south-western area of Australia's North West Shelf petroleum province. The North West Shelf is a broad continental shelf consisting of a thick, prograding wedge of Cretaceous to Cenozoic carbonate sediments on the north-western passive margin of the Australian continent. North West Shelf sediments overlie a series of Paleozoic to Mesozoic sedimentary basins, collectively called the Westralian Superbasin, which stretches from the North West Cape of Western Australia to Papua New Guinea (Figure 2.1; Edwards & Zumberge, 2005). The Westralian Superbasin consists of, from north to south, the Papuan Basin (not figured), the Timor-Banda Orogen, and the Northern Bonaparte, Browse, Roebuck (previously Offshore/Western Canning) and Northern Carnarvon Basins (Longley *et al.*, 2002; Edwards & Zumberge, 2005).

Formation of the Westralian Superbasin was instigated by the rifting and fragmentation of Gondwana which commenced during the Late Carboniferous to Early Permian (Hocking *et al.*, 1994). Rift associated crustal extension and thinning caused the separation of the 'Sibumasu' Terrane (AGSO, 1994) or 'Cimmerian Blocks' (Baillie *et al.*, 1994) from northwestern Australia and formed the epicontinental Neo-Tethys Sea. Late Triassic to Late Jurassic rifting and continental separation facilitated the deposition of thick (up to 10km) contiguous, Permian to Early Cretaceous sedimentary fill within the six closely related basins of the Westralian Superbasin (Bradshaw *et al.*, 1988).

Following continental separation, post-rift thermal sag provided accommodation space for prograding clastic deltaic to marine sequences from the Early to Late Cretaceous. As Australia moved northwards and clastic sediment supply reduced, carbonate sedimentation became dominant during the Late Cretaceous. Accumulation of thick, prograding carbonate sediments through the Cenozoic has created the current North West Shelf. The Timor-Banda Orogen resulted from the collision of the northwestern distal edge of the Westralian Superbasin with the Banda Arc System in the late Miocene (Keep *et al.*, 2002; Longley *et al.*, 2002).

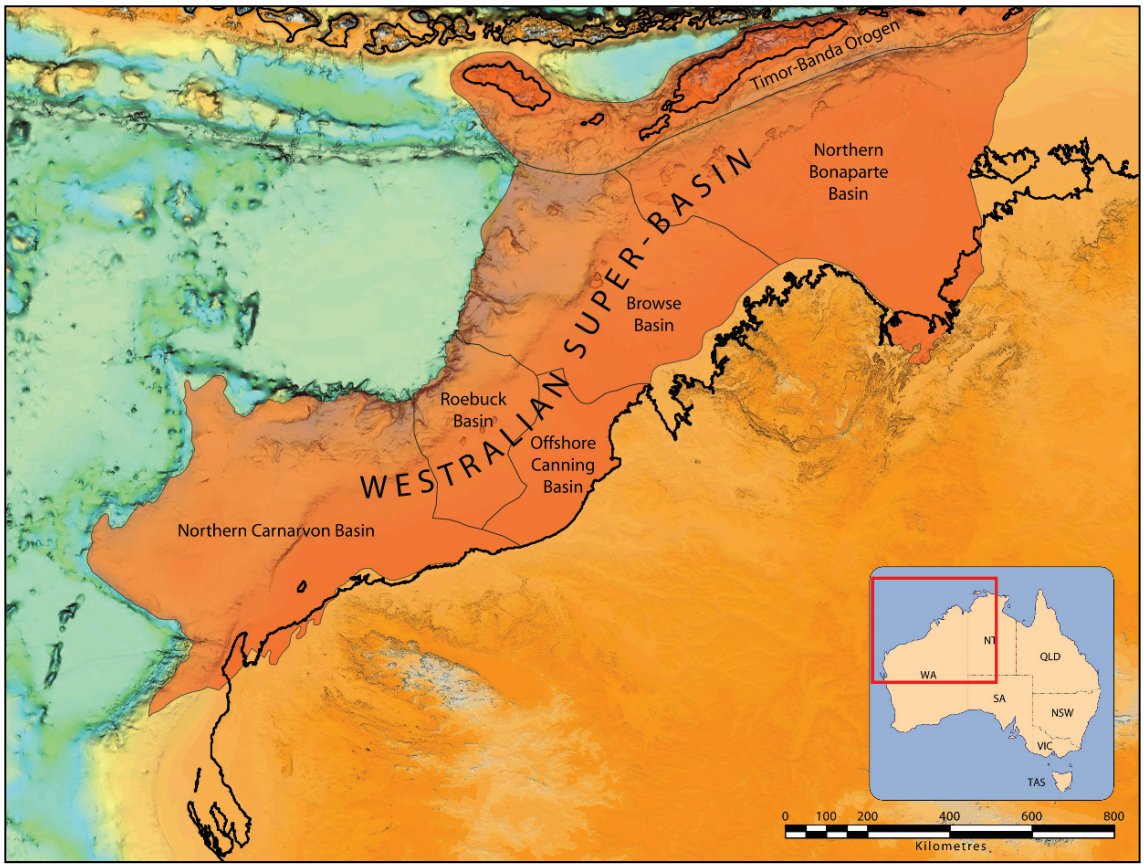

Figure 2.1: Location and components of the Westralian Superbasin.

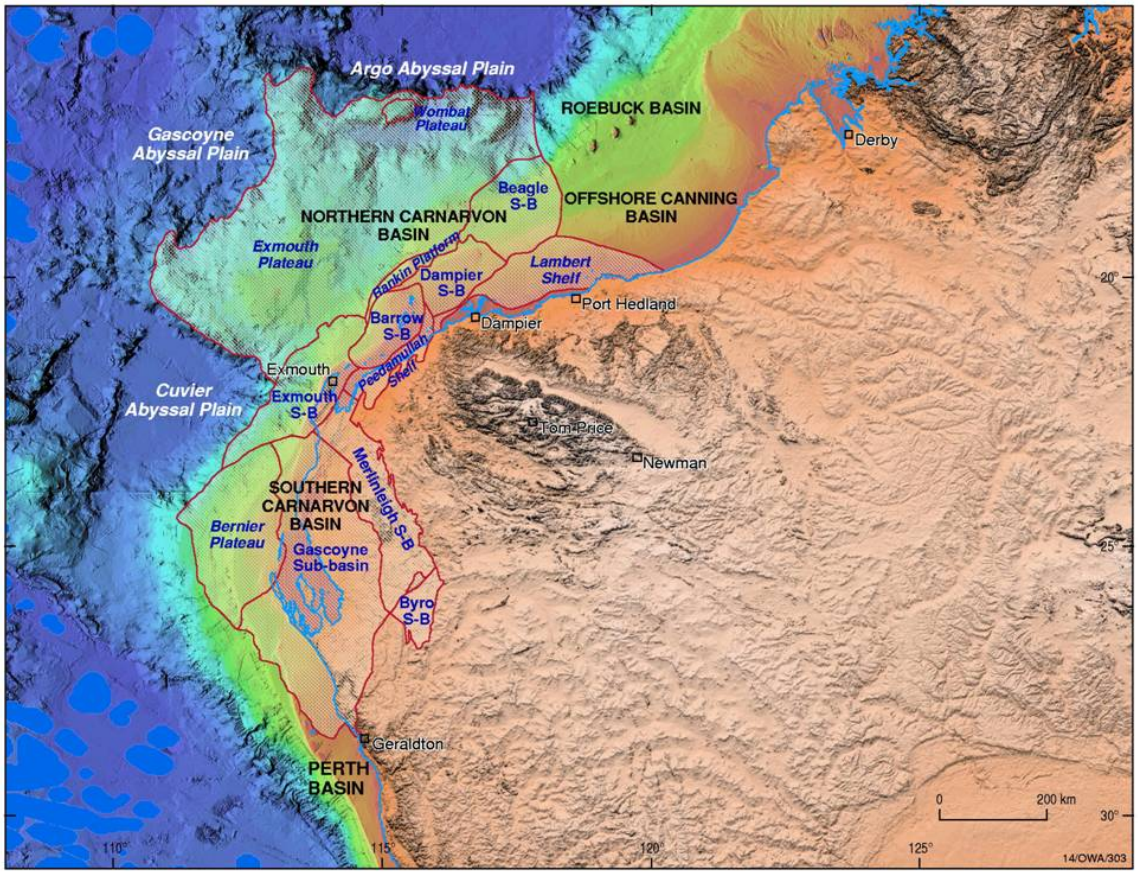

Figure 2.2: The Greater Carnarvon Basin.

From Edwards & Zumberge, 2005

2.1.2 Northern Carnarvon Basin

The Phanerozoic epicratonic Greater Carnarvon Basin is subdivided into the Southern and Northern Carnarvon Basins (Figure 2.2). The Southern Carnarvon Basin is predominantly onshore, containing up to 7km of Paleozoic-aged (Silurian to Permian) terrestrial sediments overlain by a thin veneer of Mesozoic to Cenozoic aged sediments (Hocking *et al.*, 1987; Hocking, 1988, 1994; Baillie *et al.*, 1994).

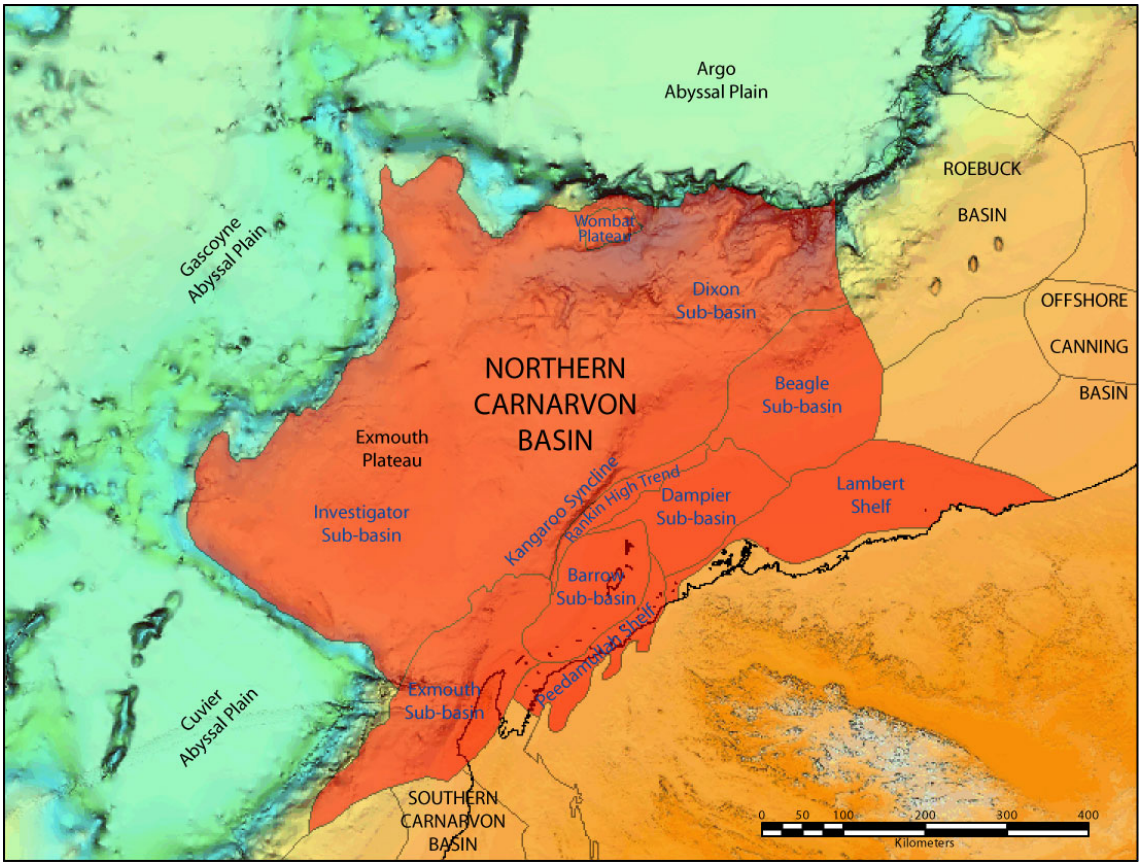

Figure 2.3: Components of the Northern Carnarvon Basin.

The predominantly offshore Northern Carnarvon Basin forms the south-western limit of the Westralian Superbasin and is transitional with the adjacent Roebuck/Offshore Canning Basin to the northeast. The Northern Carnarvon Basin comprises the major Mesozoic depocentres of the southern North West Shelf containing a thick (up to 15km) sedimentary sequence of latest Permian to Recent age (Hocking *et al.*, 1994). The Basin consists of northeast-trending sub-basins with northeast to east-trending structural fabric (Figure 2.3; Hocking *et al.*, 1987; Hocking, 1994). The Exmouth Plateau is a prominent bathymetric region bounded by the Argo, Gascoyne and Cuvier Abyssal Plains to the north, northwest and southwest respectively, and the Exmouth, Barrow, Dampier and Beagle Sub-basins to the southeast. The Plateau encompasses the Investigator and Dixon Sub-basins, the Kangaroo Syncline (or Trough) and the Rankin High Trend (or Platform; Barber, 1988; Hocking *et al.*, 1994).

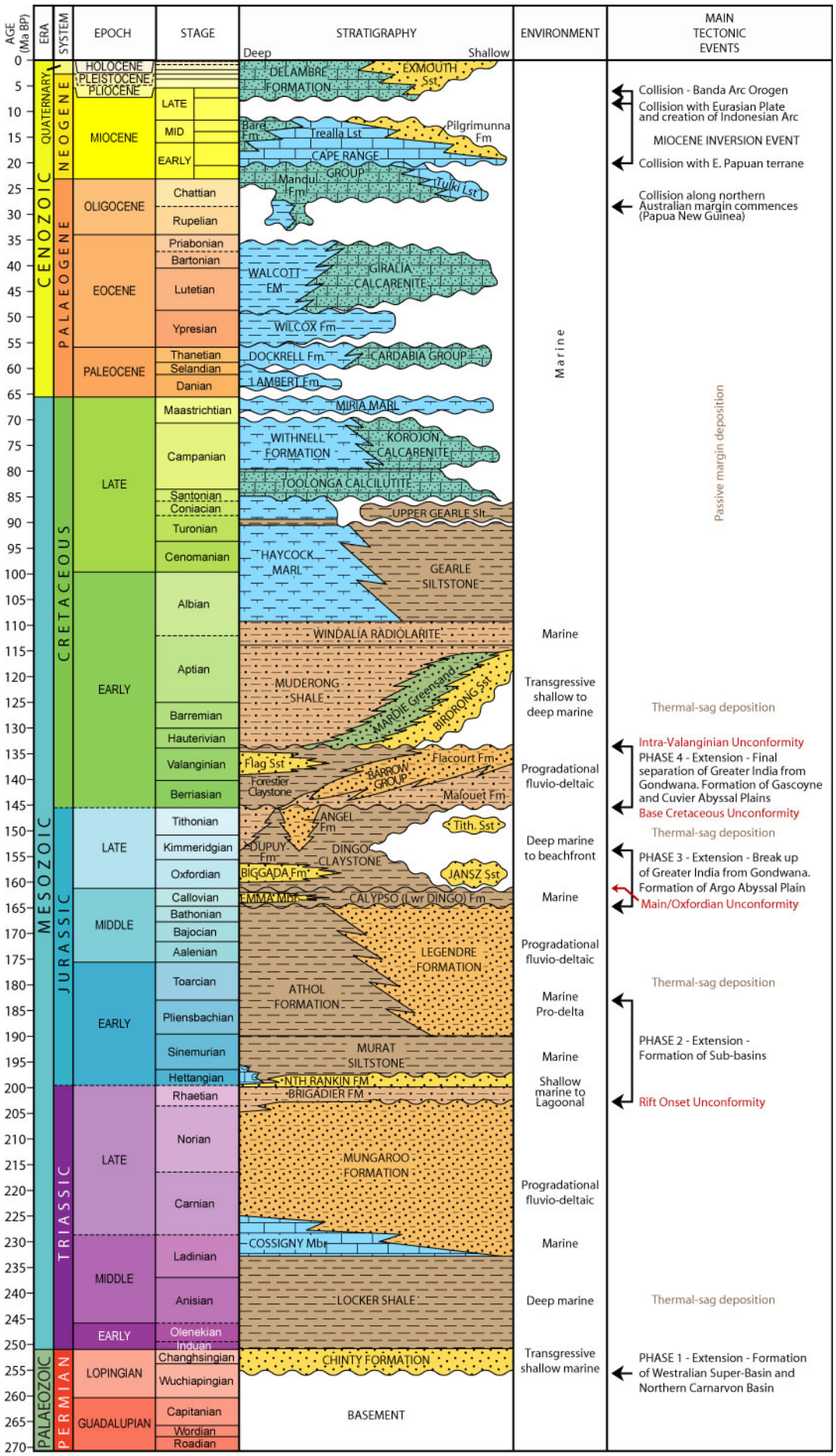

Figure 2.4: Stratigraphic and event chart for the Northern Carnarvon Basin.

The geology and formation of the Northern Carnarvon Basin has been discussed in great detail by Hocking *et al.*, 1987, 1988, 1994; Barber, 1988, 1994; Bradshaw *et al.*, 1988; Hocking, 1988, 1992, 1994; Parry & Smith, 1988; Veevers, 1988; Baillie *et al.*, 1994; Jablonski, 1997; Norvick, 2002; Jenkins *et al.*, 2003; Jablonski & Saitta, 2004; and, Edwards & Zumberge, 2005. In summary, the Northern Carnarvon Basin developed during four main successive phases of extension and thermal subsidence followed by post-rift, passive margin deposition (Figure 2.4):

Phase 1: Late Carboniferous to Permian extension caused by the initial rifting of Gondwana produced intracratonic rift basins along the northwestern margin of the Australian craton (Westralian Superbasin). Subsequent rapid thermal sag enabled the accumulation of an Late Permian to Late Triassic transgressive-regressive couplet more than 3km thick.

Phase 2: Latest Triassic (Rhaetian) to Early Jurassic (Pliensbachian) extension, the Fitzroy Movement, produced the four main depocentres: Beagle, Dampier, Barrow and Exmouth Sub-basins. The Fitzroy Movement event is expressed as the Rift Onset Unconformity. Two transgressive-regressive cycles deposited thick (over 5km) marine to deltaic sediments in a prolonged post-rift sag phase until the Callovian.

Phase 3: Mid to Late Jurassic (Callovian to Oxfordian) tectonic extension and thermal subsidence was related to the initiation of rifting of Greater India (Argo-West Burma Block) from Gondwana and the formation of the Argo Abyssal Plain through sea-floor spreading. A Callovian syn-rift associated transgression deposited widespread marine shales and mass-flow sands. A major relative sea-level regression during the Oxfordian exposed large areas of the Northern Carnarvon Basin, creating the extensive Callovian Break-up or 'Main' Unconformity. Local uplift provided the sediment source for deep-water sub-marine fan and turbiditic sands and restricted near-shore marine sands, such as the Jansz Sandstone. Adjacent low-energy, open-marine environments accumulated the silt and mudstone deposits of the Dingo Claystone.

Phase 4: Latest Jurassic (Tithonian) to Early Cretaceous (Valanginian) extension was caused by the renewed fragmentation and separation of Greater India from Gondwana. The short-lived Base Neocomian disconformity was caused by regional uplift associated with the formation of the Gascoyne abyssal plain. The resulting major relative regression instigated the rapid northward progradation of the thick (over 1,200m) Barrow Group deltaic complex. The final Greater India rifting event in the Valanginian created the Cuvier abyssal plain. Extensive regional uplift redirected the river system feeding the Barrow Delta and resulted in the short but widespread Intra-Valanginian Unconformity.

Post-rift deposition: The Tithonian–Valanginian extension generated significant post-Valanginian regional subsidence, resulting in the submergence of the Northern Carnarvon Basin. A prolonged period of tectonic subsidence and transgression with low sediment supply enabled the accumulation of transgressive sands and shelfal to open marine sediments until the Aptian. The extensive open marine Muderong Shale forms the primary regional seal throughout the Northern Carnarvon Basin. Production of the overlying Upper Aptian to Lower Albian Windalia Radiolarite signifies open marine circulation conditions from this time.

From the mid-Albian, reduced sediment supply, changed oceanic circulation patterns and the northward migration of the Australian continent resulted in the progressive, basin-wide change from siliceous- to calcareous-pelagic deposition. Carbonate-rich sediments were deposited from the Late Cretaceous to the Late Miocene as a series of north-westward prograding wedges bounded by unconformities of short duration. Bounding unconformities were the result of consecutive second-order phases of transgression and regression superimposed on a long-term global regression.

Renewed tectonic activity in the Miocene was caused by collision of the northern Westralian Superbasin with the Banda-Arc-System resulting in the Timor-Banda Orogen. Tectonic activity resulted in localised basin inversion and reactivation of some faults causing remigration of some hydrocarbon accumulations.

2.2 GEOLOGY OF THE JANSZ-IO GAS FIELD

The Jansz-Io Gas Field is located on the western limb of the Kangaroo Syncline, 250km northwest of Dampier, 70km northwest of Gorgon Gas Field, and 140km east of Scarborough Gas Field. The Kangaroo Syncline (or Trough) is a north-northeast to south-southwest trending structural downwarp across the eastern part of the Exmouth Plateau, separating the Rankin High Trend from the Exmouth Plateau mega-arch (Figure 2.5). The Kangaroo Syncline was initially formed by regional crustal extension and fault reactivation along the Rankin High Trend caused by the Oxfordian rift event of Phase 3 (described above) and progressively accentuated through preferential subsidence (Barber, 1988).

The giant Jansz-Io Gas Field covers a vast area of approximately 2,000km^2. Both a structural (fault anticline) and stratigraphic trap (reservoir pinchout) trap defining a gas-bearing reservoir up to 65m thick (Jenkins *et al.*, 2008). The Field consists of a single gas pool contained within three different aged reservoirs of Late Triassic (Rhaetian) and Late Jurassic (Oxfordian and Tithonian) age (Jenkins *et al.*, 2003). This project focuses on the volumetrically largest and

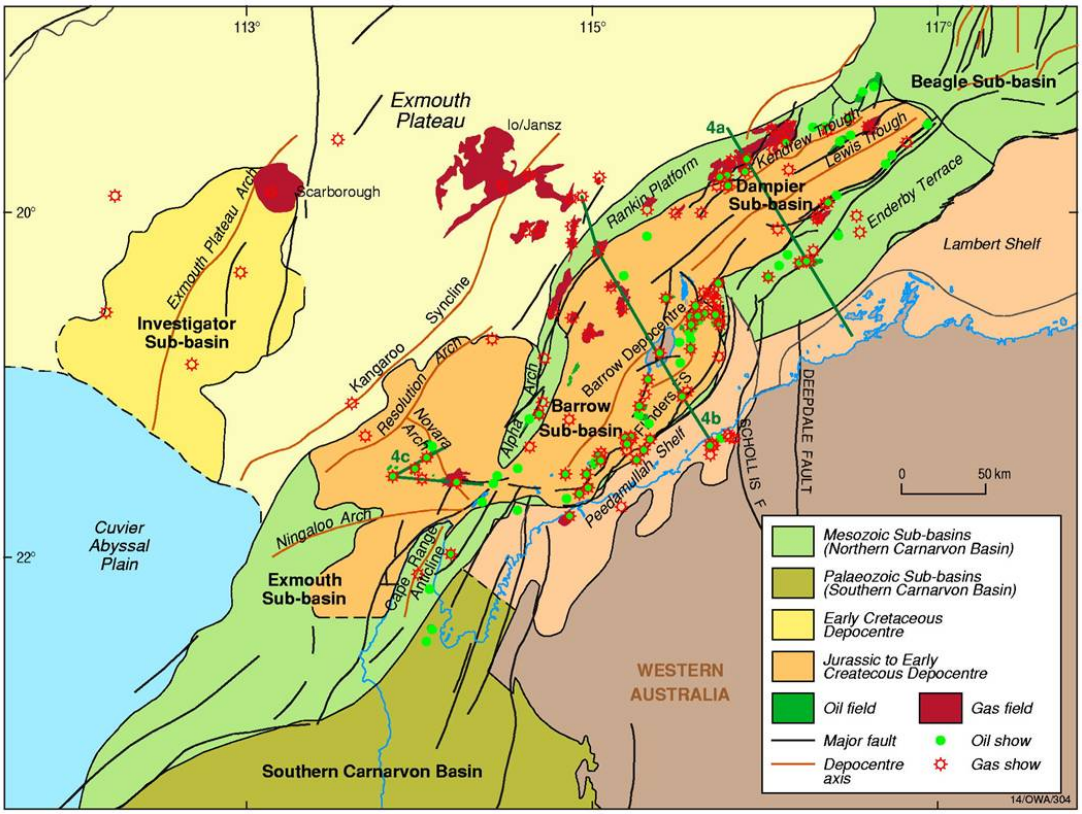

Figure 2.5: Structural elements of the Northern Carnarvon Basin and location of the Jansz-Io Gas Field. From Edwards & Zumberge, 2005

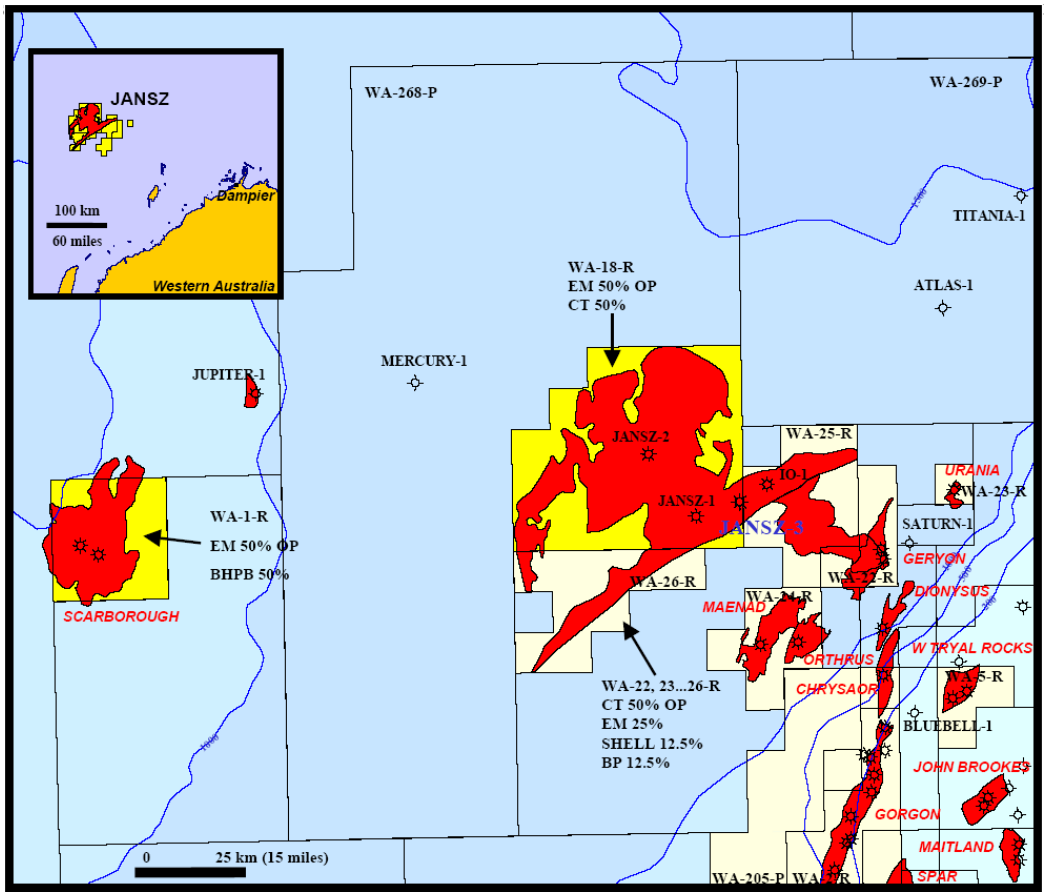

Figure 2.6: The Jansz-Io Gas Field and location of analysed wells.

From Mobil Exploration Producing Australia, 2003b

therefore most economically important reservoir, being the Oxfordian Jansz Sandstone sequence. Consequently data was analysed from the Jansz-1, -2, -3 and Io-1 wells, which all intersect the Jansz Sandstone and were available for examination at the commencement of this project (Figure 2.6).

2.2.1 Geological History

The geological history of the Jansz-Io Gas Field and characterisation of the Jansz reservoir are discussed in the Jansz-1, -2 and -3 Interpretive Well Completion Reports (Mobil Exploration Producing Australia, 2001; 2003a, b), the Io-1 Interpretive Well Completion Report (Banfield & Beattie, 2002), and three published papers: Jenkins *et al.*, 2003; Hefti *et al.*, 2006; and Jenkins *et al.*, 2008.

In summary, the Jansz Sandstone unconformably overlies the shelfal to nearshore-marine siltstone of the Callovian Calypso / Lower Dingo Formation. Oxfordian uplift of the Rankin High Trend and erosion of the Lower to Middle Jurassic Legendre / Athol and Triassic Mungaroo Formations provided the sediment source for the progradational, lower-shoreface to shelfal Jansz Sandstone. Constant uplift of the Rankin High during the Oxfordian caused the north-westward migration of the north-east to south-west oriented shoreline. This minor relative regression resulted in reworking and re-deposition of the upper-shoreface sediments, producing a coarsening- and cleaning-upward sedimentary sequence.

In the Tithonian, isostatic uplift of topographic highs adjacent to the Jansz-Io area resulted in the erosion and removal of the Oxfordian coastal plain and most of the shoreface sediments, leaving the distal lower-shoreface to open-shelf muddy sandstones preserved in the Jansz sequence. This provided the sediment supply for local deposits of coarse clastics, such as the 3m thick Tithonian sandstone (Angel Formation equivalent) at Geryon-1 which is locally in contact with the Jansz Sandstone. Subsequent post-rift thermal-sag resulted in the condensed deposition of fine-grained pro-delta mudstones of the Barrow Group over the Kangaroo Syncline, forming a minor seal for the Jansz reservoir.

During the Valanginian, the tectonic events of *Phase 4* (described above) caused a brief period of uplift and a regional depositional hiatus. The following widespread tectonic subsidence produced a major transgression and the deposition of the regionally extensive glauconitic mudstones of the Muderong Shale. The Muderong Shale forms the main economic seal to the Jansz reservoir.

2.2.2 The Jansz Sandstone

The Jansz Sandstone has been comprehensively reviewed in the recent reservoir characterisation study of Jenkins *et al.*, 2008. This study integrated all available well and seismic data collected during field exploration and appraisal and has produced a consistent interpretation for the Jansz Sandstone sequence.

In summary, the Oxfordian Jansz Sandstone consists of a coarsening- and cleaning-upward sequence of shallow-marine, highly bioturbated, glauconitic muddy sandstones deposited in a distal lower-shoreface, to open-shelf marine environment. Jenkins *et al.*, 2008 interpret two main progradational cycles separated by a short depositional hiatus informally classified as the Upper and Lower Wedge. The Upper Wedge high quality reservoir is separated from the Lower Wedge low quality reservoir by the base-of-high-permeability marker. The upper and lower boundaries of the Jansz Sandstone are defined by the Base Cretaceous Unconformity and the Oxfordian (Main) Unconformity, respectively. Laterally the sequence is constrained by depositional pinchout in north-eastern open-shelf environments and erosional truncation in the south-eastern upper-offshore, distal lower-shoreface environments.

Jenkins *et al.*, 2008 state that the Jansz Sandstone consists of three primary lithofacies in ascending order: Lithofacies S_{43}, Lithofacies S_{42}, and Lithofacies S_1.

Lithofacies S_{43} – highly bioturbated (churned), interbedded siltstone to muddy, very fine-grained sandstone. Interbeds are intensely bioturbated by ichnofauna indicative of a lower-offshore, deep water environment. The sediments are composed of quartz, with common glauconite and feldspar and rare lithics, which are moderately to well cemented by quartz overgrowths, clays, and local calcite, siderite and pyrite. Belemnites, bivalves and gastropods are common. This lithofacies forms the lower, poor quality reservoir, with moderate to high porosity (less than 25%) but very low permeability (less than 10md).

Lithofacies S_{42} – highly bioturbated (churned), thinly bedded siltstone and muddy, fine-grained sandstone. The sediments are quartzose, with common glauconite and feldspar and minor lithics, which are moderately cemented by quartz overgrowths, clays, and local calcite, siderite and pyrite. Belemnites, bivalves (frequently articulated), and gastropods are common. Intense bioturbation has removed all primary sedimentary structures, with only rare remnants of depositional bedding remaining. This lithofacies forms the primary reservoir rock of the Jansz-Io Gas Field, with high to very high porosity (greater than 25%) and moderate permeability (10-900md).

Lithofacies S_1 – poorly sorted, coarse-grained, granular to pebbly sandstones, with minor detrital clay (5-10%). No primary sedimentary structures or stratification are evident, but the beds typically display reverse-grading (coarsening upwards). The sands are predominantly quartzose, with common iron-rich oolites, clay clasts, glauconite, and mollusc and wood fragments. These sands are typically tightly cemented by early authigenic cements of either carbonate (calcite and siderite), or iron-rich amorphous clay, berthierine/chamosite and siderite, but may be weekly cemented by siderite, clays and minor pyrite. Tightly cemented sands have poor reservoir quality, with cementation precluding almost all porosity and permeability. This lithofacies is geographically restricted to the more proximal depositional localities, and stratigraphically restricted to the top of the Io-1 and Jansz-3 wells analysed in this study.

These sediments represent a progradational and aggradational sequence from more proximal to distal depositional localities, with each lithofacies intergrading and interbedding with the adjacent lithofacies. The lithofacies are time-transgressive as observed through lithofacies change along microplankton biostratigraphic and base-of-high-permeability chronostratigraphic markers.

The distinctive *Cruziana* ichnofacies assemblage, macrofossils, glauconite and the characteristic stacking pattern of the sandstones indicates that this sequence was deposited in a nearshore (upper-offshore, distal lower-shoreface) to inner-shelf (lower-offshore to open-shelf) palaeodepositional environment. A low but continuous sedimentation rate allowed the production of glauconite and homogenisation of the sediments by ichnofauna between storm-induced sediment supply. The intensity of bioturbation and absence of primary sedimentary structures indicates that the setting was at or below fair-weather wavebase with infrequent and low intensity storm events, except during Lithofacies S_1 deposition. Lithofacies S_1 is interpreted as storm-generated sandy sediment-gravity flows derived from back-beach ponds and swamps in the paralic zone, as indicated by the common occurrence of non-abraded, ferruginous ooids.

Chapter 3

PREVIOUS PALYNOLOGICAL ANALYSES

Numerous palynological studies relevant to this project are available either as published works or unpublished manuscripts and company reports. The most relevant are summarised herein.

3.1 JANSZ-IO WELL PALYNOLOGY REPORTS

Initial palynological examinations of the Jansz-Io wells involved in this study were conducted by *Morgan Palaeo and Associates* consultants for the respective Basic and Interpretive Well Completion Reports (WCR's):

Jansz-1	Hooker & Morgan, 2000a & b
Io-1	Ingram & Hooker, 2001a & b
Jansz-2	Hooker & Morgan, 2003a & b
Jansz-3	Hooker, 2003a & b

These palynological reports were commissioned to determine the biostratigraphic age, broad depositional environment and thermal maturity of the intersected sedimentary sequence.

Table 3.1 outlines the number and type of original palynological samples analysed from the four Jansz-Io wells studied herein. These samples reportedly range from Norian (Upper Triassic) to Maastrichtian (Upper Cretaceous) in age. A total of 60 palynology samples were examined from the Jansz Sandstone reservoir of these four wells. The Jansz Sandstone was found to be of Oxfordian *Wanaea spectabilis* Zone age, specifically the *Wanaea spectabilis* a and b Subzones of Morgan *et al.* (2002), and deposited in a nearshore to offshore marine environment.

Table 3.1: Type and number of original palynology samples for the Jansz-Io field wells.

WELL	CORES	CUTTINGS	SIDE WALL CORES	TOTAL	TOTAL FROM RESERVOIR
Jansz-1	19	6	40	**65**	**20 (19 CO + 1 SWC)**
Jansz-2	8	50	4	**62**	**5 (CO)**
Jansz-3	17	20	–	**37**	**15 (CO)**
Io-1	18	5	42	**65**	**20 (2 MSCT + 18 CO)**
			TOTAL	**229**	**60**

The wells Io-2 and Jansz-4 were drilled since the commencement of this project and therefore no samples or reports from these wells were incorporated in this project for confidentiality purposes.

To my knowledge, no further palynological examination has been conducted on the Jansz-Io Field until this project.

3.2 AUSTRALASIAN STUDIES

The first major Australasian Mesozoic microplankton publications were the comprehensive taxonomic works of Deflandre & Cookson (1955) and Cookson & Eisenack (1958, 1960a & b, 1962a & b) from Australia's North West Shelf (NWS) and Papua New Guinea (PNG). Edgell (1964) compiled the first Mesozoic microplankton biozonation on Lower Cretaceous sediments from the Perth Basin. Microplankton biozonation was thereafter recognised as the dominant method of correlation on the NWS.

Demand for Mesozoic microplankton biostratigraphy was subsequently driven by petroleum exploration on the NWS. The majority of microplankton research until the late 1980's was conducted by in-house palynologists and considered highly proprietary. Therefore most research was produced as unpublished company reports, with a few notable exceptions recorded in Table 3.2. The first publication of a single, unified and integrated palynological biozonation scheme for the entire Australian Mesozoic sequence was developed by Helby, Morgan & Partridge as Helby *et al.,* (1987), commonly referred to as the HMP biozonation scheme. Related taxonomic papers in the same Association of Australasian Palaeontologists Memoir (Jell, 1987) provided the essential support for this comprehensive biozonation scheme. Concurrently, Davey (1987) produced an integrated palynological biozonation for the Mesozoic of PNG, highlighting the similarities and differences between these neighbouring regions. Francis & Westermann (1993) published a comparison of the Upper Jurassic portions of these two biozonation schemes and presented important new data for ammonite-microplankton correlation for Upper Jurassic sediments of Australia, PNG and Indonesia. Burger (1996) provided further age ties for many Helby *et. al.* (1987) biozones by incorporating fresh ammonite, conodont, foraminiferal, nannofossil and ostracod evidence in his palynological analysis of NWS dredge samples.

In the late 1990's, the need for higher resolution biostratigraphy for petroleum exploration prompted the revision of the original microplankton biozonation schemes and supporting taxonomy. Davey (1999) published a revised palynological biozonation for PNG. For the NWS, Riding & Helby (2001a-h) and Helby & Partridge (2001) published a series of papers describing additional Jurassic and Cretaceous key microplankton taxa, and graphically presenting an informal alphanumeric zonal subdivision (Foster, 2001, fig. 2). Morgan, Hooker & Ingram privately distributed a parallel informal alphanumeric subzonation scheme in 2002 (Morgan *et al.*, 2002).

The HMP biozonation scheme was updated by Helby *et. al.* (2004) including a graphic comparison of the afore-mentioned informal subzonations, however formal subzones were not

resolved in the ultimate 2004 scheme. The HMP zones were subsequently tied to the 2004 Geologic Time Scale by Partridge (2006a-d). Most recently, Riding *et al.* (2010) reviewed published literature and open-file unpublished reports to refine the biostratigraphic and chronostratigraphic correlation of the HMP zones to the Northern Hemisphere Dinoflagellate Cyst Zones of Poulsen & Riding (2003) and the 2008 Geologic Time Scale, however no subzones were included. Since formal subdivision of the HMP zones with taxonomic evidence has not been published to date, recent research, such as Mantle (2009a & b) and the present study, has focused on taxonomically refining and subdividing portions of the well established HMP biozonation structure.

As mentioned in Riding *et. al.* (2010, p.544), compared to the Northern Hemisphere, relatively few publications specifically related to Australasian Jurassic microplankton taxonomy or biostratigraphy have been published. The most relevant publications to the Australasian Oxfordian *Wanaea spectabilis* Zone are listed in Table 3.2.

Table 3.2: Australasian microplankton literature relevant to the Oxfordian *Wanaea spectabilis* Zone.

PUBLICATION	AGE	LOCATION
Backhouse, 1988	Late Jurassic - Early Cretaceous	Perth Basin, Western Australia
Burger, 1994, 1996	Mesozoic	North West Shelf, offshore Western Australia
Cookson & Eisenack, 1958, 1960a & b, 1962a & b, 1974	Mesozoic - Cenozoic	Australia & Papua New Guinea
Davey, 1987, 1999	Middle Jurassic - Early Cretaceous	Papua New Guinea
Deflandre & Cookson, 1955	Late Mesozoic - Tertiary	Australia
Edgell, 1964	Early Cretaceous	Perth Basin, Western Australia
Filatoff, 1975	Jurassic	Perth Basin, Western Australia
Francis & Westermann, 1993	Late Jurassic	Australia, Papua New Guinea & Indonesia
Helby & Stover, 1987	Bathonian - Callovian	Australia & Papua New Guinea
Helby *et al.*, 1987, 2004	Mesozoic	Australia
Helby *et al.*, 1988	Middle - Late Jurassic	New Zealand
Kemp, 1976	Permian and Early Cretaceous	Officer Basin, Western Australia
Mantle, 2005, 2009a & b	Callovian	Timor
Morgan, 1975, 1980	Cretaceous	Australia
Morgan *et al.*, 2002 (unpublished)	Mesozoic	Australia
Partridge, 2006a - d	Mesozoic	Australia
Riding, 2005a & c	Late Jurassic	Australia
Riding & Fensome, 2003	Late Jurassic	Australia & Europe
Riding & Helby, 2001a - h	Middle Jurassic - Early Cretaceous	Australia & Timor
Riding *et al.*, 2010	Middle Triassic - Late Jurassic	North West Shelf, offshore Western Australia
Sarjeant *et al.*, 1992	Jurassic	Circum-Pacific
Stevens, 1987	Early Cretaceous	Western Australia
Stover & Helby, 1987a - d	Mesozoic	Australia & Papua New Guinea
Wilson & Helby, 1987	Oxfordian	New Zealand
Wiseman, 1980	Middle Jurassic - Early Cretaceous	Carnarvon Basin, Queensland
Wiseman & Williams, 1974	Early Cretaceous	North West Shelf, offshore Western Australia

3.3 WORLDWIDE STUDIES

The existence of dinoflagellate cysts in Jurassic sediments was first recorded by Ehrenberg in 1843 (Ehrenberg, 1843a, b) in sediments from Asia, Australia, Africa and Poland. Following these pioneering works, few Jurassic dinoflagellate cyst papers were published for nearly a century. Jurassic dinoflagellate cyst taxonomic and biostratigraphic studies were greatly advanced by the major publications of Deflandre (e.g., 1935, 1936, 1937, 1938, 1939, 1941, 1947b) from Late Jurassic sediments of France. These seminal works have been followed by hundreds of publications on Jurassic microplankton taxonomy and biostratigraphy from all over the globe. The most relevant taxonomic and biostratigraphic publications to the Jansz Oxfordian *Wanaea spectabilis* Zone assemblage are summarised in Table 3.3.

Table 3.3: Global microplankton literature relevant to the Oxfordian *Wanaea spectabilis* Zone.

REGION	PUBLICATION	AGE	LOCATION
Worldwide	Below, 1982a, b & c, 1987a & b, 1990	Triassic - Recent	Africa, Europe, Indonesia and Russia
	Fauconnier & Masure, 2004	Triassic - Recent	Worldwide
	Jan du Chêne *et al.*, 1986a	Triassic - Recent	Worldwide
	Riding & Sarjeant, 1984	Jurassic	Worldwide
	Riding & Thomas, 1992	Jurassic	Worldwide
	Sarjeant, 1979	Mid-Late Jurassic	Worldwide (except North America)
	Stancliffe & Sarjeant, 1988, 1990, 1996	Bathonian - Oxfordian	Worldwide
	Stover & Evitt, 1978	Triassic - Recent	Worldwide
	Stover *et al.*, 1977	Jurassic	Worldwide
	Stover & Williams, 1987	Triassic - Recent	Worldwide
	Williams *et al.*, 1993	Mesozoic - Cenozoic	Northern hemisphere
Africa	El Beialy & Ibrahim, 1997	Callovian - Oxfordian	Egypt
	Hssaïda & Morzadec-Kerfourn, 1993	Bathonian - Oxfordian	Morocco
	Ibrahim *et al.*, 2002	Jurassic - Early Cretaceous	Egypt
	Ibrahim & Schrank., 1996	Late Jurassic - Early Cretaceous	Egypt
	Jiang *et al.*, 1992	Late Jurassic	Kenya
	Msaky, 2007	Late Jurassic	Tanzania
	Schrank, 2005	Late Jurassic - Early Cretaceous	Tanzania
	Thusu & Vigran, 1985	Late Bathonian - Tithonian	Libya
Asia & The Middle East	Ashraf, 1979	Jurassic - Early Cretaceous	Afghanistan
	Gitmez & Ertug, 1999	Late Jurassic - Early Cretaceous	Turkey
	Jain *et al.*, 1984	Middle - Late Jurassic	India
	Kholeif *et al.*, 2004	Oxfordian	Qatar
	Kumar, 1986	Jurassic	India
	Wheeler & Sarjeant, 1990	Late Jurassic - Early Cretaceous	Iran
	Zhu Youhua & He Chengquan, 2007	Late Jurassic - Early Cretaceous	NE China
Europe	Alberti, 1961	Mesozoic - Tertiary	Europe
	Beju, 1971	Jurassic	Romania
	Borges *et al.*, 2011	Jurassic	Portugal
	Brenner, 1988	Oxfordian - Kimmeridgian	Germany
	Courtinat, 1989, 2006	Late Jurassic	France
	Courtinat & Gaillard, 1980	Oxfordian	France
	Davey, 1979c, 1982	Late Jurassic - Early Cretaceous	NW Europe
	Davey *et al.*, 1966a, 1969	Mesozoic - Cenozoic	United Kingdom (UK)
	Deflandre, 1935, 1936, 1937, 1938, 1939, 1941, 1947b	Middle - Late Jurassic	France

	Dodekova, 1967, 1969, 1975, 1990, 1992, 1994	Bathonian - Tithonian	Bulgaria
	Drugg, 1978	Jurassic	Europe
	Erkmen & Sarjeant, 1980	Callovian	United Kingdom
	Fensome, 1979	Middle - Late Jurassic	Greenland
	Gitmez, 1970	Kimmeridgian	UK and France
	Gitmez & Sarjeant, 1972	Kimmeridgian	UK and France
	Gocht, 1970	Bathonian	Germany
	Huault, 1999	Aalenian - Oxfordian	France
	Ioannides *et al.*, 1977	Kimmeridgian	United Kingdom
	Klement, 1960	Late Jurassic	Germany
	Kunz, 1990	Oxfordian - Tithonian	Germany
	Lund & Ecke, 1988	Middle - Late Jurassic	Germany
	Nøhr-Hansen, 1986	early Kimmeridgian	United Kingdom
	Porter, 1988	Jurassic	United Kingdom
	Poulsen, 1986, 1992, 1993, 1994a & b, 1996	Jurassic	Denmark & Poland
	Poulsen & Riding, 2003	Jurassic	NW Europe
	Prauss, 1989	Pliensbachian - Callovian	Germany
	Raynaud, 1978	Late Jurassic	northern Europe
	Riding, 1983, 1987a & b, 2005b	Jurassic	United Kingdom
	Riding *et al.*, 1985	Bathonian	United Kingdom
	Riding & Thomas, 1988	Late Jurassic	United Kingdom
	Riley & Fenton, 1982	Callovian - Oxfordian	NW Europe
	Sarjeant, 1960a & b, 1961a & b, 1962a & b,1963a & b, 1968, 1972, 1974, 1976a & b, 1978, 1980, 1982, 1984, 1985	Jurassic - Cretaceous	Europe
	Smelror, 1988a & b, 1989	Bathonian - Oxfordian	Norway and Greenland
	Stancliffe, 1989, 1991, 1996	Oxfordian	United Kingdom
	Thomas & Cox, 1988	Oxfordian - Kimmeridgian	United Kingdom
	Woollam, 1980, 1982, 1983	Jurassic	United Kingdom
	Woollam & Riding, 1983	Jurassic	United Kingdom
North America	Brideaux, 1977	Late Jurassic - Early Cretaceous	Canada
	Brideaux & Fisher, 1976	Late Jurassic - Early Cretaceous	Canada
	Davies, 1983	Jurassic - Early Cretaceous	Canada
	Johnson & Hills, 1973	Jurassic	Canada
	Olmstead *et al.*, 1996	Oxfordian - Kimmeridgian	Arizona
	Pocock, 1972	Jurassic	Canada
	Wiggins, 1975	Jurassic - Cretaceous	Alaska
	Williams, 1975	Middle Jurassic - Pleistocene	offshore eastern Canada
	Zotto *et al.*, 1987	Kimmeridgian	offshore eastern USA
Russia	Lentin & Vozzhennikova, 1990	Jurassic - Tertiary	Russia
	Riding *et al.*, 1999	Jurassic - Early Cretaceous	Russia
	Vozzhennikova, 1967	Jurassic - Tertiary	Russia
South America	Quattrocchio *et al.*, 2006	Early Cretaceous	Argentina
	Quattrocchio & Sarjeant, 1992	Callovian - Tithonian	Argentina
	Quattrocchio & Volkheimer, 1990	Jurassic - Early Cretaceous	Argentina
	Riding *et al.*, 2011	Callovian	Argentina

Chapter 4

NEW PALYNOLOGICAL ANALYSES

4.1 THE JANSZ-IO PROJECT

This project aims to produce a practical subdivision of the *Wanaea spectabilis* Zone for the Jansz Sandstone sequence intersected by conventional core. High density and equidistant samples were collected while logging conventional core from the reservoir sequence of four wells across the Jansz-Io Gas Field. Only conventional core samples were examined for biostratigraphy to minimise potential errors from caving (cuttings) or depth correlation (side wall cores). New palynological strew-slides were prepared for palynological examination to ensure accuracy of zonal subdivision and consistency of palynofacies analysis. Palynological analyses performed in this project include:

1. detailed systematics of the diverse microplankton assemblages yielded by the Jansz-Io samples;
2. identification of key marker species and bioevents;
3. improved biostratigraphic subdivision of the intersected *Wanaea spectabilis* Zone for high resolution intra-reservoir correlation;
4. detailed quantitative analysis of the microplankton and total palynodebris content (palynofacies analysis); and,
5. integration of the biostratigraphic framework with lithofacies and petrophysical data for bio-sequence stratigraphic and palaeoenvironmental syntheses of the Jansz Sandstone reservoir sequence.

The results of these analyses are presented in forthcoming chapters.

4.2 MATERIALS

ExxonMobil kindly granted access to the original palynological strew-slides and remaining kerogen residue samples produced during routine petroleum exploration sampling of the Jansz-1, -2 and -3 wells. New strew-slides prepared from pre-existing Jansz-3 core sample residues were qualitatively analysed and incorporated into taxonomic analysis, with some specimens from this material assigned as the type material of new species.

New palynological strew-slides were prepared from conventional core samples collected from the Jansz-1, -2, -3 and Io-1 wells to ensure consistency of palynofacies results and accuracy of zonal subdivision. Palynological samples were collected from conventional core at 1m intervals

where possible, and as close as possible to the meter where sampling on the meter was prevented, such as rare samples in the Io-1 core. The author personally collected the palynology samples from the Jansz-1, -2 and -3 wells. Micropalaeontologist and then Geoscience Australia Timescales Group Manager, Dr Richard Howe, kindly assisted by sampling the Io-1 conventional core at Core Laboratories in Kewdale, Perth on the author's behalf.

A list of all samples analysed is presented in Appendix 1.

4.3 METHODS

4.3.1 Core logging

Primary sedimentary structures apparent in conventional core, such as grainsize, grading, bedding surfaces and bioturbation, were recorded to assist in determining the palaeodepositional environment and provide a lithostratigraphic framework of the Jansz Sandstone reservoir sequence. Core logging conducted for Well Completion Reports during petroleum exploration provides a good overview of the core features for individual wells. However, logging reports are completed soon after each well is drilled, therefore reports for different wells of the same field may be written years apart resulting in widely varied interpretations. Consequently, it is beneficial to re-examine all available cores in the study area during palynology sampling to accumulate all available information for the most consistent and accurate environmental interpretation.

The archived portions of Jansz-1, -2 and -3 conventional core stored at Geoscience Australia were examined and logged in detail during palynological sampling for this project. Comprehensive notes on the lithology, lithological boundaries, grainsize, sorting, visible petrology, sedimentary structures, bioturbation, macrofossils, cementation, diagenesis, and palynology sample locations were recorded. Core logs generated for the Jansz wells are available in Appendix 2.

Logging of the Io-1 core was unfortunately not possible during sample collection, since the archive quota had not been received by Geoscience Australia to that date. However the core samples obtained for palynology were compared to the detailed core photographs contained in the Io-1 Well Completion Reports and the cores from the Jansz wells.

4.3.2 Palynological Sample Collection Procedures

Great care was taken when sampling for palynology to prevent contamination. Tools used for sampling raw material were thoroughly washed in distilled water and laboratory detergent between samples. During sampling, care was taken to preserve the 'face' of the valuable conventional core for future analysis. Additionally the circumference of the conventional core was avoided to prevent sample contamination by driller's mud, which contains palynomorphs from other stratigraphic units. Where possible the outer edge of the sample was removed using a diamond saw and the sample washed in clean, distilled water to remove contaminants.

Sample size collected for palynological preparation varied according to the sample lithology:

- 10g for fine-grained sediments (*e.g.* shale);
- 20g for sandstones and partially oxidised sediments;
- 30g for pebbly sandstone with fine, iron-rich, partially oxidised matrix.

Collected samples were isolated in disposable self-sealing sample bags to avoid cross contamination. Sample metadata were carefully collected, including:

- Well name;
- Sample number;
- Core Depth (m);
- Sample Type;
- Sample Weight.

4.3.3 Palynological Sample Processing Procedures

All palynological strew-slides examined in this study were prepared through the Geoscience Australia Palaeontology and Sedimentology Laboratory. Residues provided by ExxonMobil were prepared into palynological strew-slides for initial qualitative analysis. Raw conventional core samples were processed using standard palynological processing techniques summarised as follows:

1. 10-30g of sediment from each sample was sieved at 3mm and the larger fraction crushed to approximately 3mm diameter.
2. A representative sample of 10-20g was washed in xylene, acetone, dichloromethane and/or 'RigWash' industrial detergent to remove synthetic drillers mud to prevent kerogen clumping.
3. Samples were digested in 30% hydrochloric acid (HCl) for up to 12 hours to remove the carbonate mineral content, then washed and neutralised.

4. Samples were digested in 70% hydrofluoric acid (HF) for up to 12 hours to remove the silicate mineral content, then washed and neutralised.
5. Samples were then digested with hot (100-150^{o}c) 30% HCl and placed in a warm bath (53-55^{o}c) for up to 30 minutes to remove residual fluoride mineral content, then washed and neutralised.
6. Kerogen strew-slides were prepared on no.1 cover slips and mounted onto glass microscope slides using Eukitt® polyester resin.
7. A portion of the kerogen residue was sieved at either 5 or 20µm using polycarbonate sieving discs to remove fine particulate amorphous organic matter, and +5µm and +20µm fraction strew-slides were prepared as for the kerogen strew-slides.
8. Where necessary, residues were oxidised in hot (100-150^{o}c) 70% nitric acid (HNO_3) for 30-60 seconds to remove pyrite and AOM from specimens.
9. Where necessary, heavy-liquid separation using 2.1SG zinc bromide ($ZnBr_2$) was conducted to remove remaining mineral matter.
10. +5µm and/or +20µm fraction oxidised strew-slides were prepared as described above.

Samples collected from iron-rich, coarse 'Lithofacies S_1' sediments were identified as having poor palynological potential. Therefore, poorly cemented Lithofacies S_1 samples were sieved to remove the coarsest grainsizes and concentrate fine-grained sediments to 1/ reduce sample volume for palynological processing; 2/ maximise the potential kerogen recovery; and 3/ reduce potential contamination from palynomorphs contained in reworked lithoclasts. This method proved highly successful in some samples, producing the best preserved microplankton specimens of all samples.

All strew-slides (with the exception of those submitted to the Commonwealth Palaeontological Collection [CPC] as type material) and any unprocessed core samples or processed kerogen residues remaining after palynological preparation are archived in the Geoscience Australia Repository through the Geoscience Australia Palaeontology and Sedimentology Laboratory.

Well preserved samples were prepared for scanning electron microscopy (SEM) analysis by strew-mounting +20µm oxidised residue on round no.1 cover slips. The cover slips were attached to aluminium SEM stubs and spatter-coated with gold for SEM examination. SEM analyses were conducted for illustrative purposes only and SEM stubs are not archived.

4.3.4 Analysis Equipment and Techniques

All transmitted light microscopy was conducted on a Zeiss Axioplan microscope with nomarski differential interference contrast capabilities, and an Olympus DP11 digital camera in the Geoscience Australia Palaeontology and Sedimentology Laboratory. The majority of photomicrographs were taken using a 40x Plan-Neofluar oil objective, with more detailed photomicrographs taken using a 63x Plan-Apochromat oil or a 100x Plan-Neofluar oil objective. Initial sample overview analyses and photomicrographs were conducted using 20x or 40x Plan-Neofluar dry objectives. Photomicrographs of specimens illustrated herein have been adjusted for brightness and contrast, but not digitally modified or altered.

Original strew-slides or residues provided by ExxonMobil were analysed for qualitative taxonomic analysis only. These samples were not included in quantitative analyses to ensure consistency of palynological results from uniformly prepared samples.

Detailed qualitative and quantitative palynological analyses were conducted on newly prepared samples. Qualitative taxonomic analysis was completed during the first phase of sample examination to ascertain the microplankton assemblage. Quantitative palynofacies counts of 100 palynomorph and palynodebris grains were conducted on all new samples from all wells to enable palynofacies signature comparison across the field, as outlined in Chapter 7.2. Detailed quantitative biostratigraphic analysis was carried out on all Jansz-1, -2 and -3 +20µm sieved fraction samples of 250 microplankton specimens every 1m with accessory species outside the counts recorded to determine the assemblage diversity. Comparative analysis was conducted on Io-1 samples of 100 microplankton specimen counts every 3m with additional species recorded as accessories. The purpose of a reduced microplankton count at lower sample density in Io-1 was to determine if key bioevent signatures would be recognisable during routine palynological analyses for petroleum exploration.

Chapter 5

PALYNOLOGY: SYSTEMATICS AND INVENTORY

Detailed taxonomy is presented for marine microplankton, comprising dinoflagellate cysts and acritarchs, which constitute the main focus of the present study. Spores and pollen, foraminiferal test linings and other palynomorph groups were also encountered in the samples and are briefly discussed.

> ***"Paratabulation is the key to interpreting dinoflagellate taxonomy and phylogeny and these, in turn, are fundamental to meaningful biostratigraphic and ecological studies."***
>
> Fensome *et al.*, 1996, p.129.

5.1 DINOFLAGELLATE CYSTS

5.1.1 Nomenclature

Dinoflagellate cysts comprised the largest proportion of palynomorphs in the Jansz-Io preparations. The dinoflagellate cyst taxonomy presented herein follows the nomenclatorial conventions of The International Code of Botanical Nomenclature (ICBN; McNeill *et al.*, 2006) and is constrained by the following parameters:

- Newly identified taxa recorded herein as "gen. nov." or "sp. nov." are pending formal publication;
- Dinoflagellate cyst suprageneric classification follows Fensome *et al.* (1993), however, for ease of taxonomic comparison, dinoflagellate cyst descriptions are presented from the generic level and are arranged in alphabetical order;
- Generic descriptions follow the style of Stover & Evitt (1978);
- The abbreviation 'cf.' or 'aff.' preceding the specific epithet in a taxon name represents that observed specimens either visually closely resemble or have a morphological affinity with the so named published species respectively;
- The abbreviation '*s.s.*' following the specific epithet refers to '*sensu stricto*' for 'in the stricter sense', referring to a taxon as originally described;
- A question mark (?) following or within the taxon name indicates questionable assignment to the species and/or genus respectively;
- Some citations that appear only for taxon authorship are not included in the reference list. Citations for these references may be found in Fensome & Williams (2004);

- Synonymy lists presented for each species are intended to record the taxonomic history and assist taxonomic description or revision rather than present a complete list of published occurrences;
- Applied descriptive terminology follows Evitt (1985) and Williams *et al.* (2000);
- Paratabulation is presented in homologous Kofoid notation as in Fensome *et al.* (1993);
- Descriptive dimensions follow Stover & Evitt (1978), being small (<50 μm), medium / intermediate (50-100 μm), and large (>100 μm);
- Species measurements are presented as "minimum (mean) maximum" dimensions, *e.g.* 40 (50) 60 μm; where only 2 specimens are measured they are presented as "minimum, maximum" dimensions, *e.g.* 40, 50 μm;
- The abbreviation 'TLM' means Transmitted Light Microscope (/Microscopy);
- The abbreviation 'SEM' means Scanning Electron Microscope (/Microscopy);
- The abbreviation 'HMP' refers to the Helby, Morgan & Partridge biozonation scheme of Helby *et al.*, 1987 and the revised editions of Helby *et al.*, 2004, Partridge, 2006 and Riding *et al.*, 2010;
- Refer to quantitative analysis charts in Appendix 4 for observed taxon ranges.
- Previously reported species ranges are compiled from the most relevant publications and are not intended as an exhaustive list. Refer to the Palynodata database for further species ranges, accurate up to 2006 (Palynodata datafile: 2006 Version; Geological Survey of Canada, Open File 5793).
- All sample depths refer to conventional core depths in metres below rotary table (mRT(c)) as recorded during sample collection.

With respect to Plates:

- All type material figured in transmitted light microscopy plates is archived in the Commonwealth Palaeontological Collection (CPC) at Geoscience Australia, Canberra (see Appendix 3).
- Figured specimens imaged by scanning electron microscopy are presented here for illustrative purposes only and have not been archived.
- Specimen orientation follows Evitt, 1985, where:
    - 'View' indicates the direction of exterior view at high focus;
    - 'Focus' refers to the location of the detail shown.

  For example, "Dorsal view, high to low foci" refers to a focal series from "the dorsal surface in dorsal view at high focus" to "the ventral surface in dorsal view at low focus".
- A single scale bar per plate applies to all figures on that plate. Where scales differ, a scale bar is presented for each specimen, unless stated otherwise.
- The holotype of each new species is indicated by an asterisk (*).

5.1.2 Glossary of Introduced Terms

***Endosuture*:** parasuture of the endophragm.

***Endoplates*:** paraplates of the endophragm.

***Insiderae*:** noun of *Insiderate* Below (1987a, p.61; Below 1987b, pl.19, figs.1-10; Translated by Fensome *et al.,* 1993, p.866): "If processes have basal root-like divisions which fuse with the cyst surface, I term this *insiderate* (Latin *insidere* = to root)."

***Periplates*:** paraplates of the periphragm.

***Perisuture*:** parasuture of the periphragm.

***Simulate*:** shape of an intratabular process distally and/or proximally reflects the shape of the underlying paraplate, though not as clearly or completely as clypteate processes (*e.g. Areosphaeridium*). (Latin *simulo* = to make like, cause to resemble). Differs to *simulate process complex* of Lentin & Williams, 1976 (p. 175) which relates to multiple processes arranged in a plate-defined polygonal complex.

5.1.3 Systematic Descriptions

Genus ***Adnatosphaeridium*** Williams & Downie, 1966, emend. Stancliffe & Sarjeant, 1990

Type species: *Adnatosphaeridium vittatum* Williams & Downie, 1966.

***Adnatosphaeridium* sp. A**

Pl. 1, figs. A-B

Description: Skolochorate cyst of medium to large size; endophragm (central body) subspherical, smooth to scabrate; periphragm forms very thin, solid, (apparently intratabular) processes to process complexes, distally connected by a dense network of interconnecting trabeculae. Trabeculum consists of threads to ribbons to perforated membranes; supporting processes frequently indistinguishable from the trabeculum, therefore exact number of processes indeterminate. Parasulcus not observed; paracingulum appears to consistently host processes. Paratabulation not expressed apart from vague suggestion from probable intratabular arrangement of observable processes. Archeopyle apical, Type (tA).

Dimensions: (µm; 4 specimens measured)

Total length: 75 (103) 128

Total width: 81 (94) 118
Central body length (with operculum): 56 (1 specimen)
Central body length (without operculum): 52 (54) 57
Central body width: 40 (55) 88
Max. length of processes: 20 (31) 48

Comments: The thin processes are typically not strong enough to support the dense trabeculum resulting in intense folding and distortion of the trabeculum (pl. 1, fig. B). Measurements were taken on the few specimens retaining a relatively well preserved structure.

Comparison: *Adnatosphaeridium* sp. A is similar to *Adnatosphaeridium densifilosum* (Cookson & Eisenack, 1974) Stancliffe & Sarjeant, 1990 in having a complex trabecular network and paracingular processes, but *A. densifilosum* differs in possessing relatively thick and often flared processes supporting the trabeculum rather than the fine processes to process complexes observed here.

Adnatosphaeridium sp. A is also similar to *Rigaudella filamentosa* (Cookson & Eisenack, 1958) Below, 1982b, particularly observed *R. filamentosa* morphotypes with paracingular processes, but *R. filamentosa* has a much finer trabeculate network so the supporting processes and process complexes are clearly discernible.

This species is placed within *Adnatosphaeridium* due to the apparently consistent display of paracingular processes. However *Adnatosphaeridium* sp. A and *R. filamentosa* are clearly related, and future examination may well reveal more intermediate specimens to indicate that *Adnatosphaeridium* sp. A may simply be an extremely trabeculate morphotype of *R. filamentosa,* similar to the variable trabeculae observed in *R. aemula* (Deflandre, 1939) Below, 1982b.

Genus ***Aldorfia*** Stover & Evitt, 1978

Type species: Gocht, 1970, as *Gonyaulacysta aldorfensis*.

Aldorfia aldorfensis (Gocht, 1970) Stover & Evitt, 1978

Pl. 1, figs. C-E

1970 *Gonyaulacysta aldorfensis* Gocht, p.136-138, pl.30, figs.1-2, 3a-d, pl.31, figs.9a-b, 10a-c, 11, pl.32, figs.1-2, 3a-b, text-figs.5, 9a-c.

1978 *Aldorfia aldorfensis* (Gocht, 1970) Stover & Evitt, p.140.

Dimensions: (μm; 12 specimens measured)
Autophragm length: 54 (63) 78
Autophragm width: 44 (55) 65
Ectophragm length: 67 (82) 100
Ectophragm width: 54 (72) 86

Comments: Jansz-Io specimens display the same morphological characteristics and fall within the size range presented by Gocht (1970) from the type locality. However, observed Jansz-Io specimens appear to have a broader ectocoel than the figured type specimens, and predominantly display isolated projections within the ectocoel rather than septa (= muri in Stover & Evitt, 1978).

Previously reported range: Cosmopolitan: Mid-Bathonian to Mid-Oxfordian of Australia (Riding *et al.*, 2010);
Bajocian to Lower Callovian of Europe (Gocht, 1970; Sarjeant, 1979; Riley & Fenton, 1982; Riding *et al.*, 1985, 1999, 2010; Jan du Chêne *et al.*, 1986a; Prauss, 1989; Fauconnier, 1995; Fauconnier *et al.*, 1996; Poulsen & Riding, 2003);
Mid-Oxfordian to Mid-Kimmeridgian of Egypt (Ibrahim *et al.*, 2002).

Genus ***Ambonosphaera*** Fensome, 1979, emend. Prauss, 1989

Type species: *Ambonosphaera calloviana* Fensome, 1979.

Ambonosphaera? conferta sp. nov.

Pl. 1, figs. H-K; Pl. 2, figs. A-L; Pl. 108, figs. A-H

Holotype and type locality: Pl. 2, fig. J-L, Jansz-3, Core, 2811mRT(c), GA sample no. 1631225, slide no. 5, England Finder co-ordinates: T42/1, CPC no. 40583.

Derivation of name: From *confertum* (Latin): "to press close together, cram together, compressed, dense", for both the strong lenticular dorso-ventral compression and the compressed dorsal paratabulation.

Synopsis: Small to medium-sized, strongly lenticular, proximate cyst; circumcavate; endocyst ambitus circular to subpolygonal, pericyst ambitus subpolygonal with prominent lateral postcingular bulges; deep paracingular and parasulcal furrows with distinct kidney-shaped

flagellar scar; dorso-ventral surfaces vacuolate, pericoel internally displays scabrate to granulate ornament and rare interconnecting processes; archeopyle apical, probably Type tA; gonyaulacacean paratabulation, formula: Xpr, 4', ?1a, 6'', 6c, 6''', 1p, 1'''', 5s; dorsal paratabulation compressed and 1'''' constrained to ventral surface so ambital circumference encircled by parasutures.

Diagnosis:

Shape: Strongly lenticular through dorso-ventral compression. Epicyst smaller than hypocyst. Diameter of cyst typically widest at the mid-hypocyst. Endocyst ambitus circular to subpolygonal, pericyst ambitus subpolygonal. Subpolygonal shape caused by the variable development of antapical and lateral post-cingular bulges, most common on the pericyst, less frequently on the endocyst. Antapex may be slanted towards the right lateral side.

Wall Relationships: Circumcavate with endophragm and thinner periphragm appressed dorso-ventrally. Pericoel wider hypocystally than epicystally, with a small apical bulge and larger antapical and lateral post-cingular bulges varying the pericoel width.

Wall Features: TLM: Where membranes appressed, vacuoles up to 1µm diameter may be sparse or dense, evenly scattered or concentrated adjacent to the paracingulum and parasulcus. Where membranes separate, endophragm internally smooth, externally faintly scabrate to granulate in appearance; periphragm externally smooth, internally with scattered granules to rare short, thin processes. Very rarely the endophragm and periphragm are connected by thin processes, and broken processes are common.
SEM: Endophragm consists of a dense aggregate of granules forming a solid, internally smooth endocyst (pl. 108, fig. F). Periphragm composed of intertwined vermiculate elements forming a smooth but microperforate external surface and an irregular pseudo-granulate internal surface (pl. 108, fig. F, G). Rarely thin processes span the pericoel to connect the two membranes (pl. 108, fig. H).

Archeopyle: Apical, free, probably compound, Type tA. No free opercula observed; endo-operculum and peri-operculum almost certainly separate, and slight overlap of the apical paraplates seen by SEM suggests the peri-operculum may be internally compound (pl. 108, fig. E), though this is not confirmed. May have short accessory archeopyle sutures, especially at the parasulcal notch.

Paratabulation: TLM: Clearly indicated by angular archeopyle margin, and paracingular and parasulcal furrows; faintly indicated by subtle folds in the periphragm, and on dorso-ventral surfaces by slight variations in vacuole distribution.

SEM: Angular archeopyle margin and deep paracingular and parasulcal furrows clearly evident; parasutures marked by aligned, elongate perforations in narrow, shallow grooves on the periphragm surface, clearly indicating a typical gonyaulacacean paratabulation pattern, formula: Xpr, 4', ?1a, 6'', 6c, 6''', 1p, 1'''', 5s. Ventral paratabulation is enlarged and dorsal tabulation is compressed so the ambital circumference is encircled by closely aligned parasutures (pl. 108, fig. A, D, E).

Paracingulum: Distinctly evident as lateral indentations on the periphragm and a deep groove highlighted by a reduction of vacuoles on the dorso-ventral surfaces. Offset by 1 paracingulum width. Internal paracingular parasutures sometimes faintly evident in transmitted-light. SEM confirmed the presence of 6 paracingular paraplates.

Parasulcus: Longitudinal L-type; median position. Indicated by a deep parasulcal notch and a shallow vertical furrow, typically deeper hypocystally, with a conspicuous kidney-shaped flagellar scar, often highlighted by a surrounding darker 'stain' in TLM.

Size: Small to intermediate.

Dimensions: (µm; 16 specimens measured)
Periphragm length (with operculum): 43 (51) 57 (8 specimens)
Periphragm length (without operculum): 40 (49) 54
Periphragm width: 41 (49) 56
Endophragm length (with operculum): 32 (41) 47 (8 specimens)
Endophragm length (without operculum): 31 (39) 43
Endophragm width: 34 (38) 43

Comments: While *Ambonosphaera? conferta* has a standard gonyaulacacean paratabulation formula, the expression of this paratabulation is unusual. The ventral paratabulation is laterally expanded and the dorsal paratabulation is laterally compressed, resulting in a bilaterally divided paratabulation where the ambital circumference is completely encircled by parasutures (possibly excluding the apical series; pl. 108, fig. D, E). The ventral surface of the loisthocyst is constructed of two precingular paraplates (1 & 6''), two paracingular paraplates (1 & 6c), three postcingular paraplates (1, 2 & 6'''), a very large 1p, the 1'''', and the sulcal series. The dorsal surface of the loisthocyst is comprised of four precingular paraplates (2-5''), four paracingular paraplates (2-5c), and three postcingular paraplates (3-5'''). The 4''' paraplate is distinctively long and narrow allowing the 1'''' to reside entirely on the ventral surface.

This unique paratabulation arrangement is most clearly observed by SEM, however indications of this arrangement can be observed in TLM on more paratabulate specimens, specifically: the mid-dorsally positioned 3’’/4’’ parasuture (pl. 2, fig. G); slight folding of the periphragm delineating the long, narrow 4’’’ (pl. 2, fig. G); and sometimes slight folding of the periphragm (pl. 2, fig. A) or a band of reduced ornament (pl. 2, fig. D) from the flagellar scar to the left-lateral postcingular bulge defining the very long 2’’’/1p parasuture.

Ambonosphaera? conferta does not have a consistent antapical claustra and the antapex of most specimens remains intact. However some specimens display an antapical opening which is interpreted to be mechanical rupture of the fragile, antapically positioned 4’’’/1’’’’ parasuture.

Comparison: *Ambonosphaera? conferta* does not fall neatly into a single genus and is tentatively assigned to *Ambonosphaera* as displaying the most similar characteristics.

Sirmiodiniopsis Drugg, 1978, is excluded due to the absence of paired hypocystal claustra, *Polygonifera* Habib, 1972, and *Dingodinium* Cookson & Eisenack, 1958, are both excluded for being camocavate, and *Senoniasphaera* Clarke and Verdier, 1967, is discounted for having an offset parasulcus and two antapical and possible lateral horns. *Sirmiodinium* Alberti, 1961, commonly has a distinct trilobate ambitus, a single antapical claustra, and a combination (tA)@+P@ archeopyle.

Yalkalpodinium Morgan, 1980, is circumcavate, dorso-ventrally compressed and may have connecting structures between the membranes. In particular, *Ambonosphaera? conferta* is superficially similar to *Yalkalpodinium elangiana* Riding & Helby, 2001d. However, *Y. elangiana* and other *Yalkalpodinium* species are typically much larger, have a relatively narrow pericoel, the paracingulum is positioned more centrally, the parasulcal notch is more pronounced, and do not possess dorsally compressed paratabulation.

Ambonosphaera is considered the most appropriate genus for *Ambonosphaera? conferta*, with *Ambonosphaera* species having a similar size-range, ornament, paratabulation features (in TLM) and prominent, indented paracingulum. Furthermore, text-figures of the three confirmed *Ambonosphaera* species (*A. calloviana* Fensome, 1979, *A. delicata* Lebedeva & Nikitenko, 1998, and *A. hemicavata* Prauss, 1989) indicate that the antapical plate is restricted to the ventral surface. However, none of these species display the unique compressed dorsal paratabulation and aligned circumferential parasutures of *A? conferta*. Only the tentatively assigned *A? staffinensis* (Gitmez, 1970) Poulsen and Riding, 1992 is similarly dorso-ventrally compressed rather than subspherical in shape, however *A? staffinensis* is described as being circumcavate to camocavate rather than definitely circumcavate like *A? conferta*. *A. delicata* is

also circumcavate to camocavate, while *A. calloviana* is suturocavate to bicavate, and *A. hemicavata* is hypocavate. One important similarity between *A. hemicavata* and *A? conferta* is the observation of intra-pericoel ornament, including columellae (thin processes) connecting the endo- and pericysts, which clearly indicates a close relationship of these species.

Ambonosphaera? conferta may be conspecific with *Senoniasphaera* sp.1 of Davey, 1987. The brief description of *Senoniasphaera* sp.1 matches observed features of *A? conferta*, including pericoel width increasing hypocystally with postcingular and antapical extensions of the periphragm, however the poor plate quality makes confirmation difficult.

Helby *et al.*, 1988 figures specimens with similar appearance as "*Senoniasphaera?* sp.1 of Davey (1987)", especially Figs. 15E-F, however no description is provided, and these specimens may be more subspherical in shape. A more dorso-ventrally compressed specimen is figured as "*Sirmiodiniopsis?* sp. A" (Fig. 8N), though the presence of hypocystal claustra is uncertain.

Burger, 1996 figures specimens with similar appearance as "*Sirmiodiniopsis?* sp. A of Helby *et al.*, 1988" (pl. 9, figs. Q, V), though also does not provide a description.

Previously reported range: If synonymous with *Senoniasphaera* sp.1 of Davey, 1987 then rare from Upper Callovian to Lower Kimmeridgian of Papua New Guinea (equivalent to Upper Callovian to Mid-Tithonian of Partridge, 2006a).
If synonymous with "*Senoniasphaera?* sp.1 of Davey (1987)" of Helby *et al.*, 1988 then Kimmeridgian to Mid-Tithonian of New Zealand.
If synonymous with "*Sirmiodiniopsis?* sp. A" of Helby *et al.*, 1988 then Oxfordian to Kimmeridgian of New Zealand.
If synonymous with "*Sirmiodiniopsis?* sp. A of Helby *et al.*, 1988" of Burger, 1996 then common to abundant in Upper Kimmeridgian to Mid-Tithonian of the Northern Carnarvon Basin, Western Australia.

Ambonosphaera? sp. A

Pl. 1, figs. F-G

Description: Small to medium-sized proximate cyst; strongly lenticular, endocyst ambitus subcircular to subovoidal, thinner pericyst ambitus subcircular to subpolygonal with a low, conical apical perihorn; circumcavate; paracingulum indicated on periphragm by low parallel

ridges adjacent to a shallow furrow; smooth to scabrate ornament with rare granules; mechanical damage may produce antapical claustra; archeopyle apical, probably Type (tA).

Dimensions: (µm; 13 specimens measured)
Periphragm length: 46 (52) 67
Periphragm width: 39 (45) 52
Endophragm length: 36 (41) 49
Endophragm width: 31 (37) 47

Comparison: *Ambonosphaera?* sp. A is very similar to *Ambonosphaera? conferta*, however it has a much simpler appearance, having much reduced ornament, few paratabulation features, a slightly thicker, more opaque periphragm and a slightly thinner endophragm.

Genus ***Ampulladinium*** Riding, Helby & Parker *in* Riding & Helby, 2001g

Type species: *Ampulladinium variabile* Riding, Helby & Parker *in* Riding & Helby, 2001g

Ampulladinium aiax Mantle, 2009b

Pl. 3, figs. A-D

2009b *Ampulladinium aiax* Mantle, p.113-114, pl.5, figs.8-11; Text-fig.5.

Dimensions: (µm; 12 specimens measured)
Autophragm length: 28 (34) 41
Autophragm width: 30 (34) 40
Ectophragm length: 29 (35) 42
Ectophragm width: 31 (36) 41

Comments: Specimens matching the original description were very rare and limited to the base of the *Wanaea spectabilis* Zone. It is not certain if these specimens are *in situ* or if they are reworked from Callovian sediments.

Previously reported range: Upper Callovian to Lower Oxfordian of Australia and the Timor Sea (Mantle, 2009a & b; Riding *et al.*, 2010).

Ampulladinium? deltatum sp. nov.

Pl. 3, figs. E-M

Holotype and type locality: Pl. 3, fig. G-J, Jansz-3, Core, 2810 mRT(c), GA sample no. 1631224, slide no. 5, England Finder co-ordinates: C16/3, CPC no. 40590.

Derivation of name: After the triangular Greek letter *'delta'* for the rounded-triangular ambitus.

Synopsis: Cysts small; proximate; lenticular; large lateral post-cingular bulges produce a flat to slightly convex hypocyst creating a distinctive rounded-triangular ambitus; hypocyst longer than epicyst. Ornament of non-tabular short spines to short processes either entirely cover cyst or, more commonly, much reduced on dorso-ventral surfaces; ornament may be distally connected forming a partial ectophragm visible laterally. Archeopyle apical, Type (tA), operculum free.

Diagnosis:

Shape: Rounded-corner triangular ambitus formed by large lateral post-cingular bulges creating a flat to slightly convex hypocyst and smoothly tapering sides from the rounded apex. Strongly lenticular (always observed in dorso-ventral orientation).

Wall Relationships: Autophragm, sometimes with incomplete ectophragm visible laterally (pl. 3, figs. I, L).

Wall Features: Variable, non-tabular ornament of short, thin, echinate to baculate spines or very thin capitate processes either entirely cover cyst (pl. 3, figs. E-F) or are absent from the centre of dorso-ventral surfaces (pl. 3, figs. H-M). Rarely, ornament may be aligned in rows in a pseudo-radial arrangement (pl. 3, fig. H). Processes may be distally connected to form a very thin, incomplete ectophragm. Where spines or processes are absent, autophragm is scabrate.

Archeopyle: Apical, Type (tA), operculum free. No free opercula observed.

Paratabulation: Indicated by angular principal archeopyle suture, and rarely by short accessory archeopyle sutures and paracingulum if visible. Archeopyle shows epicystal tabulation is Xpr, 4', ?1a, 6"; remaining paratabulation indeterminate.

Paracingulum: Rarely observed as a reduction or absence of ornament (pl. 3, figs. H-J). Slightly closer to apex of cyst than antapex.

Parasulcus: Indicated only by parasulcal notch in the principal archeopyle suture. Very narrow as paraplate may be demarcated by short accessory archeopyle sutures at base of the parasulcal notch, slightly offset to the left lateral side (pl. 3, figs. G, H, K).
Size: Small.

Dimensions: (µm; 12 specimens measured)
Autophragm length (with operculum): 33 (36) 39 (3 specimens)
Autophragm length (without operculum): 32 (36) 39
Autophragm width: 32 (38) 42
Max. length of ornament: 1 (1.8) 2.5

Comments: The degree of ornamentation is highly variable. A complete plexus of forms was observed from specimens with very little ornament restricted to a circumferential zone to specimens entirely covered with dense spines. Densely ornamented specimens were relatively rare compared to specimens with reduced dorso-ventral ornamentation.

Comparison: This species is currently questionably attributed to *Ampulladinium* due to the generic description requiring a "prominent mid-ventral parasulcal notch", whereas in *Ampulladinium? deltatum* the parasulcal notch is slightly offset to the left lateral side. However, this may be a slight technicality, since the marked indentation of the small 6'' paraplate of *A.? deltatum* can give the general appearance of a broad mid-ventral parasulcal notch.

Ampulladinium? deltatum differs from other *Ampulladinium* species in the distinctive rounded-triangular ambitus. *Ampulladinium variabile* Riding, Helby & Parker, 2001 *in* Riding & Helby, 2001g is trilobate to subtriangular with typically concave rather than straight to slightly convex lateral margins. *Ampulladinium aiax* Mantle, 2009b has a subcircular to subtriangular ambitus, though always more rounded than *A.? deltatum*. It is possible that these three species form a morphological lineage from the subcircular to subtriangular *A. aiax* morphotypes in the Callovian, through the rounded-triangular *A.? deltatum* morphotypes in the Oxfordian, to the trilobate *A. variabile* morphotypes in the Tithonian.

Genus ***Apteodinium*** Eisenack, 1958, emend. Sarjeant, 1985, and Lucas-Clark, 1987

Type species: *Apteodinium granulatum* Eisenack, 1958.

Apteodinium? sp. A

Pl. 4, figs. A-C

Description: Intermediate-sized proximate cyst. Ambitus subcircular to subovoidal with some dorso-ventral compression; slight dextral torsion. Autophragm 1–1.5µm thick, with finely reticulate to spongeous ornament of irregularly interconnecting septa and processes. Reticulum lumina diameter variable: up to 1µm where ornament is thin; more coarsely spongeous (up to 2.5µm) where ornament is thicker, typically adjacent to the paracingulum, apices, and rarely major parasutures. Paratabulation indicated by large precingular Type P_3 archeopyle, and variably indicated by broad bands of higher ornament and/or aligned projections which may be distally linked by a fine trabeculum along some parasutures. Paracingulum indicated by a furrow of reduced ornament, though rarely thick adjacent ornament may fold over and mask this; internal paracingular tabulation rarely observed. Parasulcus indicated by reduced ornament and occasionally a faint flagellar scar; internal parasulcal tabulation faint and rarely observed. May possess a short (up to 3µm), solid, baculate apical projection which may be surrounded by higher spongeous ornament.

Dimensions: (µm; 11 specimens measured)
Autophragm length (without ornament): 64 (75) 89
Autophragm width (without ornament): 47 (62) 76
Autophragm length (with ornament): 66 (80) 95
Autophragm width (with ornament): 49 (69) 82

Comparison: *Apteodinium?* sp. A is questionably attributed to *Apteodinium* due to similar ornament (as described in Lucas-Clarke, 1987, p.168) and dextral torsion, however *A.?* sp. A does not have a large apical horn and is generally more tabulate than other *Apteodinium* species. This species could alternatively be placed in *Aldorfia* Stover & Evitt, 1978, however *A.?* sp. A does not possess a continuous ectophragm, has a much thinner covering of finer ornament, and is more tabulate than *Aldorfia aldorfensis* (Gocht, 1970) Stover & Evitt, 1978.

Apteodinium? sp. A is superficially similar to *Scriniodinium dictyotum* Cookson & Eisenack, 1960b. However, *S. dictyotum* rarely shows clear paratabulation features, and has two distinct membranes with a reticulate periphragm and hollow pericoel rather than spongeous ornament covering an autophragm as seen in *A.?* sp. A.

Genus ***Arkellea*** Below, 1990

Type species: Sarjeant, 1961a, as *Cymatiosphaera teichophera.*

Arkellea teichophera (Sarjeant, 1961a) Below, 1990

Pl. 3, figs. N-Q

1961a *Cymatiosphaera teichophera* Sarjeant, p.107-108, pl.15, fig.9; text-figs.9a-b.
1990 *Arkellea teichophera* (Sarjeant 1961a), Below, 1990, p.42-43, pl.9, figs.1-9.

Dimensions: (µm; 12 specimens measured)
Total length: 31 (45) 53
Total width: 27 (42) 53
Central body length: 28 (35) 40
Central body width: 20 (26) 31
Max. length of septa: 5 (10) 15

Comments and Comparison: Unfavourably oriented or preserved specimens of this species may potentially be attributed to the genus *Heslertonia* Sarjeant, 1966a, which has paracingular paraplates delimited by parasutural septa. However, well preserved Jansz-Io specimens are identified as *Arkellea teichophera* due to the ovoidal autophragm with conical apex and Type 2I archeopyle (pl. 3, fig. O); rigid parasutural septa with faint striations; the absence of anterior and posterior paracingular septa (pl. 3, fig. N); and the paracingular position indicated by 1/ shallow indentations on the distal septal margins (pl. 3, fig. P) and 2/ lateral displacement of continuous septa between adjacent precingular and postcingular paraplates when spanning the paracingulum (pl. 3, figs. N, O; as observed in Below, 1990, pl. 9, fig. 5, text-fig. 11).

Previously reported range: Oxfordian to Berriasian of Australia (Wiseman, 1980);
Upper Callovian to Lower Oxfordian globally (Sarjeant, 1979);
Lower Oxfordian of Papua New Guinea (Davey, 1987);
Upper Bathonian to Lower Oxfordian of Europe (Sarjeant, 1961a, 1976b; Smelror, 1988b; Kunz 1990; Stancliffe, 1991; Courtinat, 2006)

Genus ***Atopodinium*** Drugg, 1978,
emend. Masure, 1991

Type species: *Atopodinium prostatum* Drugg, 1978.

Atopodinium haromense Thomas & Cox, 1988

Pl. 4, fig. D

1988 *Atopodinium haromense* Thomas & Cox, p.319-321, 323, pl.1, figs.1-6; text-fig.4.

1991 *Atopodinium haromense* Thomas & Cox; emend. Masure, p.65-68, pl.1, figs.1-12; text-figs.1, 2.

Dimensions: (µm; 15 specimens measured)
Total length: 52 (67) 84
Total width: 53 (66) 76

Comments: Specimens observed herein align with the *Atopodinium haromense* descriptions of Thomas & Cox, 1988 and Masure, 1991, including rows of grana or gemmae and folds incompletely defining the paratabulation and more densely ornamented antapical paraplate. However, they differ from the figured type material in their more rounded subpolygonal appearance and typically unfolded paracingulum and parasulcus.

Comparison: *Atopodinium haromense* is similar to *Kallosphaeridium hypornatum* Prauss, 1989, however *K. hypornatum* has a more rounded ovoidal ambitus and does not display any indications of paratabulation other than the archeopyle and ornamented antapical paraplate.

Previously reported range: Cosmopolitan and long ranging, from the Oxfordian to Turonian (refer to Masure, 1991, p.77-78, text-figs. 8, 9).
Callovian to Kimmeridgian of Europe (Thomas & Cox, 1988; Poulsen 1996; Riding *et al.*, 1999);
Oxfordian to Lower Kimmeridgian of Egypt (Ibrahim *et al.*, 2002)

Atopodinium torum sp. nov.

Pl. 4, figs. E-I; Pl. 5, figs. A-I

Holotype and type locality: Pl. 5, fig. A-C, Jansz-3, Core, 2811mRT(c), GA sample no. 1631225, slide no. 5, England Finder co-ordinates: P36/2, CPC no. 40598.

Derivation of name: From *torus* (Latin): "any round protuberance; a mound" for the distinctive antapical node in the centre of the antapical paraplate.

Synopsis: Intermediate-sized proximate cyst; slightly dorso-ventrally compressed; polygonal to subpolygonal ambitus. May have small apical horn; antapical paraplate concave with a convex antapical protrusion in the centre. Paratabulation partially indicated by apical archeopyle and accessory sutures, cyst shape, thin parasutural folds and very rarely aligned grana; parasulcal and intraparacingular tabulation undefined. Predominantly smooth with rare grana on some parasutures or around the antapical node. Archeopyle apical, Type (tA)@.

Diagnosis:

Shape: Polygonal to subpolygonal cyst with some slight dorso-ventral compression. May have a small apical horn (up to 4 µm long; pl. 5, fig. A). Antapical paraplate concave with a distinctive antapical node in the centre, up to 8 µm wide, that protrudes to the level of the antapical paraplate margins. Cyst is frequently folded.

Wall Relationships: Autophragm only.

Wall Features: Autophragm predominantly smooth to faintly scabrate with rare scattered grana concentrated on the antapical paraplate; rarely grana may align along parasutures (pl. 5, fig. G).

Archeopyle: Apical, Type (tA)@; may have deep accessory archeopyle sutures.

Paratabulation: Incompletely indicated by the polygonal cyst shape, the angular principal archeopyle suture, deep accessory archeopyle sutures where developed, broad or thin parasutural folds, and rarely by alignment of grana. Paratabulation interpreted to be standard gonyaulacacean paratabulation, formula: Xpr, 4', ?6'', Xc, ?6''', 1p, 1'''', Xs but exact paratabulation formula indeterminate due to undefined ventral region.

Paracingulum: Indicated by the maximum cyst width and frequently highlighted by parallel parasutural folds. Intraparacingular paraplates rarely visible. Paracingular ends significantly displaced, up to 3x paracingular width.

Parasulcus: Parasulcal position may be indicated by a longitudinal fold, displacement of the paracingulum, or attachment point of the adnate archeopyle. Paratabulation not defined.

Size: Intermediate.

Dimensions: (µm; 13 specimens measured)
Total length: 66 (80) 95
Total width: 45 (68) 83

Comparison: *Atopodinium torum* is most similar to *Atopodinium haromense* Thomas & Cox, 1988. However, *A. torum* differs from this, and all other *Atopodinium* species, in having less ornament and having a concave antapical paraplate with a small convex antapical protrusion.

Genus ***Barbatacysta*** Courtinat, 1989

Type species: Erkmen & Sarjeant, 1980, as *Sentusidinium creberbarbatum*.

Barbatacysta creberbarbata (Erkmen & Sarjeant, 1980) Courtinat, 1989

Pl. 5, figs. J-M

1980 *Sentusidinium creberbarbatum* Erkmen & Sarjeant, p.52-54, text-fig.2 (holotype drawn from specimen figured by Fensome, 1979, pl.1, fig.3, as *Sentusidinium pilosum*).

1989 *Barbatacysta creberbarbata* (Erkmen & Sarjeant) Courtinat, p.186; pl.18, figs.1-3; pl.21, fig.1; pl.23, fig.14; text-fig.80A.

Dimensions: (μm; 38 specimens measured)
Autophragm length (with operculum): 40 (47) 51 (10 specimens)
Autophragm length (without operculum): 34 (44) 55 (32 specimens)
Autophragm width: 20 (26) 37
Length of apical process: 5 (7) 9 (10 specimens)
Max. length of processes: 2 (4) 6
Mean length of processes: 2 (3.5) 4

Comments: Rare specimens with an attached operculum display a longer capitate process at the extreme apex (pl.5, fig.L).

Comparison: Specimens herein attributed to *Barbatacysta creberbarbata* intergrade with *Barbatacysta* (was *Prolixosphaeridium*) *capitata* (Cookson & Eisenack, 1960b) Schrank, 2005. Both species are recorded in Australasia and typically differentiated by a higher length:width ratio and low ornament between the spines of the latter. However, both of these factors are highly variable in Jansz-Io specimens. For example, pl. 5, figs. L-M show specimens with a high length:width ratio but no proximal ornament. Shorter specimens with proximal ornament were also observed, and therefore is deemed inappropriate to differentiate between the species here. *B. creberbarbata* is the name applied here due to the dominance of proximally unornamented morphotypes.

The similarity of these two species has also been discussed by Stancliffe, 1991 and Schrank, 2005, therefore these species may be synonymous. The morphological variations may be produced by a single motile population in response to varying environmental conditions, such as salinity and temperature, as has been observed in extant dinoflagellate populations (*e.g.*, Mertens *et. al.*, 2009).

Previously reported range: Cosmopolitan: Callovian *Ternia balmei* to *Voodooia tabulata* Interval Zones of the Timor Sea (Mantle 2009b);
Upper Callovian to Tithonian of Europe (Erkmen & Sarjeant, 1980; Brenner, 1988; Dürr, 1988; Courtinat, 1989; Kunz 1990; Stancliffe, 1991; Dodekova, 1992; Poulsen, 1993; Riding *et al.*, 1999);
Kimmeridgian to Tithonian of India (Kumar, 1986);
Oxfordian to Tithonian of Africa (Jiang *et al.*, 1992; Wheeler & Sarjeant, 1990; Schrank, 2005).

Barbatacysta gemmata sp. nov.

Pl. 6, figs. A-U

Holotype and type locality: Pl. 6, fig. M-P, Jansz-3, Core, 2855mRT(c), GA sample no. 1631269, slide no. 5, England Finder co-ordinates: U23/2, CPC no. 40609.

Derivation of name: Named for the distinctive gemmate ornament.

Synopsis: Small, subspherical cyst with distinctive gemmate ornament that appears verrucate to vermiculate in plan view. Apex and parasulcus consistently host an amorphous mass. Paratabulation partially indicated by archeopyle, accessory archeopyle sutures, and rarely by thin pandasutural bands. Archeopyle apical, Type (tA)@ or Type (tA).

Diagnosis:
Shape: Subspherical.

Wall Relationships: Autophragm only.

Wall Features: Intratabular ornament of distinctive, small to large gemmae (rarely baculae; up to 3 µm long, 1 – 2 µm diameter) that are subcircular in distal cross-section. Adjacent ornament may coalesce producing a verrucate to vermiculate appearance in plan view. Ornament consistently coalesces at apex (possibly over preapical paraplates) to form a rounded mass, and

along parasulcus to form a large, flattened, elongate, amorphous mass. Thin pandasutural bands rarely visible by alignment of ornament.

Archeopyle: Apical, Type (tA)@, but sometimes Type (tA) probably due to mechanical breakage; deep accessory archeopyle sutures common.

Paratabulation: Usually indicated by principal archeopyle suture and deep accessory archeopyle sutures only; rarely incompletely indicated by thin pandasutural bands between aligned ornament. Epicystal paratabulation formula Xpr, 4', ?1a, 6"; remaining paratabulation indeterminate, but probably standard gonyaulacacean.

Paracingulum: Usually not observed; rarely indicated by pandasutural bands.

Parasulcus: Indicated by parasulcal notch, attachment point of apical operculum, and a large, elongate amorphous mass, which may contain two pits or a thin channel that may correspond to flagellar pores.

Size: small.

Dimensions: (µm; 14 specimens measured)
Autophragm length: 24 (28) 36
Autophragm width: 26 (29) 34
Max. length of processes: 1 (1.5) 3

Comments: *Barbatacysta gemmata* is a distinctive species within Jansz-Io preparations that can be identified from fragments alone due to the unique gemmate ornament.

Comparison: *Barbatacysta gemmata* differs to all other *Barbatacysta* species in the small cyst size, short ornament length and distinctive gemmate ornament. *Barbatacysta gemmata* is most similar to *Barbatacysta verrucosa* (Sarjeant, 1968) Courtinat, 1989 in having short ornament elements that produce a verrucate appearance in plan view. However, *B. verrucosa* is slightly larger, the paracingulum and parasulcus are devoid of ornament, and the short processes are branched and distally recurve.

Barbatacysta sp. A

Pl. 7, figs. A-C

Description: Small to medium-sized, spherical to subspherical, proximate cyst; robust autophragm with granulate intratabular ornament separated by very thin, unornamented pandasutural bands. Standard gonyaulacacean paratabulation, formula: Xpr, 4', 6'', 6c, 6''', 1p, 1'''', Xs. Parasulcal series not fully expressed; reduced ornament may reveal faint flagellar scar. Archeopyle apical, Type (tA) with short to long accessory archeopyle sutures.

Dimensions: (μm; 12 specimens measured)
Autophragm length (with operculum): 52 (54) 55 (3 specimens)
Autophragm length (without operculum): 46 (51) 57
Autophragm width: 44 (50) 55

Comments: Thin pandasutural bands may be barely visible on some specimens.

Comparison: *Barbatacysta* sp. A intergrades with *Barbatacysta* sp. B but encompasses specimens with lower-relief ornament of distinct elements that rarely coalesce into vermiculae.

Barbatacysta sp. B

Pl. 7, figs. D-E

Description: Small to medium-sized, spherical to subspherical, proximate cyst; robust autophragm with dense, intratabular, verrucate to vermiculate ornament separated by very narrow pandasutural bands. Standard gonyaulacacean paratabulation, formula: Xpr, 4', 6'', 6c, 6''', 1p, 1'''', Xs. Parasulcal series not fully expressed; reduced ornament may reveal faint flagellar scar. Archeopyle apical, Type (tA) with short to long accessory archeopyle sutures.

Dimensions: (μm; 12 specimens measured)
Autophragm length (with operculum): 53 (54) 56 (3 specimens)
Autophragm length (without operculum): 43 (54) 63
Autophragm width: 43 (55) 73

Comments: Thin pandasutural bands are barely visible on many specimens, but most clearly observed while changing focal depth during TLM.

Comparison: *Barbatacysta* sp. B intergrades with *Barbatacysta* sp. A, but encompasses specimens with higher relief ornament with elements that commonly coalesce into vermiculae. *Barbatacysta* sp. B also intergrades with *Lanterna reticulata* sp. nov. when coalescing vermiculae produce a pseudo-reticulum.

Genus ***Batiacasphaera*** Drugg, 1970b, emend. Morgan, 1975, and Dörhöfer & Davies, 1980

Type species: *Batiacasphaera compta* Drugg, 1970b.

Batiacasphaera macbethiae Mantle, 2009b

Pl. 7, fig. F

2009b *Batiacasphaera macbethiae* Mantle, p.100-101, pl.8, figs.1, 3-5.

Dimensions: (µm; 2 specimens measured)
Total length: 57, 60
Total width: 41, 46
Max. diameter of accumulation body: 9, 12

Comments: Very few specimens were encountered in the Jansz-Io samples, therefore this species may have been reworked from underlying Callovian-aged sediments.

Previously reported range: Bathonian to Callovian of the Timor Sea (Mantle, 2009a & b; Riding *et al.*, 2010).

Batiacasphaera **sp. A**

Pl. 7, figs. G, H

Description: Small, spherical to subspherical, proximate cyst with robust autophragm ornamented with large, isolated verrucae with little to no relief. Paracingulum not evident; paratabulation and parasulcus are only evident by deep parasulcal notch and short accessory archeopyle sutures. Archeopyle apical, Type (tA).

Dimensions: (µm; 12 specimens measured)
Total length: 26 (41) 47
Total width: 35 (41) 46
Max. length of ornament: 0.1 (0.2) 0.5
Max. diameter of ornament: 1 (2.4) 4

Comparison: *Batiacasphaera* sp. A differs from most other *Batiacasphaera* species in having large ornament elements in plan view that have little to no relief. *Batiacasphaera* sp. A is most

similar to *Batiacasphaera macrogranulata* Morgan, 1975 which has low, flat granulae to rugulae, but differs in having a larger size, a thinner autophragm, and being lenticular with a consistently offset parasulcus.

***Batiacasphaera* sp. B**

Pl. 7, figs. I-L

Description: Small to intermediate-sized, spherical to subspherical, proximate cyst with robust autophragm densely ornamented with a combination of verrucae and baculae of irregular width and length forming an uneven cyst surface. Paracingulum not evident; paratabulation and parasulcus evident by deep parasulcal notch and accessory archeopyle sutures, and sometimes by a faint flagellar scar. Archeopyle apical, Type (tA).

Dimensions: (µm; 14 specimens measured)
Total length: 38 (48) 58
Total width: 35 (47) 55
Max. length of ornament: 1.5 (2) 3
Max. diameter of ornament: 1 (1.5) 3
Mean diameter of ornament: 0.5 (0.7) 1

Comparison: *Batiacasphaera* sp. B differs from all described *Batiacasphaera* species in the combination of the above mentioned characteristics. Furthermore, *Batiacasphaera saidensis* Below, 1981 also has a robust autophragm, but is ornamented with gemmae and 'crispae'; *Batiacasphaera mica* Harding, 1990, ex Harding *in* Williams *et al.*, 1998 is microgranulate and dorso-ventrally compressed; and *Batiacasphaera granulosa* (Cookson & Eisenack, 1974) Jansonius, 1989 has an elongate cyst and narrow archeopyle.

Genus ***Broomea*** Cookson & Eisenack, 1958, emend. Lentin & Williams, 1976, and Mantle, 2009a

Type species: *Broomea ramosa* Cookson & Eisenack, 1958.

Broomea fusticula Mantle, 2009a, emend. nov.

Pl. 8, figs. A-K; Pl. 108, fig. I

2009a *Broomea fusticula* Mantle, pl. 6, figs. 1-8; Text-fig. 9.

Synopsis: Cysts large, proximate, acavate to hypo-cornucavate, elongate-ovoidal, surmounted by a long, slender, tapering apical horn, with or without paired antapical horns; endophragm and periphragm closely appressed except possibly at antapex where periphragm alone variably forms a solid to spongeous antapical boss to long, antapical horns. Scabrate to granulate ornament typically increases towards the apices; gonyaulacacean paratabulation lacking to faintly and incompletely indicated by aligned parasutural ornament, most common on paracingulum and hypocyst; archeopyle compound Intercalary, Type 2I, rarely evident.

Emended Diagnosis:

Shape: Generally club-like, being elongate ovoidal with a long, slender, tapering apical horn. Antapically variable: endophragm rounded or slightly bilobate; periphragm rounded or forms paired antapical horns. Epicyst significantly longer than hypocyst.

Wall Relationships: Endophragm and periphragm closely appressed unless spongeous pericoel is developed at antapex: acavate when periphragm is solid; hypo-cornucavate when periphragm is spongeous.

Wall Features: Cyst body scabrate to granulate, rarely verrucate, typically with increasing ornament size and density towards the apices. Apex may be surmounted by a short, narrow to irregular apicular structure. Antapically periphragm forms a solid or spongeous extension of highly variable appearance, including a rounded boss (pl. 8, fig. A), short bilobate projections (pl. 8, fig. F), to long paired antapical horns that may be dense, narrow and pointed (pl. 8, figs. D-E) to spongeous, inflated and rounded (pl. 8, figs. B-C, G-K).

Archeopyle: Intercalary, Type 2I, compound, free; rarely discernible.

Paratabulation: Occasionally indicated by 2I archeopyle, a slight paracingular lateral indentation, and incomplete alignment of granules along parasutures, most common on the paracingulum and hypocyst.

Paracingulum: May be indicated by a shallow lateral indentation with reduced ornament, adcingularly concentrated ornament and, rarely, fine paracingular ridges. Located in the lowest quarter of the endocyst; level to slightly levorotatory.

Parasulcus: Generally not indicated; rarely indicated by gap in paracingular ends or faint outline of aligned ornament.

Size: Large.

Dimensions: (μm; 32 specimens measured)
Total length: 79 (114) 145
Endophragm length: 88 (103) 137
Length of antapical ornament / horns: 2 (20) 42
Max. endophragm width: 18 (30) 44
Width of antapical horns: 11 (24) 40
Total thickness: 22 (34) 43 (7 specimens)
Paracingulum width: 4 (7) 9 (15 specimens)
Length of apical horn: 18 (31) 52

Comments: Excellently preserved specimens from Jansz-Io preparations have clarified various characteristics of *Broomea fusticula.* This species is therefore emended to: 1/ specify that cysts possess a compound 2I archeopyle; 2/ include morphotypes displaying faint paratabulation; and 3/ include morphotypes with large, spongeous, paired antapical horns resulting in hypo-cornucavation. This emended description is otherwise consistent with the original description of Mantle, 2009a.

Specimens with long, inflated, rounded and spongeous antapical horns have been included in *Broomea fusticula* as extreme examples of intraspecific variability due to the presence of a complete continuum of intermediate morphotypes.

As mentioned in Mantle 2009a, the archeopyle region appears susceptible to mechanical damage, obscuring the 2I intercalary paraplate nature in less well-preserved material.

Comparison: The holotype of *Broomea ramosa* Cookson & Eisenack, 1958 has a single intercalary archeopyle and multi-stranded antapical horns. *Broomea simplex* Cookson & Eisenack, 1958 is stated in Mantle, 2009a to possess a 2I archeopyle, however differs to *Broomea fusticula* in having hollow antapical horns.

Previously reported range: Mid-Callovian to Lower Oxfordian of Australia (Mantle, 2009a; Riding *et al.*, 2010).

Broomea ramosa Cookson & Eisenack, 1958

Pl. 8, figs. L-M

1958 *Broomea ramosa* Cookson & Eisenack, p.41-42, pl.6, figs.6-8.
1975 *Pareodinia ramosa* (Cookson & Eisenack, 1958) Wiggins, p.107.

1976 *Broomea ramosa* Cookson & Eisenack, 1958, retained by Lentin & Williams, p.144.

Dimensions: (µm; 2 specimens measured)
Total length: 153, 170
Endophragm length: 136, 140
Length of antapical horns: 42, 37
Max. endophragm width: 29, 34
Width of antapical horns: 42, 26
Paracingulum width: 7 (1 specimen)
Length of apical horn: 45, 47

Comments and Comparison: Re-examination of the *Broomea ramosa* type material confirmed the similarity of this species with *Broomea fusticula* Mantle, 2009a emend. nov. in the cyst size, shape and ornament. However, the *B. ramosa* holotype clearly shows a single intercalary archeopyle and multi-stranded antapical horns. Specimens observed in Jansz-Io preparations only differ from the type material in having thin membranes interconnecting individual strands within each antapical horn.

Previously reported range: Callovian to Oxfordian of Australia (Cookson & Eisenack, 1958), refined to Mid-Oxfordian to Mid-Tithonian of Australia (Riding *et al.*, 2010);
Mid-Oxfordian to Mid-Berriasian of Papua New Guinea (Davey, 1987).
The synthesis of Sarjeant, 1979 reported a cosmopolitan distribution from Kimmeridgian to ?Tithonian.

Genus ***Canninginopsis*** Cookson & Eisenack, 1962b, emend. Marshall, 1990

Type species: *Canninginopsis denticulata* Cookson & Eisenack, 1962b.

Canninginopsis **sp. A**

Pl. 9, fig. A

Description: Small to medium-sized, subcircular to ovoidal, proximate cyst; autophragm scabrate to granulate, with penitabular baculae to gemmae forming narrow, parallel rows delineating parasutures, most noticeable on the hypocyst; standard gonyaulacacean paratabulation, formula: Xpr, 4', 6'', Xc, 6''', 1p, 1'''', Xs; paracingular and parasulcal series not fully expressed. Horns or protrusions absent; a small, dense mass of granulae may represent

the preapical paraplates. Archeopyle apical, Type (tA) or Type (tA)@ with deep accessory archeopyle sutures dividing precingular paraplates.

Dimensions: (µm; 12 specimens measured)
Total length: 46 (64) 73
Total width: 38 (51) 65
Max. length of ornament: 1 (1.2) 2
Max. diameter of ornament: 1 (1.2) 2

Comparison: This informally described species is herein assigned to *Canninginopsis* due to the similarity of paratabulation and ornamentation to *Canninginopsis denticulata* Cookson & Eisenack, 1962b. *Canninginopsis* sp. A differs to *C. denticulata* and all other described *Canninginopsis* species in not possessing apical and antapical horns or strong dorso-ventral compression, and displaying penitabular ornament of baculae to gemmae along the parasutures of both the dorsal and ventral surfaces. *Canninginopsis intermedia* Morgan, 1980 displays penitabular ornament, although restricted to the dorsal surface.

Comments: All species currently assigned to *Canninginopsis* are Aptian or younger, making *Canninginopsis* sp. A the oldest representative of this genus recorded to date. While this species is distinctive and may be useful to support regional correlation, the Jansz-Io preparations do not contain sufficient specimens to enable formal description.

Genus ***Carnarvonodinium*** Parker, 1988

Type species: *Carnarvonodinium morganii* Parker, 1988.

***Carnarvonodinium?* sp. A**

Pl. 9, figs. B-F

Description: Cysts intermediate to large, proximate, acavate, elongate ellipsoidal narrowing towards the rounded apices; autophragm ornamented with mixed granulae, verrucae, baculae and short, irregular processes, densest surrounding the antapex; paracingulum and parasulcus not discernible. Archeopyle apical, Type (tA) or Type (tA)@ with deep accessory archeopyle sutures separating the precingular paraplates; paratabulation formula indeterminate.

Dimensions: (µm; 2 specimens measured)
Autophragm length (with operculum): 98 (1 specimen)

Autophragm length (without operculum): 75, 90

Total width: 44, 44

Max. length of ornament: 3.5, 4

Comparison: *Carnarvonodinium?* sp. A is herein questionably assigned to *Carnarvonodinium* due to the absence of an apical horn and uncertainty regarding the number of precingular paraplates: *Carnarvonodinium* typically possesses 6 precingular paraplates, however Jansz-Io specimens appear to possess only 5 (pl. 9, figs. B-F).

Carnarvonodinium? sp. A is most similar to *Carnarvonodinium morganii* Parker, 1988, although *C. morganii* has an apical horn and is ornamented with long (up to 7µm), robust processes. *C. striatigranulatum* Parker, 1988 and *C. granulatum* Jiang *in* Jiang *et al.*, 1992 both bear low relief granulate ornament only.

Genus ***Cernicysta*** Stover & Helby, 1987d

Type species: Morgan, 1980, as *Lithodinia helbyi.*

Cernicysta? janszense sp. nov.

Pl. 10, figs. A-P, Pl. 11, figs. A-Q, Pl. 12, figs. A-L

2001d *Meiourogonyaulax viriosa* Riding & Helby, figs.13C-D, G.

non 2001d *Meiourogonyaulax viriosa* Riding & Helby, p.87, 89, figs.13A-B, E-F, H-L.

Holotype and type locality: Pl. 10, fig. A-D; Pl. 11, fig. J-L, Jansz-1, Core, 2890mRT(c), GA sample no. 1631197, slide no. 4, England Finder co-ordinates: V25/3, CPC no. 40631.

Derivation of name: Named after the Jansz-1 well from which the holotype was recovered.

Synopsis: Small to intermediate, ellipsoidal cyst; ovoidal to subpolygonal ambitus. Autophragm punctate to foveolate; orange in colour with intensity increasing with wall thickness. Gonyaulacacean paratabulation indicated by smooth, closely appressed penitabular ridges with a very narrow parasutural groove; formula: ?3pr, 4', 6'', ?6c, 5''', 1p, 1'''', Xs; small 1p positioned adjacent to the ps paraplate. Archeopyle apical, Type (tA) to Type (tA)@.

Diagnosis:

Shape: Ellipsoidal cyst with subovoidal to subpolygonal ambitus. Ambital shape typically determined by autophragm thickness: flexible, thin-walled specimens have a rounded ambitus; thick-walled specimens have an angular, subpolygonal ambitus. In lateral view the apical and antapical series are usually inclined towards the ventral surface.

Wall Relationships: Autophragm only, possibly differentiated.

Wall Features: Autophragm punctate to foveolate, variably thickening into finely spongeous to solid penitabular ridges closely adjacent to paraplate margins. Penitabular ridges of neighbouring paraplates appressed, forming parallel ridges with a central, very thin parasutural groove or slit; in cross-section a narrow notch may be visible between two adjacent ridges (pl. 11, figs. B, L; pl. 12, fig. L); a small triangular void may be formed at gonal points where adjacent ridges diverge. Penitabular nature of ridges accentuated between apical and precingular paraplate series where ridges separate to form a wider pandasutural band (pl. 11, fig. N). Parasutural groove may not be visible if the penitabular ridges are fused or incompletely formed. Where ridges are not developed the parasutures may be indiscernible or rarely indicated by a faint, narrow groove directly on the autophragm.

Archeopyle: Apical, simple, Type (tA) to rarely Type (tA)@. Principal archeopyle suture slightly zigzag with deep, narrow parasulcal notch; precingular series may have short accessory archeopyle sutures.

Paratabulation: Variably expressed; indicated by penitabular ridges and thin parasutural groove where developed. Gonyaulacacean, formula: ?3pr, 4', 6'', ?6c, 5''', 1p, 1'''', Xs. Paratabular arrangement is distinctive: 1p is small and positioned adjacent to the ps paraplate; ls/1p parasuture is typically faint to absent while the 1'''/1p parasuture is commonly distinct, giving the impression of a posteriorly widening or deviating parasulcus (pl. 12, figs. F, J). Apical series rarely differentiated; preapical paraplates may be indicated by a small apical boss (pl. 10, fig. O) or rarely fully expressed (pl. 11, fig. J-K). 5 postcingular paraplates are probably 2''' - 6''' homologues with the first postcingular paraplate incorporated into the parasulcus.

Paracingulum: Laevorotatory; ends offset at least 1 paracingulum width. External and internal paracingular paratabulation partially to fully indicated by unique penitabular ridge morphology.

Parasulcus: Indicated by deep parasulcal notch and fully to incompletely outlined by unique penitabular ridge morphology; ps paraplate frequently represented; other internal paraplates rarely differentiated (pl. 11, figs. P, Q).

Size: Small to intermediate.

Dimensions: (μm; 12 specimens measured)
Autophragm length (with operculum): 61 (67) 77 (5 specimens)
Autophragm length (without operculum): 52 (64) 75
Total width: 44 (49) 63
Max. height of parasutural ornament: 1.5 (3.5) 5

Comments: The unique penitabular ridge and parasutural groove morphology is most clearly observed at high magnification; at low magnification ridges may appear as a single parasutural ridge.

Comparison: Three paratypes of *Meiourogonyaulax viriosa* Riding & Helby, 2001d (figs.13C-D, G, from 1642.50m of Jabiru-2) were re-examined for this study. These specimens were confirmed to differ to the *M. viriosa* holotype and display all characteristics of *Cernicysta? janszense* sp. nov. Consequently these specimens are herein transferred as paratypes of *C? janszense*. *M. viriosa* differs to *C? janszense* in having a subcircular ambitus, 6 postcingular paraplates, an elongate rhomboidal 1''', large ps and 1p paraplates, and paratabulation indicated by single parasutural ridges to septa.

Cernicysta? janszense is most similar in ambital shape and paratabulation formula to *Cernicysta helbyi* (Morgan, 1980) Stover & Helby, 1987d. However, *C. helbyi* possesses an autophragm and ectophragm with spongeous ectocoel, parasutural folds, and expanded ventral paratabulation (very large 1''' and 1p paraplates), whereas *C? janszense* has a possibly differentiated autophragm, a unique penitabular ridge and parasutural groove morphology, and constricted ventral paratabulation (very small 1''' and 1p paraplates). Therefore, this species is tentatively assigned to *Cernicysta.*

Genus ***Chlamydophorella*** Cookson & Eisenack, 1958, emend. Duxbury, 1983

Type species: *Chlamydophorella nyei* Cookson & Eisenack, 1958.

Chlamydophorella ectotabulata Smelror, 1989

Pl. 13, figs. A-F

1989 *Chlamydophorella ectotabulata* Smelror, p.141-143, 145, pl.1, figs.1-4; pl.2, figs.1-4; pl.3, figs.1-5; text-figs.2A-C.

Dimensions: (µm; 14 specimens measured)
Autophragm length (with operculum): 37 (41) 46 (13 specimens)
Autophragm length (without operculum): 33 (39) 43 (5 specimens)
Autophragm width: 28 (37) 42
Max. width of pericoel: 1.5 (3.1) 4
Max. width of processes: 1 (1.1) 1.5

Comments: Well-preserved specimens possessing faint ectophragmal paratabulation traces enabled the identification of this species without requiring SEM analysis. Parasutural separation of ectophragmal paraplates was visible under TLM, although convincing photographic evidence was evasive. Specimens lacking paratabulation traces but otherwise identical are probably conspecific with *Chlamydophorella ectotabulata* but were assigned to *"Chlamydophorella* spp. Type A" (refer below) in the absence of evidence.

Previously reported range: Cosmopolitan: Upper Bathonian to Upper Oxfordian of Europe (Smelror, 1988b, 1989; Fauconnier *et al.*, 1996);
Callovian to Mid-Oxfordian of The Middle East and Egypt (Ibrahim *et al.*, 2002; Kholeif *et al.*, 2004)

Chlamydophorella sp. cf. ***C. haigii*** Backhouse, 2006

Pl. 13, figs. H-L

cf. 2006 *Chlamydophorella haigii* Backhouse, p.58, 60, pl.1, figs.1-8.

Dimensions: (µm; 2 specimens measured)
Autophragm length (with operculum): 49, 55
Autophragm width: 46, 53
Max. width of pericoel: 4.5, 5
Max. width of processes: 0.8, 0.8

Comparison: Jansz-Io specimens resemble *Chlamydophorella haigii* Backhouse, 2006 in possessing numerous, very fine processes; however the dimensions of the cyst and processes are larger than in *C. haigii.*

Previously reported range: *Chlamydophorella haigii s.s.* was described from the Albian of the Southern Carnarvon Basin, Australia (Backhouse, 2006).

Chlamydophorella sp. cf. ***C. nyei*** Cookson & Eisenack, 1958

Pl. 13, fig. G

cf. 1958 *Chlamydophorella nyei* Cookson & Eisenack, p.56, pl.11, figs.1-3.

Dimensions: (µm; 12 specimens measured)
Autophragm length (with operculum): 39, 41 (2 specimens)
Autophragm length (without operculum): 32 (40) 43
Autophragm width: 34 (41) 47
Max. width of pericoel: 6 (8) 10
Max. width of processes: 1.5 (2) 2

Comparison: Specimens herein assigned to *Chlamydophorella* sp. cf. *C. nyei* resemble *Chlamydophorella nyei* Cookson & Eisenack, 1958 in size, number of processes and ambital angularity; however the holotype is figured with an apical horn which Jansz-Io specimens do not possess.

Previously reported range: *Chlamydophorella nyei s.s.* was described from the Cenomanian to Lower Turonian of Australia and Papua New Guinea (Cookson & Eisenack, 1958) and is reported from the Valanginian to Turonian of Australia (Wiseman & Williams, 1974; Kemp, 1976; Morgan, 1980) and Mid-Kimmeridgian to Tithonian(?) globally (Sarjeant, 1979).

Chlamydophorella wallala Cookson & Eisenack, 1960b

Pl. 14, figs. G-L

1960b *Chlamydophorella wallala* Cookson & Eisenack, p.255, pl.38, fig.13; pl.39, fig.11.

Dimensions: (µm; 12 specimens measured)
Autophragm length (with operculum): 33 (51) 58 (8 specimens)
Autophragm length (without operculum): 29 (50) 62
Autophragm width: 25 (32) 37
Max. width of pericoel: 5 (8) 10
Max. width of processes: 1.5 (1.9) 2.5

Comments: Morphotypes assigned to *Chlamydophorella wallala* in the literature vary considerably; therefore only specimens conforming to the type description are herein attributed to this species.

Previously reported range: Basal Callovian to Uppermost Kimmeridgian of Australia and Papua New Guinea (Cookson & Eisenack, 1960b; Davey, 1987; Riding *et al.*, 2010);
Oxfordian of New Zealand (Wilson & Helby, 1987);
Upper Callovian to Tithonian of Europe (Sarjeant, 1979; Fauconnier *et al.*, 1996);
Lower to Mid-Oxfordian of Egypt (Ibrahim *et al.*, 2002);
Oxfordian to Tithonian of Africa (Jiang *et al.*, 1992; Schrank, 2005).

Chlamydophorella sp. A

Pl. 14, figs. A-F

Description: Intermediate-sized, proximate, holocavate cyst; autophragm elongate ellipsoidal with rounded to rarely conical apices; numerous short, fine, capitate processes support a thin ectophragm; ectocoel narrow over most of cyst, extending into a short ectohorn (<3µm long) and, frequently though not consistently, two conspicuous bulges at the paracingulum. Processes intratabular with paratabulation frequently but faintly indicated by very thin pandasutural bands with rare penitabular alignment of processes; gonyaulacacean paratabulation, formula indeterminate. Archeopyle apical, Type (tA) to Type (tA)@. Parasulcus indicated by parasulcal notch only.

Dimensions: (µm; 12 specimens measured)
Autophragm length (with operculum): 52 (59) 63 (10 specimens)
Autophragm length (without operculum): 49 (56) 60 (9 specimens)
Autophragm width: 20 (26) 31
Max. width of pericoel: 2.5 (3.6) 4.5
Max. width of processes: 1

Comparison: *Chlamydophorella* sp. A bears a striking resemblance to *Gardodinium angustum* Riding, Helby & Stevens *in* Riding & Helby, 2001g in all aspects, including size, faint paratabulation and paracingular bulges, except the pronounced apical ectohorn. An elongate, parallel sided ectohorn is a generic trait of *Gardodinium*, therefore Jansz-Io specimens are herein assigned to *Chlamydophorella*. *G. angustum* ranges from the Tithonian to Berriasian of north-western Australia and neighbouring regions, therefore *Chlamydophorella* sp. A may be a direct ancestor of *G. angustum*.

Chlamydophorella spp.

Undifferentiated specimens generically attributable to *Chlamydophorella* but unable to be specifically assigned are placed in *Chlamydophorella* spp. The diversity of *Chlamydophorella* morphotypes lead to the characterisation of six informal types, *Chlamydophorella* spp. Types A – F, as outlined in Table 5.1. High variability, poor preservation (especially of fine Type A and D morphotypes) or few specimens meant further speciation was impracticable.

Table 5.1: *Chlamydophorella* spp. Types A – F

Cyst shape	Process thickness	*Chlamydophorella* spp.
Subspherical	Fine (<1µm)	Type A
	Intermediate (1-2µm)	Type B
	Robust (>2µm)	Type C
Elongate ellipsoidal	Fine (<1µm)	Type D
	Intermediate (1-2µm)	Type E
	Robust (>2µm)	Type F

Genus ***Chytroeisphaeridia*** (Sarjeant, 1962a) Downie & Sarjeant, 1965, emend. Pocock, 1972 and Davey, 1979d

Type species: Sarjeant, 1962a, as *Leiosphaeridia* subgen. *Chytroeisphaeridia chytroeides* (Acritarch).

Chytroeisphaeridia chytroeides (Sarjeant, 1962a) Downie & Sarjeant, 1965, emend. Davey, 1979d

Pl. 15, figs. A-D

1962a *Leiosphaeridia* subgen. *Chytroeisphaeridia chytroeides* (Acritarch) Sarjeant, p.493-494, pl.70, figs.13, 16.

1965 *Chytroeisphaeridia chytroeides* (Sarjeant, 1962a) Downie & Sarjeant, p.103.

1979d *Chytroeisphaeridia chytroeides* (Sarjeant, 1962a) Downie & Sarjeant, 1965, emend. Davey, p.211.

Dimensions: (µm; 24 specimens measured)

Total length: 34 (41) 47

Total width: 27 (34) 40

Length of apical horn: 0 (1) 3.5

Comments and Comparison: Observed specimens of *Chytroeisphaeridia chytroeides* displayed intraspecific variability in the development of a short, blunt apical horn (pl. 15, figs. C-D). Intergrading examples (*e.g.*, pl. 15, fig. B) confirm the common origin, and hence the morphotypes are not separated for quantitative analysis. Apart from being much smaller in size, the 'horned' morphotype is similar in shape to the larger *Chytroeisphaeridia cerastes* Davey, 1979d.

Previously reported range: Cosmopolitan: Bajocian to Mid-Oxfordian of Australia, the Timor Sea and Papua New Guinea (Filatoff, 1975; Davey, 1987; Mantle, 2009b; Riding *et al.*, 2010);
Oxfordian to Tithonian of New Zealand, (Helby *et al.*, 1988);
Aalenian to Kimmeridgian (?Tithonian) of Europe (Sarjeant, 1962a, 1968, 1972, 1979; Raynaud, 1978; Erkmen & Sarjeant, 1980; Woollam, 1980; Riding *et al.*, 1985, 1999, 2010; Nøhr-Hansen, 1986; Porter, 1988; Smelror, 1988a & b; Thomas & Cox, 1988; Prauss, 1989; Kunz 1990; Stancliffe, 1991; Poulsen, 1993; Fauconnier *et al.*, 1996; Huault, 1999; Borges *et al.*, 2011);
?Aalenian to Tithonian of The Middle East and Africa (Wheeler & Sarjeant, 1990; Jiang *et al.*, 1992; Ibrahim & Schrank, 1996; Gitmez & Ertug, 1999; Ibrahim *et al.*, 2002);
Kimmeridgian of North America (Zotto *et al.*, 1987);
Callovian of Argentina (Riding *et al.*, 2011).

Genus ***Circulodinium*** Alberti, 1961

Type species: *Circulodinium hirtellum* Alberti, 1961.

Circulodinium sp. cf. ***C. densebarbatum?*** (Cookson & Eisenack, 1960b) Fauconnier *in* Fauconnier & Masure, 2004

Pl. 15, figs. G-L

cf. 1960b *Cyclonephelium densebarbatum* Cookson & Eisenack, p.253, pl.38, figs.9-10.
cf. 2004 *Circulodinium densebarbatum* (Cookson & Eisenack, 1960b) Fauconnier *in* Fauconnier & Masure, 2004, p.114.

Dimensions: (µm; 22 specimens measured)
Autophragm length (with operculum): 48 (53) 60 (6 specimens)
Autophragm length (without operculum): 44 (52) 61
Autophragm width: 41 (50) 57
Max. length of ornament: 2.5 (5) 8

Comparison: Jansz-Io specimens are superficially similar to the *Circulodinium densebarbatum* paratype of Cookson & Eisenack 1960b figured in their pl.38, fig.9 which possesses longer circumferential processes than the holotype. Observed specimens differ to *Circulodinium densebarbatum s.s.* in possessing circumferential ornament that is distally and proximally connected to appear spongeous, and is reduced apically and antapically with maximum ornament width commonly occurring on the lateral hypocyst.

Previously reported range: *C. densebarbatum s.s.* ranges from Oxfordian to Valanginian of Australia (Cookson & Eisenack, 1960b; Helby *et al.*, 1987; Morgan *et al.*, 2002; Riding *et al.*, 2010), Kimmeridgian to Tithonian of New Zealand (Helby *et al.*, 1988), and sporadically from Lower Oxfordian to Mid-Berriasian of Papua New Guinea (Davey, 1987).

Circulodinium? sp. A

Pl. 16, figs. A-L

Description: Small to intermediate-sized, subcircular to ovoidal, strongly lenticular, proximate cyst; autophragm only; hypocyst substantially longer than epicyst, with epicyst one third of total cyst length or less; paracingular and parasulcal furrows frequently indicated by shallow lateral indentations and reduced ornament; faint kidney-shaped flagellar scar common; microverrucate to strongly vermiculate ornament, typically coarsest on ventral postcingular paraplates; standard gonyaulacacean paratabulation, formula: 4', 6'', Xc, ?6''', 1p, 1'''', Xs indicated by zigzag principal archeopyle suture and subtle changes in ornament; archeopyle apical, probably Type (tA), operculum free; short accessory archeopyle sutures common in the precingular series.

Dimensions: (µm; 12 specimens measured)
Autophragm length (without operculum): 33 (44) 52
Autophragm width: 35 (43) 53
Max. length of ornament: 0.5 (1) 1.5

Comparison: *Circulodinium?* sp. A is tentatively placed in *Circulodinium* as being most similar to *Circulodinium vermiculatum* Stover & Helby 1987c. However observed specimens differ from *C. vermiculatum* and other *Circulodinium* species in never displaying antapical or lateral protrusions, having more ornament on the dorso-ventral surfaces, a more centrally positioned parasulcus, and a very high paracingulum. Therefore specimens may ultimately be recognised as belonging to a new genus in association with *Circulodinium?* sp. B below. *Circulodinium?* sp. B differs in having a larger, more elongate cyst with a more polygonal ambitus.

Circulodinium? sp. B

Pl. 17, figs. A-L

Description: Intermediate-sized, ovoidal to polygonal, slightly lenticular, proximate cyst; autophragm only; hypocyst substantially longer than epicyst, with epicyst approximately one quarter of total cyst length; paracingular and parasulcal furrows frequently indicated by shallow lateral indentations and reduced ornament; faint kidney-shaped flagellar scar rarely observed. Ornament variable, ranging from microverrucate, strongly vermiculate to reticulate; typically coarsest on ventral postcingular paraplates. Standard gonyaulacacean paratabulation, formula: 4', 6'', Xc, ?6''', 1p, 1'''', Xs indicated by zigzag principal archeopyle suture and very subtle changes in ornament; 6'' paraplate anterior margin varies from camerate to planate; archeopyle apical, probably Type (tA), operculum free; short accessory archeopyle sutures common in the precingular series.

Dimensions: (µm; 12 specimens measured)
Total length: 58 (66) 83
Total width: 44 (55) 71

Comments: *Circulodinium?* sp. B is distinctive with its ovoidal to rectangular shape, very short epicyst and wide archeopyle. Specimens with flat apices and parallel sides have a 'boxy' appearance (pl. 17, fig. H).

Comparison: This species is tentatively placed in *Circulodinium* due to the similarity with *Circulodinium?* sp. A herein, including unequal hemicysts, ornament, paratabulation and lenticular nature. *Circulodinium?* sp. A differs in having a smaller, subcircular to ovoidal cyst with slightly more visible paratabulation.

Genus ***Clathroctenocystis*** Wiggins, 1972

Type species: *Clathroctenocystis elegans* Wiggins, 1972

Clathroctenocystis asaphes (Drugg, 1978) Stover & Helby, 1987d

Pl. 15, figs. E-F

1978 *Belodinium asaphum* Drugg, p.63-64, pl.2, figs.8-10.

1987d *Clathroctenocystis asapha* (Drugg 1978) Stover & Helby, p.277.

2004 *Clathroctenocystis asaphes* (Drugg 1978) Stover & Helby, 1987d; Fensome & Williams, p.132.

Dimensions: (μm; 12 specimens measured)
Periphragm length: 45 (69) 90
Periphragm width: 22 (36) 44
Endophragm length: 39 (58) 75
Endophragm width: 20 (32) 38

Previously reported range: Upper Callovian to Mid-Oxfordian of Europe and Russia (Drugg, 1978; Fauconnier, 1995; Huault, 1999; Riding *et al.*, 1999)

Genus ***Cleistosphaeridium*** Davey *et al.*, 1966b, emend. Eaton *et al.*, 2001

Type species: *Cleistosphaeridium diversispinosum* Davey *et al.*, 1966b.

Cleistosphaeridium? oxfordianum sp. nov.

Pl. 18, figs. A-M, Pl. 19, figs. A-F, Pl. 108, figs. J-K

Holotype and type locality: Pl. 18, fig. J-M, Jansz-3, Core, 2810mRT(c), GA sample no. 1631224, slide no. 5, England Finder co-ordinates: P28/1, CPC no. 40669.

Derivation of name: From the occurrence of this species in the Oxfordian Stage.

Synopsis: Intermediate-sized, spherical to subspherical, apteate, proximate to proximochorate cyst. Autophragm densely granulate to vermiculate with numerous non-tabular to intratabular, membranous, dolabrate (pick-like) processes, infrequently proximally linked by penitabular ridges, rarely in concentric penitabular arcs; pandasutural bands may occur. Paratabulation gonyaulacacean; archeopyle apical, Type (tA); operculum free; principal archeopyle suture zigzag; short accessory archeopyle sutures common.

Diagnosis:
Shape: Spherical to subspherical.

Wall Relationships: Autophragm only.

Wall Features: Densely ornamented with non-tabular to intratabular processes, usually the same length on individual specimens, though process length may increase at the paracingulum and antapically (pl. 18, fig. H). Processes highly variable, ranging from simple, conical or tapered to broad and membranous; distal process tips are typically asymmetrically expanded and variably furcate resulting in distinctive dolabrate (pick-like) processes; SEM shows process bases are insiderate although this is rarely evident under TLM. Individual processes are generally oriented parallel to the nearest parasuture. Processes may be proximally linked to form incomplete penitabular ridges, and very rarely aligned in concentric penitabular arcs. Ornament between processes appears microgranulate to vermiculate under TLM; SEM reveals a broadly fibro-pitted ornament with verrucate to vermiculate elements roughly radially arranged around process bases and extending into basal insiderae.

Archeopyle: Apical, Type (tA); operculum free. Principal archeopyle suture zigzag; short accessory archeopyle sutures common on operculum and precingular series. Variability common in shape and dimensions of archeopyle and isolated opercula (pl. 18, figs A-E; pl. 19, figs. A, D) possibly indicating variable precingular paratabulation.

Paratabulation: Usually indicated by principal archeopyle suture and short accessory archeopyle sutures only; rarely incompletely indicated by proximal penitabular ridges and broad pandasutural bands when developed. Gonyaulacacean; inferred formula: 4', 6(-?7)'', Xc, ?6''', 1p, 1'''', Xs. Variability in archeopyle shape and dimensions and accessory archeopyle sutures suggest variability may exist in the precingular series, ranging from 6 to 7 precingular paraplates.

Paracingulum: Rarely indicated by either or both of: 1/ proximal ridges joining adjacent processes, or 2/ increased process length.

Parasulcus: Typically indicated by parasulcal notch only but may contain shorter and simpler processes.

Size: Intermediate.

Dimensions: (μm; 12 specimens measured)
Autophragm length (without operculum): 49 (54) 60
Autophragm width: 47 (55) 69
Max. length of ornament: 6 (8) 11

Comparison: The generic assignment of this species is problematic, since it does not conform to all generic characteristics of the most similar published genera. The Jurassic to Cretaceous genus *Systematophora* Klement, 1960 contains spherical cysts with an apical archeopyle and (usually) proximally connected penitabular process complexes, but rarely display intratabular processes. Conversely, the Cenozoic genus *Cleistosphaeridium* Davey *et al.*, 1966b (emend. Eaton *et al.*, 2001) incorporates cysts with an apical archeopyle that are subspherical (weakly dorso-ventrally compressed) with distinctive dolabrate processes that may be intratabular and/or weakly proximally connected annular to arcuate process complexes. Even though *Cleistosphaeridium? oxfordianum* is spherical in shape and Oxfordian in age (therefore much older than other representative species), the distinctive intratabular dolabrate processes that may have proximal annular connections more closely align with *Cleistosphaeridium* than *Systematophora*.

An alternative genus for this species could be *Impletosphaeridium* Morgenroth, 1966 (emend. Islam, 1993). The type species of *Impletosphaeridium*, *Impletosphaeridium transfodum* Morgenroth, 1966, may be synonymous with the *Cleistosphaeridium* type species, *Cleistosphaeridium diversispinosum* Davey *et al.*, 1966b (emend. Eaton *et al.*, 2001) according to Eaton *et al.*, 2001 (p.174). However, uncertainty regarding the nature of the archeopyle of the *Impletosphaeridium transfodum* holotype, a dissimilar paratype, and unavailability of the type material for clarification, prevented official synonymy. Furthermore, Stover & Evitt, 1978 (p.232) recommended that species with a known archeopyle should be attributed to other genera, and Fauconnier & Masure, 2004 (p.337) considered *Impletosphaeridium* problematic. Therefore, attribution of new species with a known archeopyle to *Impletosphaeridium* is considered inappropriate.

Cleistosphaeridium? oxfordianum is most similar to *Cleistosphaeridium diversispinosum* in process morphology and variability, but *C. diversispinosum* differs in having longer processes on a slightly lenticular cyst body.

Genus ***Contracysta*** gen. nov.

Type species: *Contracysta variantia* gen. et. sp. nov.

Derivation of name: From *contra-* (Latin): "opposite, over against, on the opposite side", given for the opposite, 'reverse' wall relationship to other genera of similar appearance, and *cysta* referring to the cyst.

Diagnosis: Highly variable, small to large, proximate to skolochorate cysts. Endophragm consistently spherical to subspherical; smooth to scabrate. Process-forming periphragm microperforate, fenestrate to striate; microperforate ornament often appears microgranulate in TLM. Displays 'reverse' wall relationship: periphragm alone forms processes with periplates* appressed to endophragm only in intratabular areas, lifting from endophragm in penitabular areas to form 17 to 18 hollow processes of variable length, breadth and form. Processes anchored to endophragm by insiderae*. Process length and appearance highly variable: complete continuum ranging from proximate, proximochorate, to phragmochorate; extremely fenestrate processes may be reduced to annulate or simulate process complexes. Distally processes typically simulate* to clypteate. Processes may have ring and/or interlinking trabeculae. Paracingular and parasulcal processes absent; rarely paracingular or parasulcal ridges may occur. Paratabulation gonyaulacacean; process formula: 4', 6'', 0c, 5-6''', 1p, 1'''', 0s; where 5 post-cingular processes are present, the 1''' process is absent. Apical archeopyle, Type (tA); operculum free.

* Refer to the glossary of introduced terms in Chapter 5.1.2.

Comments: This genus is erected to contain species identified as possessing a 'reverse' wall relationship and that morphologically may not be assigned to existing genera. *Contracysta,* together with species observed herein as possessing a 'reverse' wall relationship questionably assigned to *Oligosphaeridium* Davey & Williams, 1966*, Perisseiasphaeridium* Davey & Williams, 1966*, Rigaudella* (Deflandre, 1939) Below, 1982b*,* and *Stiphrosphaeridium* Davey, 1982, form a continuum of morphotypes herein termed the "*Contracysta* Complex". Refer to Chapter 5.1.5 for further discussion on the "*Contracysta* Complex" and 'reverse' wall development, and interpretations of process and trabeculum development.

Comparison: *Contracysta* differs to all existing genera with intratabular processes in having a 'reverse' wall relationship, as discussed in Chapter 5.1.5. The variability observed within this genus results in the various morphotypes having a broadly similar appearance to some existing genera, which are differentiated as follows:

Proximate morphotypes: These morphotypes with little to no separation between the wall layers (pl. 99, figs A-G) are vaguely reminiscent of *Lanterna* Dodekova, 1969. However, *Lanterna* has an ornamented autophragm with pandasutural bands and never has intratabular ornamentation variations indicating the contact zones between two wall layers.

Broadly flaring proximate to proximochorate morphotypes (pl. 98, figs. A-F; pl. 99, figs. J-L; pl. 100, figs. A-H): These morphotypes are similar to *Atlantodinium* Zotto et al., 1987 and

Amphorula Dodekova, 1969. Morphotypes with annulate to simulate process complexes (pl. 100, figs. I-L) are similar to *Emmetrocysta* Stover, 1975 and *Systematophora* Klement, 1960. These genera differ from *Contracysta* in having paracingular and/or parasulcal processes where *Contracysta* extremely rarely has paracingular and parasulcal ridges without processes.

Proximochorate morphotypes with longer, narrow to broadly flaring processes (pl. 101, figs. A-I): These morphotypes are similar to proximochorate species of *Oligosphaeridium*. However, *Oligosphaeridium* is typically skolochorate, not trabeculate (apart from provisionally accepted species), and described as possessing a process on the ps paraplate. Proximochorate morphotypes intergrade with skolochorate morphotypes herein questionably attributed to *Oligosphaeridium, Rigaudella, Stiphrosphaeridium* and *Perisseiasphaeridium.* These morphotypes are differentiated according to the presence of no trabeculae, interlinking trabeculae, ring trabeculae or paracingular ridges respectively.

Contracysta variantia sp. nov.

Pl. 98, figs. A-F, Pl. 99, figs. A-L, Pl. 100, figs. A-L, Pl. 101, figs. A-I, Pl. 107, fig. J-L, Pl. 110, figs. G-J

Holotype and type locality: Pl. 98, fig. A-F, Io-1, Core, 2842mRT(c), GA sample no. 1694663, slide no. 4, England Finder co-ordinates: T24/1, CPC no. 40679.

Derivation of name: From *variantia* (Latin): "difference, variation" for the significant variability in the length and form of the processes.

Synopsis: Highly variable, small to large, proximate to skolochorate cysts. Endophragm consistently spherical to subspherical; smooth to scabrate. Process-forming periphragm microperforate, fenestrate to striate; microperforate ornament often appears microgranulate in TLM. Displays 'reverse' wall relationship: periphragm alone forms processes with periplates* appressed to endophragm only in intratabular areas, lifting from endophragm in penitabular areas to form 17 to 18 hollow processes of variable length, breadth and form. Processes anchored to endophragm by insiderae*. Process length and appearance highly variable: complete continuum ranging from proximate, proximochorate, to phragmochorate; extremely fenestrate processes may be reduced to annulate or simulate process complexes. Distally processes typically simulate* to clypteate. Processes may have ring and/or interlinking trabeculae. Paracingular and parasulcal processes absent; very rarely paracingular or parasulcal ridges may occur. Paratabulation gonyaulacacean; process formula: 4', 6'', 0c, 5-6''', 1p, 1'''',

0s; where 5 post-cingular processes are present, the 1''' process is absent. Apical archeopyle, Type (tA); operculum free.

* Refer to the glossary of introduced terms in Chapter 5.1.2.

Diagnosis:

Shape: Endophragm (central body) spherical to subspherical; processes typically of equal length, though may be uneven.

Wall Relationships: Endophragm and periphragm arranged in 'reverse' wall relationship, with variable, trabeculate ectophragm. Endophragm forms central body only; periphragm forms intratabular processes only. Walls are in contact in intratabular areas only; may be observed as slightly to markedly thickened or internally ornamented process bases. Processes proximally anchored to endophragm by thread-like to root-like insiderae. Trabeculate ectophragm typically present as distal interlinking trabeculae, rarely distal ring trabeculae. Trabeculae highly variable, ranging from fine threads, that may be broken, to broad, perforate membranes; may occur on very few to all processes on individual specimens. Refer to Chapter 5.1.5 for further discussion on trabeculum, process and 'reverse' wall development.

Wall Features: Endophragm (central body) smooth to finely scabrate with very rare, isolated granules or verrucae on some specimens. Periphragm typically microperforate to finely fenestrate, rarely smooth or strongly fenestrate. Periphragm forms 17 to 18 highly variable processes. Process length ranges from proximate (with periphragm only slightly separated from endophragm) to proximochorate. Proximally processes range from broad-based (almost penitabular) and subpolygonal (roundly simulate), to narrow-based (intratabular) and subcircular. Distally processes range from broadly flaring to narrow; most commonly angularly polygonal (angularly simulate to clypteate), rarely subcircular. Distal process margins often recurve back towards endophragm. Distal margins typically finely and irregularly loricate, though may be entire (when enclosed by ring trabeculae), stauromate (when large fenestrae intersect simulate distal margin), or irregularly digitate (when strongly fenestrate). Extremely fenestrate 'processes' with broad bases may be reduced to simulate or annulate process complexes, with digits surmounting a basal ridge. Perforate to fenestrate periphragm often visible lining the internal bases of processes as punctate, foveolate or irregularly reticulate ornament; particularly evident in broadly flaring proximate to proximochorate forms. Ornament rarely visible in bases of long processes unless suitably oriented or exposed by process breakage. In proximate to low-proximochorate morphotypes, a distinctive, narrow to broad, penitabular, granulate-looking ring is frequently visible where periphragm and endophragm intratabularly contact. The granulate ring may represent the extent of insiderae that anchor the

process to the endophragm surface. Insiderae appear as proximal verrucae surrounding the process base; root-like ridges radiating from the process base onto the endophragm; to long, thin threads proximally to medially linking the process to the endophragm surface. Parasutural features typically absent; extremely rarely observed as faint, parasuturally aligned micrograna through SEM.

Archeopyle: Apical, Type (tA); principal archeopyle suture zigzag with a prominent parasulcal notch. Deep accessory archeopyle sutures commonly developed in precingular series. Operculum simple, free.

Paratabulation: Gonyaulacacean paratabulation typically indicated by simulate intratabular processes, angular principal archeopyle suture and deep accessory archeopyle sutures only; extremely rarely observed as faint parasuturally aligned micrograna through SEM. Paratabulation formula: ?2pr, 4', 6'', 6c, 5-6''', 1p, 1'''', 5s. Process formula: 0-?2pr, 4', 6'', 0c, 5-6''', 1p, 1'''', 0s. Where 5 post-cingular processes are present, the 1''' process is absent. The 1''' paraplate may be represented by a small polygonal process, or a linear septum that may be mistaken for a distally recurved process or broken trabeculum adjacent to the 2''' paraplate.

Paracingulum: Indicated by the absence of processes and frequently by adcingular alignment of distal margins of pre- and post-cingular processes in proximate to proximochorate morphotypes; extremely rarely indicated by low (<1-3µm), distally expanded ridges. Slightly laevorotatory; offset by approximately one paracingulum width.

Parasulcus: Indicated by prominent parasulcal notch and the absence of processes; extremely rarely indicated by low (<1-3µm), irregularly shaped, distally expanded ridges.

Size: Intermediate to large.

Dimensions: (µm; 30 specimens measured)
Total length: 41 (64) 93
Total width: 38 (64) 92
Central body length (with operculum): 41 (47) 53 (6 specimens)
Central body length (without operculum): 40 (50) 65 (24 specimens)
Central body width: 36 (50) 71
Max. length of processes: 0 (12) 30

Comments: Variability within *Contracysta variantia* is extreme, including:

1. proximate morphotypes with almost flat ‘prostrate processes’ (having almost no separation between the endo- and periphragms; pl. 99, figs A-G);
2. proximochorate morphotypes with broad, variably fenestrate, simulate intratabular processes (pl. 98, figs. A-F; pl. 99, figs. J-L; pl. 100, figs. A-H);
3. proximochorate morphotypes with broad to narrow, elongate intratabular processes (pl. 101, figs. A-I) that intergrade with skolochorate cysts herein questionably attributed to existing skolochorate genera; and,
4. phragmochorate morphotypes where fenestrate ornament reduces the intratabular processes to annulate or simulate process complexes (pl. 100, figs. I-L).

All of these morphotypes are attributed to this single species based upon observation of a complete continuum between morphotypes which precludes further subdivision. The monospecific origin of these cysts is supported by observation of individual morphologically indeterminate *Contracysta* specimens displaying processes of different morphologies (pl. 99, fig. I; pl. 100, figs. I-J; pl. 107, fig. J-L).

However, for quantitative analysis and to test morphostratigraphic potential, this species has been subdivided into four informal categories: 1/ proximate; 2/ proximochorate; 3/ phragmochorate; and 4/ *Contracysta* sp. indet. Intergrading skolochorate morphotypes exhibiting a reverse wall relationship are tentatively assigned to the most relevant existing skolochorate genera to maintain the morphological and stratigraphical integrity of existing genera, and to avoid confusion when comparing existing species of similar morphology. Refer to Chapter 5.1.5 for further discussion on the “*Contracysta* Complex” and ‘reverse’ wall development, and interpretations of process and trabeculum development.

Comparison: *Contracysta variantia* differs to all existing genera with intratabular processes in having a ‘reverse’ wall relationship, as discussed in Chapter 5.1.5. Refer to the comparisons of *Contracysta* gen. nov. above for comparisons at the generic level.

The *Contracysta variantia* holotype and similar, broadly-flaring proximochorate morphotypes are most similar to *Amphorula dodekovae* Zotto *et al.*, 1987, which differs in possessing paracingular and parasulcal septa.

Proximate morphotypes with ‘prostrate processes’ are unique in their appearance, having two wall layers with the periphragm dissociating into periplates which are intratabularly attached to the endophragm with a contact area highlighted by a granulate ring. Apart from a vague similarity to single-walled genera with pandasutural bands (*e.g. Lanterna* Dodekova, 1969), no existing genus or species is known to possess these morphological characteristics.

Proximate morphotypes with very broad, low, almost penitabular processes are most similar to *Atlantodinium jurassicum* Zotto *et al.*, 1987, which differs in having low penitabular septa and possessing paracingular and parasulcal septa.

In phragmochorate morphotypes, variability in the extent of process fenestration results in the formation of simulate to annulate process complexes of highly variable morphology. This results in the similar appearance to multiple species of *Systematophora* Klement, 1960, including *S. areolata* Klement, 1960, *S. cretacea* Davey, 1979b, *S. rosenfeldii* Volkheimer & Sarjeant, 1993, *S. silybum* Davey, 1979a, *S.?prodigiosa* Dodekova, 1994 and *S. valensii* (Sarjeant, 1960a) Sarjeant, 1961. These, and all *Systematophora* species, differ in possessing paracingular and parasulcal septa.

Proximochorate morphotypes with broad to narrow, elongate intratabular processes are similar to proximochorate species of *Oligosphaeridium* Davey & Williams, 1966, including *O. complex* subsp. *brevispinum* Jain, 1977, *O. djenn* Below, 1982c, *O. poculum* Jain, 1977 and *O. porosum* Lentin and Williams, 1981. However, these species differ in not possessing ring or interlinking trabeculae.

Backhouse, 1988 figured a specimen as "*Oligosphaeridium* sp. A" (pl.37, fig.1) from the Hauterivian to Barremian of the Perth Basin. This specimen looks identical to some Jansz-Io broadly-flaring proximochorate specimens, and appears to display the characteristic *Contracysta* features, including insiderae, internally ornamented process bases and under-curved processes.

Davey, 1982 figured three specimens as *Oligosphaeridium* sp. I (p. 15, pl. 2, figs. 6-8) from the early Berriasian of Bed E, Speeton, England. These specimens are examples of proximate to proximochorate and phragmochorate morphotypes and are described as being variable in length, width and extent of fenestration, which corresponds exactly to observations of *Contracysta variantia* morphotypes. *Oligosphaeridium* sp. I appears to differ in not possessing distal trabeculae (or remnants thereof), not including proximate morphotypes with 'prostrate processes', and the presence of insiderae is uncertain. Further examination of the English material is required to determine the presence of a reverse wall relationship and enable a full comparison with *Contracysta variantia*.

Genus ***Ctenidodinium*** Deflandre, 1939,
emend. Sarjeant, 1966a, Sarjeant, 1974, Woollam, 1983, and Benson, 1985

Type species: Eisenack, 1935, as *Lithodinia jurassica* var. *ornata* (now *Ctenidodinium ancora*).

Ctenidodinium ancora Riding & Helby, 2001d

Pl. 20, figs. E-G.

2001d *Ctenidodinium ancorum* Riding & Helby, p.69,71, figs.3A-L.

2004 *Ctenidodinium ancora* Riding & Helby, 2001d; Fensome & Williams, p.169.

Dimensions: (µm; 12 specimens measured)
Autophragm length: 42 (49) 57
Autophragm width: 55 (61) 70
Autophragm breadth: 46 (52) 60
Max. length of processes: 6 (9) 12

Comments: Very few specimens of this distinctive species have been observed in the Jansz-Io preparations. *C. ancora* has a consistent range of Bathonian to Callovian with inconsistent occurrences to the Mid-Oxfordian in Riding *et. al.* (2010). Inconsistent occurrences may either reflect an intermittent extension of the taxon range or reworking. Given the evidence of Bathonian to Callovian reworking, the likelihood that these specimens are reworked is considered more probable.

Comparison: *Ctenidodinium ancora* is very similar to *Dichadogonyaulax sellwoodii* Sarjeant, 1974 with which it may intergrade, or potentially be conspecific. Mechanical damage of the fragile anchor-shaped distal process tips may produce specimens indistinguishable from *D. sellwoodii*. Specimens are only assigned to *C. ancora* if distal anchors are present.

Previously reported range: Bathonian to Callovian (inconsistent to Mid-Oxfordian) of Australia and the Timor Sea (Riding & Helby, 2001d; Partridge, 2006a; Mantle, 2009a; Riding *et al.*, 2010).

Ctenidodinium fuscibasilarum Riding & Helby, 2001d

2001d *Ctenidodinium fuscibasilarum* Riding & Helby, p.71-72, figs.4A-L.

Dimensions: Poorly preserved specimens were unsuitable for measurements.

Comments: Very few specimens of this distinctive species have been observed in the Jansz-Io preparations. *Ctenidodinium fuscibasilarum* has a recorded range of Mid-Bathonian to Upper Callovian in Riding *et. al.* (2010), therefore specimens are interpreted to be reworked to this level.

Previously reported range: Mid-Bathonian to Upper Callovian of Australia and the Timor Sea (Riding & Helby, 2001d; Mantle, 2009a).

Ctenidodinium planocristatum Riding & Helby, 2001d

Pl. 20, figs. H-I

2001d *Ctenidodinium planocristatum* Riding & Helby, p.72-73, figs.5A-O.

Dimensions: (µm; 12 specimens measured)
Total length: 61 (70) 81
Hypocyst length: 34 (51) 69
Total width: 62 (79) 102
Max. length of parasutural ridges: 1.5 (2) 3

Comments: *Ctenidodinium planocristatum* has a recorded range of Mid-Bathonian to Upper Callovian in Riding *et. al.* (2010) and has not previously been recorded from the *Wanaea spectabilis* Zone. Evidence from other species indicates that Bathonian to Callovian sediments have been reworked into the Jansz Sandstone, therefore *C. planocristatum* may also be reworked; however *in situ* occurrence cannot be discounted. Acmes of this species occur in underlying Callovian sediments and may account for the volume of specimens occurring in the Jansz-Io preparations.

Previously reported range: Mid-Bathonian to Upper Callovian of Australia and the Timor Sea (Riding & Helby, 2001d; Mantle, 2009a; Riding *et al.*, 2010).

Genus ***Cygnusicysta*** Riding & Helby, 2001e

Type species: *Cygnusicysta taltarniana* Riding & Helby, 2001e

Cygnusicysta delicata sp. nov.

Pl. 20, figs. A-D

Holotype and type locality: Pl. 20, fig. A, B, Jansz-1, Core, 2887mRT(c), GA sample no. 1631194, slide no. 4, England Finder co-ordinates: U23/2, CPC no. 40700.

Derivation of name: From *delicatus* (Latin): "delicate"; for the delicate, easily folded cyst.

Synopsis: Small, cavate cyst; scabrate to microgranulate endophragm and periphragm separated by a narrow pericoel; probably spherical to subspherical cyst but very thin walled and typically folded. Archeopyle probably apical, Type (tA) or Type (tA)@; no other paratabulation evident.

Diagnosis:

Shape: Probably originally spherical to subspherical cyst but very thin walled and typically deformed to produce a subcircular to subpolygonal ambitus.

Wall Relationships: Cavate with thin endophragm and periphragm separated by a very narrow pericoel; cavation often only visible on lateral margins or at folds.

Wall Features: Endophragm and periphragm both scabrate to microgranulate.

Archeopyle: Probably apical, Type (tA) or Type (tA)@.

Paratabulation: Not indicated other than probable apical archeopyle.

Paracingulum: Not indicated.

Parasulcus: Not indicated.

Size: Small.

Dimensions: (µm; 14 specimens measured)
Total length: 30 (42) 50
Total width: 28 (40) 46
Max. width of pericoel: 1 (1.5) 4

Comments: While *Cygnusicysta delicata* is frequently deformed and therefore often difficult to identify, the significant number of specimens necessitates the publication of this species. A dinoflagellate affiliation has been deduced through many specimens displaying a probable apical archeopyle despite the lack of other paratabulation indications.

Comparison: *Cygnusicysta delicata* differs from the generic type species, *Cygnusicysta taltarniana* Riding & Helby, 2001e, in having a smaller cyst size and a much thinner endophragm.

Genus ***Desmocysta*** Duxbury, 1983

Type species: *Desmocysta plekta* Duxbury, 1983.

Desmocysta? **sp. A**

Pl. 21, figs. A-C

Description: Small to intermediate-sized, subspherical to ovoidal cyst. Autophragm smooth to scabrate with sparsely scattered, very thin, long, possibly non-tabular filaments. Filaments distally branch and expand into amorphous distal masses; frequently entangled at antapex. Large precingular archeopyle, Type 2P; operculum free, probably compound; paratabulation formula indeterminate.

Dimensions: (μm; 12 specimens measured)
Autophragm length: 42 (49) 59
Autophragm width: 32 (45) 57
Filament length: 30 (38) 47 (8 specimens)

Comparison: *Desmocysta?* sp. A possesses scattered, possibly non-tabular filaments attached across the cyst surface (pl. 21, fig. C) rather than being restricted to the antapex, as seen in *Desmocysta plekta* Duxbury, 1983 and *Desmocysta simplex* Duxbury, 2001.

Genus ***Dichadogonyaulax*** Sarjeant, 1966a, emend. Sarjeant, 1974, Woollam, 1983 and Benson, 1985

Type species: Norris, 1965, as *Gonyaulax culmula*.

Dichadogonyaulax sellwoodii Sarjeant, 1974

Pl. 20, figs. J-K

1974 *Dichadogonyaulax sellwoodii* Sarjeant, p.52, 55, pl.1, figs.A-H; pl.2, figs.I-K; pl.3, figs.L-Q.

1978 *Ctenidodinium sellwoodii* (Sarjeant, 1974) Stover & Evitt, p.204.

1993 *Dichadogonyaulax sellwoodii* Sarjeant, 1974; retained by Lentin & Williams, p.179.

Dimensions: (µm; 12 specimens measured)
Autophragm length: 38 (53) 75
Autophragm width: 55 (68) 88
Max. length of ornament: 4 (8) 12

Comparison: *Dichadogonyaulax sellwoodii* is very similar to *Ctenidodinium ancora* Riding & Helby, 2001d with which it may intergrade, or potentially be conspecific. Mechanical damage of the *C. ancora* fragile anchor-shaped distal process tips may produce specimens indistinguishable from *D. sellwoodii*. Specimens are only assigned to *D. sellwoodii* if no distal anchors are present.

Previously reported range: Cosmopolitan: Callovian to Lower Oxfordian of Papua New Guinea (Davey, 1987);
Bajocian to Oxfordian of Europe (Sarjeant, 1974, 1979; Riley & Fenton, 1982; Riding *et al.*, 1985; Prauss, 1989; Fauconnier *et al.*, 1996; Huault, 1999; Riding *et al.*, 1999; Poulsen & Riding, 2003; Riding, 2005b);
Bathonian to Lower Oxfordian of The Middle East and Egypt (El Beialy & Ibrahim, 1997; Ibrahim *et al.*, 2002; Kholeif *et al.*, 2004)

Genus ***Dingodinium*** Cookson & Eisenack, 1958, emend. Mehrotra & Sarjeant, 1984, Stover & Helby, 1987d, and Khowaja-Ateequzzaman *et al.*, 1990

Type species: *Dingodinium jurassicum* Cookson & Eisenack, 1958.

Dingodinium jurassicum Cookson & Eisenack, 1958

Pl. 21, figs. G-I

1958 *Dingodinium jurassicum* Cookson & Eisenack, p.39, pl.1, figs.10-11.

Dimensions: (µm; 11 specimens measured)
Periphragm length: 62 (67) 72

Periphragm width: 53 (59) 65
Endophragm length: 44 (50) 56
Endophragm width: 40 (44) 49
Max. length of endophragmal ornament: 1 (2) 2.5

Previously reported range: Cosmopolitan: Lower Oxfordian to Berriasian (to Valanginian?; with a notable acme in the Tithonian) of Australia, New Zealand and Papua New Guinea (Cookson & Eisenack, 1958, 1960b; Davey, 1987; Helby *et al.*, 1987, 1988; Bint & Marshall, 1994; Morgan *et al.*, 2002; Riding *et al.*, 2010);
Upper Callovian to Mid-Tithonian of Europe (Sarjeant, 1979; Raynaud, 1978; Poulsen, 1993, 1996; Riding *et al.*, 1999);
Kimmeridgian to Tithonian of The Middle East (Gitmez & Ertug, 1999);
Tithonian of Africa (Schrank, 2005).

Dingodinium sp. cf. ***D. minutum*** Dodekova, 1975, emend. Poulsen, 1996

Pl. 21, figs. D-F

cf. 1975 *Dingodinium minutum* Dodekova, p.25, pl.5, figs.13-15.
cf. 1996 *Dingodinium minutum* Dodekova, 1975, emend. Poulsen, p.82.

Dimensions: (μm; 12 specimens measured)
Periphragm length (with operculum): 39 (46) 51 (10 specimens)
Periphragm length (without operculum): 41 (47) 52 (2 specimens)
Periphragm width: 38 (45) 54
Endophragm length (with operculum): 36 (42) 47 (10 specimens)
Endophragm length (without operculum): 35 (36) 37 (2 specimens)
Endophragm width: 34 (40) 47

Comparison: Jansz-Io specimens are most similar to *Dingodinium minutum* in cyst size and ornament, but differ from the type material in having a slightly larger endocyst, narrower pericoel, and a frequently folded periphragm with little to no paratabulation or visible apical perihorn. These differences preclude precise specific allocation; however, observed specimens are very similar to other published examples of this species, including Poulsen, 1996.

Previously reported range: *Dingodinium minutum s.s.* occurs from the Mid-Callovian to Lower Oxfordian of Australia (Riding *et al.*, 2010);

Callovian to Lower Oxfordian of Papua New Guinea (Davey, 1987);
Bathonian to Kimmeridgian of Europe (Dodekova, 1975, 1990; Sarjeant, 1979; Davey, 1982; Smelror, 1988a; Poulsen, 1993, 1996);
Callovian of the Timor Sea (Mantle, 2009b as *Dingodinium* sp. cf. *D. minutum*).

Genus ***Dissiliodinium*** Drugg, 1978, emend. Bailey & Partington, 1991, and Feist-Burkhardt & Monteil, 2001

Type species: *Dissiliodinium globulus* Drugg, 1978.

Dissiliodinium caddaense (Filatoff, 1975) Stover & Helby, 1987a

Pl. 22, figs. C-F

1975 *Chytroeisphaeridia caddaense* Filatoff, p.89, pl.29, figs.7-9.
1987 *Dissiliodinium caddaense* (Filatoff, 1975) Stover & Helby, p.107, figs.4A-L.

Dimensions: (µm; 12 specimens measured)
Hypocyst length: 42 (64) 81
Hypocyst width: 59 (89) 115
Max. length of ornament: 1 (2) 3
Length of antapical horn: 0 (5) 13

Comments: *Dissiliodinium caddaense* is restricted to the Lower to Mid-Bajocian according to Riding *et. al.* (2010); therefore specimens recorded in the Jansz-Io sequence are interpreted to be reworked from Bajocian sediments. Damaged or poorly preserved specimens may be difficult to distinguish from reworked Upper Bajocian to Lower Bathonian specimens of *Wanaea verrucosa* Riding & Helby, 2001b, therefore only specimens that can be clearly identified as *D. caddaense* have been recorded and measured.

Previously reported range: Bajocian of Australia (Filatoff, 1975, Helby *et al.*, 1987, 2004; Stover & Helby, 1987a; Morgan *et al.*, 2002; Partridge, 2006a; Riding *et al.*, 2010).

Dissiliodinium volkheimeri Quattrocchio & Sarjeant, 1992

Pl. 22, figs. A-B

1987 *Dissiliodinium* sp. Helby *et al.*, 1987, fig.16E.

1992 *Dissiliodinium volkheimeri* Quattrocchio & Sarjeant, p.70, pl.1, fig.2; pl.2, figs.1-6.

Dimensions: (µm; 12 specimens measured)
Total length: 47 (66) 88
Hypocyst length: 30 (49) 67
Total width: 60 (79) 105

Previously reported range: Bajocian to Callovian of Australia and the Timor Sea (Helby *et al.*, 1987; Mantle, 2009b); Callovian to Upper Tithonian of Argentina (Quattrocchio & Sarjeant, 1992; Riding *et al.*, 2011).

Genus ***Durotrigia*** Bailey, 1987

Type species: *Durotrigia daveyi* Bailey, 1987.

Durotrigia magna Riding & Helby, 2001d

Pl. 23, figs. C-F

2001d *Durotrigia magna* Riding and Helby, p.73, 75, figs.6A-F.

Dimensions: (µm; 12 specimens measured)
Total length: 74 (98) 115
Total width: 79 (97) 127
Length of apical horn: 0 (8) 11
Max. length of ridges: 1 (1.5) 3

Comments: *Durotrigia magna* has a recorded range of Mid-Bathonian to Upper Callovian in Riding *et. al.* (2010) and has not previously been recorded from the *Wanaea spectabilis* Zone. Evidence from other species suggests that Bathonian to Callovian sediments have been reworked into the Jansz Sandstone, therefore *D. magna* may also be reworked.

Previously reported range: Mid-Bathonian to Upper Callovian (with Lower Callovian acme) of Australia and the Timor Sea (Riding & Helby, 2001d; Mantle, 2009a; Riding *et al.*, 2010).

***Durotrigia?* sp. A**

Pl. 23, figs. A-B

Description: Intermediate-sized, subspherical cyst; autophragm densely covered by very fine baculate spines of equal length. Large precingular archeopyle, Type ?3-5P, compound, free; other paratabulation, paracingulum and parasulcus absent to indistinct.

Dimensions: (µm; 3 specimens measured)
Total length: 56 (60) 68
Hypocyst length: 39 (43) 48
Total width: 64 (70) 78

Comparison: *Durotrigia?* sp. A is tentatively assigned to *Durotrigia* due to the presence of a 3-5P archeopyle and low relief ornament but the absence of distinct parasutural elements such as ridges or septa, which distinguishes this species from published *Durotrigia* species.

Genus ***Egmontodinium*** Gitmez & Sarjeant, 1972

Type species: *Egmontodinium polyplacophorum* Gitmez & Sarjeant, 1972.

Egmontodinium elongatum Mantle 2005

Pl. 24, figs. D-J

2005 *Egmontodinium elongatum* Mantle, p.253, 255-256, pl.2. figs.1-9, text-fig.6.

Dimensions: (µm; 24 specimens measured)
Autophragm length (with operculum): 70 (77) 83 (4 specimens)
Autophragm length (without operculum): 52 (69) 88
Autophragm width: 24 (38) 57
Max. length of septa: 5 (8) 10

Comments: Jansz-Io specimens display a significant degree of intraspecific variability, particularly in septal and bi- to trifurcate process development, resulting in variably expressed paratabulation. However, all specimens conform to the original Mantle, 2005 description and hence are included therein.

Previously reported range: Mid-Callovian to Mid-Oxfordian of Australia (Mantle, 2005, 2009a; Riding *et al.*, 2010).

Egmontodinium? sp. A

Pl. 25, figs. A-L

Description: Intermediate-sized, ovoidal to elongate subpolygonal, proximochorate cysts. Autophragm scabrate with numerous, solid, parasutural to intratabular processes and short, discontinuous septa; processes are subcircular to flattened in cross-section and may be proximally and distally expanded with simple, capitate or bifurcate distal tips; processes may be isolated, connected by a proximal ridge, or merge to produce membranous to stauromate (rarely erymnate) discontinuous septa, most commonly developed along parasutures but also rarely intratabularly. Paratabulation standard gonyaulacacean, indicated by parasutural alignment of processes / septa, paracingulum, parasulcus and archeopyle margin; formula: Xpr, 4', 6'', Xc, 6''', 1p, 1'''', Xs. Paracingulum and parasulcus not subdivided and devoid of processes. Archeopyle apical, Type (tA) with zigzag margin and deeply indented parasulcal notch; operculum free.

Dimensions: (µm; 12 specimens measured)
Autophragm length (with operculum): 59 (62) 65 (3 specimens)
Autophragm length (without operculum): 57 (62) 67
Autophragm width: 27 (31) 37
Max. length of septa / processes: 4 (5) 7

Comments: Specimens attributed to *Egmontodinium?* sp. A are extremely variable in shape (ovoidal to elongate subpolygonal), paratabulation expression (parasuturally aligned processes with or without proximal ridges, to discontinuous septa) and process / septal density. Different combinations of these morphological features results in a complex continuum of morphotypes that prevent formal classification.

Comparison: Generically this species is intermediate between *Egmontodinium* and *Productodinium* Davey 1987. This species is herein questionably assigned to *Egmontodinium* based upon the combination of short, discontinuous parasutural septa and numerous processes. Specimens attributed to *Egmontodinium?* sp. A intergrade with *Productodinium chenii* Davey 1987, which differs only in never possessing parasutural or intratabular septa. This species may form part of the *P. chenii* / *E. torynum* lineage discussed by Davey 1987 (p.43).

Previously reported range: Similar specimens were recorded as "*Egmontodinium* sp. A" by Mantle 2009a from the Callovian of the Timor Sea area.

Genus ***Ellipsoidictyum*** Klement, 1960

Type species: *Ellipsoidictyum cinctum* Klement, 1960, p.78.

Ellipsoidictyum sp. A

Pl. 24, figs. A-C

Description: Small to intermediate, subspherical to ovoidal, proximochorate cysts. Autophragm with reticulum formed by interconnecting, non-tabular septa (< 3 µm high) forming roughly equidimensional lumina (< 5 µm diameter). Gonyaulacacean paratabulation typically indicated by archeopyle and parasulcal notch only, rarely by vague delineation of the paracingulum. Apical archeopyle, Type (tA). Free opercula and zigzag principal archeopyle suture indicate epicystal paratabulation formula of Xpr, 4', ?1a, 6''; remaining paratabulation indeterminate.

Dimensions: (µm; 3 specimens measured)
Autophragm length (with operculum): 49 (1 specimen)
Autophragm length (without operculum): 45 (47) 50
Autophragm width: 37 (41) 47
Total length (with operculum): 55 (1 specimen)
Total length (without operculum): 51 (53) 55
Total width: 41 (46) 53

Comparison: *Ellipsoidictyum* sp. A is very similar to *Valensiella ovulum* (Deflandre, 1947b) Eisenack, 1963, but differs in never having an ectophragm.

Genus ***Endoscrinium*** (Klement, 1960) Vozzhennikova, 1967, emend. Vozzhennikova, 1965, Gocht, 1970, and Riding & Fensome, 2003

Type species: Deflandre, 1939, as *Gymnodinium galeritum*.

Endoscrinium acroferum (Prauss, 1989) Riding & Fensome, 2003

Pl. 26, figs. A-C

1989 *Scriniodinium acroferum* Prauss, p.45-46, pl.9, figs.1-2, pl.14, figs.17-22; text-fig.21.

2003 *Endoscrinium acroferum* (Prauss, 1989) Riding & Fensome, p.21.

Dimensions: (µm; 2 specimens measured)
Periphragm length: 75, 83
Periphragm width: 90, 96
Endophragm length: 63, 76
Endophragm width: 79, 87
Max. length of ornament: 3, 3

Comments: *Endoscrinium acroferum* only occurs in Jansz-Io preparations as damaged and poorly preserved cysts; however the long, echinate spines surmounting the low parasutural septa were sufficient to provide a positive identification.

To the authors knowledge this species has not previously been recorded from the Australasian region; however the extremely rare and poorly preserved specimens suggests that the Jansz-Io specimens may not be *in situ*.

Previously reported range: Upper Bathonian to Upper Callovian of Germany (Prauss, 1989).

Endoscrinium galeritum (Deflandre, 1939) Vozzhennikova, 1967, emend. Riding & Fensome, 2003

Pl. 26, figs. D-G

1939 *Gymnodinium galeritum* Deflandre, p.167, pl.5, figs.7-9; pl.6, fig.1.
1960 *Scriniodinium galeritum* (Deflandre, 1939) Klement, p.22.
1967 *Endoscrinium galeritum* (Deflandre, 1939) Vozzhennikova, p.176.
2003 *Endoscrinium galeritum* (Deflandre, 1939) Vozzhennikova, 1967, emend. Riding & Fensome, p.20.

Dimensions: (µm; 12 specimens measured)
Periphragm length: 84 (105) 121
Periphragm width: 75 (99) 118
Endophragm length: 65 (86) 100
Endophragm width: 60 (82) 96

Previously reported range: Cosmopolitan: Oxfordian of Australia (Morgan *et al.*, 2002; Riding *et al.*, 2010);
Oxfordian of New Zealand (Wilson & Helby, 1987);
Lower Oxfordian of Papua New Guinea (Davey, 1987);

Callovian to Mid-Kimmeridgian of Europe and Russia (Deflandre, 1939; Klement, 1960; Sarjeant, 1961a, 1962a & b, 1968, 1972, 1979; Dodekova, 1967; Vozzhennikova, 1967; Gocht, 1970; Raynaud, 1978; Woollam, 1980; Riley & Fenton, 1982; Brenner, 1988; Riding & Thomas, 1988; Smelror, 1988b; Kunz 1990; Stancliffe, 1991; Poulsen, 1993, 1996; Fauconnier, 1995; Fauconnier *et al.*, 1996; Huault, 1999; Riding *et al.*, 1999, 2010; Riding, 2005b);
Upper Bathonian to Kimmeridgian of The Middle East and Africa (Conway, 1978; Ashraf, 1979; Ibrahim & Schrank, 1996; Gitmez & Ertug, 1999);
Kimmeridgian to Tithonian of India (Jain *et al.*, 1984);
Mid-Callovian to Lower Oxfordian of northern Canada (Johnson & Hills, 1973);
Callovian of Argentina (Quattrocchio & Volkheimer, 1990; Riding *et al.*, 2011).

Endoscrinium sp. cf. ***E. irregulare*** (Cookson & Eisenack, 1958) Riding & Fensome, 2003

Pl. 27, fig. F

cf. 1958 *Wetzeliella irregularis* Cookson & Eisenack, 1958, p.28-29, pl.10, figs.1-2.
cf. 1978 *Wetzeliopsis irregularis* (Cookson & Eisenack, 1958) Beju, p.4. Note: Combination not validly published: basionym not fully referenced.
cf. 1978 *Scriniodinium? irregulare* (Cookson & Eisenack, 1958) Stover & Evitt, p.188.
cf. 1983 *Tubotuberella irregularis* (Cookson & Eisenack, 1958) Davies, p.23.
cf. 2003 *Endoscrinium irregulare* (Cookson & Eisenack, 1958) Riding & Fensome, p.22.

Dimensions: (μm; 6 specimens measured)
Periphragm length: 79 (93) 108
Periphragm width: 71 (84) 99
Endophragm length: 62 (75) 90
Endophragm width: 58 (68) 80
Max. length of ornament: 5 (7) 9

Comparison: Jansz-Io specimens are most similar to *Endoscrinium irregulare* (Cookson & Eisenack 1958) Riding & Fensome 2003, and scalloped varieties of *Endoscrinium luridum* (Deflandre 1939) Gocht 1970. *Endoscrinium* sp. cf. *E. irregulare* differs to these taxa in having reduced ornamentation on dorso-ventral parasutures, and reduced apical and antapical pericoels producing a hexagonal to polygonal ambitus rather than a quadrilateral ambitus; however this may be a factor of poor preservation.

Previously reported range: *Endoscrinium.irregulare s.s.* is recorded from Upper Jurassic (Upper Oxfordian to Lower Berriasian) of Western Australia and Papua New Guinea (Cookson & Eisenack, 1958; Helby *et al.*, 1987);
Kimmeridgian of Africa (Jiang *et al.*, 1992).
Helby *et al.*, 1988 record similar specimens as "*Scriniodinium* sp. B" from Tithonian of New Zealand.

Endoscrinium kempiae (Stover & Helby, 1987a) Lentin & Williams, 1989

Pl. 27, fig. E

1987a *Scriniodinium kempiae* Stover & Helby, p.114-115, figs.14A-B, 15A-F, 16A-I.
1989 *Endoscrinium kempiae* (Stover & Helby, 1987a) Lentin & Williams, p.127.

Dimensions: (µm; 7 specimens measured)
Periphragm length: 70 (94) 122
Periphragm width: 63 (78) 98
Endophragm length: 60 (74) 88
Endophragm width: 57 (66) 78

Comments: Very few specimens of this distinctive species have been observed in the Jansz-Io preparations. *Endoscrinium kempiae* has a consistent range of Bathonian to Mid-Callovian with inconsistent occurrences to the Lower Oxfordian in Riding *et. al.* (2010). Inconsistent occurrences may either reflect an intermittent extension of the taxon range or reworking. Given the evidence of Bathonian to Callovian reworking, the likelihood that these specimens are reworked is considered more probable.

Previously reported range: Bathonian to Mid-Callovian (with inconsistent range base to Mid-Bajocian and top to Lower Oxfordian) of Australia and Papua New Guinea (Helby *et al.*, 1987; Stover & Helby, 1987a; Burger, 1996; Partridge, 2006a; Mantle, 2009a; Riding *et al.*, 2010).

Endoscrinium luridum (Deflandre, 1939) Gocht, 1970

Pl. 27, figs. A-D

1939 *Gymnodinium luridum* Deflandre, p.166, pl.5, figs.4-6.
1960 *Scriniodinium luridum* (Deflandre, 1939) Klement, p.20.
1970 *Endoscrinium luridum* (Deflandre, 1939) Gocht, p.144-146.

Dimensions: (μm; 16 specimens measured)
Periphragm length: 62 (79) 101
Periphragm width: 63 (77) 99
Endophragm length: 47 (60) 79
Endophragm width: 45 (57) 76

Comparison: As identified in Riding & Fensome, 2003, Australian *Endoscrinium luridum* specimens can be difficult to distinguish from *E. attadalense* (Cookson & Eisenack, 1958) Riding & Fensome, 2003. Refer to Riding & Fensome, 2003 (p.25) Australian for detailed discussion.

Previously reported range: Cosmopolitan: Upper Bajocian to Valanginian of Australia (Cookson & Eisenack, 1958, 1960b; Wiseman & Williams, 1974; Morgan, 1980; Wiseman, 1980; Mantle, 2009a; Riding *et al.*, 2010);
Oxfordian to Lower Tithonian of Papua New Guinea (Davey, 1987);
Bathonian to Kimmeridgian of Europe (Deflandre, 1939; Klement, 1960; Sarjeant, 1960b, 1962a & b, 1968, 1972, 1979; Dodekova, 1967; Gocht, 1970; Raynaud, 1978; Erkmen & Sarjeant, 1980; Riding *et al.*, 1985; Nøhr-Hansen, 1986; Brenner, 1988; Riding & Thomas, 1988; Kunz 1990; Stancliffe, 1991; Poulsen, 1993, 1996; Fauconnier, 1995; Fauconnier *et al.*, 1996; Riding *et al.*, 1999; Poulsen & Riding, 2003; Riding, 2005b);
Late Jurassic of The Middle East (Conway, 1978; Ashraf, 1979);
Kimmeridgian to Tithonian of Africa (Jiang *et al.*, 1992);
Lower Oxfordian to Kimmeridgian of Canada (Pocock, 1972; Brideaux & Fisher, 1976).

Endoscrinium peripentum sp. nov.

Pl. 28, figs. C-F, Pl. 29, figs. A-F

Holotype and type locality: Pl. 29, fig. A-F, Jansz-3, Core, 2811mRT(c), GA sample no. 1631225, slide no. 5, England Finder co-ordinates: S24/1, CPC no. 40732.

Derivation of name: From *peri-* for the periphragm, and *penta* (Greek): "five", referring to the pentagonal shape of the periphragmal ambitus.

Synopsis: Intermediate to large, lenticular, circumcavate cysts. Endophragm and periphragm smooth to scabrate to rarely sparsely granulate. Endophragmal ambitus subspherical; periphragmal ambitus distinctly pentagonal; small, rounded apical perihorn common; paratabulation fully expressed by low parasutural ridges, formula: Xpr, 4', 6'', 6c, 6''', 1p,

1’’’’, 5s. Suturocavation may be developed along some major parasutures. Precingular archeopyle, Type P; operculum free.

Diagnosis:

Shape: Endophragmal ambitus subspherical; periphragmal ambitus distinctly pentagonal, with triangular epi-pericyst and trapezoidal hypo-pericyst, widest at the paracingulum. Preferential orientation suggests cysts are lenticular.

Wall Relationships: Circumcavate with endophragm and thinner periphragm appressed dorso-ventrally; minor suturocavation may be developed on major dorso-ventral parasutures, particularly along the paracingulum and the 2’’’/1p, 3’’’/4’’’ and 4’’’/5’’’ parasutures. A small, rounded apical perihorn is common.

Wall Features: Both endophragm and periphragm smooth to scabrate to rarely sparsely granulate; periphragm only has narrow, low, smooth parasutural ridges.

Archeopyle: Precingular archeopyle, Type $P_{(3'')}$; operculum free; operculum may separate into endo- and peri-opercular pieces.

Paratabulation: Standard gonyaulacacean paratabulation pattern fully expressed by parasutural ridges on the periphragm, formula: Xpr, 4’, 6’’, 6c, 6’’’, 1p, 1’’’’, 5s. Paraplate 4’ is short; paraplate 6’’ is elongate and subtriangular. A small circular to ovoidal porichnion is present on the 1’/4’ parasuture at the base of the apical perihorn.

Paracingulum: Not evident on the endophragm; distinctly evident on the periphragm by a shallow furrow between parallel parasutural ridges at the widest part of the pericyst.

Parasulcus: Longitudinal L-type; median position. Clearly indicated and internally subdivided by faint parasutural ridges on the periphragm.

Size: Intermediate to large.

Dimensions: (µm; 14 specimens measured)
Periphragm length: 75 (94) 108
Periphragm width: 76 (93) 115
Endophragm length: 63 (78) 93
Endophragm width: 61 (76) 92

Comparison: *Endoscrinium peripentum* is very similar to *Leptodinium*? sp. A, in size, wall thickness and paratabulation formula. However, *Leptodinium*? sp. A differs in being circum-suturocavate (being appressed dorso-ventrally with parasutural pericoels expanding towards the circumference), having a consistently granulate periphragm, and a slightly different paratabulation expression. *E. peripentum* has a much shorter 4' paraplate than 1' paraplate, and consequentially has an elongate, subtriangular 6'' paraplate with a very long 1'/6'' parasuture and very short 4'/6'' parasuture. Conversely, *Leptodinium*? sp. A has 1' and 4' paraplates of nearly equal length, resulting in a short, polygonal 6'' paraplate with a short 1'/6'' parasuture and relatively long 4'/6'' parasuture.

Endoscrinium peripentum differs to other published *Endoscrinium* species in the distinctive pentagonal periphragmal ambitus, being partially suturocavate, and the absence of periphragmal claustra, parasutural spines or ornamentation.

Endoscrinium? sp. A

Pl. 28, figs. A-B

Description: Intermediate to large, slightly lenticular, circumcavate cysts. Thin endophragm and periphragm smooth to scabrate to rarely sparsely granulate. Endophragmal ambitus subspherical to ovoidal; periphragmal ambitus ovoidal to subpolygonal; small, rounded apical perihorn may be present; gonyaulacacean paratabulation faintly expressed by low parasutural ridges or folds, formula: 4', 6'', Xc, 6''', 1p, 1'''', Xs. Suturocavation may be developed along some major parasutures. Precingular archeopyle, Type P; operculum free.

Dimensions: (µm; 12 specimens measured)
Periphragm length: 75 (89) 98
Periphragm width: 71 (85) 100
Endophragm length: 69 (78) 85
Endophragm width: 65 (74) 83

Comparison: *Endoscrinium?* sp. A is most similar to *Endoscrinium peripentum* sp. nov., however the thin and fragile wall layers are subject to folding and damage making the ambital shape and paratabulation difficult to determine.

Genus ***Escharisphaeridia*** Erkmen & Sarjeant, 1980

Type species: Sarjeant, 1968, as *Chytroeisphaeridia pocockii*.

Escharisphaeridia mantellii (Gitmez & Sarjeant, 1972) Courtinat, 1989

Pl. 30, figs. A-C

1972 *Chytroeisphaeridia mantellii* Gitmez & Sarjeant, p.186, pl.1, figs.3-4; pl.12, fig.3.

1978 *Chytroeisphaeridia? mantellii* Gitmez & Sarjeant, 1972; Stover & Evitt, p.29.

1989 *Escharisphaeridia mantellii* (Gitmez & Sarjeant, 1972) Courtinat, p.180.

Dimensions: (µm; 13 specimens measured)

Autophragm length (with operculum): 38 (49) 67 (4 specimens)

Autophragm length (without operculum): 37 (49) 66

Autophragm width: 40 (50) 64

Max. length of ornament: 1 (2) 3

Mean length of ornament: 0.5 (0.5) 1

Comparison: Jansz-Io preparations contain a continuum of *Escharisphaeridia* species subdivided on slight differences of ornamentation as outlined in Table 5.2.

Table 5.2: Differentiation of *Escharisphaeridia* species.

Species	Important characteristics
Escharisphaeridia sp. A	Thick, microspongeous differentiated autophragm often appears two-layered in ambital cross-section.
Escharisphaeridia pocockii	Microgranulate autophragm with low and evenly distributed ornament elements of equal length.
Escharisphaeridia mantellii	Finely granulate to verrucate autophragm with rare spinose projections extending beyond mean ornament length.

Previously reported range: Callovian to Oxfordian of the Timor Sea (Mantle, 2009b);
Kimmeridgian globally (Sarjeant, 1979);
Oxfordian to Kimmeridgian of Europe (Gitmez & Sarjeant, 1972; Courtinat, 1989);
Oxfordian to Tithonian of The Middle East (Gitmez & Ertug, 1999).

Escharisphaeridia pocockii (Sarjeant, 1968) Erkmen & Sarjeant, 1980

Pl. 30, figs. D-F

1968 *Chytroeisphaeridia pocockii* Sarjeant, p.230, pl.3, fig.9.

1979d *Lithodinia pocockii* (Sarjeant, 1968) Davey, p.217.

1980 *Escharisphaeridia pocockii* (Sarjeant, 1968) Erkmen & Sarjeant, p.62.

Dimensions: (µm; 13 specimens measured)
Autophragm length (with operculum): 53, 57 (2 specimens)
Autophragm length (without operculum): 44 (50) 57
Autophragm width: 45 (55) 61
Max. length of ornament: 0.5 (0.8) 1
Mean length of ornament: 0 (0.3) 0.5

Comparison: Jansz-Io preparations contain a continuum of *Escharisphaeridia* species subdivided on slight differences of ornamentation as outlined in Table 5.2.

Previously reported range: Cosmopolitan: Bajocian to Tithonian of Australia and the Timor Sea (Filatoff, 1975; Mantle, 2009b);
Bajocian to Mid-Kimmeridgian of Europe and Greenland (Sarjeant, 1968, 1972, 1979; Gitmez, 1970; Raynaud, 1978; Fensome, 1979; Courtinat & Gaillard, 1980; Erkmen & Sarjeant, 1980; Nøhr-Hansen, 1986; Smelror, 1988a & b; Prauss, 1989; Kunz 1990; Stancliffe, 1991; Poulsen, 1993, 1996);
Callovian of The Middle East (Wheeler & Sarjeant, 1990);
Kimmeridgian to Tithonian of India (Kumar, 1986);
Upper Bathonian to Upper Oxfordian of Africa (Thusu & Vigran, 1985; El Beialy & Ibrahim, 1997; Ibrahim *et al.*, 2002);
Kimmeridgian of North America (Zotto *et al.*, 1987);
Kimmeridgian to Tithonian of Argentina (Quattrocchio & Volkheimer, 1990; Quattrocchio & Sarjeant, 1992)

Escharisphaeridia sp. A

Pl. 30, figs. G-L

Description: Intermediate-sized, subspherical, proximate cyst. Autophragm differentiated into robust (<1µm) inner layer with fine, spongeous ornament up to 2.5µm thick that appears microgranulate in plan view. Paracingulum rarely faintly observed as parallel bands of slightly thicker ornament or shallow furrow of reduced ornament. Parasulcus indicated by parasulcal notch and a frequently distinct furrow. Archeopyle apical, Type (tA) or rarely Type (tA)@; principal archeopyle suture zigzag with short accessory archeopyle sutures. Epicystal

paratabulation formula Xpr, 4', 6"; remaining paratabulation indeterminate, but probably standard gonyaulacacean.

Dimensions: (µm; 20 specimens measured)
Autophragm length: 42 (52) 64
Autophragm width: 45 (54) 65
Wall thickness: 1.5 (2.5) 3.5

Comparison: Jansz-Io preparations contain a continuum of *Escharisphaeridia* species subdivided on slight differences of ornamentation as outlined in Table 5.2.

Escharisphaeridia? sp. B

Pl. 31, figs. A-F

Description: Intermediate to large, proximate cysts. Autophragm smooth to scabrate; ambitus ovoidal with no horns or projections. Paracingulum and parasulcus rarely indicated by a narrow ridge or furrow. Archeopyle apical, Type (tA) or Type (tA)@; principal archeopyle suture slightly zigzag with deep accessory archeopyle sutures common. Epicystal paratabulation formula Xpr, 4', 6"; remaining paratabulation indeterminate, but probably standard gonyaulacacean.

Dimensions: (µm; 12 specimens measured)
Total length: 64 (91) 128
Total width: 50 (73) 105
Width of archeopyle: 28 (49) 79

Comments: The paracingulum and parasulcus of *Escharisphaeridia?* sp. B may rarely be indicated by either a smooth, unornamented ridge or a narrow, shallow furrow (pl. 31, figs. A, E, F). This unusual morphological characteristic has not previously been recorded in *Escharisphaeridia*, therefore the generic association is tentative.

Comparison: *Escharisphaeridia?* sp. B differs to all other *Escharisphaeridia* species in cyst size and archeopyle width. This species is most similar to the acritarch *Fromea fragilis* Cookson & Eisenack, 1962, in size, shape and ornament but differing in clearly having a wide, apical archeopyle with accessory archeopyle sutures rather than a narrow, circular apical pylome. Poorly preserved specimens are difficult to differentiate, therefore only specimens with a clear apical archeopyle are assigned to *Escharisphaeridia?* sp. B.

Genus ***Evansia*** Pocock, 1972,
emend. Below, 1990

Type species: *Evansia granulata* Pocock, 1972

Evansia alaskensis (Wiggins, 1975) Below, 1990

Pl. 32, figs. A-D, Pl. 109, fig. D

1975 *Pareodinia alaskensis* Wiggins, p.104, pl.2, figs.7-8.

1990 *Evansia alaskensis* (Wiggins, 1975) Below, 1990, p.72-73.

Dimensions: (µm; 13 specimens measured)

Total length: 43 (50) 59

Total width: 31 (38) 53

Previously reported range: Callovian to Mid-Kimmeridgian of Alaska (Wiggins, 1975); Upper Bathonian to Oxfordian of Europe (Smelror, 1988a & b)

Evansia? lacryma Mantle 2005

Pl. 32, figs. E-F

2005 *Evansia? lacryma* Mantle, p.250-253; pl. 1, figs 1-9; text-figs. 4, 5.

Dimensions: (µm; 12 specimens measured)

Total length: 40 (50) 66

Total width: 29 (36) 41

Length of apical horn (approx.): 4 (6) 9

Length of apical horn extension: 0 (0.5) 5

Previously reported range: Callovian of Australia (Mantle, 2005, 2009a)

Evansia zabra (Davies, 1983) Jansonius, 1986

Pl. 32, figs. G-I

1983 *Glomodinium zabra* Davies, p.18, pl.3, figs.2-12; text-figs.11A-C.

1986 *Evansia zabra* (Davies, 1983) Jansonius, p.208.

Dimensions: (µm; 22 specimens measured)
Total length: 53 (70) 87
Total width: 30 (40) 48
Length of apical horn (approx.): 7 (9) 13
Length of apical horn extension: 0 (3) 8.5

Comments: Jansz-Io specimens of *Evansia zabra* display significant intraspecific variability with respect to size, ambital shape (particularly antapically), and distribution and density of ornamentation. Ambitus is consistently lacrimoidal (teardrop-shaped) but may be smoothly rounded (pl. 32, figs. G centre and bottom), subangular (pl. 32, figs. G top, I), or rarely hypotractally constricted (pl. 32, fig. H). Ornament commonly increases antapically but may also be concentrated adcingularly.

Observed specimens differ from the original description in the absence of two rudimentary antapical horns or hypotractal bulges. However, arcuate, compressional folds are common and may be interpreted as rudimentary horns if located on the hypocyst in lateral view, as on the holotype.

Previously reported range: Bathonian to Oxfordian of North America (Davies, 1983).

Genus ***Fostericysta*** (Riding & Helby, 2001e) Riding, 2005c

Type species: Riding & Helby, 2001e, as *Fosteria eclipsiana.*

Fostericysta eclipsiana (Riding & Helby, 2001e) Riding, 2005c

Pl. 33, figs. A-D

2001e *Fosteria eclipsiana* Riding and Helby, p.114-115.
2005c *Fostericysta eclipsiana* (Riding & Helby, 2001e) Riding, p.1091.

Dimensions: (µm; 12 specimens measured)
Total length: 20 (23) 28
Total width: 20 (23) 28

Comparison: *Fostericysta eclipsiana* appears remarkably similar to *Jansonia scarffei* Tykoezinski *et al.*, 2000. Figured specimens appear identical, however the paratabulation formulas of the two species are reportedly different (*e.g.*, *F. eclipsiana* possesses 6 precingular

paraplates while *J. scarffei* possesses 7). Poorly preserved specimens observed in the Jansz-Io preparations did not enable paratabulation clarification. Reassessment of the holotypes may reveal if these species are conspecific. In this instance *J. scarffei* would be the senior synonym of *F. eclipsiana.* However, given the distinctiveness and potential biostratigraphic importance of this species, the current author recommends retaining *Fostericysta* as a distinct genus.

Previously reported range: Callovian to Mid-Oxfordian of Australia and the Timor Sea (Riding & Helby, 2001e; Mantle, 2009b; Riding *et al.*, 2010). If conspecific with *Jansonia scarffei*, then Mid- to Upper Bathonian of England (Tykoezinski *et al.*, 2000).

Genus ***Fusiformacysta*** Morgan, 1975, emend. Riding & Helby, 2001d

Type species: *Fusiformacysta salasii* Morgan, 1975.

Fusiformacysta challisiana Riding & Helby, 2001e

Pl. 34, figs. A-L

2001e *Fusiformacysta challisiana* Riding & Helby, p.117, 119, figs.4A-L.

Dimensions: (µm; 12 specimens measured)
Total length: 69 (78) 93
Total width: 60 (69) 88

Comments: As reported in the original Riding & Helby, 2001e description, significant intraspecific variability of both the cyst shape and ornamentation was also observed in the Jansz-Io preparations. Cysts varied from subspherical to subpolygonal, with or without prominent mid-ventral bulges forming a deeply indented parasulcus. Ornament ranged from finely granulate to coarsely granulate, verrucate, and vermiculate to reticulate.

Previously reported range: Lower Bathonian to Lower Kimmeridgian (with Mid- to Upper Bathonian acme) of Australia and the Timor Sea (Riding & Helby, 2001e; Helby *et al.*, 2004; Partridge, 2006a; Mantle, 2009b; Riding *et al.*, 2010).

Fusiformacysta terniana Riding & Helby, 2001d

Pl. 33, figs. K-M

2001d *Fusiformacysta terniana* Riding & Helby, p.77, 79, 81, figs.8A-L, 9A-D.

Dimensions: (µm; 12 specimens measured)
Total length: 53 (76) 94
Total width: 56 (77) 93
Length of apical horn: 0 (0.5) 2.5
Length of antapical horn: 3 (7) 10

Comments: Few specimens of this species have been observed in the Jansz-Io preparations. *Fusiformacysta terniana* has a recorded range of Upper Bajocian to Callovian of Riding *et. al.* (2010) and has not previously been recorded from the *Wanaea spectabilis* Zone, therefore specimens are interpreted to be reworked to this level.

Previously reported range: Upper Bajocian to Callovian (with Lower to Mid-Bathonian acme) of Australia and the Timor Sea (Riding & Helby, 2001d; Morgan *et al.*, 2002; Mantle, 2009b; Riding *et al.*, 2010)

Fusiformacysta **sp. A**

Pl. 33, figs. E-J

Description: Intermediate-sized, proximate cysts. Subspherical ambitus, with or without prominent mid-ventral bulges forming a deeply indented parasulcus. Autophragm thin (<1µm) and microgranulate. Large precingular archeopyle, Type 3P; possibly compound; opercular pieces free.

Dimensions: (µm; 12 specimens measured)
Total length: 52 (64) 75
Total width: 56 (64) 78

Comparison: *Fusiformacysta* sp. A is similar to *Fusiformacysta terniana* Riding & Helby, 2001d and *Fusiformacysta challisiana* Riding & Helby, 2001e, but has a thinner and paler autophragm, much finer ornament, and never possesses apical or antapical protuberances.

Gen. et. sp. indet. A

Pl. 35, figs. A-H

Description: Small to intermediate-sized, elongate ovoidal, murochorate cysts. Autophragm or closely appressed endophragm and periphragm; foveolate to pseudoreticulate ornament with distally trabeculate, spinose to fenestrate parasutural septa. Wide paracingulum fully internally subdivided; parasulcus not clearly observed; apical series undivided; a small apical boss may represent the pr paraplates. Archeopyle either anterior intercalary Type ?3I or apical Type (tA)@ with the principal archeopyle suture within a broad apical/precingular pandasutural band.

Dimensions: (µm; 4 specimens measured)
Autophragm/endophragm length (with operculum): 39 (44) 50
Autophragm/endophragm length (without operculum): 40 (1 specimen)
Autophragm/endophragm width: 21 (23) 24
Max. length of septa: 5 (7) 8

Comments: While this species is highly distinctive and may be useful to support regional correlation, the Jansz-Io preparations do not contain sufficient specimens to enable formal description. The exact paratabulation formula and nature of the archeopyle remain elusive. The archeopyle may be intercalary Type ?3I with the loss of multiple anterior intercalary paraplates; however the lack of ornamentation and differentiation of intercalary paraplates is evidence against this interpretation. Alternatively the archeopyle may be apical Type (tA)@ with the principal archeopyle suture medially positioned within a broad, unornamented pandasutural band between the apical and precingular paraplate series (as in *Egmontodinium polyplacophorum* Gitmez & Sarjeant, 1972 or *Cernicysta? janszense* sp. nov. herein). The parallel parasutural septa, reduced ornamentation, and a very faint suggestion of a medial principal archeopyle suture visible in pl. 35, fig. E are evidence for the latter interpretation, but more specimens are required to determine the precise characteristics.

Comparison: Uncertainty regarding the paratabulation and archeopyle preclude comparison with existing genera.

Gen. et. sp. indet. A appears to be identical to figured specimens of "Gen. et sp. nov. D" Helby *et al.*, 1988 (figs.6L, M; figs.9D-F; figs.14G-I) from New Zealand, however no description was included to enable detailed comparison.

This species is most similar in size and shape to Gen. et. sp. indet. B herein which differs in being coarsely reticulate and kledochorate rather than murochorate, so possessing membranous penitabular crests rather than parasutural septa.

Previously reported range: Oxfordian to Kimmeridgian of New Zealand, (Helby *et al.*, 1988 as "Gen. et sp. nov. D")

Gen. et. sp. indet. B

Pl. 35, figs. I-N

Description: Small to intermediate-sized, elongate ovoidal, kledochorate cysts. Endophragm with closely appressed, coarsely reticulate periphragm forming membranous penitabular crests to processes fully delineating paratabulation including paracingular paraplates. Crests may be closed or open adcingularly; intermediate septa may link adjacent crests, especially along parasulcus and paracingulum. Archeopyle apical Type (tA). Paratabulation probably gonyaulacacean; exact formula indeterminate.

Dimensions: (µm; 12 specimens measured)
Endophragm length (with operculum): 42 (46) 48 (3 specimens)
Endophragm length (without operculum): 35 (47) 62 (9 specimens)
Endophragm width: 22 (31) 48
Max. length of processes: 5 (11) 15

Comments: The exact paratabulation of Gen. et. sp. indet. B was difficult to determine due to the density of penitabular crests, intermediate septa and coarsely reticulate ornament; however observations suggest the paratabulation is gonyaulacacean. The reticulate ornament extends onto the penitabular crests giving the appearance of striate or foveolate processes, or process complexes interlinked by thin membranes.

Comparison: Gen. et. sp. indet. B differs to *Egmontodinium* Gitmez & Sarjeant, 1972 and Gen. et. sp. indet. A herein in being kledochorate rather than murochorate. *Amphorula* Dodekova, 1969 is also kledochorate but uncertainty regarding the paratabulation of Gen. et. sp. indet. B prevents direct comparison. Gen. et. sp. indet. B appears most similar to *Amphorula expirata* (Davey, 1982b) Courtinat, 1989 which differs in having incomplete arcuate penitabular crests to isolated processes that may rarely be striate or foveolate but otherwise lacks ornamentation.

Gen. et. sp. indet. C

Pl. 36, figs. A-C

Description: Small to intermediate, proximate cysts. Autophragm psilate to shagreenate; ambitus ovoidal; apex either conical without apical horn, or rounded with a small, rounded apical horn. Archeopyle apical, Type (tA)@, attached ventrally at parasulcus. Paratabulation only indicated by principal archeopyle suture and deep accessory archeopyle sutures revealing six precingular paraplates; apex without accessory archeopyle sutures; paracingulum not evident.

Dimensions: (µm; 5 specimens measured)
Autophragm length (with operculum): 31, 68 (2 specimens)
Autophragm length (without operculum): 25 (40) 52
Autophragm width: 20 (32) 39
Length of apical horn: 0 (3) 5

Comments: Very few specimens of Gen. et. sp. indet. C are present in the Jansz-Io preparations, therefore this species is not formally described herein.

Comparison: Gen. et. sp. indet. C differs to *Batiacasphaera* Drugg, 1970b and *Escharisphaeridia* Erkmen & Sarjeant, 1980 in having an adnate rather than free operculum and frequently an apical horn. *Kallosphaeridium* de Coninck, 1969 has an adnate operculum, but never possesses an apical horn. Gen. et. sp. indet. C is otherwise very similar to *Kallosphaeridium hypornatum* Prauss, 1989 which differs in the larger cyst size, presence of antapical ornament and absence of an apical horn. Gen. et. sp. indet. C is also similar to figured specimens of *Batiacasphaera* sp. B Helby *et al.*, 1988 (figs.13F, J) from New Zealand, however the absence of a description precludes detailed comparison.

Previously reported range: If synonymous with "*Batiacasphaera* sp. B" Helby *et al.*, 1988 then Kimmeridgian of New Zealand.

Gen. et. sp. indet. D

Pl. 36, figs. D-G

Description: Intermediate-sized cysts; strongly elongate ellipsoidal ambitus with rounded apices. Endophragm and periphragm separated by very narrow, often indistinguishable pericoel. Both wall layers psilate to scabrate except where a dense foliate mass extends from

the antapex of the periphragm, possibly restricted to the antapical paraplate. Archeopyle apical, Type (tA) or Type (tA)@; principal archeopyle suture faintly zigzag; short accessory archeopyle sutures indicate six precingular paraplates; remaining paratabulation, paracingulum and parasulcus indeterminate.

Dimensions: (µm; 4 specimens measured)
Total length (with operculum): 52, 67 (2 specimens)
Total length (without operculum): 47 (58) 66 (3 specimens)
Total width: 20 (23) 29
Max. length of ornament: 4 (9) 15

Comments: While this species is distinctive and may be useful to support regional correlation the Jansz-Io preparations do not contain sufficient specimens to enable formal description.

Comparison: Gen. et. sp. indet. D appears to be identical to figured specimens of "Gen. et sp. nov. A" Helby *et al.*, 1988 (fig.10U; fig.14F; fig.18S) from New Zealand, however no description was included to enable detailed comparison. *Wallodinium krutzschii* (Alberti, 1961) Habib, 1972 is very similar, being elongate ellipsoidal, cavate and without ornamentation, but differs in having greater cavation and never possessing an antapical foliate mass.

Previously reported range: Kimmeridgian to Tithonian of New Zealand (Helby *et al.*, 1988 as "Gen. et sp. nov. A")

Gen. et. sp. indet. E

Pl. 37, figs. A-L

Description: Intermediate-sized, proximate, holocavate cysts. Ambitus subspherical with or without small apical node; frequently damaged, compressed or folded. Autophragm with very thin ectophragm apparently supported by numerous intratabular, circular pits or 'dimples' up to 3µm in diameter in the ectophragm wall; ectocoel very narrow (<2µm); ectophragm frequently slumped onto autophragm surface so dimples are scarcely visible. Gonyaulacacean paratabulation absent to strongly evident when broad, smooth to scabrate pandasutural bands are developed; formula: Xpr, 4', 6'', Xc, ?5-6''', 1p, 1'''', Xs. Paracingulum and parasulcus not subdivided and commonly evident as shallow furrows or folds. Precingular archeopyle, possibly Type ?1-3P, compound.

Dimensions: (µm; 9 specimens measured)

Autophragm length: 54 (67) 85
Autophragm width: 51 (65) 76
Ectophragm length: 61 (72) 90
Ectophragm width: 56 (69) 82

Comments: The Jansz-Io preparations do not contain sufficient well-preserved or suitably oriented specimens to enable formal description of Gen. et. sp. indet. E. The exact nature of the archeopyle remains uncertain, however is apparently compound precingular, sequentially losing between 1 and 3 (or more) precingular paraplates.

Comparison: Gen. et. sp. indet. E is most similar to Gen. et. sp. indet. F herein, which differs in having an autophragm only and broad, thickened, striate pandasutural bands. *Fusiformacysta* Morgan, 1975 is of similar size and shape and has a Type 3P precingular archeopyle, however has an autophragm only and never displays pandasutural bands.

Gen. et. sp. indet. F

Pl. 36, figs. H-K, Pl. 109, fig. B

Description: Intermediate-sized, proximate cysts. Ambitus subspherical with or without small apical node. Robust autophragm; thinner intratabularly with greatly thickened, smooth to striate pandasutural bands. Intratabular ornament of numerous, regularly spaced, circular verrucae up to 2µm diameter that appear as positive features in TLM but revealed as pits or dimples in SEM. Paracingulum evident as an equatorial furrow; internally subdivided by pandasutural bands and a penitabular row of verrucae / dimples on each paracingular paraplate; parasulcus not observed. Gonyaulacacean paratabulation, formula: Xpr, 4', 6'', ?6c, ?5-6''', 1p, 1'''', Xs. Precingular archeopyle, number of paraplates involved uncertain.

Dimensions: (µm; 1 specimen measured)
Total length: 57
Total width: 57
Max. length of ornament: <0.5
Length of apical horn: 5
Max. wall thickness: 4

Comparison: Very few specimens of Gen. et. sp. indet. F were observed in the Jansz-Io preparations. Uncertainty regarding the paratabulation and archeopyle preclude comparison with existing genera.

Gen. et. sp. indet. F is most similar to Gen. et. sp. indet. E herein, which differs in having two wall layers (autophragm and ectophragm) and variable development of pandasutural bands. *Fusiformacysta* Morgan, 1975 has a similar size, shape, precingular archeopyle and an autophragm only, however never displays pandasutural bands.

Gen. et. sp. indet. G

Pl. 36, figs. L-M

Description: Small to intermediate-sized, subspherical to ovoidal, proximate cysts. Autophragm densely covered by non-tabular, hollow, spherical to rarely cauliflorate gemmae up to 2.5µm diameter. Gonyaulacacean paratabulation only indicated by principal archeopyle suture and accessory archeopyle sutures revealing 6 precingular paraplates. Archeopyle apical, Type (tA) or Type (tA)@; paracingulum not evident; parasulcus indicated only by parasulcal notch or occasionally ventral attachment of operculum.

Dimensions: (µm; 1 specimen measured)
Autophragm length: 40
Autophragm width: 41
Max. length of ornament: 1.5

Comparison: The Jansz-Io preparations contained very few specimens of this species. Gen. et. sp. indet. G may be attributed to *Barbatacysta* Courtinat, 1989 with low to intermediate relief ornament, however no pandasutural bands have been observed. Alternatively, Gen. et. sp. indet. G may represent an extreme example of *Sepispinula* Islam, 1993 if cyst development was interrupted prior to completion of the hollow to septate processes, comparable to the observations of Kokinos & Anderson, 1995 (p.155) on the cyst and spine development of extant *Lingulodinium polyedrum* (Stein, 1883) Dodge, 1989.

Gen. et. sp. indet. H

Pl. 38, figs. A-T

Description: Very small to small, spherical, proximate cysts. Autophragm composed of very robust, dark-coloured, strongly corrugate intratabular ornament separated by deep, distinct pandasutural bands; penitabular margins typically entire but rarely fossulae breach the margin. Standard peridiniacean paratabulation fully exhibited; formula: 2-3pr, 4', 3a, 7'', 5c, 5''', 2'''', 5s; ortho hexa combination. Paracingulum slightly laevorotatory, offset approximately half the

width; internally subdivided into five paraplates with a particularly large 3c paraplate. Parasulcus incorporates as, rs, ls, ps and t paraplates. Archeopyle uncertain, possibly combination Type (tA)@3I.

Dimensions: (µm; 12 specimens measured)
Total length: 21 (24) 28
Total width: 21 (24) 28

Comments: The membrane underlying the pandasutural bands is extremely thin and almost invisible under TLM (pl. 38, fig. T). Cyst structure is provided by the thick and robust corrugate intratabular ornament. Cysts are commonly broken along the parasutures or along intratabular fossulae if the penitabular margin is breached as the structurally weakest points.

Gen. et. sp. indet. H is a very rare but distinctive component of only five samples from Io-1.

Comparison: Gen. et. sp. indet. H represents one of the very few P-cysts observed in the Jansz-Io preparations. The restricted distribution and uncertainty regarding the archeopyle prevent formal description and thorough comparison with existing genera. However, no other known peridiniacean genus possesses the combination of small size, spherical shape, dark colour and complete paratabulation, including of the paracingular region.

Gen. et. sp. indet. I

Pl. 39, figs. A-B

Description: Small to intermediate-sized, proximate cysts. Ambitus elongate ovoidal to subpolygonal, broadest at paracingulum. Non-tabular, randomly foveolate ornament; lumina subcircular to ovoidal of variable size. Paracingulum and parasulcus may be slightly indented, paler, and highlighted by large, aligned lumina. Archeopyle apical, Type (tA), principal archeopyle suture zigzag with a prominent parasulcal notch; short accessory archeopyle sutures reveal six precingular paraplates.

Dimensions: (µm; 12 specimens measured)
Autophragm length (without operculum): 39 (48) 55
Autophragm width: 29 (36) 42
Max. diameter of lumina: 2 (4) 9

Comparison: The irregular, foveolate ornament of Gen. et. sp. indet. I is distinctive in the Jansz-Io preparations and recognisable as fragments. This species is most similar to *Ellipsoidictyum* Klement, 1960 but differs in having foveolate ornament rather than a reticulum formed by septa. This species differs to *Egmontodinium* Gitmez & Sarjeant, 1972 in the absence of parasutural to penitabular septa or processes.

Gen. et. sp. indet. J

Pl. 39, figs. C-E

Description: Intermediate to large, proximate cysts. Ambitus subcircular to ovoidal with or without small apical ectohorn; possibly lenticular. Smooth, thin autophragm overlain by a finely spongeous ectophragm up to 3µm thick. Paracingulum rarely observed as an equatorial fold; other paratabulation and parasulcus not evident. Archeopyle uncertain, possibly Type P.

Dimensions: (µm; 2 specimens measured)
Autophragm length: 59, 77
Autophragm width: 59, 81
Ectophragm length: 63, 83
Ectophragm width: 61, 87

Comparison: Very few specimens of Gen. et. sp. indet. J were observed in the Jansz-Io preparations and uncertainty regarding the archeopyle precludes association with currently described genera. This species is most similar to *Apteodinium* Eisenack, 1958, which differs in having a definite Type P archeopyle, prominent apical horn and more robust subspherical to rhomboidal shape.

Genus ***Glossodinium*** Ioannides *et al.*, 1977, emend. Courtinat *in* Courtinat & Gaillard, 1980

Type species: *Glossodinium dimorphum* Ioannides *et al.*, 1977.

Glossodinium dimorphum Ioannides *et al.*, 1977

Pl. 39, figs. F-G

1977 *Glossodinium dimorphum* Ioannides *et al.*, p.453, pl.2, figs.13-14; text-fig.8.

1978 *Dinopterygium dimorphum* (Ioannides *et al.*, 1977) Drugg, p.67, pl.2, fig.11, pl.3, figs.1-4.

1980 *Glossodinium dimorphum* Ioannides *et al.*, 1977; Courtinat *in* Courtinat & Gaillard, p.453, pl.2, figs.13-14; text-fig.8.

Dimensions: (μm; 1 specimen measured)
Periphragm length: 110
Periphragm width: 102
Endophragm length: 76
Endophragm width: 87

Previously reported range: Cosmopolitan: Basal Callovian to Lower Oxfordian of Australia (Helby *et al.*, 1987; Mantle, 2009b; Riding *et al.*, 2010);
Mid-Oxfordian of Papua New Guinea (Davey, 1987, 1999);
Tithonian of New Zealand, (Helby *et al.*, 1988);
Oxfordian to Tithonian of Europe (Ioannides *et al.*, 1977; Raynaud, 1978; Brenner, 1988; Thomas & Cox, 1988; Kunz 1990; Stancliffe, 1991; Poulsen, 1993, 1996; Fauconnier *et al.*, 1996; Huault, 1999; Riding *et al.*, 1999, 2010; Poulsen & Riding, 2003; Riding, 2005b);
Oxfordian to Kimmeridgian of North America (Zotto *et al.*, 1987; Olmstead *et al.*, 1996);
Upper Oxfordian to Tithonian of Africa (Jiang *et al.*, 1992; Ibrahim *et al.*, 2002).

Genus ***Gonyaulacysta*** Deflandre, 1964, emend. Sarjeant, 1969, Stover & Evitt, 1978, Sarjeant, 1982, and Helenes & Lucas-Clark, 1997

Type species: Deflandre, 1939, as *Gonyaulax jurassica.*

Gonyaulacysta centriconnata Riding, 1983

Pl. 40, figs. A-D

1983 *Gonyaulacysta centriconnata* Riding, p.197-200,202, pl.1, pl.2, figs.1-8; text-figs.2-3.

Dimensions: (μm; 11 specimens measured)
Periphragm length: 62 (76) 88
Periphragm width: 63 (72) 82
Endophragm length: 53 (65) 76
Endophragm width: 57 (64) 74
Epipericoel length: 5 (8) 13

Comments: Beautifully preserved specimens of *Gonyaulacysta centriconnata* observed in the Jansz-Io preparations reveal a complete gonyaulacacean paratabulation, with the formula 4', 2a, 6'', 6c, 6''', 1p, 1'''', 5s. The 1''' paraplate is incorporated into the parasulcus and the small 1a and larger 2a paraplates are located above the anterior archeopyle margin between the 2', 3', 3'' and 4'' paraplates. Contrary to the original description, intratabular contact areas indicating suturocavation were observed in the paracingular series, but the absence of contact areas within the parasulcus is confirmed. The apical perihorn frequently possesses a short (2.5µm), solid, capitate extension. Jansz-Io specimens conform to the original description in all other characteristics.

Previously reported range: Inconsistently in Basal to Mid-Oxfordian of Australia (Riding *et al.*, 2010);
Upper Callovian to Mid-Oxfordian of Europe (Riding, 1983, 2005b; Kunz 1990; Fauconnier, 1995; Huault, 1999; Riding *et al.*, 1999, 2010; Poulsen & Riding, 2003)

Gonyaulacysta dualis (Brideaux & Fisher, 1976) Stover & Evitt, 1978

Pl. 40, figs. E-G

1976 *Psaligonyaulax dualis* Brideaux & Fisher, p.18-20, pl.1, figs.4-6, 8-12; pl.2, figs.1-2.
1978 *Gonyaulacysta dualis* (Brideaux & Fisher, 1976) Stover & Evitt, p.158.

Dimensions: (µm; 12 specimens measured)
Periphragm length: 65 (80) 93
Periphragm width: 39 (48) 54
Endophragm length: 49 (60) 75
Endophragm width: 36 (43) 52
Epipericoel length: 9 (16) 18

Comments and Comparison: Intraspecific variability is observed in the development of parasutural septa and the relative length of the hypocyst. Rare specimens with minimal development of parasutural septa and a short hypocyst may resemble *Gonyaulacysta ceratophora* (Cookson & Eisenack, 1960) Riding, 2005.

Previously reported range: Lower Oxfordian to Lower Kimmeridgian of North America (Brideaux & Fisher, 1976);
Mid-Oxfordian to Kimmeridgian of Europe (Poulsen 1996; Riding *et al.*, 1999);
Oxfordian of Africa (Schrank, 2005)

Gonyaulacysta eisenackii (Deflandre, 1939) Górka, 1965, emend. Sarjeant, 1982

Pl. 41, figs. G-I

1939 *Gonyaulax eisenackii* Deflandre, p.171, pl.6, figs.7-10; text-figs.3-4.

1965 *Gonyaulacysta eisenackii* (Deflandre, 1939) Górka, p.299-300, pl.I, figs.5a-c.

1970 *Endoscrinium eisenackii* (Deflandre, 1939) Gocht, p.146-147.

1978 *Tubotuberella eisenackii* (Deflandre, 1939) Stover & Evitt, p.197.

1982 *Gonyaulacysta eisenackii* (Deflandre, 1939) Dodekova, 1967, emend Sarjeant, p.32-34. (Note: Sarjeant, 1982 mistakenly records Górka, 1965 as placing this species in *Gonyaulax*, therefore credits Dodekova, 1967 with transferring this species to *Gonyaulacysta*.)

1989 *Gonyaulacysta eisenackii* (Deflandre, 1939) Górka, 1965, Lentin & Williams, p.152.

Refer to Sarjeant, 1982 for additional synonymy.

Dimensions: (µm; 3 specimens measured)

Periphragm length: 73 (77) 85

Periphragm width: 47 (58) 74

Endophragm length: 52 (52) 52

Endophragm width: 40 (48) 61

Epipericoel length: 3 (7) 13

Comments and Comparison: Very few specimens of *Gonyaulacysta eisenackii s.s.* were observed in the Jansz-Io preparations. Only specimens possessing an S-type parasulcus and low to moderately high denticulate to echinate parasutural crests were recorded as *G. eisenackii s.s.*. Very similar but more prevalent specimens differing only in possessing a more robust endophragm and greatly reduced denticulate parasutural septa were herein recorded as *Gonyaulacysta* sp. cf. *G. eisenackii.*

Previously reported range: Cosmopolitan: Mid-Callovian to Mid-Oxfordian of Australia (Cookson & Eisenack, 1958; Riding *et al.*, 2010);

Lower Oxfordian of Papua New Guinea (Davey, 1987);

Kimmeridgian of New Zealand, (Helby *et al.*, 1988);

Bathonian to Lower Kimmeridgian of Europe (Deflandre, 1939; Sarjeant, 1962a & b, 1968, 1972, 1979; Górka, 1965; Dodekova, 1967; Gocht, 1970; Beju, 1971; Erkmen & Sarjeant, 1980; Woollam, 1980; Smelror, 1988a & b; Prauss, 1989; Kunz 1990; Fauconnier, 1995; Fauconnier *et al.*, 1996; Poulsen 1996; Huault, 1999; Riding *et al.*, 1999, 2010; Poulsen & Riding, 2003; Riding, 2005b);

Mid-Bathonian to Upper Callovian of northern Canada (Johnson & Hills, 1973)

Gonyaulacysta sp. cf. ***G. eisenackii*** (Deflandre, 1939) Górka, 1965, emend. Sarjeant, 1982

Pl. 41, figs. A-F

Refer to *Gonyaulacysta eisenackii* above for synonymy.

Dimensions: (µm; 12 specimens measured)
Periphragm length: 65 (71) 83
Periphragm width: 50 (56) 67
Endophragm length: 49 (54) 64
Endophragm width: 44 (49) 57
Epipericoel length: 4 (6) 8

Comparison: Specimens herein recorded as *Gonyaulacysta* sp. cf. *G. eisenackii* are very similar to *Gonyaulacysta eisenackii s.s.*, but differ in possessing a more robust endophragm and greatly reduced denticulate to echinate parasutural septa which are commonly more distinct at the antapex. This morphology is similar to *Tubotuberella dangeardii* (Sarjeant, 1968) Stover & Evitt, 1978 but differs in having an ovoidal subpolygonal ambitus rather than an angular subpolygonal ambitus and an S-type parasulcus rather than an L-type parasulcus.

Gonyaulacysta jurassica (Deflandre, 1939) Norris & Sarjeant, 1965, emend. Sarjeant, 1982

Pl. 42, figs. A-F, Pl. 109, fig. F

1939 *Gonyaulax jurassica* Deflandre, p.168, pl.6, figs.2-5; text-figs.1-2.
1965 *Gonyaulacysta jurassica* (Deflandre, 1939) Norris & Sarjeant, p.65.
1982 *Gonyaulacysta jurassica* (Deflandre, 1939) Norris & Sarjeant, 1965, emend. Sarjeant, 1982, p.28-30.

Refer to Sarjeant, 1982 for additional synonymy.

Dimensions: (µm; 26 specimens measured)
Periphragm length: 81 (98) 114
Periphragm width: 54 (68) 84
Endophragm length: 54 (65) 79
Endophragm width: 45 (54) 68
Epipericoel length: 16 (21) 29

Comments: A great degree of intraspecific variability is present in the Jansz-Io *Gonyaulacysta jurassica* population. Variability principally involves cyst size, cavation, and septal height, perforation and distal ornament. Distal septal ornament ranged significantly, from slightly serrate, to simply echinate, to ornately phractate and broadly erymnate, with all intermediates. Some specimens otherwise identical to typical *G. jurassica* clearly exhibit suturocavation in addition to the epi- and hypopericoels. These variations are included within *G. jurassica* for the purposes of this study.

Previously reported range: Cosmopolitan: Mid-Bathonian to Tithonian of Australia and Papua New Guinea (Cookson & Eisenack, 1958; Wiseman, 1980; Davey, 1987, 1999; Mantle, 2009b; Riding *et al.*, 2010);
Oxfordian to Tithonian of New Zealand (Wilson & Helby, 1987; Helby *et al.*, 1988);
Bajocian to Tithonian of Europe (Deflandre, 1939; Sarjeant, 1960b, 1962a & b, 1968, 1972, 1979; Dodekova, 1967; Raynaud, 1978; Erkmen & Sarjeant, 1980; Woollam, 1980; Nøhr-Hansen, 1986; Brenner, 1988; Porter, 1988; Riding & Thomas, 1988; Smelror, 1988a & b; Thomas & Cox, 1988; Prauss, 1989; Kunz 1990; Stancliffe, 1991; Poulsen, 1993, 1996; Fauconnier *et al.*, 1996; Huault, 1999; Riding *et al.*, 1999, 2010; Borges *et al.*, 2011);
Bathonian to Tithonian of The Middle East (Conway, 1978; Ashraf, 1979; Wheeler & Sarjeant, 1990; Gitmez & Ertug, 1999);
Kimmeridgian to Tithonian of India (Jain *et al.*, 1984; Kumar, 1986);
Oxfordian to Tithonian of Africa (Jiang *et al.*, 1992; El Beialy & Ibrahim, 1997; Ibrahim *et al.*, 2002);
Callovian to Upper Kimmeridgian of North America (Pocock, 1972; Johnson & Hills, 1973; Williams, 1975; Brideaux & Fisher, 1976; Zotto *et al.*, 1987; Olmstead *et al.*, 1996).

Gonyaulacysta macracantha sp. nov.

Pl. 42, figs. G-I, Pl. 43, figs. A-G

Holotype and type locality: Pl. 43, fig. A-D, Jansz-3, core, 2855.54mRT(c), GA sample no. 1440695, slide no. 4, England Finder co-ordinates: M22, CPC no. 40795.

Derivation of name: From *macr-* (Greek): "long, great, large" and *–acanth* (Greek): "spine, thorn" for the long spines surmounting the parasutural septa.

Synopsis: Intermediate-sized, proximate, slightly lenticular cysts. Endophragm subcircular to ovoidal; periphragm ovoidal to subpentagonal with a broad, tapering, rounded or blunt apical perihorn; adjacent short, angular, gonal extensions common. Epicavate with broad, low

epipericoel; slightly suturocavate elsewhere. Standard gonyaulacacean paratabulation, formula: Xpr, 4', 6'', 6c, 6''', 1p, 1'''', 5s indicated on the periphragm by low parasutural septa surmounted by long (<5µm) echinate spines. Archeopyle precingular, Type P.

Diagnosis:

Shape: Slightly lenticular through dorso-ventral compression. Endophragmal ambitus subcircular to ovoidal; periphragmal ambitus ovoidal to subpentagonal with a broad, tapering, rounded or blunt apical perihorn; short, angular, gonal extensions common between the apical and precingular series.

Wall Relationships: Endophragm and thinner periphragm; epicavate with a low, broad epipericoel; elsewhere slightly suturocavate, shown by faint penitabular contact areas, except within the parasulcus.

Wall Features: Endophragm and periphragm smooth to scabrate; periphragm only possesses low (up to 3µm), unperforated parasutural septa surmounted by long (up to 5µm), simple, echinate spines, typically longest at gonal points.

Archeopyle: Slightly reduced precingular, Type P, formed by the loss of paraplate 3''.

Paratabulation: Standard gonyaulacacean paratabulation fully expressed by parasutural septa on the periphragm; formula: Xpr, 4', 6'', 6c, 6''', 1p, 1'''', 5s. The 1''' paraplate is incorporated into the parasulcus. No anterior intercalary paraplates were observed.

Paracingulum: Clearly indicated by parallel parasutural septa; internally subdivided into six paracingular paraplates; slightly laevorotatory, offset by approximately its width.

Parasulcus: Longitudinal L-type; median position. Typically indicated by a shallow furrow surrounded by parasutural septa. Rarely fully but faintly internally subdivided by low parasutural ridges. A faint, central, flagellar scar is common.

Size: Intermediate.

Dimensions: (µm; 12 specimens measured)

Periphragm length: 69 (79) 90

Periphragm width: 63 (70) 87

Endophragm length: 62 (69) 78

Endophragm width: 55 (64) 80

Epipericoel length: 7 (9) 12
Max. length of parasutural spines: 1 (3) 5

Comparison: *Gonyaulacysta macracantha* is similar to two other *Gonyaulacysta* species, being *G. centriconnata* Riding, 1983 and *G. pectinigera* (Gocht, 1970) Fensome, 1979. *G. centriconnata* differs in having more distinct suturocavation, intratabular grana to tuberculae, and only slightly denticulate parasutural crests. *G. pectinigera* is also slightly suturocavate, but differs in being cornucavate with a narrow apical perihorn, having a foveolate periphragm and parasutural crests surmounted by spines that may be distally bifurcate.

Genus ***Herendeenia*** Wiggins, 1969

Type species: Cookson & Eisenack, 1958, as *Omatia pisciformis.*

Herendeenia sp. aff. ***H. alaskaensis*** (Stover & Evitt, 1978) Stover & Helby, 1987b

Pl. 44, figs. A-C

aff. 1969 *Herendeenia pisciformis* Wiggins, pl.1, figs.1-3.
aff. 1978 *Omatia alaskaensis* Stover & Evitt, p.178.
aff. 1987b *Herendeenia alaskaensis* (Stover & Evitt, 1978) Stover & Helby, p.155-156.

Dimensions: (µm; 3 specimens measured)
Periphragm length: 68 (78) 90
Periphragm width: 45 (50) 54
Endophragm length: 64 (71) 79
Endophragm width: 41 (46) 51
Length of apical horn: 9 (10) 11

Comparison: Observed *Herendeenia* sp. aff. *H. alaskaensis* specimens are most similar to *Herendeenia alaskaensis s.s.* but morphologically differ in being significantly shorter (restricted to the intermediate rather than large size range) with a lower length to width ratio, having a clearly defined paracingulum, microgranulate to spongeous ornament (rather than densely granulate ornament), and a slight endohorn protruding into the perihorn. These differences may be sufficient to speciate between the morphological forms, however the limited number of specimens prevents formal differentiation.

Previously reported range: *Herendeenia alaskaensis s.s.* is recorded from the Tithonian of Australia and Papua New Guinea (Cookson & Eisenack, 1958; Stover & Helby, 1987b) and Upper Hauterivian to Barremian of Alaska (Wiggins, 1969 as *Herendeenia pisciformis*).

Herendeenia sp. aff. ***H. pisciformis*** (Cookson & Eisenack, 1958) Wiggins, 1969, emend. Stover & Helby, 1987b

Pl. 44, figs. D-F

aff. 1958 *Omatia pisciformis* Cookson & Eisenack, p.61, pl.8, fig.6.

aff. 1969 *Herendeenia pisciformis* (Cookson & Eisenack, 1958) Wiggins, p.146 (*non* pl.1, figs.1-7, text-figs.3a, b).

aff. 1987b *Herendeenia pisciformis* (Cookson & Eisenack, 1958) Wiggins, 1969, emend. Stover & Helby, p.154, as a revised description.

Dimensions: (µm; 7 specimens measured)
Periphragm length: 88 (123) 164
Periphragm width: 42 (51) 58
Endophragm length: 83 (107) 144
Endophragm width: 40 (47) 56
Length of apical horn: 6 (12) 16

Comparison: *Herendeenia* sp. aff. *H. pisciformis* is most similar to *Herendeenia pisciformis s.s.* but morphologically differs in extending into the intermediate size range, possessing a spongeous, microreticulate to coarsely reticulate periphragm, a short, rounded endohorn protruding into the perihorn, and significantly increased paratabulation shown by periphragmal parasutural folds that lengthen towards the apices. Coarsely reticulate morphotypes may falsely appear to have processes supporting periphragmal parasutural folds. These differences may be sufficient to speciate between the morphological forms, however the limited number of specimens prevents formal differentiation.

Previously reported range: *Herendeenia pisciformis s.s.* is recorded from the Tithonian of Australia, New Zealand and Papua New Guinea (Cookson & Eisenack, 1958; Stover & Helby, 1987b; Helby *et al.*, 1988).

Genus ***Horologinella*** Cookson & Eisenack, 1962a, emend. Stover & Evitt, 1978 and Backhouse, 1988

Type species: *Horologinella lineata* Cookson & Eisenack, 1962a

Horologinella? **sp. A**

Pl. 45, figs. A-H, Pl. 109, fig. C

Description: Very small to small, proximate, strongly lenticular cysts. Ambitus subcircular to rounded-subpolygonal when prominent lateral postcingular and antapical lobes are developed; epicyst approximately half to one-third the length of hypocyst; subtle to prominent paracingular constriction. Autophragm only or endophragm and closely appressed, extremely thin and easily damaged periphragm. Cyst wall very dark-brown-coloured; commonly increasing in intensity on the ventral surface surrounding a slightly paler flagellar scar; smooth to scabrate ornament. Paratabulation rarely evident as faint, low and smooth parasutural ridges; typically best developed hypocystally showing 6’’’, 1p, 1’’’’; remaining paratabulation formula indeterminate. Archeopyle apical, possibly Type tA.

Dimensions: (µm; 13 specimens measured)
Total length: 18 (22) 27
Total width: 18 (22) 30
Width at paracingulum: 13 (15) 18

Comments: *Horologinella?* sp. A exhibits considerable intraspecific variability of ambital shape, ranging from subcircular morphotypes with only slight paracingular indentation to lobate morphotypes with prominent paracingular indentation and variable development of lateral mid-hypocystal lobes and a single antapical lobe usually offset to the right lateral side. Very rare specimens may show an extremely thin, psilate periphragm spanning the paracingulum (pl. 45, fig. C). The archeopyle is clearly apical, however the exact number of paraplates involved and the simple or compound nature are uncertain.

Comparison: Uncertainty regarding the archeopyle and paratabulation make generic association difficult. Jansz-Io specimens are currently questionably placed in *Horologinella* due to the typically deeply incised paracingulum and faint paratabulation indicated by smooth, low ridges. However current *Horologinella* species typically possess a partiform paratabulation pattern, a subcircular, enlarged Type $A_{4'}$ archeopyle and are pale in colour. Alternatively, the dark colour and hypocystal paratabulation may suggest a relationship to *Fostericysta eclipsiana* (Riding & Helby, 2001e) Riding, 2005c and *Jansonia scarffei* Tykoezinski *et al.*, 2000 which

are also lobate, have an apical archeopyle and sexiform hypocystal configuration, however they possess denticulate parasutural crests.

Genus ***Hystrichodinium*** Deflandre, 1935, emend. Sarjeant, 1966a and Clarke & Verdier, 1967

Type species: *Hystrichodinium pulchrum* Deflandre, 1935

***Hystrichodinium?* sp. A**

Pl. 45, figs. I-K

Description: Intermediate-sized, proximate to proximochorate cysts. Ambitus subcircular to elongate ellipsoidal with numerous (>100) tapering processes with furcate to rarely ramifying distal tips and sharply to largely curved proximal contacts. Processes hollow and open to the autocoel; approximately the same length on individual specimens; possibly located parasuturally. Autophragm very thin, pale and easily folded or damaged. Vague indications suggest precingular archeopyle, Type P. Paracingulum, parasulcus and paratabulation indeterminate.

Dimensions: (µm; 12 specimens measured)
Autophragm length (without processes): 43 (58) 71
Autophragm width (without processes): 22 (40) 62
Max. length of processes: 5 (7) 10
Max. width of processes: 2 (3) 4

Comments: *Hystrichodinium?* sp. A displays a highly variable ambitus, ranging from subcircular to elongate ellipsoidal. The thin autophragm is so pale that specimens are easily overlooked. Specimens are frequently folded or damaged, although spinose fragments are easily identifiable. No conclusive archeopyle has been observed, however specimens frequently display a paler area in the precingular region, suggesting a Type P precingular archeopyle. No specimens have been observed that would suggest an apical archeopyle.

Comparison: Observed specimens are questionably placed within *Hystrichodinium* based upon the presence of numerous hollow processes that are in direct communication with the autocoel and a probable precingular archeopyle. Elongate ellipsoidal morphotypes have a similar appearance to *Egmontodinium torynum* (Cookson & Eisenack, 1960b) Davey, 1979c and *Productodinium chenii* Davey, 1987. However, *E. torynum* and *P. chenii* possess solid,

membranous processes surmounting a continuous, robust autophragm and a confirmed apical archeopyle.

Hystrichodinium sp. B

Pl. 45, fig. L

Description: Intermediate-sized, proximochorate to chorate cysts. Autophragm thin and easily compressed and folded. Ambitus subcircular covered with numerous (<100) hollow, subconical to tapering processes with acuminate to rounded distal tips; processes roughly the same length and width on individual specimens and may be parasuturally aligned. Paracingulum rarely faintly expressed by apparently aligned processes. Vague indications suggest precingular archeopyle, Type P. Parasulcus and paratabulation indeterminate.

Dimensions: (µm; 12 specimens measured)
Autophragm length (without processes): 36 (51) 67
Autophragm width (without processes): 33 (42) 50
Max. length of processes: 10 (17) 26
Max. width of processes: 1 (3) 4

Comparison: *Hystrichodinium* sp. B is most similar to *Hystrichodinium pulchrum* Deflandre, 1935 in possessing long, hollow processes with simple distal tips, however *H. pulchrum* differs in having coarsely foveolate to pseudoreticulate intratabular ornament.

Genus ***Hystrichosphaeridium*** Deflandre, 1937, emend. Davey & Williams, 1966

Type species: Ehrenberg, 1838, as *Xanthidium tubiferum*.

Hystrichosphaeridium? sp. aff. ***H. petilum*** Gitmez, 1970

Pl. 45, fig. M

aff. 1970 *Hystrichosphaeridium petilum* Gitmez, p.289-290, pl.9, figs.1,6; text-fig.24.

Dimensions: (µm; 11 specimens measured)
Central body length (without operculum): 31 (39) 46
Central body width: 28 (37) 48

Max. length of processes: 20 (25) 29

Comparison: *Hystrichosphaeridium?* sp. aff. *H. petilum* is most similar to *Hystrichosphaeridium petilum s.s.* but morphologically differs in having a slightly larger size range, possessing solid processes that are rarely distally interconnected by thin trabeculae, and the presence of paracingular and parasulcal processes is uncertain.

Previously reported range: *H. petilum s.s.* has been reported from the Oxfordian to Berriasian of Papua New Guinea (Davey, 1987);
Oxfordian to Tithonian of New Zealand, (Helby *et al.*, 1988);
Oxfordian to Tithonian of Europe (Gitmez, 1970; Sarjeant, 1979; Thomas & Cox, 1988; Fauconnier *et al.*, 1996);
Kimmeridgian to Tithonian of The Middle East (Gitmez & Ertug, 1999).

Backhouse, 1988 has recorded a similar species with hollow processes as *Areosphaeridium?* sp. A from Valanginian to Hauterivian of the Perth Basin.

Genus ***Impletosphaeridium*** Morgenroth, 1966, emend. Islam, 1993

Type species: *Impletosphaeridium transfodum* Morgenroth, 1966.

Impletosphaeridium lumectum (Sarjeant, 1960a) Islam, 1993

Pl. 45, figs. N-O

1960 *Baltisphaeridium lumectum* Sarjeant, p.139-140, pl.6, fig.1, Text-fig.2.
1969 *Cleistosphaeridium lumectum* (Sarjeant, 1960) Davey *et al.*, p.16.
1978 *Cleistosphaeridium? lumectum* (Sarjeant, 1960) Stover & Evitt, p.32.
1993 *Impletosphaeridium lumectum* (Sarjeant, 1960) Islam, p.86.

Dimensions: (µm; 12 specimens measured)
Autophragm length: 43 (50) 59
Autophragm width: 32 (44) 57
Max. length of processes: 7 (11) 22

Previously reported range: Callovian of the Timor Sea (Mantle 2009b);

Oxfordian to Berriasian of Europe (Sarjeant, 1960a, 1962b, 1976b, 1979; Brenner, 1988; Courtinat, 1989; Dodekova, 1992; Poulsen, 1996);
Lower Cretaceous of The Middle East (Ashraf, 1979);
Callovian of South America (Quattrocchio & Sarjeant 1992)

Genus ***Kallosphaeridium*** de Coninck, 1969, emend. Jan du Chêne *et al.*, 1984

Type species: *Kallosphaeridium brevibarbatum* de Coninck, 1969.

Kallosphaeridium hypornatum Prauss, 1989

Pl. 46, figs. A-F

1989 *Kallosphaeridium hypornatum* Prauss, p.40-41, pl.6, figs.1-4; text-fig.16.

Dimensions: (µm; 12 specimens measured)
Autophragm length: 36 (56) 90
Autophragm width: 39 (51) 75
Max. length of ornament: 1 (2) 3

Comparison: *Kallosphaeridium hypornatum* is similar to *Atopodinium haromense*, however *A. haromense* has a rounded subpolygonal ambitus and has tabulation incompletely defined by rows of grana or gemmae and folds.

Previously reported range: Bajocian of Germany (Prauss, 1989)

Kallosphaeridium interstinctum sp. nov.

Pl. 46, figs. G-L

Holotype and type locality: Pl. 46, fig. G-I, L, Jansz-3, Core, 2853mRT(c), GA sample no. 1631267, slide no. 5, England Finder co-ordinates: R45/4, CPC no. 40811.

Derivation of name: From *interstinctus* (Latin): "spotted, speckled" for the evenly granulate to verrucate ornament.

Synopsis: Small to intermediate-sized, proximate cysts. Autophragm subspherical to ovoidal with evenly distributed, non-tabular granulate to verrucate ornament of little to no vertical relief; thin wall easily folded or damaged. Archeopyle apical, Type (4AI)@ or Type (5A)@; OW/CD ratio typically 0.35-0.45.

Diagnosis:

Shape: Subspherical to ovoidal ambitus. Thin membrane frequently folded or damaged.

Wall Relationships: Autophragm only.

Wall Features: Non-tabular ornament of evenly distributed, isolated grana to verrucae, 0.5-1.5µm diameter, typically with no measureable height but rarely ranging up to 0.5µm.

Archeopyle: Archeopyle apical, Type (4AI)@ or Type (5A)@, rarely detached probably due to mechanical damage. When measureable, OW/CD (operculum width to cyst diameter) ratio is typically between 0.35-0.45. Deep accessory archeopyle sutures may be present in the precingular paraplate series.

Paratabulation: Principal archeopyle suture and occasional deep accessory archeopyle sutures indicate gonyaulacacean paratabulation; epicystal formula: Xpr, 4', 1a, 6'' or Xpr, 5', 6''; remaining paratabulation indeterminate.

Paracingulum: Not indicated.

Parasulcus: Indicated only by ventral attachment of the apical operculum.

Size: Small to intermediate.

Dimensions: (µm; 12 specimens measured)
Autophragm length: 46 (53) 59
Autophragm length (without operculum): 32 (41) 52
Autophragm width: 37 (47) 61
Max. length of ornament: 0 (0.2) 0.5
Max. diameter of ornament: 0.5 (0.7) 1.5

Comparison: Observed specimens conform to the emended generic description of Jan du Chêne *et al.*, 1984 in possessing a typically adnate apical archeopyle of Type (4AI)@ or Type (5A)@ with a low OW/CD ratio and hence are placed unquestionably within *Kallosphaeridium*.

Kallosphaeridium interstinctum differs to all other *Kallosphaeridium* species in possessing granulate to verrucate ornament of little to no relief. The granulate *Kallosphaeridium* species *K.? granulatum* (Norvick *in* Norvick & Burger, 1976) Stover & Evitt, 1978 and *K. capulatum* Stover, 1977 display more variable ornament with consistently measureable vertical relief.

Specimens with small grana to verrucae may intergrade with *Kallosphaeridium microgranulatum* sp. nov., but the latter species encompasses specimens with scabrate to microgranulate ornament and are separated herein for the stratigraphic potential of *K. interstinctum*.

Kallosphaeridium microgranulatum sp. nov.

Pl. 48, figs. A-F

Holotype and type locality: Pl. 48, fig. D-F, Jansz-1, Core, 2891mRT(c), GA sample no. 1631198, slide no. 4, England Finder co-ordinates: N20, CPC no. 40816.

Derivation of name: In reference to the microgranulate ornament.

Synopsis: Small to intermediate-sized, proximate cysts. Autophragm subspherical to ovoidal with evenly distributed, non-tabular scabrate to microgranulate ornament; thin wall easily folded or damaged. Archeopyle apical, Type (4AI)@ or Type (5A)@; OW/CD ratio typically 0.3-0.4.

Diagnosis:

Shape: Subspherical to ovoidal ambitus. Thin membrane frequently folded or damaged.

Wall Relationships: Autophragm only.

Wall Features: Non-tabular scabrate to microgranulate ornament typically less than 0.5µm in length and diameter, but very rarely possessing isolated fine, short baculae or clavae ranging up to 2µm.

Archeopyle: Archeopyle apical, Type (4AI)@ or Type (5A)@, rarely visible and often detached due to folding or mechanical damage. When visible, OW/CD (operculum width to cyst diameter) ratio is typically between 0.3-0.4. Deep accessory archeopyle sutures may be present in the precingular paraplate series.

Paratabulation: Principal archeopyle suture and occasional deep accessory archeopyle sutures indicate gonyaulacacean paratabulation; epicystal formula: Xpr, 4', 1a, 6'' or Xpr, 5', 6''; remaining paratabulation indeterminate.

Paracingulum: Not indicated.

Parasulcus: Indicated only by ventral attachment of the apical operculum.

Size: Small to intermediate.

Dimensions: (μm; 13 specimens measured)
Autophragm length: 35 (49) 61
Autophragm width: 35 (50) 65
Max. length of ornament: 0.2 (0.7) 2
Mean length of ornament: 0 (0.1) 0.5

Comparison: The extremely high abundance of *Kallosphaeridium microgranulatum* specimens in the Jansz-Io preparations has enabled the classification of this fragile and easily damaged species. Specimens with a visible operculum are very rare, but suitably oriented and preserved specimens possess a Type (4AI)@ or Type (5A)@ with a low OW/CD ratio and hence are placed unquestionably within *Kallosphaeridium*.

Kallosphaeridium microgranulatum differs to most *Kallosphaeridium* species in not being predominantly ornamented with spines, baculae, clavae or hair-like projections. *K. microgranulatum* is most similar to *K? granulatum* (Norvick *in* Norvick & Burger, 1976) Stover & Evitt, 1978, which possesses more variable ornament of grana, baculae or clavae with variable density and distribution. *K. yorubaense* Jan du Chêne & Adediran, 1985 differs in possessing short, slender, elongate projections which impart a somewhat punctoreticulate to granulate texture, a more angular archeopyle and more robust autophragm.

K. microgranulatum may intergrade with *K. interstinctum* sp. nov., but the latter species encompasses specimens with isolated grana to verrucae with little to no vertical relief and are separated herein for the stratigraphic potential of *K. interstinctum*.

Kallosphaeridium villosum sp. nov.

Pl. 47, figs. A-L

Holotype and type locality: Pl. 47, fig. D-F, I, Jansz-3, Core, 2811mRT(c), GA sample no. 1631225, slide no. 5, England Finder co-ordinates: O38/4, CPC no. 40818.

Derivation of name: From *villosus* (Latin): "shaggy, hairy" for the distinctive hairy appearance produced by the finely spinose ornament.

Synopsis: Intermediate-sized, proximate cysts. Autophragm ovoidal; easily folded. Densely ornamented with non-tabular, fine, hair-like spines typically 1-1.5µm (max. 2µm) long. Archeopyle apical, Type (4AI)@ or Type (5A)@; OW/CD ratio typically 0.35-0.4.

Diagnosis:

Shape: Ovoidal ambitus. Membrane frequently folded or damaged.

Wall Relationships: Autophragm only.

Wall Features: Dense, non-tabular ornament of very fine, hair-like, acicular spines, typically 1-1.5µm long and of equal length on individual specimens; microgranulate appearance in plan view.

Archeopyle: Archeopyle apical, Type (4AI)@ or Type (5A)@, rarely detached due to mechanical damage. When measureable, OW/CD (operculum width to cyst diameter) ratio is typically between 0.35-0.4. Deep accessory archeopyle sutures may be present in the precingular paraplate series.

Paratabulation: Principal archeopyle suture and occasional deep accessory archeopyle sutures indicate gonyaulacacean paratabulation; epicystal formula: Xpr, 4', 1a, 6'' or Xpr, 5', 6''; remaining paratabulation indeterminate.

Paracingulum: Not indicated.

Parasulcus: Indicated only by ventral attachment of the apical operculum.

Size: Intermediate.

Dimensions: (µm; 12 specimens measured)
Autophragm length: 51 (60) 65
Autophragm width: 40 (51) 58
Max. length of ornament: 0.5 (1.5) 2

Comments: The ornamentation of *Kallosphaeridium villosum* is unique in the Jansz-Io preparations and can therefore be identified as fragments. The dense covering of very short, hair-like spines produces a fuzzy ambital outline when viewed at low TLM magnifications, with the spinose nature evident above 400x magnification.

Comparison: *Kallosphaeridium villosum* is most similar to *K? romaense* (Burger, 1980a) Burger, 1980b, which has numerous short spinules <1µm high but differs in having a smaller cyst size and an apical archeopyle of uncertain operation. *K. brevibarbatum* de Coninck, 1969 also possesses dense hair-like ornament but differs in having longer spines of approximately 4µm long.

Genus ***Kalyptea*** Cookson & Eisenack, 1960b

Type species: *Kalyptea diceras* Cookson & Eisenack, 1960b.

Kalyptea diceras Cookson & Eisenack, 1960b

Pl. 48, figs. G-I

1960b *Kalyptea diceras* Cookson & Eisenack, p.256-257, pl.39, fig.1.

Dimensions: (µm; 12 specimens measured)
Autophragm length: 78 (87) 101
Autophragm width: 21 (36) 55
Length of apical horn: 12 (19) 28
Length of antapical horn: 6 (12) 20

Comments: Two *Kalyptea diceras* morphotypes occur in the Jansz-Io preparations: the predominant 'classic' variety with rounded horns and broad cyst (pl. 48, figs. H-I); and the 'pointed' variety with pointed horns and narrow cyst (pl. 48, fig. G) similar to those figured by Wiggins, 1975. The 'pointed' morphotype may be more appropriately separated from the 'classic' morphotype, however so few specimens of the 'pointed' variety were recorded that separation was not considered necessary.

Previously reported range: Bathonian to Tithonian globally (Sarjeant, 1979);
Tithonian of Australia and Papua New Guinea (Cookson & Eisenack, 1960b);
Upper Callovian to Kimmeridgian of Europe (Woollam, 1980; Smelror, 1988a; Poulsen, 1993);
Oxfordian to Tithonian of The Middle East (Wheeler & Sarjeant, 1990; Gitmez & Ertug, 1999).

Genus ***Lagenadinium*** Piel, 1985

Type species: *Lagenadinium callovianum* Piel, 1985.

Discussion: According to Courtinat, 1999 (p.177), *Lagenadinium* is the taxonomic junior synonym of *Stephanelytron* Sarjeant, 1961a, and is recorded as such in the Fensome & Williams, 2004 *Lentin & Williams Index*. However, Fauconnier & Masure, 2004 contains entries for both *Lagenadinium* (by Fauconnier) and *Stephanelytron* (by Courtinat & De Cruz), with neither generic entry citing Courtinat, 1999 and the generic emendment, new species or new combinations proposed therein. Therefore, *Lagenadinium* is interpreted as retained by implication by Fauconnier (in collaboration with Courtinat & De Cruz) *in* Fauconnier & Masure, 2004. Note that the *Stephanelytron* species *S.? brontes* Courtinat, 1999 and *S. ceto* Courtinat, 1999 are legitimately published. However, their exclusion from the list of attributed *Stephanelytron* species by Courtinat & De Cruz *in* Fauconnier & Masure, 2004 is curious, and demonstrates that a review of these species and their attribution is necessary.

Furthermore, *Lagenadinium* was later officially retained by Mantle, 2009b (p.111) on the basis of the distinctly different type species: The type species of *Stephanelytron, S. redcliffense* Sarjeant, 1961a, emend. Stover *et al.*, 1977, possesses a single antapical corona and parasuturally aligned processes that may support a thin ectophragm. Conversely, the *Lagenadinium* type species*, L. callovianum* Piel, 1985, possesses one or two coronas positioned hypoventrally (on the hypocystal ventral surface, possibly 1p +/- ?2’’’, or 1’’’ +/- 2’’’) and non-tabular processes supporting a robust ectophragm. While these type species are clearly substantially different, both genera contain attributed species that possess characteristics more suited to the alternate genus. For example, *Stephanelytron* contains species with non-tabular processes and *Lagenadinium* contains species with paratabulation. Therefore, the primary criterion for generic separation generally appears to be the presence and position of one or two coronas, with paratabulation and presence or absence of an ectophragm being of lesser importance. On this basis, species observed in the Jansz-Io preparations have been generically assigned accordingly, with species possessing one or more hypoventral coronas placed in *Lagenadinium* and those with a single antapical corona placed in *Stephanelytron,* and speciated further according to presence or absence of paratabulation and an ectophragm.

Lagenadinium callovianum Piel, 1985

Pl. 49, figs. A-P

1985 *Lagenadinium callovianum* Piel, p.108, 110, 112, pl.1, figs.1-9; pl.2, figs.1-8; pl.3, figs.1-5; text-figs.1a-d, 2a-c, 3.

1999 *Stephanelytron callovianum* (Piel 1985) Courtinat, p.177.

2004 *Lagenadinium callovianum* Piel 1985, Fauconnier *in* Fauconnier & Masure, p.369, retained by implication.

2009b *Lagenadinium callovianum* Piel 1985, Mantle, p.111.

Dimensions: (μm; 20 specimens measured)

Autophragm length (with operculum): 34 (41) 53 (11 specimens)

Autophragm length (without operculum): 29 (35) 43 (15 specimens)

Autophragm width: 21 (26) 31

Ectophragm length (with operculum): 40 (48) 62 (11 specimens)

Ectophragm length (without operculum): 34 (39) 54 (15 specimens)

Ectophragm width: 26 (33) 37

Max. width of pericoel: 3 (4) 7

Height of corona: 3 (3.5) 5 (11 specimens)

Max. diameter of corona 1: 4.5 (8) 12 (17 specimens)

Max. diameter of corona 2: 5 (6) 8 (3 specimens)

Comments: Observed specimens conform to the original description of *Lagenadinium callovianum* in size, hypoventral position of one to three coronas, and possessing an ectophragm. The ectophragm may be mechanically broken, and rarely some processes may align to indicate individual parasutures but full paratabulation is never displayed.

Previously reported range: Callovian of Europe (*e.g.* Piel 1985; Riding *et al.*, 1999)

Lagenadinium sp. A

Pl. 50, figs. A-F

Description: Small to intermediate-sized, proximate, holocavate cyst. Autophragm elongate ellipsoidal with rounded antapex and rounded to truncated-conical apex. Numerous (>300) short (typically 3.5μm long), fine (<1μm wide), capitate processes support a thin ectophragm. Processes intratabular and parasutural to penitabular, faintly indicating gonyaulacacean paratabulation, formula: Xpr, 4', 6'', Xc, 6''', 1p, 1'''', Xs. A single subcircular to ovoidal, membranous corona is located hypoventrally, probably on the 2''' paraplate. Archeopyle apical, Type (tA) to Type (tA)@; principal archeopyle suture slightly zigzag. Parasulcus indicated by parasulcal notch and possibly outlined by parasuturally aligned processes.

Dimensions: (µm; 12 specimens measured)
Autophragm length (with operculum): 40 (44) 48 (8 specimens)
Autophragm length (without operculum): 34 (40) 47 (7 specimens)
Autophragm width: 24 (27) 34
Max. width of pericoel: 2.5 (3.5) 5
Max. diameter of corona: 8 (9) 10
Height of corona: 3.5 (2 specimens)

Comments: Only a single hypoventral corona was observed on *Lagenadinium* sp. A, however additional coronas may potentially occur.

Comparison: *Lagenadinium* sp. A is similar to the generic type species *Lagenadinium callovianum* Piel, 1985, but differs in displaying near complete paratabulation. *Lagenadinium* sp. B differs in possessing processes within the corona and not displaying paratabulation, and *Lagenadinium?* sp. C differs in having one or two pseudo-coronas comprised of a ring of processes.

Lagenadinium sp. B

Pl. 49, figs. Q-T

Description: Small to intermediate-sized, proximate, holocavate cyst. Autophragm elongate ellipsoidal with rounded apices. Numerous (>300) non-tabular, short (typically 4µm long), fine (<1µm wide), capitate processes support a very thin ectophragm. A single subcircular to ovoidal, membranous corona is located hypoventrally, probably on the 2''' paraplate; internally possesses few (<10) processes. Archeopyle apical, Type (tA) to Type (tA)@; principal archeopyle suture slightly zigzag. Parasulcus, paracingulum and paratabulation indeterminate.

Dimensions: (µm; 7 specimens measured)
Autophragm length (with operculum): 41 (46) 51 (7 specimens)
Autophragm length (without operculum): 38 (41) 43 (3 specimens)
Autophragm width: 27 (31) 35
Ectophragm length: 47 (52) 60
Ectophragm width: 33 (37) 41
Max. width of pericoel: 3 (4) 6
Height of corona: 3 (4) 4.5 (3 specimens)
Max. diameter of corona: 8 (11) 13

Comparison: *Lagenadinium* sp. B differs to all other *Lagenadinium* species in possessing processes within the corona. *Lagenadinium* sp. A further differs in displaying paratabulation.

Lagenadinium? sp. C

Pl. 50, figs. G-N

Description: Small to intermediate-sized, proximate, holocavate cyst. Autophragm ovoidal with rounded apices and a short, blunt apical horn. Numerous (>200) non-tabular to rarely incompletely parasuturally aligned, short (typically 3.5µm long), fine (<1µm wide), capitate processes support a thin ectophragm. One to two pseudo-coronas comprised of a ring of processes are located hypoventrally. Archeopyle apical, Type (tA) to Type (tA)@; principal archeopyle suture slightly zigzag. Parasulcus, paracingulum and paratabulation indeterminate.

Dimensions: (µm; 12 specimens measured)
Autophragm length (with operculum): 32 (36) 39 (9 specimens)
Autophragm length (without operculum): 30 (32) 37 (6 specimens)
Autophragm width: 19 (25) 29
Ectophragm length: 36 (43) 47
Ectophragm width: 26 (31) 34
Max. width of pericoel: 3 (3.5) 5
Height of corona: 3 (3.5) 4 (8 specimens)
Max. diameter of corona: 5 (7) 8 (3 specimens)

Comparison: The arrangement of processes into a circular pseudo-corona indicates that this species may be a phylogenetic intermediate between *Lagenadinium* and *Chlamydophorella* Cookson & Eisenack, 1958. The absence of a true corona may result in this species being placed in *Chlamydophorella* Cookson & Eisenack, 1958 if the process-ring pseudo-coronas are not observed. However, the position of the pseudo-coronas shows a direct association with *Lagenadinium* and hence is questionably placed herein. This unique feature differentiates *Lagenadinium?* sp. C from all *Lagenadinium* and *Chlamydophorella* species.

Genus ***Lanterna*** Dodekova, 1969, emend. Courtinat, 1989

Type species: *Lanterna bulgarica* Dodekova, 1969.

Lanterna reticulata sp. nov.

Pl. 51, figs. A-L

Holotype and type locality: Pl. 51, fig. E–F, Jansz-3, Core, 2811mRT(c), GA sample no. 1631225, slide no. 5, England Finder co-ordinates: L34/3, CPC no. 40837.

Derivation of name: In reference to the reticulate ornament.

Synopsis: Small to intermediate-sized, spherical to subspherical, proximate cyst. Autophragm only; reticulate to rarely pseudo-reticulate intratabular ornament with entire penitabular margins separated by distinct, unornamented pandasutural bands. Standard gonyaulacacean paratabulation, formula: Xpr, 4', 1a, 6'', 6c, 6''', 1p, 1'''', Xs. Parasulcal series not fully expressed; reduced ornament may reveal faint flagellar scar. Archeopyle apical, Type (tA), rarely with short to long accessory archeopyle sutures.

Diagnosis:

Shape: Spherical to subspherical.

Wall Relationships: Autophragm only.

Wall Features: Reticulate to pseudo-reticulate intratabular ornament with small to large (0.5-4µm diameter) lumina; lumina size typically uniform on individual specimens. Very rare pseudo-reticulate ornament created when discontinuous anastomosing ridges form an incomplete reticulum. Penitabular margins typically entire, forming penitabular ridges of the same height and thickness as the reticulum. Intratabular ornament separated by distinct, smooth to scabrate pandasutural bands.

Archeopyle: Apical, Type (tA); operculum free. Principal archeopyle suture zigzag with a broad parasulcal notch; accessory archeopyle sutures rarely occur in precingular series.

Paratabulation: Standard gonyaulacacean paratabulation fully indicated by pandasutural bands and intratabular ornament; formula: Xpr, 4', 1a, 6'', 6c, 6''', 1p, 1'''', Xs. The 1''' paraplate is incorporated into the parasulcus. A small anterior intercalary paraplate is faintly to clearly evident between the 2', 3', 3'' and 4'' paraplates (pl. 51, fig. C).

Paracingulum: Strongly laevorotatory; ends offset one to two times the paracingulum width. Fully internally subdivided into six paracingular paraplates delineated by reticulate ornament and pandasutural bands.

Parasulcus: Indicated by parasulcal notch and outlined by pandasutural bands; not internally subdivided. A small, faint flagellar scar may be located within a narrow furrow with reduced ornamentation.

Size: Small to intermediate.

Dimensions: (µm; 44 specimens measured)
Autophragm length (with operculum): 50 (56) 60 (6 specimens)
Autophragm length (without operculum): 41 (50) 60
Autophragm width: 40 (48) 61
Mean diameter of lumina: 0.5 (2) 4

Comments: *Lanterna reticulata* exhibits significant intraspecific variability with respect to lumina diameter, producing very finely to very coarsely reticulate morphotypes with all intermediaries. The pseudo-reticulate morphotype is particularly rare, but included within this spectrum as an extreme end member.

Comparison: Finely reticulate morphotypes intergrade with *Barbatacysta* sp. B herein, which differs in having verrucate to vermiculate intratabular ornament separated by very narrow, faint, pandasutural bands. *Lanterna reticulata* differs to *Lanterna?* sp. A and *Lanterna?* sp. B herein in having reticulate rather than foveolate or spongeous ornament respectively.

Lanterna? sp. A

Pl. 52, figs. A-F

Description: Small to intermediate-sized, spherical to subspherical, proximate cyst. Autophragm only; thick, irregularly foveolate intratabular ornament separated by unornamented pandasutural bands. Standard gonyaulacacean paratabulation, formula: Xpr, 4', 1a, 6'', 6c, 6''', 1p, 1'''', Xs. Parasulcal series not fully expressed; reduced ornament may reveal faint flagellar scar. Archeopyle apical, Type (tA) rarely with short to long accessory archeopyle sutures.

Dimensions: (µm; 21 specimens measured)
Autophragm length (with operculum): 44 (47) 50 (3 specimens)
Autophragm length (without operculum): 40 (49) 55
Autophragm width: 40 (46) 55

Comments: *Lanterna?* sp. A exhibits densely foveolate intratabular ornament separated by distinct pandasutural bands. The ornamentation reflects the underlying paraplate shape; however an entire penitabular margin is not distinguishable.

Comparison: This species is questionably placed within *Lanterna* rather than *Barbatacysta* Courtinat, 1989 due to the similar cyst size, paratabulation and ornamentation style as *Lanterna reticulata* sp. nov.

***Lanterna?* sp. B**

Pl. 52, figs. G-I

Description: Small to intermediate-sized, spherical to subspherical, proximate cyst. Autophragm only; thick, finely spongeous intratabular ornament separated by unornamented pandasutural bands. Standard gonyaulacacean paratabulation, formula: Xpr, 4', 1a, 6'', 6c, 6''', 1p, 1'''', Xs. Parasulcal series not fully expressed; reduced ornament may reveal faint flagellar scar. Archeopyle apical, Type (tA) rarely with short to long accessory archeopyle sutures.

Dimensions: (µm; 12 specimens measured)
Autophragm length (with operculum): 52 (55) 57 (4 specimens)
Autophragm length (without operculum): 42 (50) 55
Autophragm width: 39 (47) 58

Comments: *Lanterna?* sp. B exhibits densely spongeous intratabular ornament separated by distinct pandasutural bands. The ornamentation reflects the underlying paraplate shape; however an entire penitabular margin is not distinguishable.

Comparison: This species is questionably placed within *Lanterna* rather than *Barbatacysta* Courtinat, 1989 due to the similar cyst size and paratabulation as *Lanterna reticulata* sp. nov.

Genus ***Leberidocysta*** Stover & Evitt, 1978

Type species: Cookson & Eisenack, 1962b, as *Hexagonifera chlamydata*.

Leberidocysta endogranulata sp. nov.

Pl. 53, figs. A-L, Pl. 54, figs. A-L

Holotype and type locality: Pl. 53, fig. E-H, Jansz-3, core, 2855.54mRT(c), GA sample no. 1440695, slide no. 4, England Finder co-ordinates: R26, CPC no. 40844.

Derivation of name: In reference to the granulate ornament on the endophragm.

Synopsis: Small to intermediate-sized, proximate, cavate cyst. Endophragm spherical to subspherical with densely granulate to rarely verrucate ornament; very thin, psilate periphragm with low, parallel paracingular folds, commonly folded or damaged. Archeopyle apical, Type (tA) or Type (tA)@; principal archeopyle suture zigzag. Parasulcus indicated by parasulcal notch and rarely by a shallow furrow of reduced ornament.

Diagnosis:

Shape: Relatively thick endophragm and very thin periphragm both spherical to subspherical; periphragm commonly folded or damaged.

Wall Relationships: Cavate with endophragm and periphragm separated by a narrow pericoel. Periphragm often deformed, therefore pericoel width is highly variable. Cyst possibly camocavate if walls are in contact at the parasulcus; however this is yet to be confirmed.

Wall Features: Endophragm with dense, finely to coarsely granulate to rarely verrucate ornament; periphragm psilate, with low, parallel paracingular folds when well preserved.

Archeopyle: Apical, Type (tA) or Type (tA)@; principal archeopyle suture zigzag; short accessory archeopyle sutures rare.

Paratabulation: Gonyaulacacean paratabulation typically indicated by principal archeopyle suture only; rarely by parallel low, smooth paracingular folds on the periphragm; epicystal paratabulation formula: Xpr, 4', ?1a, 6''. Paraplates 1' and 4' nearly of equal length, producing a wide parasulcal notch.

Paracingulum: Infrequently indicated by low, smooth, parallel folds on the periphragm; often not visible due to damage of the fragile periphragm.

Parasulcus: Indicated by broad parasulcal notch; often indicated by a shallow furrow of reduced ornament on the endophragm; very rarely indicated by a furrow or folds on the periphragm.

Size: Small to intermediate.

Dimensions: (µm; 12 specimens measured)
Endophragm length (with operculum): 49 (53) 56 (4 specimens)
Endophragm length (without operculum): 36 (49) 57
Endophragm width: 39 (52) 63
Periphragm length (with operculum): 52 (57) 63 (4 specimens)
Periphragm length (without operculum): 41 (54) 63
Periphragm width: 45 (56) 69

Comments: Intraspecific variability was mainly observed in the width of the pericoel, from wide to barely visible, which is further accentuated when the periphragm is folded or broken through mechanical damage.

Comparison: *Leberidocysta endogranulata* differs to all described *Leberidocysta* species in frequently possessing faint paracingular folds on the periphragm. *Leberidocysta endogranulata* is otherwise most similar to the generic type species *L. chlamydata* (Cookson & Eisenack, 1962b) Stover & Evitt, 1978, which differs in having an ellipsoidal endophragm with consistently verrucate ornament and a wider pericoel. *L? flagellichnia* Schiøler, 1993and the possibly synonymous *L? microverrucosa* Slimani, 1994 are much smaller with verrucate to microverrucate ornamentation.

Leberidocysta? strigosa Mantle, 2009b

Pl. 52, figs. J-L

2009b *Leberidocysta? strigosa* Mantle, p.109-110, pl.13, figs.11-13, text-fig.4.

Dimensions: (µm; 12 specimens measured)
Total length (with operculum): 49 (60) 65
Total length (without operculum): 50 (53) 56
Total width: 45 (53) 64
Max. width of pericoel: 0 (2) 7.5

Comments: The numerous *Leberidocysta? strigosa* specimens observed in the Jansz-Io preparations conform to the original description of Mantle, 2009b. Furthermore, well-oriented and well-preserved specimens suggest a possible Type (2A)@ archeopyle involving the 2' and 3' paraplates attached at the 1'/2' and 3'/4' parasutures (pl. 52, fig. K). Irregular tears, possibly from mechanical damage, may further extend from the principal archeopyle suture onto the ventral surface.

Previously reported range: Callovian to Mid-Oxfordian of Australia and the Timor Sea (Mantle, 2009b; Riding *et al.*, 2010).

Genus ***Leptodinium*** Klement, 1960, emend. Sarjeant, 1966a, Wall, 1967, Sarjeant, 1969, Stover & Evitt, 1978, and Sarjeant, 1982

Type species: *Leptodinium subtile,* Klement, 1960.

Leptodinium? ancoralium Mantle, 2005

Pl. 57, figs. A-C

2005 *Leptodinium? ancoralium* Mantle, 2005, p.256, 258-260, pl.3, figs.1-9; text-figs.7-8.

Dimensions: (µm; 12 specimens measured)
Cyst length (without ornament): 45 (52) 60
Cyst width (without ornament): 39 (44) 50
Max. length of septa: 1 (2.5) 3
Max. length of processes: 3 (5) 8

Comments: Mantle, 2005 noted a high degree of intraspecific variability in the original *Leptodinium? ancoralium* description. Further variability was observed in process and septal length and apical perihorn development. Jansz-Io specimens commonly possess longer processes arising from very low septa or directly from the parasutures, and the perihorn is frequently completely absent.

Previously reported range: Callovian to Mid-Oxfordian of Australia (Mantle, 2005, 2009a; Riding *et al.*, 2010)

Leptodinium subtile Klement, 1960

Pl. 55, figs. A-F

1960 *Leptodinium subtile* Klement, p.46-47, pl.6, figs.1-4; text-figs.23-24.

Dimensions: (µm; 5 specimens measured)
Periphragm length: 85 (98) 118

Periphragm width: 69 (89) 104
Endophragm length: 77 (88) 111
Endophragm width: 63 (80) 94

Comments: Klement, 1960 described *Leptodinium subtile* as acavate, however the figured holotype and paratypes (Klement, 1960, pl. 6, figs. 1-4) appear to be suturocavate. Observed Jansz-Io specimens that are identical to the suturocavate type material are herein recorded as *L. subtile.* As the generic type species, a re-examination of the *L. subtile* type material is recommended to clarify the wall relationships, and if necessary emend the generic description to permit species with two wall layers.

Previously reported range: Cosmopolitan: Upper Callovian to Tithonian of Europe (Klement, 1960; Sarjeant, 1979; Riley & Fenton, 1982; Brenner, 1988; Kunz 1990; Poulsen, 1993; Fauconnier, 1995; Fauconnier *et al.*, 1996; Riding *et al.*, 1999; Poulsen & Riding, 2003; Riding, 2005b);
Lower Oxfordian to Tithonian(?) of North America (Brideaux & Fisher, 1976; Zotto *et al.*, 1987; Olmstead *et al.*, 1996);
Kimmeridgian to Tithonian of Africa (Jiang *et al.*, 1992).

Leptodinium? sp. A

Pl. 56, figs. A-G

Description: Intermediate to large, lenticular, circum-suturocavate cysts. Endophragm smooth to scabrate; ambitus subspherical to subpolygonal. Thinner periphragm granulate to rarely verrucate; closely appressed to endophragm on dorso-ventral surfaces with suturocavation increasing circumferentially to produce a subpolygonal ambitus. A small, conical apical perihorn may represent the preapical paraplates. Standard gonyaulacacean paratabulation fully expressed on periphragm by low parasutural ridges or folds caused by suturocavation, formula: Xpr, 4', 6'', 6c, 6''', 1p, 1'''', 5s; paraplate 4' is elongate and broad; paraplate 6'' is short and polygonal. Precingular archeopyle, Type P; operculum free.

Dimensions: (µm; 11 specimens measured)
Periphragm length: 69 (83) 98
Periphragm width: 62 (78) 95
Endophragm length: 60 (72) 83
Endophragm width: 57 (69) 82

Comments: *Leptodinium*? sp. A is circum-suturocavate, meaning the endo- and periphragms are appressed dorso-ventrally and parasutural pericoels expand towards the circumference. Suturocavation may extend onto the dorso-ventral surfaces along major parasutures such as the paracingulum and 2’’’/1p. The pericoels may be inflated and broad, clearly showing the recurving periphragm at the apices and paracingulum (pl. 56, figs. E-F), or deflated and narrow forming loose parasutural folds (pl. 56, figs. B-C).

Comparison: *Leptodinium*? sp. A is very similar to *Endoscrinium peripentum* sp. nov. in size, wall thickness and paratabulation formula. However, *E. peripentum* differs in being circumcavate with minor suturocavation, having a smooth to scabrate periphragm, and a slightly different paratabulation. *E. peripentum* has a much shorter 4’ paraplate than 1’ paraplate, and consequentially has an elongate, subtriangular 6’’ paraplate with a very long 1’/6’’ parasuture and very short 4’/6’’ parasuture. Conversely, *Leptodinium*? sp. A conforms to the typical *Leptodinium* paratabulation arrangement with paraplates 1’ and 4’ of nearly equal length, resulting in a short, polygonal 6’’ paraplate with a short 1’/6’’ parasuture and relatively long 4’/6’’ parasuture.

Despite the apparent overall similarity to *E. peripentum* this species is not placed in *Endoscrinium* since this genus is restricted to circumcavate species. *Leptodinium*? sp. A possesses the typical *Leptodinium* paraplate arrangement as discussed in the emended generic descriptions of Stover & Evitt, 1978 (p.169-170) and Sarjeant, 1982 (p.37-38), but differs in being clearly cavate, therefore is questionably assigned to this genus. However, the figured holotype of the generic type species, *L. subtile* Klement, 1960 also appears to be suturocavate, *L. flammeolum* Morgan, 1980 is described as suturocavate, and *L. arcuatum* Klement, 1960 is recorded as suturocavate by Jan du Chêne, 1986a, (p.217) despite being officially described as acavate, so cavate species may ultimately be acceptable in this genus.

Leptodinium? sp. A differs from all published *Leptodinium* species in being circum-suturocavate. Furthermore, *L. subtile* differs in having smooth intratabular areas, *L. arcuatum* is smooth to finely microgranulate, and *L. flammeolum* is densely and coarsely granulate.

Genus ***Limbodinium*** Riding, 1987b

Type species: Drugg, 1978, as *Dinopterygium absidatum.*

Limbodinium absidatum (Drugg, 1978) Riding, 1987b

Pl. 57, figs. D-L

1978 *Dinopterygium absidatum* Drugg, p.66-67, pl.4, figs.7-9.

1987a *Dinopterygium? absidatum* (Drugg, 1978) Riding, p.260.

1987b *Limbodinium absidatum* (Drugg, 1978) Riding, p.60, 62.

Dimensions: (µm; 10 specimens measured)
Total length: 43 (73) 97
Total width: 57 (76) 90
Max. flange width: 10 (14) 19

Previously reported range: Callovian to Mid-Oxfordian of Australia (Riding *et al.*, 2010); Upper Callovian to Mid-Oxfordian of Europe (Drugg, 1978; Woollam, 1980; Riley & Fenton, 1982; Riding, 1987b, 2005b; Brenner, 1988; Huault, 1999; Riding *et al.*, 1999, 2010; Poulsen & Riding, 2003); Callovian of Argentina (Riding *et al.*, 2011).

Genus ***Lithodinia*** Eisenack, 1935, emend. Gocht, 1975, and Williams *et al.*, 1993

Type species: *Lithodinia jurassica* Eisenack, 1935.

Lithodinia jurassica Eisenack, 1935, emend. Eisenack & Klement, 1964, and Gocht, 1975

Pl. 58, figs. A-C

1935 *Lithodinia jurassica* Eisenack, p.175-177, pl.4, figs.5-10; text-figs.1-4.

1964 *Lithodinia jurassica* Eisenack, 1935, emend. Eisenack & Klement, p.505.

1975 *Lithodinia jurassica* Eisenack, 1935, emend. Gocht, p.355.

Dimensions: (µm; 4 specimens measured)
Autophragm length (without operculum): 40 (45) 50
Autophragm width: 43 (51) 58
Max. length of ornament: 2 (2.5) 3

Previously reported range: Oxfordian to Tithonian of New Zealand, (Helby *et al.*, 1988); Bajocian to Oxfordian of Europe (Eisenack, 1935; Gocht, 1970; Raynaud, 1978; Sarjeant, 1979; Riding *et al.*, 1985; Smelror, 1988a & b; Prauss, 1989; Kunz 1990; Poulsen, 1993; Huault, 1999);
Kimmeridgian to Tithonian of India (Jain *et al.*, 1984);

Callovian to Tithonian of The Middle East and Egypt (Gitmez & Ertug, 1999; Ibrahim *et al.*, 2002; Kholeif *et al.*, 2004).

Lithodinia protothymosa Riding & Helby, 2001d

Pl. 58, figs. D-G

2001d *Lithodinia protothymosa* Riding and Helby, p.81-83, figs.10A-L.

Dimensions: (μm; 14 specimens measured)
Autophragm length (without operculum): 59 (71) 80
Autophragm width: 50 (65) 78
Max. length of ornament: 7.5 (10) 15

Comments: Observed Jansz-Io specimens displayed the same high degree of intraspecific variability as discussed in the original description.

Lithodinia protothymosa has a consistent range of Bathonian to Callovian with inconsistent occurrences to the Lower Oxfordian in Riding *et. al.* (2010). Inconsistent occurrences may either reflect an intermittent extension of the taxon range or reworking. Evidence from other species suggest that Bathonian to Callovian sediments have been reworked into the Jansz Sandstone, therefore specimens recorded in the Jansz-Io sequence are interpreted to be reworked. Acmes of this species occur in underlying Callovian sediments and may account for the volume of specimens occurring in the Jansz-Io preparations.

Previously reported range: Bathonian to Callovian (inconsistently to Lower Oxfordian) of Australia and the Timor Sea (Riding & Helby, 2001d; Helby *et al.*, 2004; Mantle, 2009a; Riding *et al.*, 2010).

Genus ***Meiourogonyaulax*** Sarjeant, 1966a

Type species: *Meiourogonyaulax valensii* Sarjeant, 1966a (after Valensi, 1953, as *Gonyaulax* sp.)

Meiourogonyaulax baculata Mantle, 2009a

Pl. 59, figs. A-B

2009a *Meiourogonyaulax baculata* Mantle, p.59, pl.14, figs.4-6; text-fig.12C.

Dimensions: (µm; 12 specimens measured)
Autophragm length (without operculum): 43 (55) 70
Autophragm width: 51 (62) 79
Max. length of ornament: 3 (4.5) 6

Comments: *Meiourogonyaulax baculata* was recently described from Callovian sediments from the Timor Sea region. This species is a rare and sporadic component of the Jansz-Io preparations, therefore these occurrences may either reflect an intermittent extension of the taxon range or reworking. Given the evidence of Bathonian to Callovian reworking, the likelihood that these specimens are reworked is considered more probable.

Previously reported range: Bathonian to Callovian of Australia (Mantle, 2009a; Riding *et al.*, 2010)

Meiourogonyaulax penitabulata Riding & Helby, 2001d

Pl. 59, figs. C-G

2001d *Meiourogonyaulax penitabulata* Riding and Helby, p.83, 85, 87, figs.11A-M, 12A-I.

Dimensions: (µm; 5 specimens measured)
Autophragm length (without operculum): 41 (49) 70
Autophragm width: 49 (56) 78
Max. length of septa: 2 (4) 6

Comments: *Meiourogonyaulax penitabulata* has a consistent range of Basal to Uppermost Callovian with inconsistent occurrences to the Lower Oxfordian according to Riding *et. al.* (2010). Inconsistent occurrences may either reflect an intermittent extension of the taxon range or reworking. Evidence from other species suggest that Callovian sediments have been reworked into the Jansz Sandstone, therefore the rare specimens of *M. penitabulata* observed in the Jansz-Io preparations may also be reworked.

Comparison: *Meiourogonyaulax penitabulata* appears to intergrade with *Meiourogonyaulax viriosa* Riding & Helby, 2001d, therefore specimens with any penitabular septal development are included herein.

Previously reported range: Basal to Uppermost Callovian (inconsistent to Lower Oxfordian) of Australia and the Timor Sea (Riding & Helby, 2001d; Helby *et al.*, 2004; Mantle, 2009a).

Meiourogonyaulax viriosa Riding & Helby, 2001d

Pl. 60, figs. A-I

2001d *Meiourogonyaulax viriosa* Riding and Helby, p.87, 89, figs.13A-B, E-F, H-L.

non 2001d *Meiourogonyaulax viriosa* Riding and Helby, figs.13C-D, G.

Dimensions: (μm; 12 specimens measured)
Autophragm length (with operculum): 64, 67 (2 specimens)
Autophragm length (without operculum): 53 (61) 80
Autophragm width: 45 (61) 86
Max. length of septa: 2 (3.5) 5

Comments and Comparison: Three *Meiourogonyaulax viriosa* paratypes figured in Riding & Helby, 2001d (figs.13C-D, G from 1642.50m of Jabiru-2) are here transferred to *Cernicysta? janszense* sp. nov. The type material of *M. viriosa* was re-examined to confirm that these three specimens differ from the *M. viriosa* holotype in having a more elongate ovoidal ambitus, 5 postcingular paraplates, and displaying the characteristic ventral paratabulation configuration and penitabular ridge and parasutural groove morphology of *C? janszense*.

Specimens assigned to *Meiourogonyaulax viriosa* herein display variable parasutural ornament ranging from low, smooth ridges to ornately fenestrate and perforate septa. This species appears to intergrade with *Meiourogonyaulax penitabulata* Riding & Helby, 2001d, and only specimens with no penitabular septal development are included herein.

Previously reported range: Upper Bathonian to Lower Oxfordian of Australia and the Timor Sea (Riding & Helby, 2001d; Mantle, 2009a; Riding *et al.*, 2010).

Genus ***Mendicodinium*** Morgenroth, 1970, emend. Bucefalo Palliani *et al.*, 1997

Type species: *Mendicodinium reticulatum* Morgenroth, 1970.

Mendicodinium granulatum Kumar, 1986

Pl. 60, fig. J

1986 *Mendicodinium granulatum* Kumar, p.393, pl.3, fig.6; text-fig.7.

Dimensions: (μm; 14 specimens measured)
Autophragm length: 64 (74) 82
Autophragm width: 56 (72) 90
Previously reported range: Lower Kimmeridgian to Tithonian of India (Kumar, 1986)

Mendicodinium groenlandicum (Pocock & Sarjeant, 1972) Davey, 1979c

Pl. 60, figs. K-L

1972 *Thuledinium groenlandicum* Pocock & Sarjeant, p.352-354, pl.2, figs.1-9; text-fig.2.
1979c *Mendicodinium groenlandicum* (Pocock & Sarjeant, 1972) Davey, p.64.

Dimensions: (μm; 12 specimens measured)
Autophragm length: 38 (70) 86
Autophragm width: 52 (70) 89

Previously reported range: Cosmopolitan: Bajocian to Mid-Tithonian of Australia and the Timor Sea (Mantle, 2009b; Riding *et al.*, 2010);
Callovian to basal Valanginian of Papua New Guinea (Davey, 1987);
Mid-Bathonian to Kimmeridgian of Europe (Pocock & Sarjeant, 1972; Davey, 1979c; Woollam, 1980; Riley & Fenton, 1982; Smelror, 1988a & b; Prauss, 1989; Kunz 1990; Poulsen, 1993; Fauconnier, 1995; Fauconnier *et al.*, 1996; Riding *et al.*, 1999, 2010; Riding, 2005b; Borges *et al.*, 2011);
Upper Bathonian to ?Valanginian of The Middle East (Gitmez & Ertug, 1999; Kholeif *et al.*, 2004);
Bathonian to Tithonian of Africa (Jiang *et al.*, 1992; Ibrahim *et al.*, 2002);
Callovian of Argentina (Riding *et al.*, 2011).

Genus ***Microdinium*** Cookson & Eisenack, 1960a, emend. Slimani 1994

Type species: *Microdinium ornatum* Cookson & Eisenack, 1960a.

Microdinium exutum sp. nov.

Pl. 61, figs. A-P

Holotype and type locality: Pl. 61, fig. H-L, Jansz-1, Core, 2886mRT(c), GA sample no. 1631193, slide no. 4, England Finder co-ordinates: O16/4, CPC no. 40876.

Derivation of name: From *exutum* (Latin): "to lay aside, put off, put away" or "to strip, deprive of a thing" in reference to the absence of substantial parasutural ornamentation.

Synopsis: Small, proximate cysts with ovoidal to pear-shaped ambitus. Robust autophragm variably internally vacuolate. Partiform gonyaulacacean paratabulation rarely faintly indicated by very low, thin parasutural ridges. Archeopyle apical, Type (tA) or Type (tA)@.

Diagnosis:

Shape: Ambitus ovoidal to pear-shaped with a rounded epicyst tapering into the wider hypocyst.

Wall Relationships: Autophragm only; relatively thick (1-2µm).

Wall Features: Autophragm wall contains non-tabular vacuoles up to 1µm diameter, variably concentrated within the cyst wall. Externally, autophragm very rarely possesses low, thin, smooth, incomplete parasutural ridges.

Archeopyle: Apical, typically Type (tA)@ or sometimes Type (tA), possibly due to mechanical detachment; may have short (<3µm) accessory archeopyle sutures in the precingular paraplate series.

Paratabulation: Generally not indicated. Very rarely partiform gonyaulacacean paratabulation faintly and incompletely indicated by parasutural ridges; exact paratabulation formula indeterminate.

Paracingulum: Typically indicated only by the contoured transition between the epicyst and hypocyst. Rarely incompletely indicated by faint parasutural ridges.

Parasulcus: Typically not evident. Rarely indicated by small parasulcal notch or ventral attachment of apical operculum.

Size: Small.

Dimensions: (µm; 12 specimens measured)
Autophragm length (with operculum): 31 (34) 39 (6 specimens)
Autophragm length (without operculum): 30 (33) 36 (8 specimens)
Autophragm width: 24 (27) 30

Comments: Vacuoles within the autophragm appear to be a consistent morphological trait of this species. Although formation of vacuoles during preservation or sample preparation cannot be discounted, given that other species rarely show similar vacuoles, they are considered to be a primary morphological feature within this species.

The exact paratabulation formula could not be extrapolated from observed specimens. However, paratabulation traces confirm a partiform gonyaulacacean arrangement which appears to be identical to the contemporaneous *Microdinium jurassicum* Riding & Helby, 2001e.

Comparison: This species is placed in *Microdinium* due to the similarity of cyst size, shape, and apparent paratabulation to *Microdinium jurassicum*, which differs in possessing microreticulate ornament and low parasutural septa. *Microdinium? tantillum* sp. nov. differs in being smaller, spherical to ovoidal with psilate, micropunctate to microgranulate ornamentation. *Microdinium exutum* differs to all other *Microdinium* species in the absence of parasutural septa and/or intratabular ornamentation.

Microdinium jurassicum Riding & Helby, 2001e

Pl. 61, figs. Q-T, Pl. 109, fig. E

2001e *Microdinium jurassicum* Riding & Helby, p.120, 122-123, figs.6A-T.

Dimensions: (µm; 48 specimens measured)
Autophragm length (with operculum): 26 (36) 47 (36 specimens)
Autophragm length (without operculum): 23 (34) 46
Autophragm width: 22 (30) 43

Comments: Riding & Helby (2001, p.122) noted that the smallest *Microdinium jurassicum* morphotypes consistently occur in the Callovian *Rigaudella aemula* Zone (now *Ctenidodinium ancorum* to *Voodooia tabulata* Zones of Helby *et. al.,* 2004 – Riding *et. al.,* 2010) and this may be stratigraphically significant. To test the stratigraphic utility of *M. jurassicum*, Jansz-Io specimens were informally subdivided into four types according to size:

Microdinium jurassicum Type 1: 25 - < 30µm

Microdinium jurassicum Type 2: 30 - < 35µm

Microdinium jurassicum Type 3: 35 - < 40µm

Microdinium jurassicum Type 4: 40 - < 50µm

Measurements of Jansz-Io specimens confirm that *M. jurassicum* does display a correlation between size and stratigraphic interval, with the largest morphotypes being stratigraphically younger. The mean *M. jurassicum* size is smallest and the total size range is narrowest at its stratigraphic range base. Both the mean specimen size and total size range increase gradually towards the stratigraphic range top. Rare occurrences of the smallest morphotypes (<30um) have been observed in samples containing the largest morphotypes (>40um), but the largest morphotypes are restricted to the stratigraphically younger section. Therefore the largest morphotypes represent the most useful stratigraphic indicator, signifying the younger section of this species range.

Previously reported range: Mid-Callovian to Mid-Oxfordian of Australia (Riding & Helby, 2001e; Morgan *et al.*, 2002; Helby *et al.*, 2004; Mantle, 2009a; Riding *et al.*, 2010);
Oxfordian to Tithonian of New Zealand (Wilson & Helby, 1987 and Helby *et al.*, 1988 as *Microdinium* sp. A).

Microdinium? tantillum sp. nov.

Pl. 62, figs. A-X

Holotype and type locality: Pl. 62, fig. G-I, M, Jansz-3, Core, 2843mRT(c), GA sample no. 1631257, slide no. 4, England Finder co-ordinates: O45/1, CPC no. 40882.

Derivation of name: From *tantillus* (Latin): "so little, so small" for the very small cyst size.

Synopsis: Very small, proximate cysts with spherical to ovoidal ambitus. Autophragm only or endophragm and closely appressed, very thin periphragm; psilate, micropunctate to microgranulate ornament. Archeopyle apical, Type (tA) or Type (tA)@; principal archeopyle suture slightly zigzag with smooth to crenulate margin.

Diagnosis:

Shape: Spherical to ovoidal.

Wall Relationships: Autophragm only, or endophragm and closely appressed, very thin periphragm. Very rarely a possible periphragm may be visible extending across the principal archeopyle suture (pl. 62, fig. M).

Wall Features: Ornament ranges from psilate, micropunctate to microgranulate; very rarely with low, thin, smooth incomplete parasutural ridges.

Archeopyle: Apical, Type (tA)@ or Type (tA), possibly due to mechanical detachment; principal archeopyle suture slightly zigzag with smooth (pl. 62, fig. X) to crenulate (pl. 62, fig. F) margin. Polygonal archeopyle shape indicates the presence of multiple anterior intercalary paraplates.

Paratabulation: Generally not indicated. Very rarely, presumably partiform gonyaulacacean paratabulation faintly and incompletely indicated by parasutural ridges; exact paratabulation formula indeterminate. Multiple anterior intercalary paraplates suggested by polygonal archeopyle shape.

Paracingulum: Generally not visible. Rarely incompletely indicated by faint parasutural ridges.

Parasulcus: Rarely indicated by broad, shallow parasulcal notch or ventral attachment of apical operculum.

Size: Very small.

Dimensions: (μm; 71 specimens measured)
Autophragm length: 18 (23) 33
Autophragm width: 18 (22) 30

Comparison: Evidence of partiform gonyaulacacean paratabulation and multiple anterior intercalary paraplates suggests a close generic relationship with *Microdinium*; however uncertainty regarding the exact paratabulation necessitates tentative generic attribution. *Microdinium? tantillum* is most similar to *Microdinium exutum* sp. nov. which differs in having a larger size range and a vacuolate autophragm with an ovoidal to pear-shaped ambitus. This species differs to all other existing *Microdinium* species in the smaller cyst size and absence of parasutural septa or ornamentation.

Microdinium? tantillum appears very similar to "*Batiacasphaera* sp. E" Helby *et al.*, 1988 (fig.5A) from New Zealand, however the shape of the apical archeopyle is not evident and no description was included to enable detailed comparison. "*Batiacasphaera* sp. E" Helby *et al.*, 1988 is reportedly abundant in the Oxfordian of New Zealand which corresponds to observations of *Microdinium? tantillum* at Jansz-Io.

Previously reported range: If synonymous with "*Batiacasphaera* sp. E" Helby *et al.*, 1988 then Oxfordian to Kimmeridgian of New Zealand.

Genus ***Nannoceratopsis*** Deflandre, 1939, emend. Evitt, 1961, Piel & Evitt, 1980, Poulsen, 1992 and Riding & Helby, 2001a

Type species: *Nannoceratopsis pellucida* Deflandre, 1939.

Nannoceratopsis pellucida Deflandre, 1939, emend. Evitt, 1961

Pl. 63, figs. A-C

1939 *Nannoceratopsis pellucida* Deflandre, p.183, pl.8, figs.8-12.

1961 *Nannoceratopsis pellucida* Deflandre, 1939, emend. Evitt, 1961, p.312.

Dimensions: (µm; 22 specimens measured)
Autophragm length: 70 (93) 106
Autophragm width: 44 (53) 62
Length of antapical horns: 14 (34) 51

Previously reported range: Cosmopolitan: Mid-Bathonian to Berriasian of Australia and the Timor Sea (Cookson & Eisenack, 1958, 1960b; Wiseman, 1980; Morgan *et al.*, 2002; Mantle, 2009b; Riding *et al.*, 2010);
Callovian to basal Tithonian of Papua New Guinea (Davey, 1987);
Oxfordian to Tithonian of New Zealand (Wilson & Helby, 1987; Helby *et al.*, 1988);
Mid-Bajocian to Mid-Kimmeridgian of Europe (Deflandre, 1939; Sarjeant, 1960b, 1962a & b, 1968, 1972, 1979; Gocht, 1970; Raynaud, 1978; Woollam, 1980; Riley & Fenton, 1982; Riding *et al.*, 1985, 1999, 2010; Brenner, 1988; Porter, 1988; Riding & Thomas, 1988; Smelror, 1988a & b; Thomas & Cox, 1988; Prauss, 1989; Kunz 1990; Stancliffe, 1991; Fauconnier, 1995; Fauconnier *et al.*, 1996; Huault, 1999; Poulsen & Riding, 2003; Riding, 2005b);

Upper Callovian to Lower Oxfordian of The Middle East (Wheeler & Sarjeant, 1990);
Kimmeridgian to Tithonian of India (Jain *et al.*, 1984);
Mid-Bathonian to Oxfordian of northern Canada (Johnson & Hills, 1973; Brideaux & Fisher, 1976);
Callovian of Argentina (Quattrocchio & Volkheimer, 1990; Riding *et al.*, 2011).

Nannoceratopsis reticulata Mantle, 2005

Pl. 63, figs. D-I

2005 *Nannoceratopsis reticulata* Mantle, p.260, 262, pl.4, figs.1-9.

Dimensions: (μm; 12 specimens measured)
Autophragm length: 81 (92) 108
Autophragm width: 41 (58) 79
Length of antapical horns: 20 (33) 46

Previously reported range: Callovian to Mid-Oxfordian of Australia and the Timor Sea (Mantle, 2005, 2009b; Riding *et al.*, 2010).

Genus ***Oligosphaeridium*** Davey & Williams, 1966, emend. Davey, 1982

Type species: White, 1842, as *Xanthidium tubiferum* var. *complex*.

Oligosphaeridium? sp. cf. ***O. complex*** (White, 1842) Davey & Williams, 1966

Pl. 102, figs. A-B

cf. 1842 *Xanthidium tubiferum* var. *complex* White, p.39, pl.4, fig.11.
cf. *Xanthidium complex* (White, 1842) Bronn, 1848, p.1375.
cf. *Hystrichosphaeridium complex* (White, 1842) Deflandre, 1946, p.111.
cf. *Oligosphaeridium complex* (White, 1842) Davey & Williams, 1966, p.71-74.
Holotype: White, 1842, pl.4, fig.11, lost according to Davey & Williams (1966, p.74).
Neotype: Davey & Williams, 1966, pl.7, fig.1, designated by Davey & Williams (1966, p.71).

Dimensions: (µm; 12 specimens measured)
Total length: 83 (117) 139
Total width: 98 (126) 165
Central body length (with operculum): 66 (1 specimen)
Central body length (without operculum): 45 (55) 69
Central body width: 43 (56) 84
Max. length of processes: 38 (47) 57

Comments: *Oligosphaeridium?* sp. cf. *O. complex* specimens are herein identified as possessing a 'reverse' wall relationship as described for the *Contracysta* complex (refer to Chapter 5.1.5), but are otherwise similar to *Oligosphaeridium complex s.s*. Skolochorate specimens are assigned to *Oligosphaeridium?* sp. cf. *O. complex* that possess narrow, trumpate processes with proximal insiderae*, and expanded, sparsely spinose distal margins with minimal process fenestration, with or without incomplete trabeculate remnants. Distal process margins are highly variable and frequently asymmetrical, but never deeply fenestrate.

* Refer to glossary of introduced terms in Chapter 5.1.2.

Comparison: *Oligosphaeridium?* sp. cf. *O. complex* specimens intergrade with *Contracysta* complex morphotypes as differentiated in Chapter 5.1.5. Specimens assigned to *Oligosphaeridium?* sp. cf. *O. pulcherrimum* (Deflandre & Cookson, 1955) Davey & Williams, 1966 / *O. diluculum* Davey, 1982 differ in having more fenestrate processes.

Previously reported range: The oldest known occurrence of *Oligosphaeridium complex s.s.* in Australia was recorded from the Valanginian of Western Australia (Wiseman & Williams, 1974; Backhouse, 1988) and ranges to the Cenomanian (Cookson & Eisenack, 1958, 1974; Morgan, 1980; Stover & Helby, 1987c & d).
Elsewhere *O. complex* is recorded as having a cosmopolitan distribution from the Tithonian to Early Cretaceous (Sarjeant, 1979);
Berriasian to Lower Aptian of Egypt (Ibrahim & Schrank, 1996);
Hauterivian to Aptian of Papua New Guinea (Davey, 1987). Davey (1987, 1999) also sporadically records *Oligosphaeridium* cf. *complex* with 'somewhat irregular' processes from the Upper Tithonian through the Early Cretaceous, as well as *Oligosphaeridium* sp. 1, a similar species with very variable processes, from the Kimmeridgian to Berriasian. An *Oligosphaeridium* spp. acme is also recorded in the Mid-Oxfordian of Australia (Helby *et al.*, 2004), although these forms are not described.

Oligosphaeridium? sp. cf. ***O. pulcherrimum*** (Deflandre & Cookson, 1955) Davey & Williams, 1966 **/ *O. diluculum*** Davey, 1982

Pl. 102, figs. C-F, Pl. 103, figs. A-F, Pl. 111, figs. A-B

cf. 1955 *Hystrichosphaeridium pulcherrimum* Deflandre & Cookson, 1955, p.270-271, pl.1, fig.8; text-figs.21-22.

cf. 1966 *Oligosphaeridium pulcherrimum* (Deflandre & Cookson, 1955) Davey & Williams, p.75-76.

cf. 1982 *Oligosphaeridium diluculum* Davey, p.14-15, pl.2, figs.1-5.

Dimensions: (µm; 22 specimens measured)

Total length: 81 (117) 147

Total width: 97 (118) 149

Central body length: 43 (53) 68

Central body width: 41 (51) 58

Max. length of processes: 31 (47) 60

Comments: Skolochorate specimens assigned to this species are extremely variable and defy clear classification. Specimens possess strongly fenestrate and irregular processes most similar to *Oligosphaeridium pulcherrimum* and *Oligosphaeridium diluculum s.s.*, but differ in possessing more variable processes and a 'reverse' wall relationship as described for the *Contracysta* complex (refer to Chapter 5.1.5). Specimens are assigned to *Oligosphaeridium?* sp. cf. *O. pulcherrimum/diluculum* that possess narrow to broad, strongly fenestrate to faintly striate, trumpate processes with proximal insiderae* and expanded distal margins, with or without incomplete trabeculate remnants or very rare, individual interlinking trabeculae. Distal process margins are highly variable, frequently asymmetrical, and may be deeply fenestrate with fenestrae occasionally extending close to the proximal process base.

These specimens are divided into two morphotypes for quantitative analysis: *Oligosphaeridium?* sp. cf. *O. pulcherrimum/diluculum* as described above; and, *Oligosphaeridium?* sp. cf. *O. pulcherrimum/diluculum* – tethered, for rare specimens possessing 'tether' trabeculae[#] that attach a distal process tip to an endosuture*.

[#] Refer to trabeculum discussion in Chapter 5.1.5; * refer to glossary in Chapter 5.1.2.

Comparison: *Oligosphaeridium?* sp. cf. *O. pulcherrimum/diluculum* specimens intergrade with *Contracysta* complex morphotypes as differentiated in Chapter 5.1.5. Specimens assigned to *Oligosphaeridium?* sp. cf. *O. complex* differ in having narrow, less fenestrate processes.

Previously reported range: The oldest known *O. pulcherrimum* occurrence in Australia was recorded from the Berriasian of Western Australia (Wiseman & Williams, 1974) with a range through to the Cenomanian (Kemp, 1976; Morgan, 1980; Wiseman, 1980; Stover & Helby, 1987c & d; Backhouse, 1988).

Elsewhere *O. pulcherrimum* has been reported from Kimmeridgian to Tithonian globally (Sarjeant, 1979);

Kimmeridgian of Europe (Gitmez, 1970);

Oxfordian to Tithonian of The Middle East (Gitmez & Ertug, 1999);

Kimmeridgian to Tithonian of India (Jain *et al.*, 1984; Kumar, 1986).

O. diliculum is recorded from the Tithonian of New Zealand, (Helby *et al.*, 1988) and has a sporadic range from Mid-Oxfordian to Mid-Valanginian of Papua New Guinea (Davey, 1987).

Genus ***Paragonyaulacysta*** Johnson & Hills, 1973, emend. Dörhöfer & Davies, 1980, and Below, 1990

Type species: *Paragonyaulacysta calloviensis* Johnson & Hills, 1973.

Paragonyaulacysta warrenii (Albert *et al.*, 1986) comb. and emend. nov.

Pl. 64, figs. A-L, Pl. 65, figs. A-I, Pl. 109, fig. G

1986 *Lacrymodinium warrenii* Albert *et al.*, p.307-308, 310, pl.1, figs.1-12; pl.2, figs.1-13; text-fig.3.

Synopsis: Small to intermediate-sized, proximate cysts. Differentiated autophragm or closely appressed endophragm and periphragm; ambitus lacrimoidal (teardrop-shaped) with short to long apical horn. Partiform gonyaulacacean paratabulation fully expressed by simple to fibrous parasutural septa. Intratabular areas smooth to scabrate. Kofoid paratabulation formula: Xpr, $3'_{[*1', 2', 3']}$, 2a, 6'', 6c, 6''', $2''''_{[*1p, *1'''']}$, $5s_{[as, ras, *rs, ls, *ps]}$. Anterior intercalary archeopyle, Type 2I; compound; opercular pieces free.

Emended Diagnosis:

Shape: Ambitus lacrimoidal (teardrop-shaped = pyriform of Albert *et al.*, 1986) with rounded to subangular antapex and short to long, distally rounded apical horn, with or without an apicular extension of varying size and shape. Equatorial cross-section subcircular.

Wall Relationships: Differentiated autophragm only, or closely appressed robust endophragm and very thin, fibrous periphragm. Bi-layered arrangement rarely observed when damage of the outer layer reveals a paler membrane beneath (pl. 64, fig. E).

Wall Features: TLM: Intratabular areas smooth to scabrate with very thin, fibrous (fringe-like), flexuous parasutural septa, often folded onto cyst surface.
SEM: Cyst externally covered by a dense mat of countless, very fine (approx. 0.1µm thick), intertwined fibrous elements, which align perpendicularly to paraplate margins and extend into fibrous, flexuous parasutural septa, often distally recurved or folded onto cyst surface. Rare, small (up to 1µm diameter), circular depressions are sparsely and randomly distributed across intratabular areas.

Archeopyle: Anterior intercalary, Type 2I; compound; opercular pieces free. May rarely appear as Type I if an opercular piece (typically the 2a) remains in place.

Paratabulation: Partiform gonyaulacacean paratabulation fully expressed by parasutural septa, Kofoid paratabulation formula: Xpr, 3'$_{[*1', 2', 3']}$, 2a, 6'', 6c, 6''', 2''''$_{[*1p, *1'''']}$, 5s$_{[as, ras, *rs, ls, *ps]}$ (*asterisks indicate paraplate homologues). Distinctive parasulcal configuration: the small *1' is exsert and effectively forms the anterior limit of the parasulcus; the ras, rs and ps paraplates are enlarged and posteriorly displaced; the *rs is particularly elongated and displaces the *ps and 6''' to directly contact the 2'''' (= *1''''); and the variable, small, narrow ls paraplate may contact the 1c and as paraplates or be precluded by the ras contacting the 1c or 1''' paraplates. Both anterior intercalary paraplates are pentagonal with the 1a/2a parasuture adjoining the 4'' paraplate resulting in a planate 3'' and camerate 4'' anterior paraplate margin (Figure 5.1).

Paracingulum: Laevorotatory; ends offset approximately 1 paracingulum width. 1c strongly curved adjacent to the parasulcus.

Parasulcus: Topographically indicated by narrow, shallow furrow. Internally, distinctive paratabular arrangement fully subdivided by parasutural septa.

Size: Small to intermediate.

Dimensions: (µm; 12 specimens measured)
Total length: 47 (59) 70
Total width: 36 (46) 53
Max. length of septa: 1 (3) 4

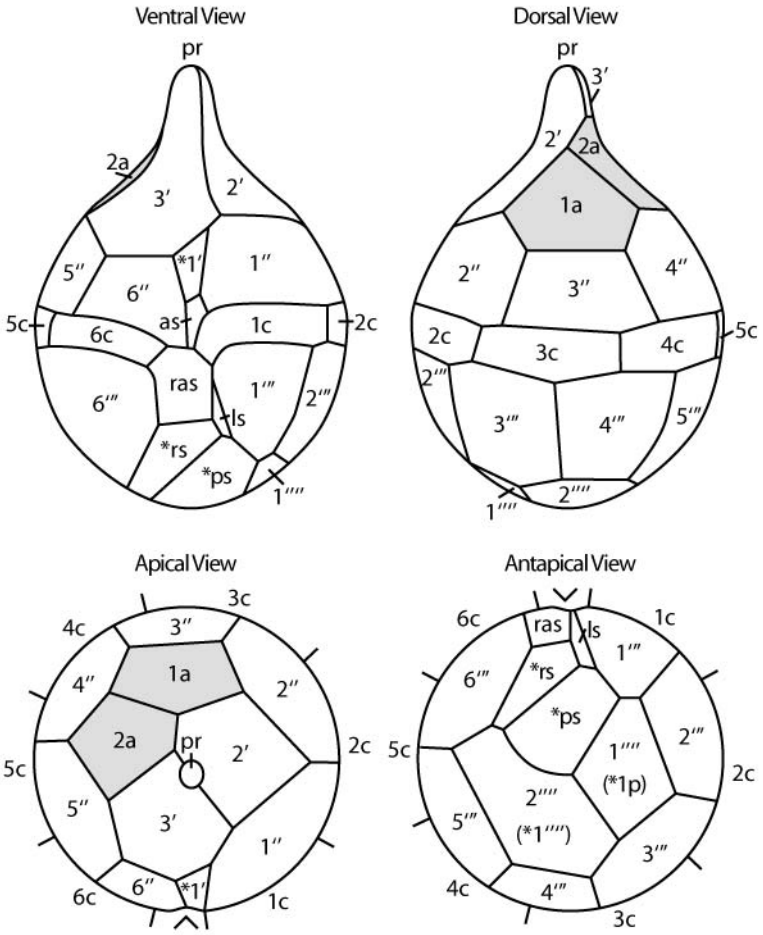

Figure 5.1: Paratabulation of *Paragonyaulacysta warrenii.* Paratabulation indicated by standard Kofoid notation with plate homologues indicated by asterisks (*).

Comments: Intraspecific variability was observed in A/ the ambital shape, B/ apical horn length, C/ size and shape of the apicular extension, D/ absence of rare intratabular 'hair-like' processes, and E/ size, shape and paraplate contacts of the ls paraplate. Variability of these features was discussed by Albert *et al.*, 1986 and fall within reasonable variation limits of the type material as previously described, hence Jansz-Io specimens are considered synonymous with the type material.

Justification for emendment and transfer: This species is herein emended to recognise the Type 2I compound archeopyle, the possession of 6 (not 7) paracingular paraplates, and clarify paraplate homologues and hence the paratabulation formula.

The large Type 2I compound archeopyle is evident in well-oriented specimens (pl. 64, fig. C-D; pl. 65, figs. A-C). The compound nature was deduced from very rare specimens which retained one opercular piece in place, and one specimen (pl. 64, fig. C) where the 2a opercular piece is suspended within the cyst from the 2a/5'' parasuture.

The original interpretation of 7 precingular paraplates may be the result of an artefact produced by "artificial" parasutures, as discussed by Albert *et al.*, 1986 (p. 308). These artificial paracingular parasutures are evident in the figured specimens of Albert *et al.*, 1986 (pl. 2, figs. 3, 12) but not all are included in the ultimate paratabulation interpretation. Observed Jansz-Io specimens do not possess artificial paracingular parasutures or evidence for a divided 5c paraplate (equivalent to Albert *et al.*, 1986 ei and eu paraplates), therefore this species is emended to possess 6 paracingular paraplates.

The paratabulation interpretation of Albert *et al.*, 1986 was deduced by "hypothesising an explanation that involves the least substantial departures from known topological patterns" (p. 312). Paraplates were interpreted not to have moved position, but rather enlarged through fusion of adjacent paraplates, or additional paraplates created through division of existing paraplates. However, intraspecific variability of the ls paraplate and, on a broader scale, variability of the paratabular arrangement between similar species and genera, is evidence that paraplate size and position is not entirely static. Therefore, this author takes the alternate view, that the fusion and division of paraplates is less likely than the enlargement and rearrangement of existing paraplates. Consequently, the paratabulation formula is emended herein to reflect a 'standard' partiform gonyaulacacean paratabulation. Kofoid notation is adopted according to the example of Below, 1990, with plate homologues represented according to Fensome *et al.*, 1993.

A full comparison of the paratabulation and paraplate homologues between Albert *et al.*, 1986 and the current study are outlined in Table 5.3. The major differences between these two interpretations are:

1. the apical paraplate C is equivalent to Kofoid anterior intercalary 1a, resulting in this species possessing 2 anterior intercalary paraplates rather than 1 as previously described;
2. the ei and eu paracingular paraplates are equivalent to a single 5c paracingular paraplate;
3. the 'fused' fu+li parasulcal paraplate is equivalent to a single, enlarged ras parasulcal paraplate; and,
4. the 'divided' posterior sulcal paraplate into the Zi and Zu paraplates are equivalent to enlarged and displaced rs and ps parasulcal paraplates respectively.

Albert *et al.*, 1986 originally erected *Lacrymodinium* to encompass species with a Type I archeopyle, 1 anterior intercalary and 7 paracingular paraplates. The emendment of this species to possess a Type 2I compound archeopyle, 2 anterior intercalary and 6 paracingular paraplates

determines that this species is more appropriately attributed to *Paragonyaulacysta* Johnson & Hills, 1973, and is here transferred accordingly.

Table 5.3: Comparison of Paraplate Series between Albert *et al.*, 1986 and the current study.

Current Study Paraplate Series																		
Preapical	Apical			Anterior Intercalary		Precingular						Paracingular						
pr	*1’	2’	3’	1a	2a	1’’	2’’	3’’	4’’	5’’	6’’	1c	2c	3c	4c	5c		6c
P	1u	A	B	C	4v	2	3	4h	5	6	1i	au	b	c	d	ei	eu	fi
Preapical	Apical			AI		Precingular						Paracingular						
Albert *et al.*, 1986 Paraplate Series																		

Current Study Paraplate Series												
Postcingular						Antapical		Parasulcal				
1’’’	2’’’	3’’’	4’’’	5’’’	6’’’	1’’’’ (*1p)	2’’’’ (*1’’’’)	as	ras	ls	*rs	*ps
Iu	II	III	IV	V	VI	X	Y	ai	fu+li	lm	Zi	Zu
Postcingular						Antapical		Parasulcal				
Albert *et al.*, 1986 Paraplate Series												

Comparison: *Paragonyaulacysta warrenii* differs to all other published *Paragonyaulacysta* species in the distinctive parasulcal arrangement outlined herein, and in possessing 2 pentagonal intercalary paraplates rather than a quadrilateral 1a paraplate and a hexagonal 2a paraplate. This species is visually most similar to *P? borealis* (Brideaux & Fisher, 1976) Stover & Evitt, 1978 and *P? capillosa* (Brideaux & Fisher, 1976) Stover & Evitt, 1978, which differ in reportedly having 4 apical paraplates. Furthermore, *P? capillosa* is significantly larger and has dense ‘hairlike’ intratabular ornamentation with faint, low parasutural ridges indicating the paratabulation. These species were questionably attributed to *Paragonyaulacysta* by Below, 1990 (p.60) due to uncertainty regarding their apical paratabulation. In the future, further analysis and paratabulation clarification may determined that either or both of these species are synonymous with *P. warrenii*.

The most similar parasulcal paratabular arrangement is that of *P. retiphragmata* Dörhöfer & Davies, 1980 (emend. Below, 1990; p. 61, Text-fig. 17), which depicts a slightly elongated rs paraplate posteriorly extending between the 6’’’ and ps paraplates. This evidence supports the interpretation that the previously named Zi paraplate equates to a greatly extended rs paraplate rather than a divided ps paraplate as previously interpreted. (Note: the 7c+FM paraplates of Below, 1990; p. 61, Text-fig. 17 equate to the ras of *P. warrenii*.)

Previously reported range: Upper Bathonian to Mid-Callovian of Europe (Smelror, 1988b); Callovian to Valanginian of North America (Albert *et al.*, 1986).

Similar looking specimens assigned to *Pluriarvalium?* sp. A have been recorded from Callovian to Tithonian of New Zealand, (Helby *et al.*, 1988).

Genus ***Pareodinia*** Deflandre, 1947b, emend. Gocht, 1970, Johnson & Hills, 1973, Wiggins, 1975, Stover & Evitt, 1978, and Below, 1990

Type species: *Pareodinia ceratophora* Deflandre, 1947b.

Pareodinia aphelia Cookson & Eisenack, 1958, emend. Below, 1990

Pl. 66, figs. G-I

1958 *Pareodinia aphelia* Cookson & Eisenack, p.60, pl.12, figs.3, 4, 9.

1990 *Pareodinia aphelia* Cookson & Eisenack, 1958, emend. Below, p.66.

Dimensions: (µm; 12 specimens measured)
Total length: 80 (88) 96
Total width: 40 (46) 56
Length of apical horn (approx.): 14 (19) 25
Length of apical horn extension: 0 (2.8) 7.5

Comparison: Specimens herein attributed to *Pareodinia aphelia* are most similar to the strongly granulate morphotype figured by Cookson & Eisenack, 1958, pl. XII, fig. 9. Jansz-Io specimens have a long, tapering apical horn and strongly granulate ornament, but have a thicker, more robust autophragm similar to the smooth morphotypes figured in Cookson & Eisenack, 1958, pl. XII, figs. 3-4. Observed specimens differ from *Imbatodinium kondratjevii* Vozzhennikova, 1967 which has a narrower cyst, antapical bulges or horns and a clearly defined paracingulum.

Previously reported range: Callovian to Aptian of Australia (Cookson & Eisenack, 1958; Wiseman & Williams, 1974; Kemp, 1976); Aptian of Germany (Below, 1990); Callovian of Egypt (Ibrahim *et al.*, 2002).

Pareodinia ceratophora Deflandre, 1947b, emend. Gocht, 1970

Pl. 66, figs. D-F

1947b *Pareodinia ceratophora* Deflandre, p.4, text-figs.1-3.

1970 *Pareodinia ceratophora* Deflandre 1947b, emend. Gocht, p.153-156.

Dimensions: (μm; 12 specimens measured)

Total length: 63 (79) 99

Total width: 28 (42) 50

Length of apical horn (approx.): 8 (14) 22

Length of apical horn extension: 0 (0.5) 2

Previously reported range: Cosmopolitan: Aalenian to Albian of Australia (Cookson & Eisenack, 1958; Wiseman & Williams, 1974; Filatoff, 1975; Morgan, 1980; Helby *et al.*, 1987; Stover & Helby, 1987d; Backhouse, 1988; Burger, 1996; Mantle, 2009a; Riding *et al.*, 2010);
Aalenian to Tithonian of Europe (Deflandre, 1947b; Sarjeant, 1960b, 1961a, 1962a & b, 1968, 1972, 1979; Alberti, 1961; Gocht, 1970; Woollam, 1980; Riding *et al.*, 1985; Nøhr-Hansen, 1986; Porter, 1988; Smelror, 1988a & b; Prauss, 1989; Kunz 1990; Stancliffe, 1991; Poulsen, 1993; Fauconnier *et al.*, 1996; Huault, 1999; Riding *et al.*, 1999, 2010; Borges *et al.*, 2011);
Bathonian to Tithonian of Russia (Riding *et al.*, 1999);
Bajocian to ?Valanginian of The Middle East and Egypt (Ashraf, 1979; El Beialy & Ibrahim, 1997; Gitmez & Ertug, 1999; Ibrahim *et al.*, 2002; Kholeif *et al.*, 2004);
Kimmeridgian to Tithonian of Africa (Thusu & Vigran, 1985; Jiang *et al.*, 1992);
Kimmeridgian to Tithonian of India (Jain *et al.*, 1984; Kumar, 1986);
Callovian to Upper Kimmeridgian of North America (Pocock, 1972; Johnson & Hills, 1973; Brideaux & Fisher, 1976; Zotto *et al.*, 1987);
Callovian to Berriasian of Argentina (Quattrocchio & Volkheimer, 1990; Riding *et al.*, 2011).

Pareodinia halosa (Filatoff, 1975) Prauss, 1989

Pl. 66, figs. A-C

1975 *Kalyptea halosa* Filatoff, 1975, p.91, pl.29, figs.10-12.

1980 *Kalyptea? halosa* (Filatoff, 1975) Fenton *et al.*, p.164.

1981 *Caddasphaera halosa* (Filatoff, 1975) Lentin & Williams, p.31.

1980 *Pterocystidiopsis halosa* (Filatoff, 1975) Courtinat *in* Courtinat & Gaillard, p.80.

1989 *Pareodinia halosa* (Filatoff, 1975) Prauss, p.42.

Dimensions: (µm; 13 specimens measured)
Total length: 32 (46) 63
Total width: 27 (38) 51
Max. width of kalyptra: 8 (16) 30

Previously reported range: Bajocian to Barremian (with Mid-Bajocian to Lower Bathonian acme) of Australia (Filatoff, 1975; Helby *et al.*, 1987; Stover & Helby, 1987c & d; Mantle, 2009a; Riding *et al.*, 2010);
Toarcian to Tithonian of Europe and Russia (Smelror, 1988a & b; Prauss, 1989; Kunz 1990; Poulsen, 1993; Huault, 1999; Riding *et al.*, 1999, 2010; Borges *et al.*, 2011).

Genus ***Perisseiasphaeridium*** Davey & Williams, 1966

Type species: *Perisseiasphaeridium pannosum* Davey & Williams, 1966.

***Perisseiasphaeridium?* sp. A**

Pl. 106, figs. A-C

Description: Intermediate to large skolochorate cyst with a reverse wall relationship. Endophragm alone forms central body; periphragm alone forms 17-18 intratabular processes and paracingular and parasulcal ridges. Endophragm subspherical; smooth to scabrate. Processes are narrow to broad, typically hollow, rarely solid, tubiform to trumpate and faintly striate. Distal process tips are highly variable: sparsely to densely fenestrate funnels, with entire to deeply furcate, asymmetrical margins; very rarely possesses ring trabeculae. Proximal process bases may be thickened; under-curving[#] processes may be distinct or obscured by pronounced tapering; surrounded by faint to prominent insiderae*. Paracingular and parasulcal ridges low (<3µm), narrow (<2µm), smooth to distally expanded and proximally faintly insiderate; 1 ridge per paraplate; parasulcal 'ridges' may be simulate. Standard gonyaulacacean paratabulation, formula: 4', 6'', 6c, 6''', 1p, 1'''', 5s. Archeopyle apical, Type (tA); operculum free; principal archeopyle suture zigzag; accessory archeopyle sutures common.

[#] Refer to reverse wall relationship discussion in Chapter 5.1.5; * refer to glossary in Chapter 5.1.2.

Dimensions: (µm; 13 specimens measured)
Total length: 81 (103) 144
Total width: 90 (111) 145

Central body length (with operculum): 65 (2 specimens)
Central body length (without operculum): 40 (53) 63
Central body width: 43 (56) 63
Max. length of processes: 20 (40) 60

Comparison: *Perisseiasphaeridium?* sp. A intergrades with *Contracysta* complex morphotypes as differentiated in Chapter 5.1.5. This species is differentiated from all *Perisseiasphaeridium* species in possessing a 'reverse' wall relationship[#] and paracingular and parasulcal ridges rather than multiple long, solid processes. The most similar published species is *P. ingegerdiae* Nøhr-Hansen, 1986, which has very similar processes including insiderae, originally described as "supporting roots", but differs in having paired paracingular processes. *P. inusitatum* Stevens & Helby, 1987 is also shown to have thickened process bases and insiderae, originally described as "short radial striations evident at the bases of the larger processes". However, *P. inusitatum* differs in having shorter processes and paired paracingular processes.

Genus ***Pilosidinium*** Courtinat, 1989

Type species: Gitmez & Sarjeant, 1972, as *Tenua echinata*.

Comments: According to Courtinat, 1989 and Courtinat *in* Fauconnier & Masure, 2004, *Pilosidinium* is distinguished from *Sentusidinium* Sarjeant & Stover, 1978 (emend. Courtinat, 1989) by the complete absence of paratabulation apart from the zigzag principal archeopyle suture and accessory archeopyle sutures, whereas *Sentusidinium* may possess parasuturally aligned ornament, particularly at the paracingulum.

Pilosidinium disessum sp. nov.

Pl. 67, figs. A-I

Holotype and type locality: Pl. 67, fig. G-I, Jansz-3, Core, 2848mRT(c), GA sample no. 1631262, slide no. 5, England Finder co-ordinates: L19, CPC no. 40917.

Derivation of name: From *disessum* (Latin): "to sit apart, be distant", for the widely-spaced distribution of non-tabular spines.

Synopsis: Small, spherical to subspherical, apteate, proximate to proximochorate cyst. Autophragm scabrate to microgranulate with numerous (100-200) non-tabular, subconical to

tapering spines, distally capitate in cross-section, bi- to trifurcate in plan view. Archeopyle apical, Type (tA)@, attached ventrally; principal archeopyle suture slightly zigzag. Paracingulum indeterminate.

Diagnosis:

Shape: Spherical to subspherical.

Wall Relationships: Autophragm only.

Wall Features: Numerous (100-200), non-tabular spines; relatively long (maximum length 8µm), approximately the same length on individual specimens, randomly spaced approximately 2-8µm apart. Spine shafts subconical to tapering with sharply to largely curved proximal contacts, distally capitate in cross-section, bi- to trifurcate to rarely aculeate in plan view visible at high-magnification. Spines typically solid but may be proximally hollow. Ornament between the spines scabrate to microgranulate.

Archeopyle: Apical, Type (tA)@, attached ventrally; principal archeopyle suture zigzag; short accessory archeopyle sutures rare.

Paratabulation: Gonyaulacacean paratabulation indicated by principal archeopyle suture and rare short accessory archeopyle sutures; epicystal paratabulation formula: Xpr, 4', ?1a, 6''. One or more anterior intercalary paraplates suggested by opercular shape.

Paracingulum: Not indicated.

Parasulcus: Indicated only by ventrally attached apical operculum.

Size: Small.

Dimensions: (µm; 12 specimens measured)
Autophragm length: 26 (31) 41
Autophragm width: 32 (34) 37
Max. length of processes: 5 (6.5) 8

Comparison: *Pilosidinium disessum* is most similar to *P. equispinum* sp. nov., which differs in having more numerous (>300), shorter spines with simply capitate distal tips. The most similar published species is *P. aptiense* (Burger, 1980a) Courtinat *in* Fauconnier & Masure, 2004, which differs in having shorter (1-4µm), consistently hollow spines with acuminate to bifid

distal tips and a free apical operculum. The generic type species, *P. echinatum* (Gitmez & Sarjeant, 1972) Courtinat, 1989, has a larger cyst size-range with shorter and broader conical processes. *P. fensomei* Courtinat, 1989 has hollow, conical spines with acuminate distal tips and enlarged proximal contacts. For additional comparisons, refer to Courtinat *in* Fauconnier & Masure, 2004, p.447-453.

Pilosidinium equispinum sp. nov.

Pl. 68, figs. D-L

Holotype and type locality: Pl. 68, fig. G, H, Jansz-3, Core, 2810mRT(c), GA sample no. 1631224, slide no. 5, England Finder co-ordinates: R11/1, CPC no. 40919.

Derivation of name: Derived from *aequi-, aequus* (Latin): "equal", and *spineus* (Latin): "of thorns, thorny" for the dense cover of spines of equal length and of the same morphology.

Synopsis: Small, spherical to subspherical, apteate, proximate to proximochorate cyst. Autophragm densely covered with numerous (>300) non-tabular, subconical to tapering spines with capitate distal tips, typically of the same length and morphology on individual specimens. Archeopyle apical, Type (tA)@, attached ventrally; principal archeopyle suture slightly zigzag; accessory archeopyle sutures common. Paracingulum indeterminate.

Diagnosis:

Shape: Spherical to subspherical.

Wall Relationships: Autophragm only.

Wall Features: Dense cover of numerous (>300) non-tabular, subconical to tapering spines, with sharply to largely curved proximal contacts and capitate distal tips, maximum length 3-6µm, spaced approximately 2µm apart, usually the same length and morphology on individual specimens. Spines typically solid but may be proximally hollow. Ornament between the spines scabrate.

Archeopyle: Archeopyle apical, Type (tA)@, attached ventrally; principal archeopyle suture slightly zigzag; deep accessory archeopyle sutures common.

Paratabulation: Gonyaulacacean paratabulation indicated by principal archeopyle suture and accessory archeopyle sutures; epicystal paratabulation formula: Xpr, 4', ?1a, 6''. One or more anterior intercalary paraplates suggested by opercular shape.

Paracingulum: Not indicated.

Parasulcus: Indicated only by ventrally attached apical operculum.

Size: Small.

Dimensions: (µm; 37 specimens measured)
Autophragm length: 27 (37) 48
Autophragm width: 26 (38) 51
Max. length of processes: 3 (4) 6

Comparison: *Pilosidinium equispinum* is most similar to *P. disessum* sp. nov., which differs in having fewer (100-200), longer (up to 8µm) spines that are distally capitate in cross-section and bi- to trifurcate in plan view. The most similar published species is *P. aptiense* (Burger, 1980a) Courtinat *in* Fauconnier & Masure, 2004, which differs in having slightly shorter (1-4µm), consistently hollow spines with acuminate to bifid distal tips and a free apical operculum. The generic type species, *P. echinatum* (Gitmez & Sarjeant, 1972) Courtinat, 1989, has a larger cyst size-range with shorter and broader conical spines. *P. fensomei* Courtinat, 1989 has hollow, conical spines with acuminate distal tips and enlarged proximal contacts. For additional comparisons, refer to Courtinat *in* Fauconnier & Masure, 2004, p.447-453.

Pilosidinium evanescum sp. nov.

Pl. 69, figs. A-L

Holotype and type locality: Pl. 69, fig. I-L, Jansz-3, Core, 2826mRT(c), GA sample no. 1631240, slide no. 5, England Finder co-ordinates: J33/3, CPC no. 40925.

Derivation of name: From *evanesco* (Latin): "to vanish, disappear, pass away", referring to the ornament that is visible in plan view but difficult to see laterally.

Synopsis: Small, spherical to subspherical, apteate, proximate to proximochorate cyst. Autophragm densely covered with numerous (>300), short, solid, non-tabular spines, clearly visible in plan view, barely discernible laterally. Ornament includes conical to subconical

spines, broad-based tapering spines, fine hair-like spines, and rare baculae; typically distally acuminate, very rarely faintly capitate. Archeopyle apical, Type (tA)@, attached ventrally; principal archeopyle suture slightly zigzag; accessory archeopyle sutures common. Paracingulum indeterminate.

Diagnosis:

Shape: Spherical to subspherical.

Wall Relationships: Autophragm only.

Wall Features: Dense cover of numerous (>300) non-tabular, solid spines, clearly visible in plan view, barely discernible laterally. Ornament includes conical to subconical spines, broad-based tapering spines, fine hair-like spines, and rare baculae; typically distally acuminate, very rarely faintly capitate; maximum length 1-2µm, spaced 1-3µm apart, usually the same length on individual specimens.

Archeopyle: Archeopyle apical, Type (tA)@, attached ventrally; principal archeopyle suture slightly zigzag; deep accessory archeopyle sutures common.

Paratabulation: Gonyaulacacean paratabulation indicated by principal archeopyle suture and accessory archeopyle sutures; epicystal paratabulation formula: Xpr, 4', ?1a, 6''. One or more anterior intercalary paraplates suggested by opercular shape.

Paracingulum: Not indicated.

Parasulcus: Indicated only by ventrally attached apical operculum.

Size: Small.

Dimensions: (µm; 15 specimens measured)
Autophragm length: 27 (31) 38
Autophragm width: 27 (30) 37
Max. length of processes: 1 (1.5) 2

Comparison: *Pilosidinium evanescum* appears most similar to the generic type species, *P. echinatum* (Gitmez & Sarjeant, 1972) Courtinat, 1989, which differs in having a much larger cyst with only conical to subconical ornament. The ornament of *Pilosidinium evanescum* is most similar to *P. asymmetrum* (Fenton *et al.*, 1980) Courtinat *in* Fauconnier & Masure, 2004,

but the latter species differs in having a much larger cyst with ornament gradationally concentrated antapically. *P. cactosum* Quattrocchio & Sarjeant, 1992 has a similar cyst size and ornament length, but possesses greater variation in ornament elements, including "verrucae and tuberculae to spines with acuminate, capitate, buccinate, flared or briefly bifurcate distal endings" (Quattrocchio & Sarjeant, 1992, p.91) which are more clearly visible laterally. For additional comparisons, refer to Courtinat *in* Fauconnier & Masure, 2004, p.447-453.

***Pilosidinium* sp. A**

Pl. 67, figs. J-L, Pl. 68, figs. A-C

Description: Small, spherical to subspherical, apteate, proximate to proximochorate cyst. Autophragm exhibits two levels of spinose ornament: dense cover of innumerable fine, hair-like spines 1-2µm long (setose); and fewer (100-200), longer (2-6µm), non-tabular, baculae to acuminate spines randomly spaced approximately 2-8µm apart; both levels of ornament most apparent laterally. Archeopyle apical, Type (tA) to Type (tA)@, attached ventrally; principal archeopyle suture slightly zigzag; deep accessory archeopyle sutures common. Gonyaulacacean epicystal paratabulation, formula: Xpr, 4', ?1a, 6''. Paracingulum indeterminate.

Dimensions: (µm; 12 specimens measured)
Autophragm length: 26 (33) 39
Autophragm width: 27 (36) 61
Max. length of tall processes: 2 (3.5) 6
Max. length of short processes: 1 (1.5) 2

Comparison: *Pilosidinium* sp. A differs to all other *Pilosidinium* species in having two types of spinose ornament on the one cyst. This species is most similar to *P. myriatrichum* (Fensome, 1979) Courtinat, 1989, which differs in having setose ornament only without any longer spines. For additional comparisons, refer to Courtinat *in* Fauconnier & Masure, 2004, p.447-453.

Genus ***Productodinium*** Davey, 1987

Type species: *Productodinium chenii* Davey, 1987.

Productodinium chenii Davey, 1987

Pl. 70, figs. A-K, Pl. 109, fig. H

1987 *Productodinium chenii* Davey, p.44, pl.8, figs.4-6, 9.

Dimensions: (µm; 12 specimens measured)
Autophragm length (with operculum): 56 (1 specimen)
Autophragm length (without operculum): 47 (54) 61
Autophragm width: 22 (30) 37
Max. length of ornament: 3 (4.5) 6

Comments: In the original description Davey 1987 (p.44) states that "a broad range of intraspecific variability is accepted for this species and there appears to be a complete gradation from one basic morphotype to another". Observations of Jansz-Io specimens support this statement, with variability expressed in ambital shape (ovoidal to elongate subpolygonal), paratabulation expression (paracingulum only to fully parasuturally aligned processes) and process shape, density and distribution.

Comparison: Specimens attributed to *Productodinium chenii* intergrade with *Egmontodinium?* sp. A herein, and may form part of the *P. chenii* / *E. torynum* lineage discussed by Davey 1987 (p.43).

Previously reported range: Callovian to Lower Kimmeridgian of Australia and the Timor Sea (Mantle, 2009b; Riding *et al.*, 2010); Oxfordian to Mid-Kimmeridgian of Papua New Guinea (Davey, 1987).

Genus ***Pyxidiella*** Cookson & Eisenack, 1958

Type species: *Pyxidiella pandora* Cookson & Eisenack, 1958

Pyxidiella pandora Cookson & Eisenack, 1958

Pl. 71, figs. B-E

1958 *Pyxidiella pandora* Cookson & Eisenack, p.52, pl.6, figs.10-11.

Dimensions: (µm; 12 specimens measured)
Autophragm length: 38 (44) 53
Autophragm width: 19 (23) 31

Comments: Many observed *Pyxidiella pandora* specimens display broad and shallow pre- and postcingular constrictions to produce an ambital shape resembling a 'jelly baby' confection (pl. 71, fig. C). The ratio of constricted to non-constricted specimens is roughly 1:1, though one morphotype may predominate in individual samples.

Intraspecific variability was also noted in the archeopyle shape, with the posterior archeopyle margin ranging from straight to concave (pl. 71, figs. D-E). Whether this feature is an artefact of orientation or preservation is uncertain; however the frequency of occurrence on undamaged specimens suggests this is a primary feature. One figured *P. pandora* specimen by Helby *et al.* (1988, fig.8I) from New Zealand shows the same archeopyle shape as observed on the Jansz-Io specimens, although the figured cyst does not display any constriction so the lateral margins are parallel.

Previously reported range: Consistent occurrences from Callovian to Tithonian with inconsistent occurrences to Valanginian of Australia and New Zealand (Cookson & Eisenack, 1958; Wiseman, 1980; Helby *et al.*, 1987, 2004; Wilson & Helby, 1987; Helby *et al.*, 1988; Riding *et al.*, 2010).

Genus ***Reutlingia*** Drugg, 1978, emend. Below, 1987a

Type species: *Reutlingia gochtii*, Drugg, 1978.

Reutlingia gochtii Drugg, 1978, emend. Below, 1987a

Pl. 71, fig. A

1978 *Reutlingia gochtii* Drugg, p.72-73, pl.7, figs.7-10.

1987a *Reutlingia gochtii* Drugg, 1978, emend. Below, 1987a, p.137-138.

Dimensions: (µm; 2 specimens measured)
Total length: 22, 29
Total width: 21, 22

Previously reported range: Callovian of Europe (Drugg, 1978; Huault, 1999); Oxfordian of New Zealand (Helby *et al.*, 1988).

Genus ***Rhynchodiniopsis*** Deflandre, 1935,
emend. Below, 1981, Sarjeant, 1982 and Jan du Chêne *et al.*, 1985

Type species: *Rhynchodiniopsis aptiana* Deflandre, 1935.

Rhynchodiniopsis cladophora (Deflandre, 1939) Below, 1981

Pl. 71, figs. F-I

1939 *Gonyaulax cladophora* Deflandre, p.173-176, pl.7, figs.1-5; text-figs.5-6.
1967 *Gonyaulacysta cladophora* (Deflandre, 1939) Dodekova, p.17-18.
1978 *Hystrichogonyaulax cladophora* (Deflandre, 1939) Stover & Evitt, p.162.
1981 *Rhynchodiniopsis cladophora* (Deflandre, 1939) Below, p.118.

Dimensions: (µm; 12 specimens measured)
Autophragm length: 85 (104) 138
Autophragm width: 78 (91) 103
Max. length of processes: 8 (11) 15
Length of apical horn: 8 (13) 20

Comments and Comparison: Significant intraspecific variability was observed in cyst size, wall thickness, and parasutural ornament. Parasutural spines are typically isolated with bi- to trifurcate distal tips, though rarely few adjacent spines may connect distally. Very rarely numerous adjacent spines connect to produce erymnate parasutural septa, though never to the extent developed by *Rhynchodiniopsis fimbriata* (Duxbury, 1980) Sarjeant, 1982.

Previously reported range: Cosmopolitan: Mid-Callovian to Mid-Kimmeridgian of Australia (Morgan *et al.*, 2002; Riding *et al.*, 2010);
Callovian to Oxfordian of New Zealand (Wilson & Helby, 1987; Helby *et al.*, 1988);
Bathonian to Kimmeridgian of Europe (Deflandre, 1939; Sarjeant, 1960b, 1961a, 1962b, 1968, 1972, 1979; Dodekova, 1967; Raynaud, 1978; Erkmen & Sarjeant, 1980; Woollam, 1980; Riley & Fenton, 1982; Nøhr-Hansen, 1986; Brenner, 1988; Porter, 1988; Smelror, 1988a & b; Thomas & Cox, 1988; Kunz 1990; Stancliffe, 1991; Poulsen, 1993, 1996; Fauconnier, 1995; Fauconnier *et al.*, 1996; Huault, 1999; Riding *et al.*, 1999, 2010; Riding, 2005b);
Lower Oxfordian of The Middle East and Egypt (El Beialy & Ibrahim, 1997; Kholeif *et al.*, 2004);
Mid-Bathonian to Upper Kimmeridgian of Canada (Pocock, 1972; Johnson & Hills, 1973; Williams, 1975; Brideaux & Fisher, 1976);
Callovian of Argentina (Riding *et al.*, 2011).

Genus ***Rigaudella*** (Deflandre, 1939) Below, 1982b

Type species: Deflandre, 1939, as *Hystrichosphaeridium aemulum*.

Rigaudella aemula (Deflandre, 1939) Below, 1982b

Pl. 104, figs. A-F, Pl. 105, figs. A-F

1939 *Hystrichosphaeridium aemulum* Deflandre, p.187-189, pl.9, fig.12; pl.10, figs.5-8; pl.11, figs.1, 7.

1947a *Cannosphaeropsis aemula* (Deflandre, 1939) Deflandre, p.1576.

1969 *Adnatosphaeridium aemulum* (Deflandre, 1939) Williams & Downie, p.17.

1982b *Rigaudella aemula* (Deflandre, 1939) Below, p.139-140.

Dimensions: (µm; 13 specimens measured)

Total length: 79 (115) 149

Total width: 95 (122) 157

Central body length (with operculum): 53 (1 specimen)

Central body length (without operculum): 41 (53) 62

Central body width: 42 (51) 62

Max. length of processes: 35 (45) 60

Comments: Jansz-Io specimens are identified as possessing a 'reverse' wall relationship as described for the *Contracysta* complex (refer to Chapter 5.1.5), but are otherwise identical to *Rigaudella aemula s.s*. *R. aemula* occurs consistently in Oxfordian sediments, and presenting a new name for an otherwise identical species would lead to unnecessary biostratigraphic confusion. Therefore, specimens with a reverse wall relationship are attributed to *R. aemula* for biostratigraphic consistency. However, re-examination of the type material needs to be conducted to determine the wall relationship of the type material and confirm the common origin.

Significant intraspecific variability was observed in Jansz-Io *R. aemula* specimens, including solid and hollow processes, extent of distal process flaring, fenestration, interlinking and ring trabeculation, and presence or absence of simulate* distal margins. Similar variability was recorded by Davey 1987 (p.44-45), who described four *R. aemula / R. filamentosa* group morphotypes from Papua New Guinea. Davey commented that some variants were more consistent at certain stratigraphic levels, and recommended research into the potential stratigraphic utility of these variants. The variants within Jansz-Io preparations were not found to be individually stratigraphically useful and hence are grouped into a single, broad species.

However, more research needs to be conducted to determine the stratigraphic utility of variants over the species' entire stratigraphic range.

* Refer to the glossary of introduced terms in Chapter 5.1.2.

Comparison: Specimens herein attributed to *Rigaudella aemula* intergrade with *Contracysta* complex morphotypes as differentiated in Chapter 5.1.5.

This species also intergrades with *Rigaudella filamentosa* (Cookson & Eisenack, 1958) Below, 1982b, which differs in having thinner, solid processes or process complexes, including paracingular processes, and a finer trabeculate network. Occurrences of *R. aemula* and *R. filamentosa* are frequently combined under "*R. aemula / R. filamentosa* complex" or variations of this title (*e.g.* Davey, 1987; Courtinat, 2006). Therefore the intergradation of these species is well established.

Extremely trabeculate specimens of *R. aemula* (pl.105, figs.E-F) are similar to *Adnatosphaeridium densifilosum* (Cookson & Eisenack, 1974) Stancliffe & Sarjeant, 1990 in having a complex trabecular network supported by relatively thick and often flared processes. However, *A. densifilosum* differs in possessing paracingular processes which *R. aemula* does not. The relationship of these two species is analogous to that of *R. filamentosa* and *Adnatosphaeridium* sp. A herein, supporting the theory that paracingular processes are variable and these genera may intergrade or be synonymous.

Previously reported range: Cosmopolitan: Recently interpreted to range from Mid-Callovian to Tithonian in Australia (Helby *et al.*, 1987, 2004; Morgan *et al.*, 2002; Partridge, 2006a; Mantle, 2009b; Riding *et al.*, 2010) though previously reported from Bathonian? to Hauterivian (Cookson & Eisenack, 1958; Wiseman, 1980; Burger, 1996).
Elsewhere reported from Upper Callovian to Lower Tithonian (reworked into Upper Tithonian to Upper Valanginian) of Papua New Guinea (Davey, 1987);
Oxfordian to Tithonian of New Zealand (Wilson & Helby, 1987; Helby *et al.*, 1988);
Mid-Bathonian to Mid-Kimmeridgian of Europe (Deflandre, 1939; Sarjeant, 1960b, 1962a, 1968, 1979; Raynaud, 1978; Erkmen & Sarjeant, 1980; Woollam, 1980; Riley & Fenton, 1982; Brenner, 1988; Smelror, 1988a & b; Thomas & Cox, 1988; Prauss, 1989; Kunz 1990; Stancliffe, 1991; Fauconnier, 1995; Fauconnier *et al.*, 1996; Huault, 1999; Riding *et al.*, 1999, 2010; Poulsen & Riding, 2003; Riding, 2005b);
Kimmeridgian to Tithonian of India (Jain *et al.*, 1984);
Oxfordian to Lower Tithonian of Africa (Jiang *et al.*, 1992; Schrank, 2005).

Rigaudella filamentosa (Cookson & Eisenack, 1958) Below, 1982b

Pl. 72, figs. A-F

1958 *Cannosphaeropsis filamentosa* Cookson & Eisenack, p.47-48, pl.7, figs.8-9; pl.8, figs.1-2.

1969 *Adnatosphaeridium filamentosum* (Cookson & Eisenack, 1958) Williams & Downie, p.17.

1982b *Rigaudella filamentosa* (Cookson & Eisenack, 1958) Below, p.148.

Dimensions: (µm; 23 specimens measured)

Total length: 75 (99) 135

Total width: 81 (104) 141

Central body length (with operculum): 48 (50) 52 (3 specimens)

Central body length (without operculum): 37 (46) 63

Central body width: 39 (47) 62

Max. length of processes: 24 (37) 45

Comments: All specimens observed in the Jansz-Io preparations that otherwise match the emended description of Below, 1982b also possessed thin paracingular processes.

Comparison: *Rigaudella filamentosa* may be a transitional species between the genera *Rigaudella,* without paracingular processes, and *Adnatosphaeridium* Williams & Downie, 1966, with paracingular processes. Observations from the Jansz-Io preparations confirm that *R. filamentosa* intergrades with both *R. aemula* (Deflandre, 1939) Below, 1982b, which differs in having heavier, funnel-forming, trumpate processes without paracingular processes, and *Adnatosphaeridium* sp. A herein, which has fine processes to process complexes, including paracingular processes, with a more complex distal trabeculum. The similarity of these species suggests that the presence of paracingular processes may be variable and these genera may intergrade or be synonymous.

Previously reported range: Frequently recorded combined with *Rigaudella aemula* in a species complex (Davey, 1987). Where recorded independently the range is cosmopolitan:
Callovian to Tithonian of Australia (Cookson & Eisenack, 1958; Wiseman, 1980; Mantle, 2009b);
Lower Callovian to Oxfordian of Europe (Sarjeant, 1962a, 1979; Porter, 1988; Riding, 2005b);
Callovian of The Middle East (Wheeler & Sarjeant, 1990);
Kimmeridgian to Tithonian of India (Kumar, 1986);
Mid-Callovian to Lower Tithonian of Africa (Jiang *et al.*, 1992; El Beialy & Ibrahim, 1997; Schrank, 2005)

Genus ***Scriniodinium*** Klement, 1957, emend. Prauss, 1989 and Riding & Fensome, 2003

Type species: Deflandre, 1939, as *Gymnodinium crystallinum*.

Scriniodinium crystallinum (Deflandre, 1939) Klement, 1960, emend. Riding & Fensome, 2003

Pl. 73, fig. D-F, Pl. 109, fig. A

1939 *Gymnodinium crystallinum* Deflandre, p.165, pl.5, figs.1-3.

1960 *Scriniodinium crystallinum* (Deflandre, 1939) Klement, p.18.

2003 *Scriniodinium crystallinum* (Deflandre, 1939) Klement, emend. Riding & Fensome, p.12-13.

Dimensions: (μm; 13 specimens measured)
Periphragm length: 71 (86) 102
Periphragm width: 65 (81) 91
Endophragm length: 60 (68) 79
Endophragm width: 54 (63) 70

Comments: Observed specimens displayed significant intraspecific variability with respect to the ambital shape (smoothly ovoidal to angular subpolygonal), apical perihorn development, and paratabulation expression (absent to evident as faint parasutural ridges).

Specimens frequently possess radially arranged linear thickenings and/or thinned ovoidal patches where the endo- and periphragms detach to form the circumferential pericoel, with extreme examples forming a narrow pseudo-reticulate band.

Previously reported range: Cosmopolitan: *Scriniodinium crystallinum* is the basal key marker for the *Wanaea spectabilis* Zone (HMP microplankton scheme) which commences in the Lower Oxfordian. Previously recorded from Upper Callovian to Tithonian (inconsistent to Valanginian) of Australia and the Timor Sea (Cookson & Eisenack, 1958; Wiseman & Williams, 1974; Wiseman, 1980; Helby *et al.*, 1987, 2004; Partridge, 2006a; Mantle, 2009b; Riding *et al.*, 2010);
Upper Callovian to Kimmeridgian (inconsistent to Lower Tithonian) of Papua New Guinea (Davey, 1987, 1999);
Oxfordian to Tithonian of New Zealand (Wilson & Helby, 1987; Helby *et al.*, 1988);

Callovian to Lower Kimmeridgian of Europe (Deflandre, 1939; Klement, 1960; Sarjeant, 1960b, 1961a, 1962a, 1968, 1979; Dodekova, 1967; Raynaud, 1978; Woollam, 1980; Brenner, 1988; Riding & Thomas, 1988; Thomas & Cox, 1988; Kunz 1990; Stancliffe, 1991; Fauconnier, 1995; Fauconnier *et al.*, 1996; Poulsen 1996; Huault, 1999; Riding *et al.*, 1999, 2010; Poulsen & Riding, 2003);
Oxfordian to Kimmeridgian of The Middle East (Gitmez & Ertug, 1999);
(?Upper Callovian) Oxfordian to Upper Kimmeridgian of northern Canada (Johnson & Hills, 1973; Brideaux & Fisher, 1976);
Callovian of Argentina (Riding *et al.*, 2011).

Scriniodinium dictyotum Cookson & Eisenack, 1960b

Pl. 73, fig. A-C

1960b *Scriniodinium dictyotum* Cookson & Eisenack, p. 248-249, pl.37, figs.8-9.
1971 *Scriniocassis dictyotus* (Cookson and Eisenack, 1960b) Beju, p.299.
1982 *Aldorfia dictyota* (Cookson and Eisenack, 1960b) Davey, p.25.
2003 *Scriniodinium dictyotum* Cookson & Eisenack, 1960b; retained by Riding & Fensome, p.16.

Dimensions: (µm; 12 specimens measured)
Periphragm length: 65 (74) 85
Periphragm width: 55 (69) 80
Endophragm length: 55 (65) 74
Endophragm width: 45 (59) 70

Comments: Jansz-Io *Scriniodinium dictyotum* specimens displayed a high degree of intraspecific variability in ambital shape (smoothly ovoidal to angular subpolygonal), apical perihorn development, size of reticular lumina, and paratabulation expression (absent to evident as subtle variations of the reticulum).

Previously reported range: Cosmopolitan: Callovian to Berriasian of Australia, the Timor Sea and Papua New Guinea (Cookson & Eisenack, 1960b; Davey, 1987; Mantle, 2009b; Riding *et al.*, 2010);
Oxfordian to Tithonian of New Zealand (Wilson & Helby, 1987; Helby *et al.*, 1988);
Callovian to Kimmeridgian of Europe (Sarjeant, 1962a & b, 1968, 1972, 1979; Raynaud, 1978; Erkmen & Sarjeant, 1980; Woollam, 1980; Riley & Fenton, 1982; Nøhr-Hansen, 1986; Smelror, 1988a; Thomas & Cox, 1988; Stancliffe, 1991; Poulsen, 1993; Fauconnier, 1995; Fauconnier *et al.*, 1996; Huault, 1999; Riding *et al.*, 1999, 2010);

Mid-Callovian to Kimmeridgian of North America (Brideaux & Fisher, 1976; Zotto *et al.*, 1987; Olmstead *et al.*, 1996);
Kimmeridgian to Tithonian of Africa (Jiang *et al.*, 1992).

Genus ***Sepispinula*** Islam, 1993

Type species: Cookson & Eisenack, 1960a, as *Hystrichosphaeridium ancoriferum*.

Sepispinula sp. cf. ***S. ancorifera*** (Cookson & Eisenack, 1960a) Islam, 1993

Pl. 74, figs. A-F

cf. 1960a *Hystrichosphaeridium ancoriferum* Cookson & Eisenack, p.8, pl.2, fig.11.
cf. 1966b *Cleistosphaeridium ancoriferum* (Cookson & Eisenack, 1960a) Davey *et al.*, p.167.
cf. 1968 *Cleistosphaeridium ancoriferum* (Cookson & Eisenack, 1960a) Davey *et al.*, 1966b, emend. Cookson & Eisenack, p.119-120.
cf. 1993 *Sepispinula ancorifera* (Cookson & Eisenack, 1960a) Islam, p.88.

Description: Intermediate-sized, ovoidal to elongate ellipsoidal, holocavate, proximochorate cyst. Endophragm smooth to scabrate; periphragm alone forms numerous (100-200) non-tabular, tubiform, internally septate, distally closed processes with cylindrical to tapering shafts and widely flaring distal tips; adjacent processes interconnect to form a very thin, smooth ectophragm, frequently broken into polygons covering a few adjacent processes (pl. 74, fig. F) or isolated processes (pl. 74, figs. B, E), commonly recurving towards cyst surface (pl. 74, fig.E). Archeopyle apical, Type (tA), free; principal archeopyle suture zigzag, deep accessory archeopyle sutures common. Gonyaulacacean epicystal paratabulation, formula: Xpr, 4', ?1a, 6''. Parasulcus indicated by parasulcal notch only; paracingulum indeterminate.

Dimensions: (µm; 8 specimens measured)
Endophragm length (with operculum): 63, 64 (2 specimens)
Endophragm length (without operculum): 36 (52) 61
Endophragm width: 30 (39) 43
Min. length of processes: 3 (4.5) 6
Max. length of processes: 5 (7.5) 10
Min. width of process bases: 1
Max. width of process bases: 2.5 (2.9) 3

Comparison: *Sepispinula* sp. cf. *S. ancorifera* specimens are most similar to *Sepispinula ancorifera s.s.* in cyst and process morphology, but differ in being ovoidal to elongate ellipsoidal rather than spherical to subspherical, and significantly stratigraphically older.

Previously reported range: *Sepispinula ancorifera s.s.* has an Australasian distribution from the Albian to Cenomanian (Cookson & Eisenack, 1960a, 1968; Davey *et al.*, 1966b; Backhouse, 1988; Islam, 1993).

Sepispinula florida sp. nov.

Pl. 74, figs. G-L, Pl. 75, figs. A-L, Pl. 76, figs. A-L, Pl. 77, figs. A-O

Holotype and type locality: Pl. 76, fig. A-C, Jansz-3, Core, 2810mRT(c), GA sample no. 1631224, slide no. 5, England Finder co-ordinates: P27, CPC no. 40959.

Derivation of name: From *floridus* (Latin): "flowery, blossoming; made of or rich in flowers" in reference to the distinctive flower-like secate to arboriform distal process tips.

Synopsis: Intermediate-sized, spherical to subspherical, proximate to proximochorate cyst. Endophragm smooth to scabrate; periphragm alone forms numerous (100-200) non-tabular, tubiform processes with narrow to wide, cylindrical to tapering shafts, distally flaring to 'V' or 'U'-shaped ends, often recurving towards cyst body; internally septate, rarely solid or hollow, distally closed. Distal process tips distinctively secate to arboriform in plan view giving a flower-like appearance. Paratabulation gonyaulacacean; archeopyle apical, Type (tA), free; principal archeopyle suture zigzag, deep accessory archeopyle sutures common; rare incomplete pandasutural bands may occur.

Diagnosis:

Shape: Spherical to subspherical.

Wall Relationships: Endophragm and process-forming periphragm.

Wall Features: Endophragm smooth to scabrate; periphragm alone forms numerous (100-200) non-tabular processes. Processes tubiform with cylindrical to tapering shafts, sharply to largely curved proximal bases and broadly flared, characteristically 'V' or 'U'-shaped distal ends; internally septate, rarely solid or hollow, distally closed; typically isolated but may distally interconnect (Figure 5.2). Distal process tips distinctively secate to arboriform in plan view giving a flower-like appearance; very thin and most apparent at high-magnification; may

recurve towards cyst surface. Process width variable on individual specimens; process length is approximately equal, rarely shorter at the parasulcus (pl. 77, fig. J), very rarely longer at the parasutures, particularly the paracingulum (pl. 75, fig. K).

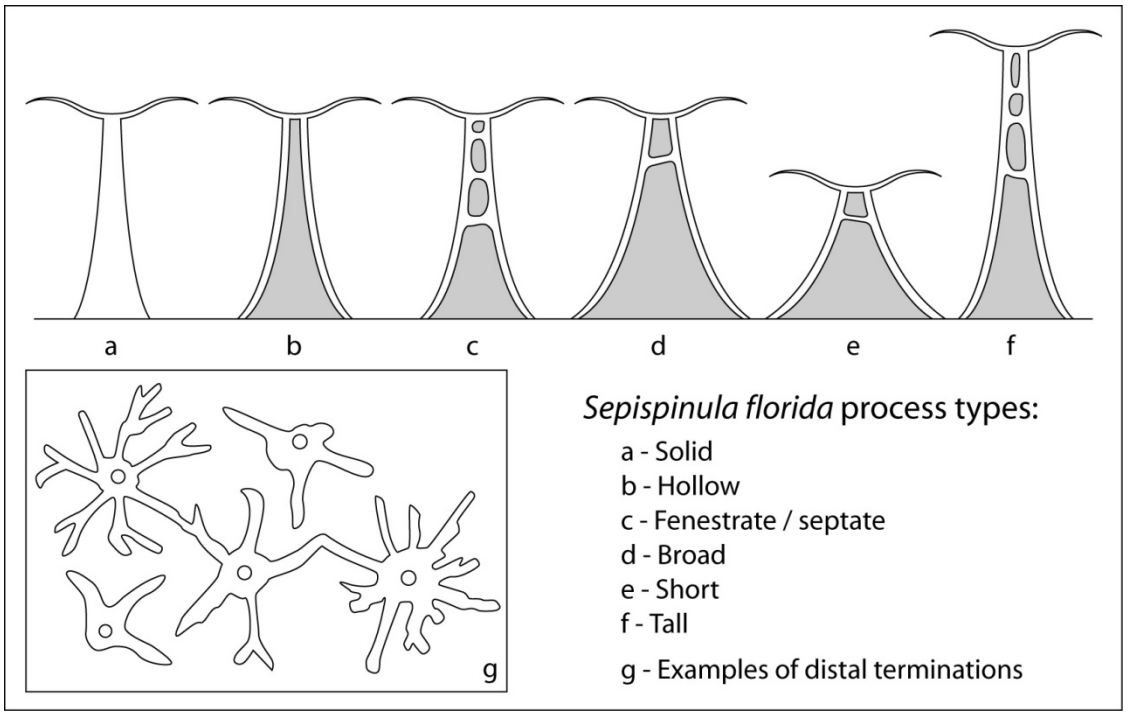

Figure 5.2: Variation in *Sepispinula florida* processes

Archeopyle: Apical, Type (tA), operculum free; principal archeopyle suture zigzag, deep accessory archeopyle sutures common.

Paratabulation: Typically indicated by principal archeopyle suture and accessory archeopyle sutures only; rarely indicated by pandasutural bands up to 4µm wide (pl. 75, fig. G; pl. 77, fig. O); commonly incompletely developed on individual specimens. Gonyaulacacean paratabulation, formula: Xpr, 4', ?1a, 6'', ?6c, 6''', 1p, 1'''', Xs. At least one anterior intercalary paraplate is indicated by the principal archeopyle suture and opercular shape.

Paracingulum: Typically not evident; very rarely indicated by incomplete pandasutural bands or slightly longer processes.

Parasulcus: Typically indicated by parasulcal notch only; very rarely evident by slightly shorter processes in apical view.

Size: Small to intermediate.

Dimensions: (µm; 17 specimens measured)

Endophragm length (without operculum): 41 (46) 50
Endophragm width: 37 (45) 53
Min. length of processes: 2.5 (4) 5
Max. length of processes: 5 (6.5) 9.5
Min. width of process bases: 0.5 (1) 2.5
Max. width of process bases: 2.5 (4.5) 8

Comments: *Sepispinula florida* exhibits intraspecific variability in archeopyle shape, process lengths and pandasutural band development. Free opercula reveal that the archeopyle ranges from slightly elongate dorso-ventrally (pl. 77, fig. C) to roughly equidimensional (pl. 77, fig. E). The extent to which the 4' paraplate extends between the 5'' and 6'' paraplates ranges from shallow and broad (pl. 77, fig. H) to very deep and narrow with an angular termination which may be confused with the parasulcal notch (pl. 75, fig. D; pl. 77, fig. K, L). Pandasutural bands range from indiscernible to 4µm wide (pl. 77, fig. O). Typically pandasutural bands are incompletely developed on individual specimens and most evident when processes are out of focus (pl. 75, fig. G). Processes are usually of roughly the same length on individual specimens, averaging 6µm long with a deviation of approximately 2-3µm between the shortest and longest processes. Very rarely process variation may reflect paratabulation, especially the paracingulum (pl. 75, fig. K), or processes may be different lengths on opposing surfaces (pl. 76, fig.I).

Comparison: *Sepispinula florida* differs to all currently attributed *Sepispinula* species in the distinctive secate to arboriform (flower-like) distal process tips. This species is most similar to the Albian to Cenomanian *S. ancorifera* (Cookson & Eisenack, 1960a) Islam, 1993 in process height, form and possession of septa, but which differs in having entire, membranous distal process tips. *S. pertusa* (Davey, 1969) Masure *in* Fauconnier &Masure, 2004 differs in having a smaller cyst body with subconical processes terminating in two distal spines recurving towards the cyst surface.

Genus ***Stephanelytron*** Sarjeant, 1961a, emend. Stover *et al.*, 1977

Type species: *Stephanelytron redcliffense* Sarjeant, 1961a.

Discussion: Refer to *Lagenadinium* Piel, 1985 above for discussion regarding the generic separation of *Stephanelytron* and *Lagenadinium*.

Stephanelytron sp. A

Pl. 78, figs. A-I

Description: Small to intermediate-sized, proximate, holocavate cyst. Autophragm elongate ellipsoidal with rounded apices. Numerous (>300) non-tabular, short (typically 4.5µm long), capitate processes support a robust ectophragm; ectocoel narrow over most of cyst, rarely extending into a short, conical ectohorn (<3µm long) and two bulges at the paracingulum. A single subcircular to ovoidal, straight to flared, striate, membranous corona is located antapically, sometimes slightly proximally thickened. Archeopyle apical, Type (tA) to Type (tA)@; principal archeopyle suture slightly zigzag. Parasulcus indicated by parasulcal notch and rarely by ventral archeopyle attachment; paratabulation indeterminate.

Dimensions: (µm; 12 specimens measured)
Autophragm length (with operculum): 48 (54) 59 (7 specimens)
Autophragm length (without operculum): 46 (51) 55 (10 specimens)
Autophragm width: 29 (34) 39
Ectophragm length: 53 (60) 65
Ectophragm width: 26 (40) 48
Max. width of pericoel: 2.5 (4.5) 6
Height of corona: 3 (6) 9
Max. diameter of corona: 8 (15) 22.5

Comments and Comparison: As outlined in the generic discussion under *Lagenadinium* above, this species is placed in *Stephanelytron* due to the antapical position of the corona. *Stephanelytron* sp. A is most similar to *S. scarburghense* Sarjeant, 1961a, which has a single, straight, striate antapical corona with both parasutural and intratabular processes, but differs in not having an ectophragm. Within the Jansz-Io preparations, this species appears most similar to *Chlamydophorella* sp. A, which has an elongate ellipsoidal autophragm, robust ectophragm, and non-tabular processes, but differs in having more numerous, finer processes and not possessing an antapical corona.

Previously reported range: Wilson & Helby, 1987 (pl. 1, fig. 14) figured one apparently identical specimen from the Oxfordian of New Zealand as "*Chlamydophorella wallala* Cookson & Eisenack".

Genus ***Stiphrosphaeridium*** Davey, 1982

Type species: Cookson & Eisenack, 1958, as *Hystrichosphaeridium dictyophorum.*

Stiphrosphaeridium? **sp. A**

Pl. 106, figs. D-F

Description: Intermediate to large skolochorate cyst with a reverse wall relationship. Endophragm alone forms central body; periphragm alone forms 17-18 intratabular processes. Endophragm subspherical; smooth to finely granulate. Processes are broad, hollow, tubiform to broadly trumpate and fenestrate to striate. Distal process tips are broadly flared and densely fenestrate, with subtly simulate* margins encircled by ring trabeculae. Proximal process bases may be thickened; under-curving[#] processes may be distinct or obscured by pronounced tapering; surrounded by faint to prominent insiderae*. Standard gonyaulacacean paratabulation, formula: 4', 6'', 6c, 6''', 1p, 1'''', 5s; process formula: 4', 6'', 0c, 5-6''', 1p, 1'''', 0s; where 5 post-cingular processes are present, the 1''' process is absent. Archeopyle apical, Type (tA); operculum free; principal archeopyle suture zigzag; accessory archeopyle sutures common.

[#] Refer to reverse wall relationship discussion in Chapter 5.1.5; * refer to glossary in Chapter 5.1.2.

Dimensions: (µm; 3 specimens measured)
Total length: 101 (117) 132
Total width: 95 (116) 136
Central body length: 51 (58) 64
Central body width: 49 (64) 93
Max. length of processes: 42 (45) 50

Comparison: *Stiphrosphaeridium?* sp. A intergrades with *Contracysta* complex morphotypes as differentiated in Chapter 5.1.5. This species is differentiated from all *Stiphrosphaeridium* species in possessing a 'reverse' wall relationship[#]. Jansz-Io specimens are very similar to *Stiphrosphaeridium* sp. 1 specimens of Davey, 1987, although the Jansz-Io specimens rarely have individual or remnant interconnecting trabeculae that were not mentioned by Davey, 1987.

Previously reported range: *Stiphrosphaeridium* sp. 1 of Davey, 1987 ranges from the Mid- to Upper Tithonian of Papua New Guinea.

Genus ***Systematophora*** Klement, 1960,
emend. Brenner, 1988, Stancliffe & Sarjeant, 1990, and Riding & Helby, 2001e

Type species: *Systematophora areolata* Klement, 1960.

Systematophora geminus Riding & Helby, 2001e

Pl. 79, figs. A-L

2001e Riding & Helby, p.123-126, figs.7A, 8A-I, 9A-I.

Dimensions: (μm; 12 specimens measured)
Autophragm length (with operculum): 54 (56) 58 (2 specimens)
Autophragm length (without operculum): 42 (52) 63 (10 specimens)
Autophragm width: 45 (53) 78
Max. length of processes: 10 (14) 21

Comments and Comparison: Observed specimens of *Systematophora geminus* displayed significant intraspecific variability, principally in the length, number and interconnectivity of processes within each process complex. The characteristic paired sets of processes per paracingular paraplate discussed in the original description are rarely observed, and linear paracingular ridges may occur, frequently possessing numerous processes along its length. Specimens with few processes per annulate complex and minimal distal connections may be confused with *Systematophora areolata* Klement, 1960 with which this species may intergrade.

Previously reported range: Upper Callovian to Mid-Oxfordian of Australia and the Timor Sea (Riding & Helby, 2001e; Morgan *et al.*, 2002; Helby *et al.*, 2004; Partridge, 2006a; Mantle, 2009b; Riding *et al.*, 2010).

Genus ***Tehamadinium*** Jan du Chêne *et al.*, 1986

Type species: Below, 1982a, as *Occisucysta brixii*.

Tehamadinium sp. cf. ***T. konarae*** Dodekova, 1992

Pl. 81, figs. A-C

cf. 1992 *Tehamadinium konarae* Dodekova, p.60-61, pl.10, figs.4-8.

Dimensions: (μm; 12 specimens measured)
Total length: 50 (61) 69
Total width: 42 (55) 72
Length of apical horn: 4 (6) 8
Max. length of septa / parasutural ornament: 2.5 (3) 4

Comparison: Specimens assigned to *Tehamadinium* sp. cf. *T. konarae* closely resemble *T. konarae* Dodekova, 1992, but differ in having a smaller size range and slightly more distinct paratabulation.

Previously reported range: *Tehamadinium konarae s.s.* was described from the Lower Oxfordian to Lower Kimmeridgian of Bulgaria (Dodekova, 1992).

Tehamadinium mediseptatum sp. nov.

Pl. 80, figs. A-L

Holotype and type locality: Pl. 80, fig. I-L, Jansz-3, Core, 2810mRT(c), GA sample no. 1631224, slide no. 5, England Finder co-ordinates: N28, CPC no. 40980.

Derivation of name: From *medius* (Latin): "middle, midmost, mid; intervening, central, neutral, intermediate", and *saeptum* (Latin): "fence" for the intermediate morphology of the parasutural ornament between spinose parasutural ridges and continuous parasutural septa.

Synopsis: Intermediate-sized, proximate cyst. Autophragm ambitus subspherical to slightly ovoidal. Gonyaulacacean fully paratabulation indicated by parasuturally aligned spines, distally linked by a fine, smooth trabeculum, and sometimes proximally by low ridges; intratabular areas densely covered with isolated spines, rarely proximally linked to form a pseudoreticulum. Ornament extends into a short apical horn. Precingular archeopyle, Type 2P; compound; opercular pieces free.

Diagnosis:
Shape: Spherical to subspherical.

Wall Relationships: Autophragm only.

Wall Features: Densely ornamented with trabeculate parasutural spines to septa and intratabular spines. Parasuturally aligned spines consistently distally linked by a fine, smooth

trabeculum to form delicate fence-like parasutural septa; spine proximal contacts vary from angular to largely curved, frequently proximally coalescing into low parasutural ridges. Intratabular areas densely covered with isolated spines of equal length as parasutural septa, rarely proximally linked to form a pseudoreticulum, very rarely forming concentric ridges, particularly on the ventral surface (pl. 80, fig. H). Ornament extends into a short, rounded apical horn.

Archeopyle: Precingular, Type $2P_{(2''+3'')}$; compound; opercular pieces free.

Paratabulation: Standard gonyaulacacean paratabulation fully expressed by parasutural ornament; formula: Xpr, 4', 6'', 6c, 6''', 1p, 1'''', 5s.

Paracingulum: Clearly indicated by parallel parasutural septa; internally subdivided into six paracingular paraplates; laevorotatory, offset by approximately its width.

Parasulcus: Longitudinal L-type; indicated by an elongate, shallow furrow with deep flagellar scar; may be fully subdivided by parasutural ornament or parasulcal paratabulation may be reduced.

Size: Intermediate.

Dimensions: (μm; 12 specimens measured)
Total length: 51 (64) 77
Total width: 50 (59) 71
Length of apical horn: 5 (7) 8
Max. length of septa / parasutural ornament: 3 (4) 6

Comparison: *Tehamadinium mediseptatum* is most similar to *T. daveyi* Jan du Chêne *et al.*, 1986, which differs in having thick, solid parasutural septa. The generic type species, *T. brixii* (Below, 1982a) Jan du Chêne *et al.*, 1986, has parasutures indicated by the alignment of distally connected arches but very rare to no intratabular spines. *T. dodekovae* Jan du Chêne *et al.*, 1986 differs in having a larger size range and fenestrate parasutural septa, and *T. evittii* (Dodekova, 1969) Jan du Chêne *et al.*, 1986 differs in having a larger size range and irregularly perforate parasutural septa with denticulate crests.

Tehamadinium mediseptatum is also very similar to figured specimens of both *Tehamadinium* sp. cf. *T. evittii* Helby *et al.*, 1988 (figs.19M-N; apparently with isolated intratabular processes) and *Tehamadinium?* sp. A Helby *et al.*, 1988 (figs.7A-B; apparently with proximally linked

intratabular processes) from New Zealand, however the absence of descriptions precludes detailed comparison. Each of the New Zealand species may correspond to extreme end-members of intraspecific variability of *T. mediseptatum*.

Previously reported range: If synonymous with *Tehamadinium* sp. cf. *T. evittii* Helby *et al.*, 1988, and/or *Tehamadinium?* sp. A Helby *et al.*, 1988 then Kimmeridgian to Tithonian of New Zealand.

Tehamadinium sp. cf. ***T. sousensis*** (Below, 1981) Jan du Chêne *et al.*, 1986

Pl. 81, figs. D-L

cf. 1981 *Occisucysta sousensis* Below, p.61-62, pl.8, figs.1a-b,2.

cf. 1986b *Tehamadinium sousensis* (Below, 1981) Jan du Chêne *et al.*, p.21 (emend. p.27-28).
Note: listed as *Tehamadinium sousense* in Fensome & Williams, 2004.

Dimensions: (µm; 12 specimens measured)
Total length: 51 (61) 74
Total width: 48 (58) 73
Length of apical horn: 3 (4.5) 8
Max. length of septa / parasutural ornament: 2 (3) 4

Comparison: Specimens assigned to *Tehamadinium* sp. cf. *T. sousensis* closely resemble *T. sousensis* (Below, 1981) Jan du Chêne *et al.*, 1986b, but differ in having a punctate to microfoveolate autophragm (rather than vacuolate) with more numerous intratabular spines.

Previously reported range: *Tehamadinium konarae s.s.* was described from the Aptian of Morocco (Below, 1981).

Genus ***Tenua*** Eisenack, 1958, emend. Sarjeant, 1968, Pocock, 1972 and Sarjeant, 1985

Type species: *Tenua hystrix* Eisenack, 1958.

Tenua monteilii sp. nov.

Pl. 82, figs. A-M, Pl. 110, fig. E

Holotype and type locality: Pl. 82, fig. J-M, Jansz-3, Core, 2810mRT(c), GA sample no. 1631224, slide no. 5, England Finder co-ordinates: R31/1, CPC no. 40987.

Derivation of name: Named in honour of Dr. Eric Monteil.

Synopsis: Small, proximate, subcircular to rounded-subpolygonal, strongly lenticular, variably circumcavate cyst. Endophragm and periphragm closely appressed over most of cyst; pericoel typically widest hypocystally. Periphragm alone forms numerous, non-tabular to very rarely penitabular, hollow to solid, narrow to broad, simple to deeply furcate, distally truncated spines, increasing in length and density circumferentially; dorso-ventral surfaces and paracingulum may be devoid of spines; ornament between spines finely punctate. Archeopyle apical, Type (tA), operculum free; parasulcal notch slightly offset to the left lateral side.

Diagnosis:

Shape: Subcircular to rounded-subpolygonal with flat, parallel apices; strongly lenticular as indicated by preferential preservational orientation.

Wall Relationships: Variably circumcavate with endophragm and periphragm closely appressed over most of cyst. Pericoel width variable; may be indiscernible; where visible, typically widest hypocystally; most apparent beneath spines where pericoel may extend into the hollow processes (pl. 82, figs. H, I).

Wall Features: Periphragm alone forms numerous, non-tabular to rarely penitabular spines. All spines typically distally blunt-ended, otherwise spines highly variable, including hollow or solid, narrow or broad, proximally sharply or largely curved, cylindrical or tapering stems, and distally simple, expanded or deeply bi- to trifurcate. Dorso-ventral surfaces and paracingulum may be devoid of spines; spines increase in length and density circumferentially. Spines distally truncated approximately equidistant from the endophragm except slightly shorter at the apex; individual spine length is relative to pericoel width, being shortest where pericoel is widest (pl. 82, fig. K). Ornament between spines finely punctate.

Archeopyle: Archeopyle apical, Type (tA), operculum free. Principal archeopyle suture zigzag; very short accessory archeopyle sutures rare.

Paratabulation: Standard gonyaulacacean paratabulation indicated by slightly zigzag principal archeopyle suture and rare, very short accessory archeopyle sutures; incompletely indicated by penitabular alignment of spines (pl. 82, figs. A-C); formula: 4', 6'', Xc, 6''', 1p, 1'''', Xs.

Paracingulum: May be evident by adcingularly aligned spines (pl. 82, fig. C), a broad band devoid of spines (pl. 82, fig. J), or rarely a shallow lateral indentation (pl. 82, figs. F, K).

Parasulcus: Indicated only by deep, broad parasulcal notch, slightly offset to the left lateral side.

Size: Small.

Dimensions: (µm; 12 specimens measured)
Endophragm length (with operculum): 39 (45) 48 (4 specimens)
Endophragm length (without operculum): 33 (40) 48
Endophragm width: 30 (39) 46
Max. length of ornament: 3 (3.5) 5

Comments: The two-walled nature of this species is not always apparent. When cavation is weekly developed the spines may appear to extend directly from an autophragm surface or be proximally interconnected by membranous septa; however the two wall layers are usually distinguishable at high magnification.

Comparison: Contrary to the emendment of Sarjeant, 1985, Courtinat *in* Fauconnier & Masure, 2004 states that *Tenua* Eisenack, 1958 possesses intratabular to sometimes penitabular ornament. Furthermore, Duxbury, 2002 (p. 78, during the retention of *Cerbia* Below, 1981) states that the mid-dorsal and mid-ventral areas of *Tenua* are essentially devoid of ornament. Therefore, this species is assigned to *Tenua* as the most suitable genus, despite differing from the generic description by being variably circumcavate.

Tenua monteilii differs to all published *Tenua* species in having evidence of two wall layers and variable circumcavation. This species is most similar to the generic type species, *T. hystrix* Eisenack, 1958a, which differs in being considerably larger and possessing an autophragm only. *Ampulladinium aiax* Mantle, 2009b is superficially similar, but differs in having an autophragm with or without an ectophragm, a smaller size range and shorter ornamentation elements.

Previously reported range: Oxfordian of New Zealand as "*Cyclonephelium* sp." of Wilson & Helby, 1987.

Genus ***Ternia*** Helby & Stover, 1987

Type species: *Ternia balmei* Helby & Stover, 1987.

Ternia balmei Helby & Stover, 1987

Pl. 83, figs. M-N

1987 *Ternia balmei* Helby & Stover, p.135-136,138-139, figs.2A-C, 3A-I, 4A-C, 5B, 6A-F, 7A-B.

Dimensions: (µm; 12 specimens measured)
Total length: 73 (100) 121
Total width: 55 (74) 100
Autophragm length: 61 (68) 87
Autophragm width: 38 (51) 60

Comments: Rare, favourably oriented Jansz-Io *Ternia balmei* specimens faintly suggest that the archeopyle may be epicystal, with the principal archeopyle suture immediately anterior to the paracingular trabeculum. This may be supported by some SEM figures in the original description (Helby & Stover, 1987, figs.3C, F); however more observations are required to confirm this interpretation.

This species range is restricted to the Bathonian to Mid-Callovian of Riding *et. al.* (2010), therefore the rare specimens encountered in the Jansz-Io preparations are interpreted to be reworked.

Previously reported range: Bathonian to Mid-Callovian of Australia and the Timor Sea (Helby & Stover, 1987; Helby *et al.*, 1987, 2004; Morgan *et al.*, 2002; Partridge, 2006a; Mantle, 2009b; Riding *et al.*, 2010).

Genus ***Tringadinium*** Riding & Helby, 2001e

Type species: *Tringadinium bjaerkei* Riding & Helby, 2001e

Tringadinium bjaerkei Riding & Helby, 2001e

Pl. 83, fig. A-F, Pl. 110, figs. C-D

2001e *Tringadinium bjaerkei* Riding & Helby, 2001e, p.128, 130-131, figs.10A-T, 11A-T.

Dimensions: (µm; 12 specimens measured)
Autophragm length: 20 (27) 32
Autophragm width: 20 (24) 29
Width at paracingulum: 11 (15) 18

Comments and Comparison: Minor intraspecific variability was observed amongst Jansz-Io *Tringadinium bjaerkei* specimens, mainly in the concentration of ornament, constriction at the paracingulum, and the size of the intratabular protuberances. Ornamented specimens with reduced intratabular protuberances may be difficult to separate from *Tringadinium comptum* Riding & Helby, 2001e which coexists with *T. bjaerkei*.

Jansz-Io specimens differ from the original description in possessing 7 precingular paraplates rather than 6 (pl. 83, fig. E) however re-examination of the type material would be necessary to ascertain if this is intraspecific variability or a specific characteristic.

Previously reported range: Upper-Callovian to Tithonian-Berriasian of Australia (Riding & Helby, 2001e; Mantle, 2009b; Riding *et al.*, 2010);
Kimmeridgian to Tithonian of New Zealand (Helby *et al.*, 1988, as "Gen. et sp. nov. B").

Tringadinium comptum Riding & Helby, 2001e

Pl. 83, fig. G-L, Pl. 110, figs. A-B

2001e *Tringadinium comptum* Riding & Helby, p.131, 133, figs.12A-T.

Dimensions: (µm; 12 specimens measured)
Autophragm length: 20 (24) 27
Autophragm width: 16 (21) 25
Width at paracingulum: 10 (14) 18

Comments and Comparison: Jansz-Io *Tringadinium comptum* specimens displayed intraspecific variability in the concentration and distribution of ornament, constriction at the paracingulum, and the slight development of intratabular protuberances. Specimens with reduced ornament and relatively well developed intratabular protuberances may be difficult to separate from *Tringadinium bjaerkei* Riding & Helby, 2001e which coexists with *T. comptum*.

Previously reported range: Mid-Callovian to Mid-Oxfordian of Australia (Riding & Helby, 2001e; Mantle, 2009b; Riding *et al.*, 2010).

Genus ***Tubotuberella*** Vozzhennikova, 1967, emend. Brideaux, 1977, Sarjeant, 1982, and Dodekova, 1990

Type species: *Tubotuberella rhombiformis* Vozzhennikova, 1967.

Tubotuberella apatela (Cookson & Eisenack, 1960b) Ioannides *et al.*, 1977, emend. Sarjeant, 1982

Pl. 84, figs. A-C

1960b *Scriniodinium apatelum* Cookson & Eisenack, p.249, pl.37, figs.12-13.

1969 *Psaligonyaulax apaleta (sic)* (Cookson & Eisenack, 1960b) Sarjeant, p.15.

1977 *Tubotuberella apatela* (Cookson & Eisenack, 1960b) Ioannides *et al.*, 1977, p.464; pl.5, figs. 6, 7. (Note: Illustrated specimens referable to *Tubotuberella rhombiformis* according to Sarjeant, 1982, p.42).

1977 *Glabridinium apatelum* (Cookson & Eisenack, 1960b) Brideaux, p.35-36.

1982 *Tubotuberella apatela* (Cookson & Eisenack, 1960b) Ioannides *et al.*, 1977, emend. Sarjeant, p.42.

Refer to Sarjeant, 1982 for additional synonymy.

Dimensions: (µm; 12 specimens measured)
Periphragm length: 66 (78) 93
Periphragm width: 40 (49) 61
Endophragm length: 48 (53) 59
Endophragm width: 40 (47) 60
Length of apical horn: 2.5 (5.5) 8
Length of antapical pericoel: 21 (31) 45

Previously reported range: Cosmopolitan: Callovian to Valanginian of Australia and Papua New Guinea (Cookson & Eisenack, 1960b; Wiseman, 1980; Davey, 1987, 1999; Burger, 1996; Mantle, 2009b; Riding *et al.*, 2010);
Oxfordian to Tithonian of New Zealand, (Helby *et al.*, 1988);
Mid-Bathonian to Valanginian of Europe (Sarjeant, 1969, 1972, 1979, 1982; Raynaud, 1978; Woollam, 1980; Riley & Fenton, 1982; Nøhr-Hansen, 1986; Brenner, 1988; Dürr, 1988; Smelror, 1988a; Prauss, 1989; Kunz 1990; Stancliffe, 1991; Dodekova, 1992; Riding &

Thomas, 1992; Poulsen, 1993; Fauconnier *et al.*, 1996; Huault, 1999; Riding *et al.*, 1999, 2010; Riding, 2005b);

Kimmeridgian to Tithonian of India (Jain *et al.*, 1984; Garg *et al.*, 2003);

Upper Kimmeridgian to Tithonian of Africa (Wheeler & Sarjeant, 1990; Jiang *et al.*, 1992; Schrank, 2005).

Tubotuberella dangeardii (Sarjeant, 1968) Stover & Evitt, 1978, emend. Sarjeant, 1982

Pl. 84, figs. D-I

1968 *Gonyaulacysta dangeardii* Sarjeant, p.226-227, pl.1, fig.21; pl.3, figs.8, 15; text-fig.3.

1977 *Dimidiadinium dangeardii* (Sarjeant, 1968) Brideaux, p.37-38.

1978 *Tubotuberella dangeardii* (Sarjeant, 1968) Stover & Evitt, p.197.

1981 *Dimidiadinium dangeardii* (Sarjeant, 1968) Lentin & Williams, p.83.

1982 *Tubotuberella dangeardii* (Sarjeant, 1968) Stover & Evitt, 1978, retained and emend. Sarjeant, p.42-43; pl.7, figs.3, 4, 9, 10; pl.8, figs.1, 2, 4-7; text-fig. 5.

Refer to Sarjeant, 1982 for additional synonymy.

Dimensions: (μm; 12 specimens measured)

Periphragm length: 63 (75) 95

Periphragm width: 45 (52) 64

Endophragm length: 42 (51) 63

Endophragm width: 42 (48) 58

Length of apical horn: 2.5 (8) 11

Length of antapical pericoel: 15 (24) 43

Comments: Some Jansz-Io specimens possess a broad, rounded antapical endohorn protruding into the hypopericoel (*e.g.*, pl.84, figs.E, G). Since the length of this protrusion is variable and frequently absent (*e.g.*, pl.84, fig.F), this feature is considered intraspecific variability.

Previously reported range: Cosmopolitan: Upper Callovian to Mid-Kimmeridgian of Australia, the Timor Sea and Papua New Guinea (Davey, 1987, 1999; Mantle, 2009b), refined to Basal Callovian to Mid-Oxfordian (inconsistent to Mid-Kimmeridgian) of Australia (Riding *et al.*, 2010);

Bajocian to Mid-Kimmeridgian of Europe and Russia (Sarjeant, 1968, 1979; Riley & Sarjeant, 1972; Erkmen & Sarjeant, 1980; Riding *et al.*, 1985, 1999, 2010; Porter, 1988; Riding & Thomas, 1988; Thomas & Cox, 1988; Courtinat, 1989; Prauss, 1989; Dodekova, 1990; Kunz 1990; Fauconnier, 1995; Huault, 1999; Borges *et al.*, 2011);

Lower Oxfordian to Mid-Kimmeridgian of The Middle East and Africa (Ashraf, 1979; Thusu & Vigran, 1985; Jiang *et al.*, 1992; El Beialy & Ibrahim, 1997; Ibrahim *et al.*, 2002; Kholeif *et al.*, 2004);
Tithonian of India (Kumar, 1986);
Oxfordian to Kimmeridgian of North America (Olmstead *et al.*, 1996);
Callovian of Argentina (Riding *et al.*, 2011).

Genus ***Valensiella*** Eisenack, 1963, emend. Courtinat, 1989

Type species: Deflandre, 1947b, as *Membranilarnax ovulum*.

Valensiella ovulum (Deflandre, 1947b) Eisenack, 1963, emend. Courtinat, 1989

Pl. 85, figs. A-L

1947b *Membranilarnax ovulum* Deflandre, p.9-10; text-figs.22-23.
1963a *Favilarnax ovulum* (Deflandre, 1947b) Sarjeant, p.720.
1963 *Valensiella ovulum* (Deflandre, 1947b) Eisenack, p.101.
1989 *Valensiella ovulum* (Deflandre, 1947b) Eisenack, 1963, emend. Courtinat, p.183.

Dimensions: (µm; 21 specimens measured)
Autophragm length (with operculum): 47 (51) 59 (10 specimens)
Autophragm length (without operculum): 40 (48) 60 (13 specimens)
Autophragm width: 32 (45) 50
Max. width of pericoel: 2.5 (4) 6

Comments: Jansz-Io specimens of *Valensiella ovulum* display significant intraspecific variability with respect to the autophragm and ectophragm thickness, pericoel width, paratabulation reflection, and the density and completeness of the reticulate ornamentation. Comparable variability was discussed by Valensi, 1953 (translated in Fensome *et al.*, 1995, p. 1935) who outlined four informal 'groups' to encompass the variety of morphotypes. Five similar groups were used during Jansz-Io quantitative analysis; however no stratigraphic benefit was derived from maintaining separate morphotypes, therefore all observed morphotypes are combined under the single broad species *V. ovulum*.

Contrary to the emendment of Courtinat, 1989, all observed specimens exhibited an ectophragm of variable thickness and entirety.

Comparison: Specimens attributed to *Valensiella ovulum* are most similar to *Valensiella* sp. A, which differs in having a smaller reticulum with subcircular to subpolygonal lumina. *Ellipsoidictyum* sp. A differs in never having an ectophragm.

Previously reported range: Cosmopolitan: Bathonian to ?Valanginian of Australia and the Timor Sea (Burger, 1996; Mantle, 2009b);
Upper Bajocian to Mid-Tithonian of Europe (Deflandre, 1947b; Sarjeant, 1962a & b, 1963a, 1968, 1972, 1979; Gocht, 1970; Erkmen & Sarjeant, 1980; Woollam, 1980; Nøhr-Hansen, 1986; Porter, 1988; Smelror, 1988a & b; Courtinat, 1989; Prauss, 1989; Kunz 1990; Poulsen, 1993, 1996; Fauconnier *et al.*, 1996; Riding, 2005b; Borges *et al.*, 2011);
Bathonian to Tithonian of The Middle East and Africa (Jiang *et al.*, 1992; Gitmez & Ertug, 1999; Ibrahim *et al.*, 2002; Kholeif *et al.*, 2004);
Middle to Late Jurassic of North America (Williams, 1975; Zotto *et al.*, 1987).

Valensiella sp. A

Pl. 86, figs. A-L

Description: Small to intermediate, lenticular, subspherical to ovoidal, proximochorate cysts. Hypocyst significantly longer than epicyst. Autophragm reticulate: interconnecting, non-tabular septa (<6 µm high) produce subpolygonal to subcircular lumina; lumina largest in the lateral pre- and postcingular areas and smallest within and around the parasulcus. Reticulum supports very thin, smooth ectophragm; very fragile, easily damaged. Parasulcus indicated by a prominent parasulcal notch and a broad longitudinal furrow with reduced ornament. Paracingulum vaguely indicated by slightly higher ornament adjacent to a shallow latitudinal furrow, forming small lateral bulges; laevorotatory, offset by approximately its width. Archeopyle apical, Type (tA), operculum free. Gonyaulacacean paratabulation incompletely indicated by free opercula, zigzag principal archeopyle suture, short accessory archeopyle sutures and slight variations in the reticulum and lumina size; epicystal paratabulation formula: Xpr, 4', 6''; remaining paratabulation indeterminate.

Dimensions: (µm; 12 specimens measured)
Autophragm length (without operculum): 46 (52) 60
Autophragm width: 40 (55) 70
Max. width of pericoel: 3 (4) 6

Comparison: *Valensiella* sp. A appears very similar to *Ellipsoidictyum fenestellum* Mantle, 2009b, but is described as having a reticulate ectophragm supported by numerous short, solid processes, rather than a thin, smooth ectophragm supported by a reticulate autophragm. These species may ultimately be shown to be synonymous, but are separated until the described differences can be clarified.

Genus ***Valvaeodinium*** Morgenroth, 1970, emend. Below, 1987b

Type species: *Valvaeodinium armatum* Morgenroth, 1970.

Valvaeodinium vermicylindratum Below, 1987b

Pl. 87, figs. A-I

1987b *Valvaeodinium vermicylindratum* Below, p.79-80, pl.25, figs.1-18.

Dimensions: (µm; 12 specimens measured)
Autophragm length: 48 (54) 63
Autophragm width: 21 (25) 32

Comments: Jansz-Io specimens are recorded as *Valvaeodinium vermicylindratum* due to the distinctive vermiculate spinose ornament and traces of paratabulation.

Comparison: *V. vermicylindratum* may intergrade with *Valvaeodinium spinosum* (Fenton *et al.*, 1980) Below, 1987b, which differs in having shorter, simple spinose elements; therefore may frequently be recorded as such in biostratigraphic reports.

Previously reported range: Oxfordian of New Zealand (Wilson & Helby, 1987 as "*Kylindrocysta* cf. *spinosa*"); Bajocian of Europe (Below, 1987b).

Genus ***Voodooia*** Riding & Helby, 2001d

Type species: *Voodooia tabulata* Riding & Helby, 2001d

Voodooia tabulata Riding & Helby, 2001d

Pl. 87, fig. K

2001d *Voodooia tabulata* Riding & Helby, p.95-97, figs.17A-B; figs.18A-O.

Dimensions: (μm; 3 specimens measured)
Autophragm length: 92 (97) 103
Autophragm width: 28 (30) 33
Length of antapical horns: 9 (11) 12

Comments: Very few specimens of this distinctive species have been observed in the Jansz-Io preparations. *Voodooia tabulata* has a recorded range of Mid- to Upper Callovian in Riding *et. al.* (2010), therefore specimens are interpreted to be reworked to this level.

Previously reported range: Mid- to Upper Callovian of Australia (Riding & Helby, 2001d; Morgan *et al.*, 2002; Helby *et al.*, 2004; Partridge, 2006a; Mantle, 2009a; Riding *et al.*, 2010).

Genus ***Wallodinium*** Loeblich Jr. & Loeblich III, 1968, emend. Riding, 1994

Type species: Cookson & Eisenack, 1960b, as *Diplotesta glaessneri*.

Wallodinium krutzschii (Alberti, 1961) Habib, 1972

Pl. 87, fig. J

1961 *Diplotesta krutzschii* Alberti, p.21, pl.7, figs.19-21; pl.12, figs.6-7.
1972 *Wallodinium krutzschii* (Alberti, 1961) Habib, p.378.

Dimensions: (μm; 12 specimens measured)
Periphragm length: 60 (79) 96
Periphragm width: 24 (27) 36
Endophragm length: 49 (55) 61
Endophragm width: 20 (24) 33

Previously reported range: Callovian to Barremian of Australia and the Timor Sea (Backhouse, 1988; Mantle, 2009b; Riding *et al.*, 2010); Oxfordian to Tithonian of New Zealand (Helby *et al.*, 1988); Oxfordian to Berriasian of Europe (Poulsen, 1993; Riding *et al.*, 1999);

Barremian of Europe (Alberti, 1961).

Genus ***Wanaea*** Cookson & Eisenack, 1958, emend. Fensome, 1981, and Riding & Helby, 2001b

Type species: *Wanaea spectabilis* Cookson & Eisenack, 1958.

Wanaea acollaris Dodekova, 1975, emend. Riding & Helby, 2001b

Pl. 88, figs. A-G

1975 *Wanaea acollaris* Dodekova, p.20-21, pl.2, figs.9-10; pl.3, figs.1-7, 9; text-fig.2.

1978a *Energlynia acollaris* (Dodekova, 1975) Sarjeant, p.14.

2001b *Wanaea acollaris* Dodekova, 1975, retained and emend. Riding & Helby, p.37.

Dimensions: (μm; 7 specimens measured)
Length of hypocyst: 61 (70) 75
Width of hypocyst: 70 (85) 98
Length of antapical horn: 4 (7) 11
Length of antapical horn extension: 0 (4.5) 6

Comments: Specimens assigned to *Wanaea acollaris* are consistent with the emendation of Riding & Helby, 2001b. Variability was observed in the extent of paratabulation expression, from paracingular ridges and isolated parasutures only (pl. 88, figs. A-B) to complete and detailed paratabulation, including the parasulcus (pl. 88, figs E-G). The deduced paratabulation formula is ?3pr, 4', ?1a, 6'', ?6c, 6''', 1p, 1'''', 5s, with two small flagellar marks between the ras and 1'' paraplates. The paratabulation formula is 'standard' gonyaulacacean, however the paratabular arrangement is unusual: the paratabulation is ventrally condensed, with markedly distorted paraplates with curved parasutures, presumably to produce the conical hypocystal shape. In particular, the 1'', 1''' and 2''' paraplates are very small and the 5'', 3''' and 4''' paraplates are large to compensate.

This is the first recorded occurrence of *Wanaea acollaris* in Australasia.

Previously reported range: Upper Bajocian to Lower Oxfordian of Europe (Dodekova, 1975; Drugg, 1978; Sarjeant, 1979; Woollam, 1980; Riley & Fenton, 1982; Porter, 1988; Prauss,

1989; Fauconnier, 1995; Fauconnier *et al.*, 1996; Riding *et al.*, 1999, 2010; Riding, 2005b; Borges *et al.*, 2011);

Mid-Bathonian to Lower Oxfordian of The Middle East (Gitmez & Ertug, 1999);

Upper Callovian to Lower Oxfordian of Africa (Thusu & Vigran, 1985; Ibrahim *et al.*, 2002 as *W. cf. acollaris*; Msaky, 2007);

Callovian of Argentina (Riding *et al.*, 2011).

Burger, 1996 recorded "*Wanaea indotata* (now *W. acollaris*)" from the ?Bathonian to Hauterivian of Australia's North West Shelf, however Burger, 1996 Text-fig. 2 shows the *W. indotata* Zone has been renamed the *W. acollaris* Zone, therefore the exact identification of this species is uncertain since specimens may be attributable to *W. indotata*.

Wanaea digitata Cookson & Eisenack, 1958, emend. Woollam, 1982

Pl. 89, figs. A-H

1958 *Wanaea digitata* Cookson & Eisenack, p.58, pl.9, figs.2-5.

1982 *Wanaea digitata* Cookson & Eisenack 1958, emend. Woollam, p.48, Fig.1Bi.

Dimensions: (µm; 16 specimens measured)

Length of hypocyst: 62 (70) 77

Width of hypocyst: 60 (86) 107

Thickness of hypocyst: 70 (83) 93 (4 specimens)

Max. width of posterior paracingular flange: 5 (9) 14

Max. width of anterior paracingular flange: 5 (7) 12

Length of antapical horn: 6 (11) 17

Comments: Observed specimens of *Wanaea digitata* display significant intraspecific variability with respect to ornamentation, principal archeopyle suture appearance, flange width, and development of an anterior paracingular flange.

Rare specimens display dense, granulate to verrucate ornament, predominantly on the hypocyst. Such specimens are interpreted to be morphological variants in response to environmental conditions.

The paracingular flange width is markedly variable, ranging from 5-14µm. Typically the characteristic three-part flange (proximal processes, medial trabeculum and distal processes) is observable, however rarely the proximal processes may be absent so that the distal processes

surmount a paracingular septa. Morphotypes with the narrowest flanges are commonly stratigraphically lower, and therefore useful for morphostratigraphy.

Many Jansz-Io specimens possess an anterior paracingular flange in addition to the characteristic posterior paracingular flange (pl. 89, fig. C-D, G-H). The anterior flange has a simpler and finer morphology, consisting of thin proximal processes distally linked by a narrow trabeculum, terminating level with the medial trabeculum on the posterior flange. The distal margin is typically smooth and entire, though may rarely exhibit slight, irregular protrusions or fine spines, or may very rarely be distally fenestrate, possibly due to mechanical damage. Occasionally the anterior flange distal margin and the posterior flange medial trabeculum appear to be laterally connected by tiny processes or a very thin, fenestrate membrane. The superimposition of the anterior and posterior flanges results in the finer anterior flange being obscured by the coarser posterior flange, and may be difficult to observe except on high magnification. Many specimens possess an irregular echinate to undulate principal archeopyle suture, which may be caused by the presence and distribution of the proximal process bases of the anterior paracingular flange.

Previously reported range: Cosmopolitan: Mid-Callovian to Upper Oxfordian of Australia (Cookson & Eisenack, 1958; Helby *et al.*, 1987, 2004; Morgan *et al.*, 2002; Partridge, 2006a; Mantle, 2009b), refined to Basal Callovian to Mid-Oxfordian of Australia (Riding *et al.*, 2010);
Callovian to Mid-Oxfordian of Papua New Guinea (Davey, 1987, 1999);
Oxfordian of New Zealand (Wilson & Helby, 1987);
Upper Callovian to Oxfordian of Europe (Sarjeant, 1968, 1972, 1979; Raynaud, 1978; Erkmen & Sarjeant, 1980; Woollam, 1980; Riley & Fenton, 1982; Porter, 1988; Smelror, 1988b);
Upper Callovian to Lower Oxfordian of Africa (Thusu & Vigran, 1985; Ibrahim *et al.*, 2002; Msaky, 2007);
Oxfordian to Tithonian of The Middle East (Gitmez & Ertug, 1999);
Upper Callovian of northern Canada (Johnson & Hills, 1973).

Wanaea indotata Drugg, 1978

Pl. 92, figs. A-B

1978 *Wanaea indotata* Drugg, p.74-75, pl.8, figs.11-14.

Dimensions: (µm; 12 specimens measured)
Length of hypocyst: 53 (71) 83
Width of hypocyst: 62 (78) 98

Max. width of flange: 1.5 (2.5) 4
Length of antapical horn: 4 (9) 14

Comparison: *Wanaea indotata* specimens with a densely 'fuzzy' paracingular fringe may intergrade with *Wanaea macula* sp. nov. Only specimens with amorphous foliate adcingular ornament are included in *W. indotata*, while specimens with a distally entire, mesh-like flange are included in *W. macula*.

Previously reported range: Lower Bathonian to Kimmeridgian (inconsistent to Valanginian) of Australia (Helby *et al.*, 1987, 2004; Morgan *et al.*, 2002; Partridge, 2006a; Mantle, 2009b), refined to Lower Bathonian to Mid-Oxfordian of Australia (Riding *et al.*, 2010);
Upper Callovian to Lower Oxfordian of Papua New Guinea (Davey, 1987);
Oxfordian of Africa (Msaky, 2007);
Bajocian to Callovian of Europe (Drugg, 1978; Riding *et al.*, 2010).

Wanaea macula sp. nov.

Pl. 90, figs. A-F, Pl. 91, figs. A-F

Holotype and type locality: Pl. 90, fig. D-F, Jansz-3, Core, 2841mRT(c), GA sample no. 1631255, slide no. 4, England Finder co-ordinates: M21/4, CPC no. 41019.

Derivation of name: From *macula* (Latin): "the mesh of a net" in reference to the characteristic reticulate mesh-like nature of the flange on this species.

Synopsis: Intermediate to large, acavate, proximate cyst. Hypocyst conical with a short, rounded antapical horn which may be slightly inclined; epicyst essentially flat; ambitus in apical view subcircular with a slightly indented parasulcus. Autophragm typically smooth, rarely sparsely microgranulate to 'fuzzy'; may be concentrated in patches, typically densest adcingularly. Paracingulum displays a prominent (4-11µm wide), irregularly reticulate to spongeous paracingular flange; distal margin entire, rarely with broad, angular projections possibly indicating paracingular gonal positions. Remaining gonyaulacacean paratabulation variably expressed by incomplete parasutural ridges to aligned grana. Archeopyle epicystal, Type E@ (Type (tAtP)@).

Diagnosis:

Shape: Conical hypocyst with a short, distally blunt and rounded antapical horn. Antapical horn typically parallel to the polar axis but may be slightly ventrally inclined. Epicyst flat to

slightly convex. Ambitus in lateral view triangular to subtriangular; ambitus in polar view subcircular to ovoidal, slightly ventrally indented at the parasulcus.

Wall Relationships: Autophragm only.

Wall Features: Prominent (4-11µm wide) paracingular flange comprised of an irregularly reticulate to spongeous mesh; may be thin, positioned on the posterior paracingular parasuture only, or thick, spanning the entire cingulum width, widest at the paracingular parasutures with a shallow medial furrow. Distal flange margin entire, formed by aligned reticulate to spongeous ornament or terminating in a narrow distal trabeculum. Flange width may be extended by broad, angular or rounded projections possibly indicating paracingular gonal positions. Remaining parasutures variably reflected by incomplete, smooth, narrow parasutural ridges to aligned grana. Intratabular areas typically smooth, rarely sparsely microgranulate to 'fuzzy' (as for *Wanaea indotata* Drugg, 1978); may be concentrated in patches, typically densest adcingularly, very rarely paraplate delineated (pl. 91, fig. D).

Archeopyle: Epicystal, Type E@ (also written Type (tAtP)@); typically attached ventrally; rarely detached due to mechanical damage. Principal archeopyle suture smoothly circular, immediately anterior to the anterior paracingular flange where present; accessory archeopyle sutures not observed.

Paratabulation: Consistently indicated by paracingular flange; remaining gonyaulacacean paratabulation incompletely and variably expressed by discontinuous parasutural ridges or aligned ornamentation; formula: ?3pr, 4', 6'', ?6c, 6''', 1p, 1'''', 5s. Paraplate 1'' is very small and paraplate 5'' is very large (pl. 91, fig. E) indicating a condensed ventral paratabulation arrangement as discussed for *Wanaea acollaris* Dodekova, 1975 above.

Paracingulum: Clearly indicated by prominent paracingular flange (described above) located on either the posterior paracingular parasuture only or both the posterior and anterior paracingular parasutures. Broad angular or rounded projections on the flange may indicate paracingular gonal positions (pl. 90, fig. E; pl. 91, figs. A-D).

Parasulcus: Consistently indicated by a shallow mid-ventral depression and interruption of the flange; variably indicated by incomplete parasutural ornament.

Size: Intermediate to large.

Dimensions: (µm; 14 specimens measured)

Length of hypocyst: 60 (77) 96 (11 specimens)
Width of hypocyst: 68 (90) 110
Thickness of hypocyst: 66 (73) 88 (5 specimens)
Max. width of flange: 4.5 (6) 11
Length of antapical horn: 6 (9) 12

Comments: Significant intraspecific variability was observed with respect to flange width, flange thickness, presence of angular to rounded gonal projections on the flange, extent of paratabulation, and density of intratabular ornamentation.

Angular to rounded gonal projections on the flange are interpreted as reflections of paracingular gonal points due to their consistent location, distribution and morphology between specimens where present. Individual specimens rarely possess projections at all paracingular gonal points. Specimens with the densest intratabular ornament are interpreted to be morphological variants in response to environmental conditions, as discussed for *Wanaea digitata* Cookson & Eisenack 1958 above. Conversely, flange thickness appears to increase with stratigraphic depth. Thick, spongeous morphotypes apparently intergrade with the older *Wanaea indotata* Drugg, 1978, and thin, finely reticulate morphotypes apparently intergrade with the younger *Wanaea talea* Riding & Helby, 2001b.

Comparison: *Wanaea macula* is differentiated from other species of *Wanaea* by the distinctive, irregularly reticulate to spongeous flange. Morphologically and stratigraphically this species is intermediate between *Wanaea indotata* Drugg, 1978 and *Wanaea talea* Riding & Helby, 2001b. *Wanaea indotata* differs in having amorphous 'fuzzy' paracingular ornament in place of a distally entire, spongeous to reticulate flange. *W. talea* has a thin, narrow flange, but is comprised of simple, slender processes distally connected by a continuous trabeculum. Riding & Helby (2001b, p.47) state that *W. talea* processes rarely bifurcate or interconnect, and that small irregular areas may occur within the flange, which are usually solid or sparsely to irregularly vacuolate. Similarly, rare *W. macula* specimens may have short segments of the flange that display simple, *W. talea*-style processes. All other *Wanaea* species are either cavate, have broad flanges, or are energlynioid forms without flanges.

Wanaea talea Riding & Helby, 2001b

Pl. 92, figs. C-D

2001b *Wanaea talea* Riding & Helby, p.45, 47, 49, figs.7C, 8A-I.

Dimensions: (µm; 1 specimen measured)
Length of hypocyst: 75
Width of hypocyst: 65
Max. width of flange: 7

Comments: Only a single specimen of *Wanaea talea* was recovered from the Jansz-Io preparations. This species is typically restricted to the very top of the *Wanaea spectabilis* zone. This specimen may either 1/ indicate down-hole contamination from stratigraphically younger sediments; 2/ be a highly degraded *Wanaea digitata* Cookson & Eisenack 1958 specimen with all distal digits removed from the paracingular flange; or 3/ represent the oldest record of *W. talea*. Down-hole contamination is considered unlikely in a core sample, especially considering no other contamination has been confirmed in the Jansz-Io preparations. A degraded *W. digitata* specimen seems improbable since, apart from being folded, the remainder of the cyst is relatively well preserved. Therefore this specimen may potentially represent the oldest record of *W. talea* to date.

Previously reported range: Upper Oxfordian of Australia (Riding & Helby, 2001b; Morgan *et al.*, 2002; Helby *et al.*, 2004; Partridge, 2006a), refined to Mid-Oxfordian of Australia (Riding *et al.*, 2010);
Oxfordian of Africa (Msaky, 2007).

Wanaea verrucosa Riding & Helby, 2001b

Pl. 92, figs. E-F

1987 "*Wanaea* sp. (granulate species)" Helby *et. al*., Fig.17B & C.
1996 "*Wanaea* sp. A "granulate species" of Helby *et. al*. 1987" Burger, pl.15, figs. A, B, K-M.
2001b *Wanaea verrucosa* Riding & Helby, p.49, 51, figs.9A-L.

Dimensions: (µm; 12 specimens measured)
Length of hypocyst: 56 (67) 75
Width of hypocyst: 60 (87) 116
Max. length of ornament: 0.2 (2) 4
Length of antapical horn: 5 (9) 14

Comments and Comparison: Damaged or poorly preserved specimens may be difficult to distinguish from reworked Bajocian specimens of *Dissiliodinium caddaense* (Filatoff, 1975)

Stover & Helby, 1987a, therefore only specimens have been recorded and measured that can be clearly identified as *W. verrucosa*.

Wanaea verrucosa is restricted to the Upper Bajocian to Lower Bathonian according to Riding *et. al.* (2010), therefore specimens recorded in the Jansz-Io sequence are interpreted to be reworked from Bajocian to Bathonian sediments. Specimens may be difficult to distinguish from poorly-preserved, reworked Lower to Mid-Bajocian specimens of *Dissiliodinium caddaense* (Filatoff, 1975) Stover & Helby, 1987a, therefore only specimens that can be clearly identified as *W. verrucosa* have been recorded and measured.

Previously reported range: Upper Bajocian to Lower Bathonian of Australia (Helby *et al.*, 1987, 2004; Riding & Helby, 2001b; Morgan *et al.*, 2002; Partridge, 2006a; Riding *et al.*, 2010).

Genus ***Wanneria*** Below, 1987a

Type species: *Wanneria misolensis* Below, 1987a.

Wanneria listeri (Stover & Helby, 1987a) Below, 1987a

Pl. 93, figs. A-C

1987a *Suessia listeri* Stover & Helby, p.121-122, 124, figs.21A-C, 22A-D, 23A-L.
1987a *Wanneria listeri* (Stover & Helby, 1987a) Below, p.77, 80.

Dimensions: (µm; 12 specimens measured)
Autophragm length: 30 (41) 48
Autophragm width: 39 (48) 64
Max. length of ornament: 2 (4) 6

Comments: This distinctive species known range is confined to the Late Triassic, therefore the rare specimens observed in the Jansz-Io preparations are interpreted to be reworked to this level.

Previously reported range: Late Triassic (Norian to Rhaetian) of Australia (Stover & Helby, 1987a; Helby *et al.*, 1987; Stover & Helby, 1987a; Riding *et al.*, 2010).

Genus ***Woodinia*** Riding & Helby, 2001d

Type species: *Woodinia pedis* Riding & Helby, 2001d

Woodinia bensonii Riding & Helby, 2001e

Pl. 93, figs. D-G, Pl. 110, fig. F

2001e *Woodinia bensonii* Riding & Helby, p.133,135-136, figs.13A-T.

Dimensions: (μm; 12 specimens measured)
Autophragm length: 24 (30) 38
Autophragm width: 20 (28) 35
Max. length of ornament: 0 (1) 2

Previously reported range: Uppermost Callovian to Oxfordian with a notable acme in Mid-Oxfordian of Australia and the Timor Sea (Riding & Helby, 2001e; Morgan *et al.*, 2002; Mantle, 2009b; Riding *et al.*, 2010).

***Woodinia?* sp. A**

Pl. 93, figs. H-R

Description: Small, proximate, strongly lenticular cysts. Autophragm only; large lateral post-cingular bulges produce a flat to slightly concave hypocyst creating a distinctive subpolygonal to rarely rounded-triangular ambitus; hypocyst typically rounded-rectangular with sub-parallel lateral margins; epicyst smoothly rounded to rounded-triangular. Non-tabular granulate to verrucate ornament, increases in length and concentration on the lateral post-cingular bulges or 'pads'. Archeopyle apical, Type (tA)@, attached ventrally at the as paraplate and frequently also the 6'' paraplate; deep accessory archeopyle sutures common. Standard gonyaulacacean paratabulation, epicystal formula: 4', 1a, 6''. Paracingulum rarely observed as a shallow indent on the lateral margins; hypocyst slightly longer than epicyst. Parasulcus offset to the left lateral side.

Dimensions: (μm; 12 specimens measured)
Autophragm length (with operculum): 39 (43) 48
Autophragm length (without operculum): 39 (43) 46 (6 specimens)
Autophragm width: 36 (41) 46
Max. length of ornament: 1 (1.5) 3

Comments: Intraspecific variability was observed primarily in the ambital shape. Rare specimens with an unoperated archeopyle have a rounded-triangular ambitus, whereas operation

of the archeopyle and development of deep accessory archeopyle sutures expands the epicyst to produce the distinctive 'boxy' subpolygonal ambitus.

Comparison: *Woodinia?* sp. A is questionably placed in *Woodinia* based upon similar morphological characteristics to *W. pedis* Riding & Helby, 2001d and *W. bensonii* Riding & Helby, 2001e. In particular the small cyst size, development of large lateral post-cingular bulges that produce a flat to slightly concave hypocyst, and the longest ornament concentrated on lateral bulges or 'pads'. This species differs from the generic *Woodinia* description in having a longer and broader epicyst producing a larger cyst size, evenly distributed non-tabular ornament over the majority of the cyst, an inconspicuous paracingulum, and a left laterally offset parasulcus. However, observed specimens of *W. bensonii* also appear to have a slightly left laterally offset parasulcus.

The rounded-triangular morphotype is most similar in ambital shape to *Ampulladinium? deltatum* sp. nov., which differs in having a consistently rounded-triangular ambitus with a flat to convex antapical margin, a typically free apical operculum, variable ornament of spines to short processes, and frequently possessing incomplete paratabulation, reduced ornament on the dorso-ventral surfaces, and a partial ectophragm.

Genus ***Yalkalpodinium*** Morgan, 1980
emend. Riding & Helby, 2001d

Type species: *Yalkalpodinium scutum* Morgan, 1980

Yalkalpodinium elangiana Riding & Helby, 2001d

Pl. 95, figs. A-H

2001d *Yalkalpodinium elangiana* Riding & Helby, p.101-102, figs.20A-P.

Dimensions: (µm; 6 specimens measured)
Endophragm length (with operculum): 56 (1 specimen)
Endophragm length (without operculum): 44 (51) 60
Endophragm width: 47 (53) 61
Periphragm length (with operculum): 64 (1 specimen)
Periphragm length (without operculum): 48 (57) 64
Periphragm width: 53 (60) 68

Comments: Observed specimens differ slightly from the original description in having a smaller cyst size than the type material.

Previously reported range: Callovian to Lower Oxfordian of Australia and the Timor Sea (Riding & Helby, 2001d; Mantle, 2009b; Riding *et al.*, 2010).

Yalkalpodinium playfordii Mantle, 2009b

2009b *Yalkalpodinium playfordii* Mantle, p.98, pl.7, figs.1-5, text-fig.1A-B.

Dimensions: (μm; 1 specimen measured)
Endophragm length (without operculum): 69
Endophragm width: 68
Periphragm length (without operculum): 81
Periphragm width: 74

Comments: Specimens matching the original description were very rare in the Jansz-Io preparations. It is not certain if these specimens are *in situ* or if they are reworked from Callovian sediments. However, *Yalkalpodinium playfordii* has a recorded range of Mid- to Upper Callovian in Riding *et. al.* (2010). Given previous evidence of Bathonian to Callovian reworking, the likelihood that these specimens are reworked is considered more probable.

Previously reported range: Mid- to Upper Callovian of Australia and the Timor Sea (Mantle, 2009b; Riding *et al.*, 2010).

Yalkalpodinium proteiformum sp. nov.

Pl. 94, figs. A-F

Holotype and type locality: Pl. 94, fig. C, D, Jansz-3, Core, 2858mRT(c), GA sample no. 1631272, slide no. 5, England Finder co-ordinates: L38/2, CPC no. 41038.

Derivation of name: After the Greek God *Proteus*, a god of the sea with the power of changing himself into different shapes, in reference to the intergrading continuum of morphotypes or forms attributed to this marine dinoflagellate species.

Synopsis: Intermediate-sized, lenticular cysts with subcircular to subpolygonal ambitus. Highly variable wall relationship: typically circumcavate endophragm and periphragm with variable low relief to coarsely spongeous ornament within pericoel; rarely ranging to spongeous differentiated autophragm when periphragm incomplete or absent exposing spongeous ornament. Paracingulum rarely indicated by increased pericoel width. Parasulcus indicated by prominent parasulcal notch and narrow, deep, ventral furrow. Archeopyle apical, Type tA or Type (tA); operculum free; gonyaulacacean paratabulation, epicystal formula: Xpr, 4', 6''.

Diagnosis:

Shape: Ambitus subcircular to subpolygonal; strongly lenticular (always observed in dorso-ventral orientation); hypocyst longer than epicyst. A single specimen with operculum in place shows a low, broad perihorn over a smoothly rounded endophragm.

Wall Relationships: Highly variable. Typically robust autophragm and thinner periphragm; circumcavate with a narrow pericoel, often widest at paracingulum. Rarely periphragm is absent, leaving a differentiated autophragm with coarsely spongeous ornament (pl. 94, figs. E-F).

Wall Features: Where membranes appressed, dorso-ventral surfaces frequently appear granulate to irregularly vacuolate. Where membranes separate, endophragm internally smooth, externally ornamented; periphragm externally smooth, internally ornamented. Intra-pericoel ornament frequently interconnects the membranes; consists of scattered granae, verrucae, baculae, simple processes, anastomosing low ridges, to coarsely pseudoreticulate to spongeous ornament. When periphragm is absent, autophragm typically possesses irregularly foveolate to spongeous ornament. Very rarely, broad periphragmal parasutural folds and ornamentation variation may incompletely indicate paratabulation, usually of the dorsal pre- or postcingular parasutures.

Archeopyle: Apical, Type tA or Type (tA); operculum free, possibly compound; principal archeopyle suture zigzag; short accessory archeopyle sutures very rare.

Paratabulation: Typically indicated by zigzag principal archeopyle suture only; rarely incompletely indicated by periphragmal folds and ornamentation variation. Gonyaulacacean paratabulation, epicystal formula: Xpr, 4', 6''; remaining paratabulation indeterminate.

Paracingulum: Rarely indicated laterally by increased pericoel width; very rarely indicated by latitudinal band of slightly reduced ornament.

Parasulcus: Longitudinal L-type; median position. Indicated by a prominent parasulcal notch and a narrow, deep, vertical furrow, typically more prominent hypocystally.

Size: Intermediate.

Dimensions: (μm; 14 specimens measured)
Endophragm length (without operculum): 57 (67) 78
Endophragm width: 60 (69) 80
Periphragm length (without operculum): 63 (74) 88
Periphragm width: 69 (78) 92

Comments: *Yalkalpodinium proteiformum* displays significant intraspecific variability with respect to wall relationships, ornamentation and paratabulation expression. All morphological types are included within this one species based upon observation of a complete continuum of intergrading morphotypes in the Jansz-Io preparations. Ornament elements supporting the periphragm are of highly variable morphology and distribution, therefore this species is interpreted as circumcavate rather than holocavate.

Comparison: This species is assigned to *Yalkalpodinium* Morgan, 1980 (emend. Riding & Helby, 2001d) as being an intermediate-sized, lenticular cyst typically possessing an endo- and periphragm which may have interconnecting ornament elements, faint paratabulation, and absent to reduced paracingular projections. *Y. proteiformum* is most similar to *Y. elangiana* Riding & Helby, 2001d, which differs in having more distinct paratabulation, possibly bearing antapical claustra, having fewer ornament elements interconnecting the endo- and periphragms, and never having spongeous ornament within the pericoel. *Y.? areolatum* (Cookson and Eisenack, 1960b) Riding & Helby, 2001d has a finely vermiculate to areolate circumferential ornament with numerous periphragm support structures to approach holocavation.

Y. proteiformum intergrades with intermediate to large specimens of *Yalkalpodinium?* sp. A, which is also extremely variable, but differs in being subspherical and effectively holocavate. This species also appears very similar to figured specimens of "*Yalkalpodinium?* sp. D" Helby *et al.*, 1988 (figs.11F, L) from New Zealand, however the absence of a description precludes detailed comparison.

Yalkalpodinium? sp. A

Pl. 95, figs. I-L, Pl. 96, figs. A-F, Pl. 97, figs. A-F

Description: Small to intermediate-sized cysts with robust endophragm and thinner periphragm; longer hypocyst than epicyst; apex with low, broad, subconical perihorn. Cysts may be subspherical to slightly lenticular; holocavate to circumcavate and variably suturocavate; and possess non-tabular to parasutural / penitabular and intratabular ornament. Periphragm smooth to scabrate; autophragm ornamented with scattered granae, verrucae, baculae and very fine to thick (<1µm), simple, tapered processes with sharply or largely curved proximal contacts that may align parasuturally or penitabularly, and may be proximally linked by low ridges delineating the paratabulation; circumcavate morphotypes appear coarsely foveolate to pseudoreticulate with subcircular lumina in dorso-ventral intratabular areas, with processes supporting the periphragm parasuturally and laterally. Paracingulum variably indicated by increased pericoel width with a narrow, medial furrow in the periphragm, and a band of reduced ornamentation with adcingularly aligned processes with or without proximal ridges. Parasulcus consistently indicated by prominent, deep parasulcal notch; variably indicated by a vertical furrow of reduced ornamentation, possibly enclosed by aligned processes with or without proximal ridges; kidney shaped flagellar scar rare. Standard gonyaulacacean paratabulation, formula: Xpr, 4', 6'', Xc, 6''', 1p, 1'''', Xs. Archeopyle apical, Type tA or Type (tA); operculum free, possibly compound; principal archeopyle suture zigzag; accessory archeopyle sutures not observed.

Dimensions: (µm; 12 specimens measured)
Endophragm length (with operculum): 58 (62) 65 (2 specimens)
Endophragm length (without operculum): 43 (54) 67
Endophragm width: 47 (54) 65
Periphragm length (with operculum): 64 (68) 72 (2 specimens)
Periphragm length (without operculum): 48 (60) 70
Periphragm width: 52 (60) 71

Comments: *Yalkalpodinium?* sp. A displays highly variable morphology in cyst size, shape, ornamentation and paratabulation expression. All morphotypes are included within this broad species due to the observation of a full continuum of intergrading morphotypes. In general, paratabulation expression becomes more pronounced with increased cyst size; however large specimens with reduced paratabulation intergrade with *Yalkalpodinium proteiformum* sp. nov. and hence may bias the distribution.

Comparison: The morphological variability of this species makes generic assignment problematic. Small, non-tabulate morphotypes appear similar to *Fibradinium variculum* Stover and Helby, 1987d, which differs in having a fibrous, vacuolate ectophragm and a small, subcircular to slightly angular archeopyle without mention of a prominent parasulcal notch.

Larger morphotypes, particularly subspherical specimens, could be assigned to *Chlamydophorella* Cookson & Eisenack, 1958. However *Chlamydophorella* is consistently holocavate, typically possesses regularly spaced processes of a single size and morphology without additional ornament elements, and is never lenticular with reduced ectocoel width on dorso-ventral surfaces.

This species is questionably placed within *Yalkalpodinium* which contains circumcavate to pseudo-holocavate species with variable ornament and structures interconnecting the membranes. This assignment is supported by the similarity to *Y. proteiformum* sp. nov., with which large, slightly lenticular, non-tabular specimens intergrades, but which differs in having a more lenticular cyst, more variable intra-pericoel ornament and faint paratabulation traces. *Yalkalpodinium?* sp. A appears very similar to figured specimens of "*Yalkalpodinium?* sp. B" Helby *et al.*, 1988 (figs.17F, S) from New Zealand, however the absence of a description precludes detailed comparison.

5.1.4 Additional Dinoflagellate Cyst Genera

The following additional dinoflagellate cyst genera were also observed in Jansz-Io preparations. They are represented either by individual or very few unidentifiable specimens, or multiple, highly morphologically variable specimens. Therefore these genera are not discussed in taxonomic detail.

Batioladinium? Brideaux, 1975
Canningia? Cookson & Eisenack, 1960b
Cassiculosphaeridia Davey, 1969
Cometodinium? Deflandre & Courteville, 1939
Cribroperidinium? Neale & Sarjeant, 1962
Cyclonephelium? Deflandre & Cookson, 1955
Hystrichosphaerina? Alberti, 1961
Korystocysta? Woollam, 1983
Phallocysta Dörhöfer & Davies, 1980
Sentusidinium Sarjeant & Stover, 1978
Trichodinium? Eisenack & Cookson, 1960

5.1.5 The *Contracysta* Complex

A complete continuum of morphotypes with intratabular processes is observed in the Jansz-Io preparations. Each of these species possesses evidence of a reverse wall relationship, including one or more of the indicative characteristics of insiderae, ornamented or thickened process bases, or under-curved processes (see following sections). This continuum includes:

- *Contracysta variantia* sp. nov., including proximate, proximochorate, phragmochorate and 'indeterminate' morphotypes;
- *Oligosphaeridium?* sp. cf. *O. complex* (White, 1842) Davey & Williams, 1966;
- *Oligosphaeridium?* sp. cf. *O. pulcherrimum* (Deflandre & Cookson, 1955) Davey & Williams, 1966 / *O. diluculum* Davey, 1982;
- *Perisseiasphaeridium?* sp. A;
- *Rigaudella aemula* (Deflandre, 1939) Below, 1982b; and,
- *Stiphrosphaeridium?* sp. A.

No clear division exists between *C. variantia* and the skolochorate morphotypes, which are differentiated according to the characteristics outlined in Table 5.4. However, apart from the reverse wall relationship, the skolochorate morphotypes are directly attributable to existing genera. Rather than retain skolochorate morphotypes in *C. variantia* on the basis of the wall relationship alone, the skolochorate morphotypes are attributed to the most morphologically similar genus in order to:

A. avoid confusion when comparing with described species of similar appearance; and,
B. maintain the morphological and stratigraphical integrity of existing skolochorate genera rather than erect a new genus containing species or morphotypes that are almost identical to existing species.

In the future, re-examination of these skolochorate genera may reveal that a reverse wall relationship is common to many, or all, of the currently attributed species. Therefore, these skolochorate morphotypes may ultimately be synonymous with previously described species. Similarly, additional chorate to skolochorate genera may also be recognised to possess a reverse wall relationship and be incorporated into the *Contracysta* complex.

Intergradation between skolochorate genera is well documented, with morphological complexes considered as potential phylogenetic lineages (*e.g.* Davey, 1982; Evitt, 1985; Stancliffe & Sarjeant, 1990; Poulsen, 1996). Determining the presence of a reverse wall relationship in existing genera may provide new insights into the phylogenetic lineages of skolochorate cysts.

Table 5.4: Differentiation of morphotypes attributed to the *Contracysta* Complex.

Species	Processes	Ring trabeculae	Interlinking trabeculae	Paracingular ridges
Contracysta variantia – proximate	Open, flat-lying over endophragm	Absent	Remnant threads to broad perforate membranes	Absent
Contracysta variantia – proximochorate	Proximally broad to narrow, distally broadly-flared to narrow bell-shaped	Rarely present	Remnant threads to broad perforate membranes	Very rarely present
Contracysta variantia – phragmochorate	Simulate to annulate complexes	Rarely present	Broad membranes	Absent
Oligosphaeridium? sp. cf. *O. complex*	Elongate, tubular, broad to narrow; minimal fenestration	Absent	Remnant threads common	Absent
Oligosphaeridium? sp. cf. *O. pulcherrimum* / *O. diluculum*	Elongate, tubular, broad to narrow; strongly fenestrate	Absent	Remnant threads common	Absent
Perisseiasphaeridium? sp. A	Elongate, tubular, broad to narrow; strongly fenestrate	Rarely present	Remnant threads common	Present
Rigaudella aemula	Broadly-flaring tubular to elongate, solid; strongly fenestrate	Present or absent	Threads, perforate membranes, to complex trabeculate networks	Absent
Stiphrosphaeridium? sp. A	Elongate, tubular, broad to narrow; strongly fenestrate	Present	Absent to remnant threads	Absent

Non-chorate generic and specific complexes were discussed by Backhouse, 2006 (p. 58) to "illustrate the problems of an overly rigid morphologic interpretation of taxa at species level, and the importance of considering a large population when circumscribing taxa". This statement is supported by the recent observations of Rochon *et al.*, 2009. These authors documented an intergrading 'complex' of 16 cyst-species attributable to 7 cyst-genera that were produced by a single population of the extant motile dinoflagellate *Gonyaulax spinifera*. The morphological variability related to process length and/or trabecular development is remarkably similar to that observed between *Contracysta variantia* morphotypes. Rochon *et al.* determined that the cyst variability was triggered by certain salinity conditions (25-30psu at 12°C).

All morphotypes in the *Contracysta* complex are considered to fall within intraspecific variability limits displayed for a single motile dinoflagellate population, as displayed by Rochon *et al.*, 2009. However, although cyst-speciation may not reflect true species boundaries, differentiation is useful where individual morphotypes have biostratigraphic significance. For the *Contracysta* complex, the skolochorate morphotypes are separated into existing genera as outline above. The proximate, proximochorate and phragmochorate morphotypes of *Contracysta variantia* are combined into a single cyst-species since these morphotypes do not individually have stratigraphic significance.

5.1.5.1 Process Development

The broad continuum of observed *Contracysta variantia* morphotypes has provided insights into the process development of *Contracysta* complex species. The interpreted method of process development accounts for the observed intergradation of proximate to skolochorate cysts (Figure 5.3 and Figure 5.4).

- The endocyst size ranges of *Contracysta* complex species are consistent across all morphotypes and endocyst size does not change during process development.
- Proximate 'closed' specimens (pl. 99, figs. A-B) reveal that the endophragm is initially closely surrounded by an entire, microperforate periphragm. Penitabular to intratabular granulate ornament (interpreted as primitive insiderae*) connects the membranes of all paraplates except the paracingulum and parasulcus, effectively producing a suturocavate cyst, although cavation may not be discernible.
- Thickening of the penitabular granulate rings widens the pericoel, inducing the periphragm to dissociate or 'open' along perisutures* (pl. 99, figs. C-D). Paracingular and parasulcal periplates* dissociate and are lost. Incomplete separation of adjacent periplates and residual fragments of the paracingular and parasulcal periplates form the foundation of interlinking trabeculae.
- Distal edges of the periplates lift away from the endophragm while intratabular areas remain in contact. This produces a single, proximate intratabular process on each endoplate* except for the paracingulum and parasulcus (pl. 99, figs. F-L; pl. 107, fig. A). The margins of the processes are angular and exactly simulate the associated endoplate. The proximal width and shape of each process is determined by the size of the contact zone between the two membranes. As the processes lift, adjacent grana of the granulate ring stretch to form short proximal insiderae (pl. 110, figs. H-J).
- As process height increases, there is a corresponding increase in the distance between distal process margins, interlinking trabecular length, insiderae length and prominence, and process fenestration (pl. 100, figs. A-H; pl. 107, fig. B). Large fenestrae may intersect the distal process margins masking their simulate* shape (pl. 100, fig. J). In extreme examples fenestrae extend to the process bases producing simulate to annulate process complexes reminiscent of *Systematophora* (pl. 100, figs. I-L).
- Further lengthening of the processes results in increasingly elongate, tubular processes (pl. 101, figs. A-I; pl. 110, fig. G). The simulate nature of the distal process tips becomes increasingly difficult to observe, as fenestrae and broken trabeculae may cause processes to appear digitate. The process width is determined by A/ the relative size of the intratabular contact zone (specimens with large, almost penitabular contact zones produce the widest, broadly-flaring processes); and B/ the size of the corresponding endoplate (the smallest endoplates possess the narrowest processes, which is useful for cyst orientation). Processes

frequently appear striate due to elongation of fenestrae and insiderae that fuse to the process surface (pl. 101, figs. H-I; pl. 111, figs. C-D).

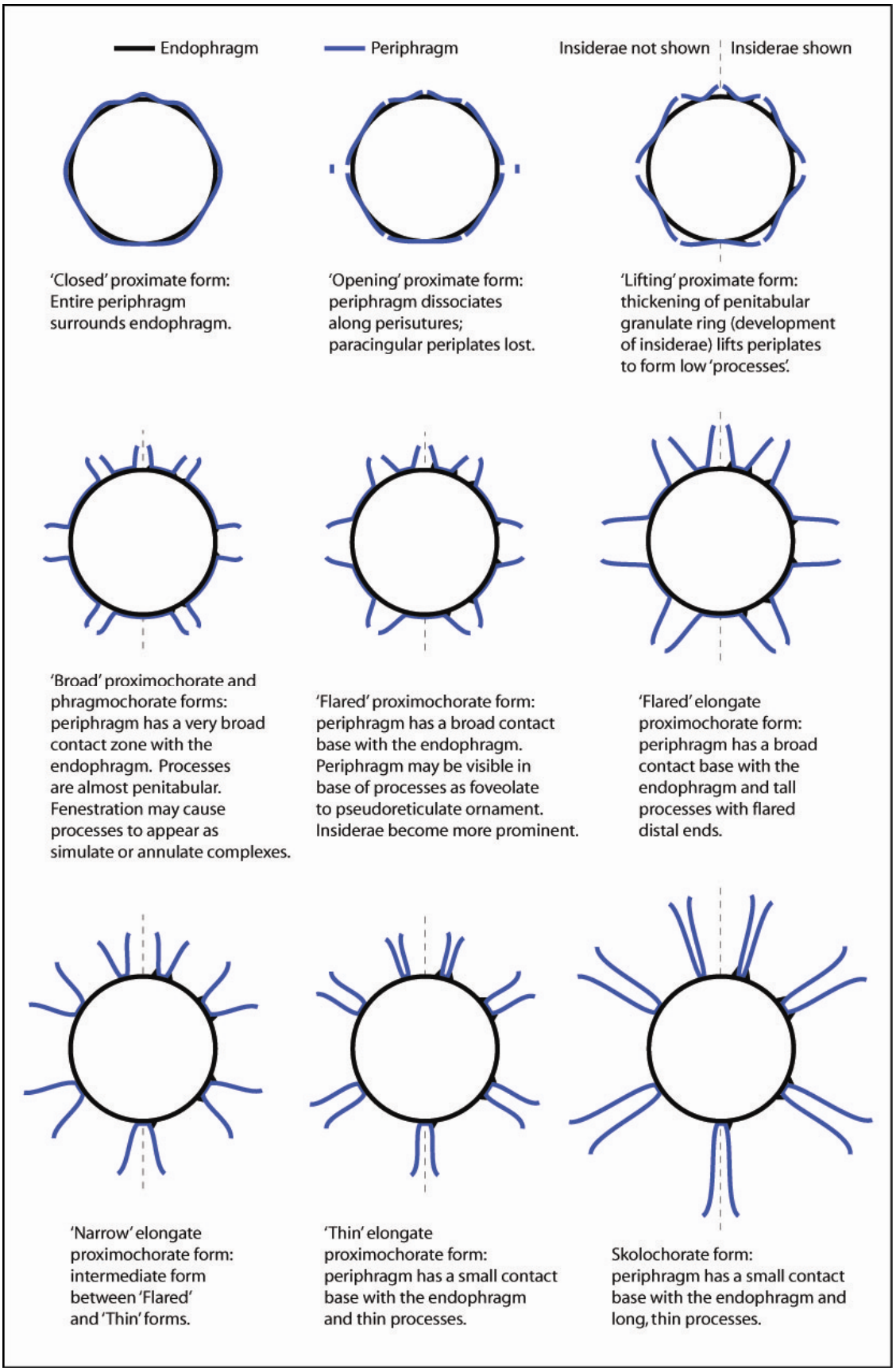

Figure 5.3: Progression of process development in *Contracysta* complex species

- Skolochorate morphotypes are produced by continued process stretching, as indicated by elongation of fenestrae and insiderae. Extension appears to be restricted to the process shafts, with the process bases constrained by their intratabular contact zones and distal tips by the original periplate size. This results in process shafts being medially constricted, producing the proximal and distal tapering which gives the impression of a 'normal' wall relationship.

* Refer to the glossary of introduced terms in Chapter 5.1.2.

The process development interpretation presented here was developed after the examination of over 500 well-preserved specimens of all *Contracysta* complex morphotypes. This centrifugal method of process development (processes extending radially outwards) is independently supported by recent research into the encystment of live dinoflagellate cultures (*e.g.* Kokinos & Anderson, 1995; Lewis & Hallet, 1997; Zonneveld & Susek, 2007; Mertens *et al.*, 2009; Rochon *et al.*, 2009). In particular, Mertens *et al.*, 2009 (p. 67) observed viscoelastic dinosporin stretching out in a radial direction during process formation on extant *Lingulodinium machaerophorum* cysts. Evidence of process stretching was preserved on *L. machaerophorum* cysts as proximal process striations, similar to the striations and insiderae observed in *Contracysta*-style processes.

However, evidence for both centrifugal and centripetal methods of skolochorate process formation exists in the fossil record. Evitt, 1985 (p. 77; Figure 4.3 I-K) discussed an undescribed *Hystrichokolpoma*-like cyst, where intraspecific variability ranges from cavate specimens with a nearly spherical pericyst and very wide pericoel, to skolochorate specimens with well developed intratabular processes. In this case the intratabular processes are formed by the periphragm centripetally collapsing onto the endophragm except in intratabular areas. These processes can be differentiated from *Contracysta*-style processes by being distally closed.

Therefore, the *Contracysta*-style, centrifugal method of intratabular process development presented here is not believed to be representative of all skolochorate cysts. Determining the method of process development, and hence the presence of a reverse wall relationship, may provide new insights into the phylogenetic lineages of skolochorate cysts.

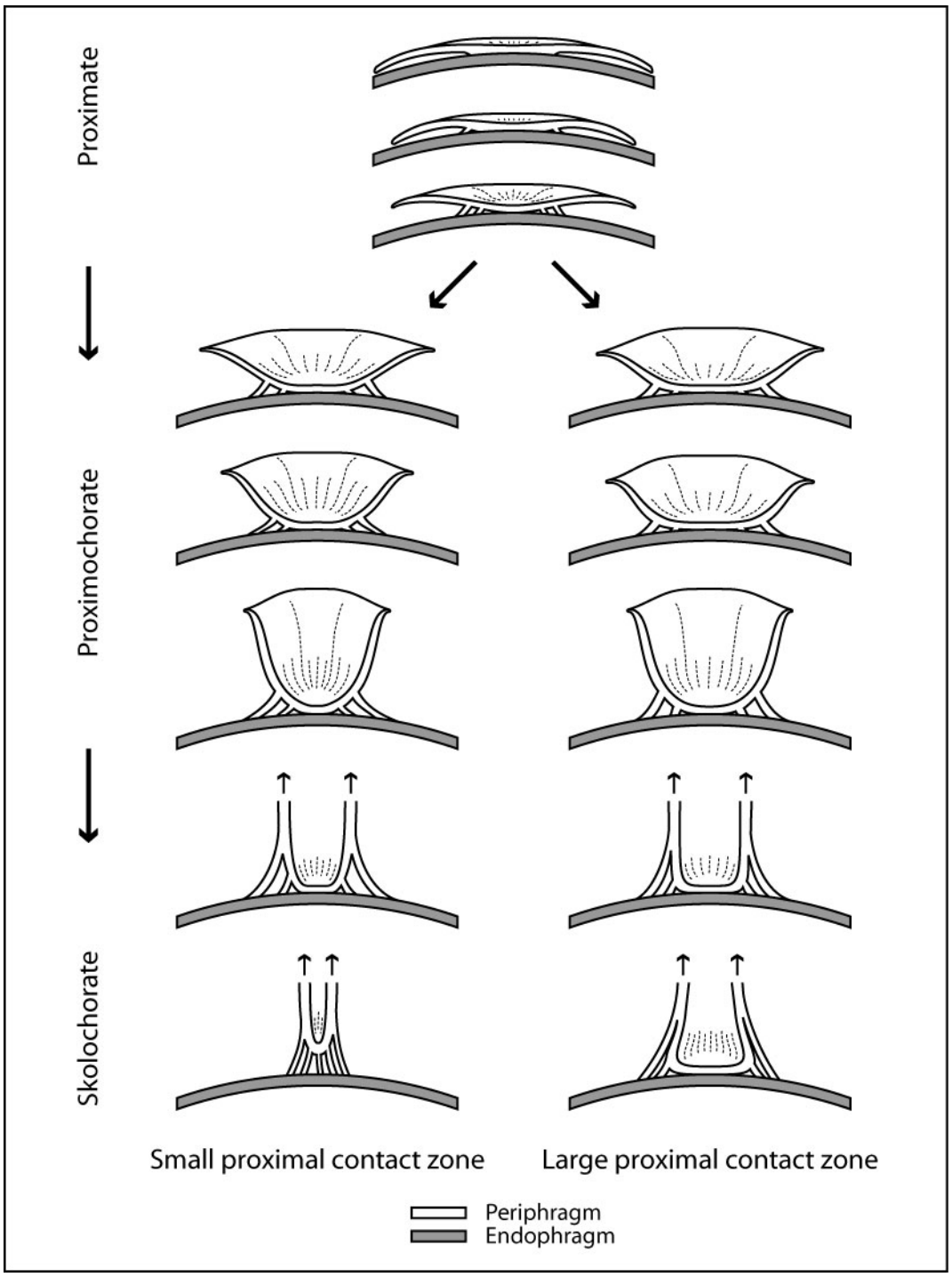

Figure 5.4: Process development and process morphology in *Contracysta* complex species. This method of process development results in the variety of *Contracysta* complex morphotypes represented in Figure 5.3.

5.1.5.2 'Reverse' Wall Relationship

The method of process development outlined above indicates that *Contracysta* complex morphotypes possess an opposite (or 'reverse') wall relationship to that typically described for similar skolochorate genera.

The typical (or 'normal') wall relationship for *Oligosphaeridium, Perisseiasphaeridium* and *Stiphrosphaeridium* (as described in the compilation of selected chorate genera by Fauconnier & Masure, 2004) is a periphragm closely appressed to the endophragm forming a two-layered central body except where the periphragm alone forms processes. The same wall relationship is presented for *Hystrichokolpoma*, however *Rigaudella* is stated to possess an autophragm only.

A 'reverse' wall relationship (as observed through the process development of *Contracysta* complex morphotypes) is where the endophragm alone forms a single-layered central body and the periphragm alone forms processes, with the processes only appressed to the central body in intratabular areas and anchored by insiderae (Figure 5.5).

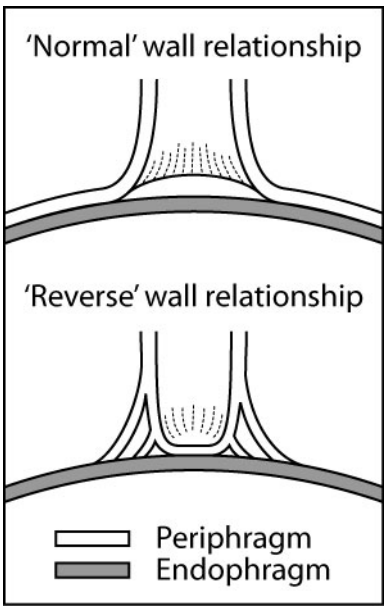

Figure 5.5: 'Normal' versus 'Reverse' wall relationship. 'Normal' is an endophragm and periphragm closely appressed forming a two-layered central body except where the periphragm alone forms processes. 'Reverse' is where the endophragm alone forms a single-layered central body and the periphragm alone forms processes, with the processes appressed to the central body in intratabular areas and anchored by insiderae.

The main evidence for a reverse wall relationship is:

1. **Internally ornamented process bases:** the microperforate to fenestrate periphragm produces a punctate (may appear microgranulate) to foveolate ornament on intratabular contact zones in clear contrast to the smooth to scabrate endophragm of the central body. This is most clearly observed in proximate to proximochorate morphotypes (pl. 98, fig. B; pl. 99, figs. D, F; pl. 100, figs. A, C, H; pl. 111, fig. G). Skolochorate morphotypes rarely exhibit foveolate internal process bases (pl. 103, fig. D; pl. 107, fig. H), and usually display proximally thickened internal bases (pl. 104, fig. F; pl. 106, fig. C) which may be reduced to a thickened ring (pl. 105, fig. D).
2. **'Under-curving' process bases:** the periphragm is often observed to curve beneath the process bases. Proximochorate morphotype processes frequently appear to rest on the

endophragm surface like bowls (pl. 98, fig. D; pl. 100, fig. B; pl. 107, fig. B; pl. 110, fig. J). Skolochorate morphotypes with thickened process bases may rarely display a distinct demarcation line between the endo- and periphragms which can be seen by TLM (pl. 107, figs. E, G). Under-curving is most apparent when insiderae are sparse, highlighting the periphragmal curvature and revealing an inwardly-curving acute angle at the junction of the endo- and periphragms (pl. 103, fig. E; pl. 107, figs. C, E-G; pl. 111, figs. E, H, I).

3. **Insiderae:** root-like insiderae apparently assist in securing the processes to the endophragm. On proximochorate morphotypes insiderae appear as a 'fringe' of fibres surrounding each process proximally (pl. 100, fig. F; pl. 110, figs. H-J; pl. 111, figs. C, D). On skolochorate morphotypes the insiderae usually appear as long, thin strands stretching between the lower portion of each process and the adjacent endophragm surface (pl. 107, figs. C, E), though they may anastomose to form 'buttress' insiderae (as in buttress-roots; pl. 111, fig. I) or coalesce into perforate 'aprons' (pl. 111, fig. E). If insiderae completely coalesce, the insiderate origin may be difficult to determine and the specimen may appear to have a 'normal' wall relationship (pl. 111, fig. F). In plan view, insiderae produce an irregular radial pattern extending from the proximal process bases onto the endophragm surface (pl. 107, figs. H, I).
4. **Striate processes:** striations may be faint to distinct. They are formed as processes stretch, by elongation and narrowing of periphragmal fenestrations, and elongation of insiderae which may appress the process shaft (pl. 101, figs. H, I; pl. 102, fig. F; pl. 111, figs. C, E).

The most convincing evidence for a reverse wall relationship is where a process formed by the under-curving periphragm is disconnected from the endophragm completely and is only anchored to the central body by insiderae (pl. 107, fig. D). Insiderae are the most consistent and distinctive evidence for a reverse wall relationship, often visible when other indications of a reverse wall relationship are masked by poor preservation or process shape. For example, narrowing of the medial process shafts during stretching often causes insiderae to appress to process shafts, concealing the under-curving periphragm, and produces a largely curved proximal contact, giving the appearance of a 'normal' wall relationship (pl. 107, fig. F). However, the presence of insiderae extending onto the endophragm surface, along with thickened process bases and striate shafts, enable identification of the 'reverse' wall relationship.

Based on these observations, cysts with a 'reverse' wall relationship consist of a central body composed of an endophragm only, except where the process-forming periphragm is proximally attached to the endophragm surface in intratabular positions. Proximally the periphragm curves under each process, so the internal process bases are lined by both the endophragm and periphragm. The processes are anchored to the endophragm by root-like insiderae (Figure 5.6).

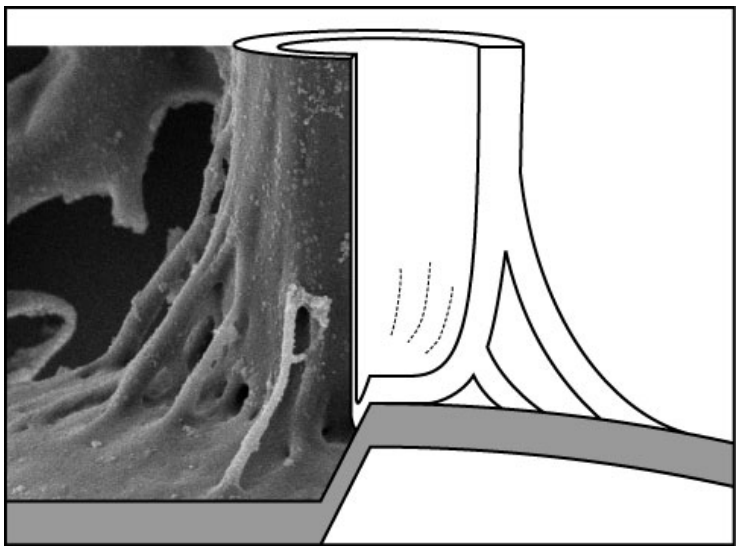

Figure 5.6: Cut away representation of the 'reverse' wall relationship

Skolochorate cysts with a reverse wall relationship are interpreted to have arisen from suturocavate gonyaulacacean dinoflagellate cysts, similar to *Gonyaulacysta centriconnata* and *Pentadinium* spp. (Figure 5.7 top). As demonstrated by the method of process development above, proximate *Contracysta* complex morphotypes initially resemble a suturocavate cyst, then transform into a cyst with intratabular processes when perisutural dissociation results in the isolation of each periplate (Figure 5.7 base).

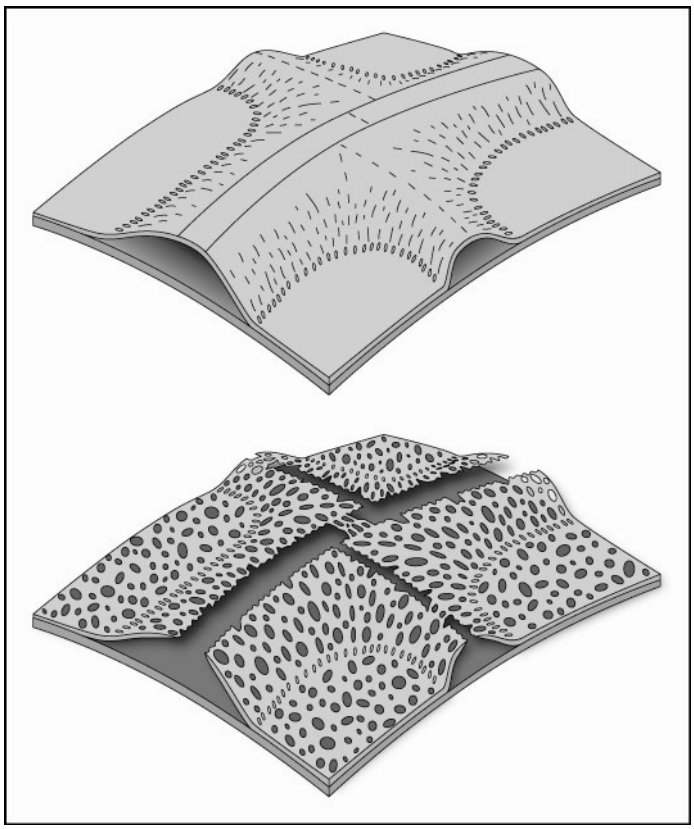

Figure 5.7: Comparison of wall of *Contracysta variantia* sp. nov. to suturocavate cysts, *e.g. Pentadinium.* Note the intratabular contact of the endophragm and periphragm, and separation of the periphragm along the parasutures resulting in intratabular processes. Incomplete periphragmal parasutural separation results in trabeculae between adjacent processes. (*Pentadinium* image [top] modified after Evitt, 1985, fig. 7.5S.)

A reverse wall relationship has not previously been reported in skolochorate cysts. However, some genera and individual species figured in the literature clearly show insiderae, providing evidence that other genera may also possess this wall relationship. The most notable examples are *Kilwacysta* Schrank 2005, and some *Oligosphaeridium* Davey & Williams 1966 and *Perisseiasphaeridium* Davey & Williams 1966 species (*e.g. O. pulcherrimum sensu* Backhouse 1988, *O. swanense* Riding & Helby, 2001f and *P. ingegerdiae* Nøhr-Hansen 1986). Observed *Contracysta* complex morphotypes intergrade with each of these taxa, including:

1. morphotypes that display deeply fenestrate processes similar to *Kilwacysta* spp. and *O. pulcherrimum sensu* Backhouse 1988 and *O. swanense*; and,
2. morphotypes reminiscent of *P. ingegerdiae* that show low cingular protrusions or ridges but lack the typical, true cingular processes of that species.

These intergrading morphotypes strongly support a close phylogenetic relationship between *Contracysta* complex morphotypes and these published taxa.

5.1.5.3 Trabeculum Development

Significant variability is observed in the *Contracysta* complex with respect to interlinking trabeculae. Variability includes:

- individual, fine threads that may be partially formed or broken (pl. 101, figs. A, G; pl. 102, figs. E-F; pl. 103, fig. B);
- thin, membranous ribbons (pl. 99, fig. J; pl. 104, figs A-F);
- converging and anastomosing threads that may form complex trabeculate networks (pl. 98, figs. A, F; pl. 99, fig. D; pl. 100, fig. E; pl. 105, figs. E-F); and
- broad, perforate membranes (pl. 105, figs. A, D).

Interlinking trabeculae may extend between very few processes or all processes on an individual specimen. Broken trabeculae are common and appear as elongate digits or irregular tendrils extending from distal process tips (pl. 100, figs. C, G; pl. 102, figs. D, F), or wider membranes that cause the processes to appear distally asymmetrical (pl. 101, fig. H; pl. 103, fig. A; pl. 111, fig. D). The trabeculae may interconnect:

1. processes on adjacent paraplates (pl. 98, fig. A; pl. 102, fig. E; pl. 104, figs. A-F);
2. processes across the paracingulum or parasulcus which are not on physically adjacent paraplates (*e.g.* pl. 98, fig. A, F; pl. 99, fig. D; pl. 100, fig I; pl. 105, figs. A-D); and,
3. very rarely, distal process tips to the endophragm surface (pl. 101, fig. C; pl. 103, figs. C, F).

The progression from proximochorate to skolochorate *Contracysta* complex morphotypes has enabled the following interpretation of the origin and development of interlinking trabeculae in skolochorate cysts:

- Where trabeculae link processes on adjacent paraplates, the location of trabeculae appears to be the result of incomplete separation of adjacent periplates (pl. 98, fig. A; pl. 99, fig. J).
- Trans-cingular or -sulcal trabeculae frequently occur at the same locations on numerous specimens. These locations appear to coincide with gonal positions of paracingular and parasulcal periplates. These trabeculae may be produced by irregular tearing or disintegration of the perforate paracingular and parasulcal periplates during perisutural dissociation resulting in the connection of non-adjacent periplates (pl. 98, figs A, F; pl. 99, fig. D; pl. 105, fig. A).
- Trabeculae that tether the distal process tip to the endophragm surface are extremely rare. These 'tether' trabeculae typically anchor to a paracingular or parasulcal endosuture*, though rarely attach to other endosutures. Tether trabeculae may be formed by the fusion of a periplate fragment with the endophragm surface, similar to insiderae (pl. 101, fig. C; pl. 103, figs. C, F).

In each instance, the positions of trabeculae appear to be determined by the incomplete or irregular dissociation of the perisutures. Where periplates remain connected, these periplate fragments stretch or grow concurrently with process development to form interlinking trabeculae. Therefore, the number and location of trabeculae appear to be established at the time of periplate dissociation in the proximate cyst development phase.

* Refer to the glossary of introduced terms in Chapter 5.1.2.

5.2 ACRITARCHS

Acritarchs are the fossilised cysts of aquatic unicellular protists of unknown phylogeny (Strother, 1996, p. 81). As such, no detailed systematic lineage can be reproduced. This study divides the observed acritarchs into two broad groups as outlined in Backhouse (1988, p. 51): Spinose Acritarchs for small spinose forms; and Non-spinose Acritarchs for the remaining acritarch genera.

5.2.1 Spinose Acritarchs

Spinose acritarchs as a broad group are useful environmental indicators as they may dominate near-shore, restricted marine or brackish environments (Wall, 1965; Sarjeant, 1968; Stancliffe & Sarjeant, 1990). The large diversity of observed forms determined that identification to species level was impractical. Therefore spinose acritarch occurrences are recorded in the broad groups of *Veryhachium* Deunff, 1954, *Michrystridium* Deflandre, 1937 and *Dorsennidium* Wicander, 1974 on the basis of spine number and cyst size. Of these, the most recognisable and proportionally most significant representative in the present counts is *Dorsennidium* sp. A. This species may be preferentially represented in the Jansz-Io samples due to the larger cyst size, and therefore may have been retained in the relatively coarsely sieved fraction while the smaller genera were mostly lost.

Genus ***Dorsennidium*** Wicander, 1974,
emend. Sarjeant & Stancliffe, 1994

Type species: *Dorsennidium patulum* Wicander, 1974.

***Dorsennidium* sp. A**

Pl. 112, figs. A-D

Description: Small to intermediate-sized acritarch with a subspherical to subpolygonal vesicle bearing 5-10 long, narrow, tapered, distally pointed spines, arranged in more than one plane. Spines proximally open to the vesicle interior. Eilyma apparently single-layered; smooth to scabrate. Spines of equal length to significantly longer than vesicle body.

Dimensions: (μm; 12 specimens measured)
Vesicle body length: 15 (18) 20

Vesicle body width: 15 (17) 21
Max. length of spines: 20 (25) 30
Number of spines: 5 (7) 10

Comments: Many *Dorsennidium* species have been formally described (refer to Stancliffe & Sarjeant 1996 for attributed species and comparisons). However Jansz-Io specimens are informally grouped into *Dorsennidium* sp. A since further speciation is unnecessary for the stratigraphic purposes of this study.

5.2.2 Non-spinose Acritarchs

Non-spinose acritarchs, although of questionable biologic affinity, may individually be of biostratigraphic importance akin to dinoflagellate cysts. As such, stratigraphically useful acritarch taxa are recorded here and described in accordance with the dinoflagellate cyst conventions outlined above and using acritarch-specific terminology where applicable.

Acritarch Gen. et. sp. indet. A

Pl. 112, figs. E-F

Description: Small, spherical, proximate vesicle. Eilyma single-layered, very dark, with strongly fossulate to corrugate ornament; ridges and fossulae typically <2µm wide, <8µm long and highly anastomosing. Rarely a possible excystment structure of a pale, narrow, subcircular to subangular irregular ring-shaped furrow (up to 30µm diameter) may be observed on one surface.

Dimensions: (µm; 7 specimens measured)
Total length: 21 (27) 35
Total width: 20 (26.5) 34

Comments: This unknown genus is classified as an acritarch in the absence of a clear archeopyle, paratabulation or other unequivocal dinoflagellate characteristics. Rare observations of a subcircular to subangular irregular fissure may be interpreted as an irregular archeopyle. However, the fissure outline is not consistent between specimens, and the outline does not correspond to any currently known dinoflagellate paratabulation arrangement; therefore a dinoflagellate affinity is not assumed at this stage.

Comparison: Acritarch Gen. et. sp. indet. A is most similar to the dinoflagellate cyst Gen. et. sp. indet. H herein, with dark wall and corrugate to fossulate ornament. However; Gen. et. sp. indet. H differs in having a clear dinoflagellate affiliation, with distinct peridinioid paratabulation and a probable combination Type (tA)@3I archeopyle.

Genus ***Fromea*** Cookson & Eisenack, 1958, emend. Yun Hyesu, 1981

Type species: *Fromea amphora* Cookson & Eisenack, 1958.

Comments: Jansonius, 1989, attributed *Fromea* as a dinoflagellate cyst. However, as stated by Jansonius, 1989 (p. 65), many authors retain this genus within Acritarcha because of the lack of clear paratabulation. Lentin & Williams, 1989 and 1993 recorded *Fromea* as a dinoflagellate; however, Williams *et al.*, 1998 and Fensome & Williams, 2004 included *Fromea* in Appendix A "for genera not considered to be dinoflagellates" (Fensome & Williams, 2004, p. 16). Therefore the current author is following common convention regarding attribution of this genus.

Fromea amphora Cookson & Eisenack, 1958

Pl. 112, figs. I-J

1958 *Fromea amphora* Cookson & Eisenack, p.56, pl.5, figs.10-11.

Dimensions: (μm; 12 specimens measured)
Total length: 75 (81) 89
Total width: 33 (42) 55
Width of pylome: 9 (12) 17

Comments: Observed *Fromea amphora* specimens varied from the type material only in the typically narrower body and pylome width.

Previously reported range: Hauterivian to Cenomanian of Australia (Cookson & Eisenack, 1958; Wiseman & Williams, 1974; Kemp, 1976; Morgan, 1980; Stover & Helby, 1987c & d); Mid-Oxfordian to Mid-Kimmeridgian of England (Thomas & Cox, 1988; Riding *et al.*, 1999); Kimmeridgian to Tithonian of India (Jain *et al.*, 1984)
The synthesis of Sarjeant, 1979 reported a cosmopolitan distribution from Mid-Kimmeridgian (to ?Tithonian).

Fromea fragilis **(**Cookson & Eisenack, 1962b) Stover & Evitt, 1978

Pl. 113, figs. A-B

1962b *Palaeostomocystis fragilis* Cookson & Eisenack, p.496-497, pl.7, figs.10-11.

1978 *Fromea fragilis* **(**Cookson & Eisenack, 1962b) Stover & Evitt, p.48.

Dimensions: (µm; 12 specimens measured)
Total length: 86 (103) 122
Total width: 56 (84) 96
Width of pylome: 18 (22) 27

Comments: Intraspecific variability was observed in cyst size, wall thickness and pylome smoothness. The majority of specimens were large, thin-walled with a ragged-edged pylome (pl. 114, fig. D). Rare, smaller, thicker-walled specimens with a smoothly rounded pylome (pl. 114, fig. C) were included in this species as morphological end members based upon observation of a morphological continuum between forms.

Comparison: *Fromea fragilis* is most similar to the dinoflagellate cyst *Escharisphaeridia?* sp. B herein, in size, shape and ornament but differing in clearly having a narrow, circular apical pylome rather than a wider, apical archeopyle with accessory archeopyle sutures. Poorly preserved specimens are difficult to differentiate, therefore only specimens with a clear apical pylome are assigned to *F. fragilis*.

Previously reported range: Aptian to Albian of Australia (Cookson & Eisenack, 1962b; Helby *et al.*, 1987);
Albian to Maastrichtian of North America (Firth, 1993; Harris & Tocher, 2003; Oboh-Ikuenobe *et al.*, 2007);
Aptian to Cenomanian of Canada (Manum & Cookson, 1964; Brideaux, 1971; Singh, 1971);
Coniacian to Maastrichtian of Russia (Lebedeva, 2006);
Maastrichtian of Europe (Schiøler *et al.*, 1997).

Fromea tornatilis (Drugg, 1978) Lentin & Williams, 1981

Pl. 112, figs. G-H

1978 *Palaeostomocystis tornatilis* Drugg, p.71-72, pl.7, figs.4-6.

1981 *Fromea tornatilis* (Drugg, 1978) Lentin & Williams, p.107.

Dimensions: (µm; 3 specimens measured)
Total length: 54 (61) 72
Total width: 50 (57) 66
Width of pylome: 10 (10) 11

Previously reported range: Cosmopolitan: Bathonian to Lower Oxfordian of Europe (Drugg, 1978; Riley & Fenton, 1982; Smelror, 1988a & b; Kunz 1990; Stancliffe, 1991; Riding *et al.*, 1999; Riding, 2005b; Borges *et al.*, 2011);
Bajocian to Tithonian of The Middle East (Gitmez & Ertug, 1999).

Genus ***Nummus*** Morgan 1975, emend. Backhouse, 1988

Type species: *Nummus monoculatus* Morgan 1975

Nummus apiculus Riding & Helby, 2001d

Pl. 113, figs. C-D

2001d *Nummus apiculus* Riding & Helby, p.102-104, figs.21A-P.

Dimensions: (µm; 12 specimens measured)
Total length: 55 (69) 80
Total width: 48 (63) 76

Comments: *Nummus apiculus* has a consistent range of Bathonian to Callovian with inconsistent occurrences to the Mid-Oxfordian in Riding *et. al.* (2010). Inconsistent occurrences may either reflect an intermittent extension of the taxon range or reworking. Evidence from other species suggests that Bathonian to Callovian sediments have been reworked into the Jansz Sandstone, therefore the likelihood that these specimens are reworked is considered more probable. Acmes of this species occur in underlying sediments and may account for the volume of specimens occurring in the Jansz-Io preparations.

Previously reported range: Bathonian to Callovian (inconsistent to Mid-Oxfordian) of Australia and the Timor Sea (Riding & Helby, 2001d; Mantle, 2009b; Riding *et al.*, 2010).

Nummus parvus Backhouse 1988

Pl. 114, fig. A

1988 *Nummus* sp. C Helby *et. al.* 1988, Figs.3S, 12K.

1988 *Nummus parvus* Backhouse, p.112, pl.43, figs.13-16, Fig. 33C.

Dimensions: (µm; 12 specimens measured)

Total length: 27 (40) 55

Total width: 21 (33) 46

Comments: The maximum dimension of observed specimens is slightly larger than the original type material, however are determined to be within acceptable limits for the species.

Previously reported range: Valanginian to Barremian of the Perth Basin, Australia (Backhouse, 1988); Callovian to Kimmeridgian of New Zealand (Helby *et al.*, 1988 as "*Nummus* sp. C").

Nummus similis (Cookson & Eisenack, 1960b) Burger, 1980b

Pl. 113, figs. E-F

1960b *Leiosphaeridia similis* Cookson & Eisenack, p.254-255, pl.38, fig.14.

1980b *Nummus similis* (Cookson & Eisenack, 1960b) Burger, p.275.

Dimensions: (µm; 1 specimen measured)

Total length: 78

Total width: 77

Comments: While Jansz-Io specimens do not clearly possess a flat, thickened equatorial rim with a disintegrated ventral surface, observed specimens are herein attributed to *Nummus similis* due to their similar appearance to the holotype (Cookson & Eisenack, 1960b, pl. 38, fig. 14) and figured specimens of Helby *et al.*, 1987 (Fig. 23F) and Helby *et al.*, 1988 (Fig. 4N).

Previously reported range: Upper Oxfordian to Barremian of Australia and Papua New Guinea (Cookson & Eisenack, 1960b; Burger, 1980b; Wiseman, 1980; Davey, 1987; Helby *et al.*, 1987; Backhouse, 1988; Morgan *et al.*, 2002; Partridge, 2006a); Oxfordian of New Zealand, (Helby *et al.*, 1988).

Genus ***Schizocystia*** Cookson & Eisenack, 1962b

Type species: *Schizocystia rugosa* Cookson & Eisenack, 1962b.

Schizocystia rara Playford & Dettmann, 1965

Pl. 114, figs. B-C

1965 *Schizocystia rara* Playford & Dettmann, p.160-161, pl.17, figs.67-69.

Dimensions: (µm; 1 specimen measured)
Hemicyst length: 30
Hemicyst width: 54

Previously reported range: Triassic (Rhaetian) to Early Jurassic of South Australia (Playford & Dettmann, 1965); Callovian of the Timor Sea (Mantle, 2009b); Bathonian to Callovian of Russia (Riding *et al.*, 1999).

Genus ***Triovalium*** gen. nov.

Refer to Addendum regarding recent reattribution.

Type species: *Triovalium attenuatum* gen. et sp. nov.

Derivation of name: From *trēs* (Latin): "three", and *ova* (Latin): "eggs", in reference to the three, ovoidal membranes arranged concentrically.

Diagnosis: Intermediate to large, proximate, cavate, strongly lenticular vesicles composed of three, concentrically arranged, ovoidal to ellipsoidal membranes. Eilyma smooth to faintly ornamented, devoid of spines, processes or projections. One or more dark, amorphous accumulation bodies common. Faint latitudinal and longitudinal folds common. No pylome or other vesicle opening observed.

Comments: In the absence of unequivocal dinoflagellate characteristics, such as an archeopyle or clear paratabulation, this genus is currently classified as an acritarch. However, the size, shape, presence of accumulation bodies and common longitudinal and latitudinal folds on this genus are suggestive of a dinoflagellate cyst affinity. Therefore, additional evidence may lead this genus to be reassigned in the future.

Comparison: No known acritarch genera or species are described as possessing three wall layers. Very few genera or species of known algal origin (such as dinoflagellate cysts) possess three or more distinct wall layers: the majority being Peridinioid genera or attributed species of *Cepadinium* Duxbury, 1983, *Chatangiella* Vozzhennikova, 1967, *Isabelidinium* Lentin & Williams, 1977, *Lasagniella* Brinkhuis *et al.*, 2000, *Luxadinium* Brideaux & McIntyre, 1975, *Manumiella* Bujak & Davies, 1983 and *Trithyrodinium* Drugg, 1967; and a single Gonyaulacoid dinoflagellate cyst genus, *Triphragmadinium* Van Simaeys *et al.*, 2005. Each of these examples differ from *Triovalium* gen. nov. in being clearly identifiable as dinoflagellate cysts.

Triovalium attenuatum sp. nov.

Pl. 114, figs. D-E

Refer to Addendum regarding recent reattribution.

Holotype and type locality: Pl. 114, fig. D, Jansz-3, Core, 2810mRT(c), GA sample no. 1631224, slide no. 5, England Finder co-ordinates: W23, CPC no. 41056.

Derivation of name: From *attenuatus* (Latin): "simply, without ornament" in reference to the thin, simple, unornamented membranes.

Synopsis: Intermediate-sized, proximate, cavate, strongly lenticular vesicles. Three, concentrically arranged, ovoidal eilyma; extremely pale, thin and easily folded or broken. Eilyma smooth to scabrate; faint latitudinal and longitudinal folds common. One or more dark, amorphous accumulation bodies common; one typically centrally located at the junction of latitudinal and longitudinal folds. No pylome or other vesicle opening observed.

Diagnosis:

Shape: Ovoidal; very strongly lenticular.

Wall Relationships: Three concentric eilyma; extremely pale, thin and easily folded or broken; middle body cavity (<6µm) typically slightly narrower than outer body cavity (<8µm).

Wall Features: Eilyma smooth to scabrate. Faint latitudinal and longitudinal folds may represent dinoflagellate cyst paracingulum and parasulcus. One or more dark, amorphous accumulation bodies common; one typically centrally located at the junction of latitudinal and longitudinal folds. No pylome or other vesicle opening observed.

Size: Intermediate.

Dimensions: (µm; 12 specimens measured)
Total length: 72 (85) 94
Total width: 49 (61) 76

Comments: As for the generic description, this species is currently classified as an acritarch in the absence of unequivocal dinoflagellate characteristics, such as a clear archeopyle or paratabulation. However, the size, shape, presence of accumulation bodies and common longitudinal and latitudinal folds on this genus are suggestive of a dinoflagellate cyst affinity. Therefore, this taxon may be reassigned in the future.

Comparison: No known acritarch genera or species are described as possessing three wall layers; therefore there are no directly comparative species. *Pterospermella* algal cysts have two wall layers of a robust central vesicle and a thinner outer vesicle with radial folds. All dinoflagellate cysts with three wall layers are clearly shown by their shape, paratabulation or archeopyle to be of dinoflagellate origin. *Triovalium attenuatum* vesicle size, shape and circumcavation is vaguely reminiscent of *Endoscrinium* (Klement, 1960) Vozzhennikova, 1967 and *Scriniodinium* Klement, 1957, which differ in having two walls only, faint to distinct paratabulation and a precingular Type P archeopyle. Within the Jansz-Io preparations *Triovalium attenuatum* is most similar to *Leberidocysta? strigosa* Mantle, 2009b in being strongly lenticular, pale, thin and unornamented. However, *L.? strigosa* differs in having a smaller size, subcircular ambitus, only two wall layers and a definite apical archeopyle.

Genus ***Wuroia*** Stover & Helby, 1987a

Type species: *Wuroia capnosa* Stover & Helby, 1987a.

Wuroia capnosa Stover & Helby, 1987a

Pl. 114, figs. F-G

1987a *Wuroia capnosa* Stover & Helby, p.129-130, fig.28A-D.

Dimensions: (µm; 1 specimen measured)
Total length: 128
Total width: 36

Comparison: This species is attributed to *Wuroia capnosa* rather than *Wuroia unciformis* Marshall, 1989 because the crescentic shape of Jansz-Io specimens is interpreted to be the result of folding. This species is not attributed to *Wuroia tubiformis* Marshall, 1989 due to the absence of a thickened rim surrounding a truncated apex.

Comments: This species range is restricted to the Mid-Callovian of Partridge (2006a-d) and Riding *et. al.* (2010), therefore the rare specimens encountered in the Jansz-Io preparations are interpreted to be reworked.

Previously reported range: Mid-Callovian of Australia and Papua New Guinea (Helby *et al.*, 1987; Stover & Helby, 1987a; Riding *et al.*, 2010).

5.3 SPORES AND POLLEN

Spores and pollen were frequently encountered in the Jansz-Io palynological samples, although this group does not constitute the main focus of this study and so are not discussed in systematic detail. However, the spore-pollen content was broadly examined to determine the stratigraphic origin of the sporomorph content.

Many taxa, such as *Alisporites similis, Araucariacites australis*, *Callialasporites dampieri*, *Dictyophyllidites harrisii, Classopollis torosa, Contignisporites cooksoniae* and *Cyathidites* spp. are long-ranging Mesozoic species consistent with the *Murospora florida* spore-pollen zone and an Oxfordian age.

Conversely, the presence of *Aratrisporites parvispinosus*, *Cycadopites stonei*, *Enzonalasporites vigens*, *Ephedripites macistriatus*, *Falcisporites australis*, *Minutosaccus crenulatus* and *Playfordiaspora velata* from the Triassic (Norian) *Minutosaccus crenulatus* Zone are clear evidence of reworking. A Norian age for this reworked material is supported by the rare occurrence of the Late Triassic dinoflagellate *Wanneria listeri*. Additionally, unidentified striate pollen, which commonly occur in the Permian, are often observed in these samples, providing circumstantial evidence for Permian reworking.

5.4 MICROFORAMINIFERAL TEST LININGS

5.4.1 Nomenclature

The organic (probably chitinous) linings of very small foraminiferal tests, known as 'microforaminiferal test linings' or 'palynoforaminifera', were frequently observed in the Jansz-Io palynological preparations. The presence of microforaminiferal test linings in palynological preparations is indicative of normal marine coastal environments and euryhaline conditions (Tyson, 1995). The high diversity of morphotypes prompted closer analysis of this infrequently studied group to determine their biostratigraphic utility within the Jansz-Io reservoir.

Formal classification was proposed by Mackó (1963) and Deák (1964), who introduced the suprageneric term 'Scytinascia' for microforaminiferal linings. This formal classification was rejected by Tappan & Loeblich (1965), although the term 'Scytinascia' remains in use by some authors (*e.g.* Courtinat & Méon, 1991). Pantic & Bajraktarevic (1988) erected the "Informal Division: Palynoforaminifera" in the foraminiferal classification scheme. However, this scheme was rejected by Stancliffe (1989) as "a separate and unnecessary classification scheme within foraminiferal systematics" because "microforaminiferal linings are the organic remains of very small Foraminifera which do not merit a separate formal classification". As an alternative, Stancliffe (1989) erected an informal 'descriptive' classification system to encourage consistency in the description and reporting of microforaminiferal linings without the erection of a formal scheme.

Stancliffe (1996) has since determined that generic classification of microforaminiferal linings is impossible following observations that the tests of different foraminiferal genera contain morphologically identical linings. Mitsuru & Koutsoukos (1998) conversely state that the establishment of parental relationships is possible to generic and/or species level (although no evidence is available in their published extended abstract). Also, while Lebedeva & Nikitenko (1998) agree with Stancliffe (1996) that parental relationships are impossible to identify, they nevertheless erected a formal generic classification scheme under "Order Foraminiferida; Incertae sedis". The intention of developing this artificial classification scheme is to relate microforaminiferal morphologies with their most similar macroforaminiferal genera so microforaminiferal linings can be more effectively used for biostratigraphy and palynofacies analysis. Future development of the Lebedeva & Nikitenko (1998) system may potentially produce some benefit. However, considering this scheme is currently undeveloped, and considering the vast diversity of morphologies within the relatively low volume of microforaminiferal linings observed in the Jansz-Io samples, application of this scheme would be impractical for the purposes of this project. Therefore the 'descriptive' classification system

of Stancliffe (1989) is used herein as a foundation to broadly differentiate the forms encountered in the Jansz-Io reservoir.

The Jansz-Io samples contained many of the microforaminiferal lining morphologies described in the Stancliffe (1989) scheme with a few exceptions and additions as discussed below. Alongside the morphotype name, an indication of the progression of chamber wall thickness is indicated as either 'solid', where all chambers typically have the same wall thickness, or 'thinning', where the chamber walls get progressively thinner away from the proloculus.
(Note: commonly broken specimens and the variation of morphologies within these broad groupings means specimen measurements are irrelevant.)

5.4.2 Informal Descriptions

5.4.2.1 Stancliffe (1989) morphotypes observed at Jansz-Io

Morphotypes observed in Jansz-Io samples that are comparable to morphotypes described in Stancliffe (1989) are:

Uniserial type I – solid & thinning

Pl. 115, fig. A-C

Description: A uniserial morphotype where the amphora-shaped chambers are distinct and clearly separated by necks, which often contain obturacula.

Planispiral type III – solid

Pl. 115, fig. F-G

Description: A planispiral morphotype which has sickle-shaped chambers that do not overlap and are wide with respect to their length. The second whorl is generally not appressed to the first whorl.

Planispiral type IV – thinning

Pl. 115, fig. H

Description: A planispiral morphotype which has chambers that do not overlap. The second whorl is appressed to the first whorl.

Trochospiral type I – solid

Pl. 115, fig. I-J

Description: A trochospiral form in which the chambers generally slightly to strongly overlap and the chambers commonly have proximal connections with the succeeding and preceding chambers. Outer whorls are closely appressed to the inner whorls.

Trochospiral type cf II – thinning

Pl. 116, fig. A-B

Description: This morphotype has discrete chambers in the primary whorl, where necks are obscured from visibility giving the appearance that each chamber connects directly with the proloculus. Second whorl not observed.

Comments: This morphotype is recorded as 'cf.' due to the similarity of Jansz-Io specimens to the Stancliffe (1989) description, but the lack of specimens retaining a second whorl to confirm the trochospiral nature.

5.4.2.2 Stancliffe (1989) morphotypes not observed at Jansz-Io

The following morphotypes described in Stancliffe (1989) were not observed in the Jansz-Io samples:

- Single Chamber, type I – This morphotype has not distinctly been recorded here. Specimens may have been mistaken for either a large chamber broken off another microforaminiferal lining, or (less likely) recorded as an acritarch.
- Uniserial, type II
- Biserial, types I & II
- Planispiral types I, II & V
- Coiled Uniserial
- 'True' Coiled Biserial – Coiled Biserial morphotypes with a coiled whorl entirely encircling the proloculus prior to commencement of the biserial arrangement, rather than the half coiled whorl observed in Jansz-Io morphotypes.

5.4.2.3 Additional morphotypes

Additional morphotypes observed in the Jansz-Io samples to those described in Stancliffe (1989) are:

Trochospiral type III – solid

Pl. 116, fig. C-G

Description: A trochospiral morphotype in which the chambers generally do not overlap and the larger chambers commonly have proximal connections with the succeeding and preceding chambers. Outer whorls overlap preceding whorls greater than inner whorls. (Whorl overlap increases distally). Chamber walls are equally solid.

Comments: Large volumes of this variety encouraged differentiation from the 'thinning' variety of this morphotype group.

Trochospiral type III – thinning

Pl. 116, fig. H

Description: A trochospiral morphotype in which the chambers generally do not overlap and the larger chambers commonly have proximal connections with the succeeding and preceding chambers. Outer whorls overlap preceding whorls greater than inner whorls. (Whorl overlap increases distally). The chambers progressively thin away from the proloculus.

Comments: Large volumes of this variety encouraged differentiation from the 'solid' variety of this morphotype group.

Compound – Half-coiled Biserial

Pl. 115, fig. D-E

Description:

An initial half-whorl or 'half-coil' of chambers is succeeded by others in a biserial arrangement. This morphotype is otherwise very similar to the Compound Coiled Biserial morphotype of Stancliffe (1989).

5.5 OTHER PALYNOMORPH GROUPS

The following palynomorph groups constitute very rare components of the Jansz-Io preparations and so are not discussed in detail. However, these groups are recorded to provide a complete account of the palynomorphs encountered in the Jansz-Io reservoir.

5.5.1 Other Algae

Non-dinoflagellate algal remains were rarely encountered in the Jansz-Io preparations. These include undifferentiated simple, diaphanous leiospheres, the fresh- to brackish-water colonial

algae, *Botryococcus*, and the marine prasinophyte phycomata *Cymatiosphaera, Pterospermella* and *Tasmanites*.

5.5.2 Scolecodonts

Scolecodonts are the fossilised segments of organic proboscidal armatures (jaw parts) of marine polychaetous annelids (Szaniawski, 1996). Their morphology is distinctive but variable, usually consisting of elongate, straight or curved elements that are smooth on one side and denticulate on the other.

5.5.3 Fungal remains

Fungal remains encountered in the Jansz-Io preparations consisted of simple fungal spores and hyphae. The spores were identified as fungal on the basis of their much darker colour than other sporomorphs and having no distinguishing sporomorph characteristics, such as surface sculpture or laesurae (linear germination apertures).

Chapter 6

BIOSTRATIGRAPHY

6.1 THE *WANAEA SPECTABILIS* MICROPLANKTON ZONE

Qualitative and quantitative analyses were conducted on Jansz-Io palynological preparations to assess the microplankton stratigraphic ranges and assemblage variations within the interval of the *Wanaea spectabilis* Zone intersected by the Jansz Sandstone. The *W. spectabilis* Zone (Figure 6.1) as currently defined is summarised as follows:

***Wanaea spectabilis* Interval Zone (Helby *et al.*, 1987, revised Riding *et al.*, 2010).**

Base: First Appearance Datum (FAD) of *Scriniodinium crystallinum.*

Top: FAD of consistent *Wanaea clathrata.*

Associated spore-pollen zone: Upper *Murospora florida* Zone (Filatoff, 1975, modified Helby *et al.*, 1987).

Age: Early to early Late Oxfordian (Riding *et al.*, 2010).

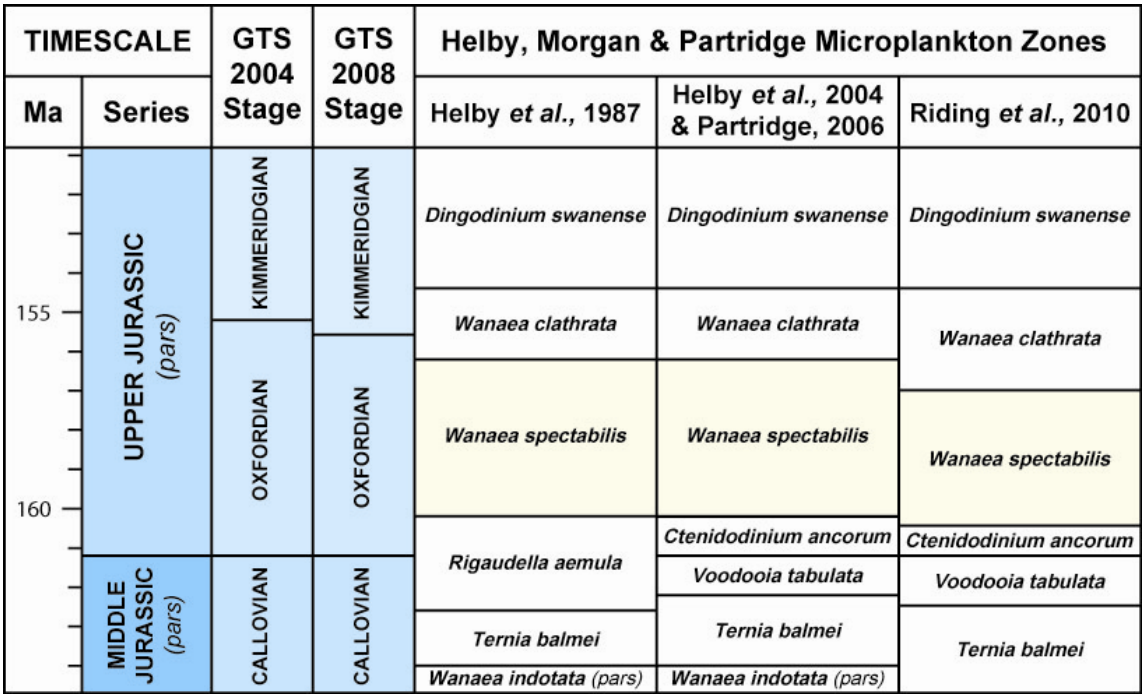

Figure 6.1: Comparison of the *W. spectabilis* Zone of each HMP edition and the chronostratigraphic correlation to the ICS Geologic Time Scale 2004 and 2008 timescales.

The base of the *W. spectabilis* Zone marks a floral turn over from the *Pareodinia ceratophora* Superzone to the *Pyxidiella* Superzone. This zone is marked by a significant increase in dinoflagellate cyst diversity, with stratigraphically important datums including the range tops of

Fostericysta eclipsiana, Systematophora geminus, Wanaea digitata and consistent *Microdinium jurassicum*, the range bases of *Dingodinium jurassicum, Gonyaulacysta ceratophora, Oligosphaeridium* spp., *Wanaea spectabilis* and *Wanaea talea*, and acmes of *Cygnusicysta taltarniana, Oligosphaeridium* spp., and *Woodinia bensonii*. *Wanaea spectabilis* itself is now understood not to extend throughout the entire zone as figured in Helby *et. al.* (1987), but rather is confined to the upper part of this zone with inconsistent occurrences in the base of the overlying *Wanaea clathrata* Zone.

Cosmopolitan taxa present in this zone include *Chytroeisphaeridia cerastes, Clathroctenocystis asaphes, Ellipsoidictyum cinctum, Endoscrinium galeritum, Endoscrinium luridum, Fromea tornatilis, Gonyaulacysta centriconnata, Gonyaulacysta eisenackii, Gonyaulacysta jurassica, Leptodinium ambiguum, Leptodinium mirabile, Limbodinium absidatum, Mendicodinium groenlandicum, Nannoceratopsis pellucida, Pareodinia* spp., *Rhynchodiniopsis cladophora, Rigaudella aemula, Scriniodinium crystallinum, Scrinodinium dictyotum, Sentusidinium* spp., *Stephanelytron–Lagenadinium* spp., *Tubotuberella apatela, Tubotuberella dangeardii* and *Wanaea digitata/fimbriata*. However, a significant proportion of the assemblage consists of endemic Australasian taxa, including *Cassiculosphaeridia solida, Chlamydophorella wallala, Cygnusicysta taltarniana* (acme), *Dingodinium jurassicum, Dingodinium swanense, Fostericysta eclipsiana, Fusiformacysta challisiana, Gonyaulacysta ceratophora, Microdinium jurassicum, Nummus tithonicus* (acritarch), *Oligosphaeridium swanense, Productodinium chenii, Prolixosphaeridium capitatum, Pyxidiella pandora, Systematophora geminus, Tringadinium bjaerkei, Tringadinium comptum, Wanaea spectabilis, Wanaea talea, Woodinia bensonii* and *Yalkalpodium elangiana*.

Mantle (2009b, p. 129) recommended that the uppermost part of the *Ctenidodinium ancorum* Zone (7aia of Foster, 2001, fig. 2) be included in the *W. spectabilis* Zone. Mantle states that the 7aia subzone assemblage is more similar to the *W. spectabilis* Zone than the underlying *C. ancorum* 7aib subzone although the basal key marker *S. crystallinum* is absent. Riding *et. al.* (2010, p. 565) indicates that the ambiguously constrained *C. ancorum* Zone may ultimately be divided between the underlying *Voodooia tabulata* Zone and overlying *W. spectabilis* Zone. Further examination of the entire *C. ancorum* Zone needs to be conducted before placement of these assemblages and the exact extent of the *W. spectabilis* Zone can be resolved. Until then, the current boundary of the *W. spectabilis* Zone remains the first stratigraphic occurrence of *S. crystallinum*.

Until now, two informal subzonation schemes of the *W. spectabilis* Zone have been developed:

1. Foster, 2001, with alphanumeric codes and supporting taxonomy (published in Laurie & Foster, 2001), although without subzone definitions; and,

2. Morgan *et al.* (2002), with alphanumeric codes and key bioevents presented in an unpublished but widely distributed report.

An approximate comparison of these informal subzonation schemes was published on the HMP biozonation charts by Helby *et. al.* (2004) and Partridge (2006a). A slightly modified comparison of the informal subzonation schemes and the key species occurrences (or bioevents) common to both schemes are presented in (Figure 6.2).

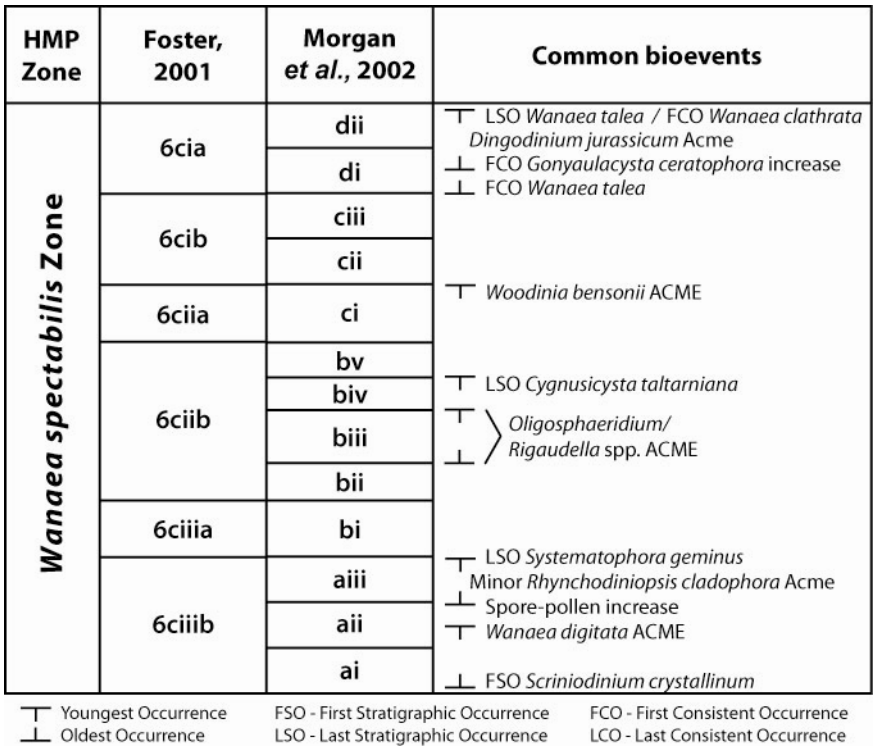

Figure 6.2: Comparison of the *W. spectabilis* Zone informal subzones.

6.2 JANSZ-IO MICROPLANKTON BIOSTRATIGRAPHY

Palynological preparations from 155 conventional core samples from the Jansz Sandstone reservoir of four Jansz-Io wells yielded a highly diverse assemblage of dinoflagellate cysts and acritarchs of good to excellent preservation. Sampling of the cored Jansz Sandstone reservoir sequence at 1m intervals enabled the identification of minor bioevents that may not have been evident at wider sampling intervals. Therefore, greater resolution could be achieved in intra-reservoir biostratigraphic correlation than is possible through a typical petroleum exploration sampling regime.

A comparison of quantitative methods (100 grain palynofacies counts and 250 specimen counts every 1m in Jansz-1, -2 and -3, versus 100 grain palynofacies counts every 1m and 100 specimen counts every 3m in Io-1) reveals that a 250 specimen count is advantageous in highly

diverse assemblages, since subtle abundance signatures are difficult to identify in a 100 specimen count. However, for routine palynological analyses, a 100 specimen count at high density sampling intervals will often enable more accurate biostratigraphic correlation of reservoir sequences than 250 specimen counts at wider intervals.

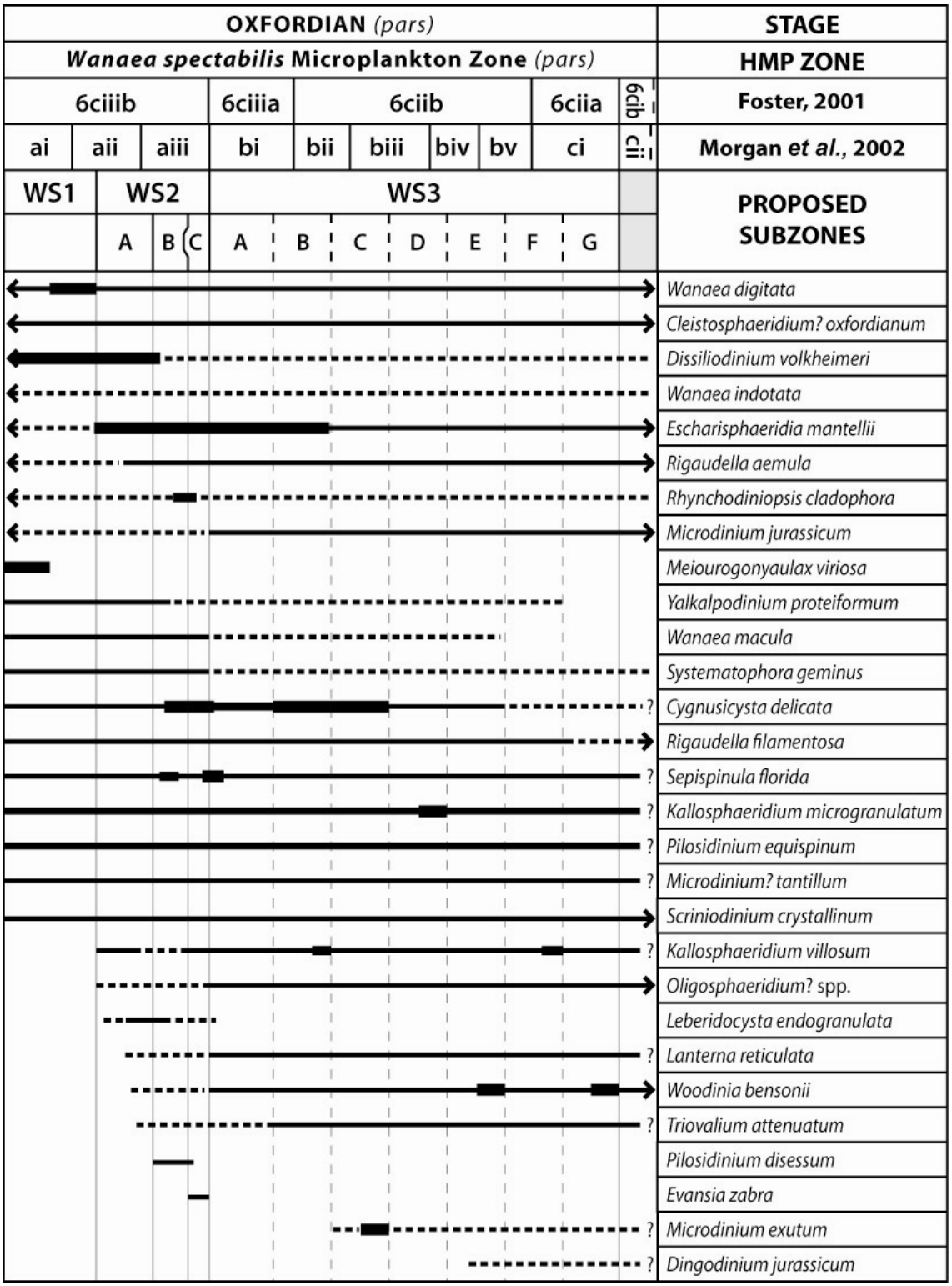

Figure 6.3: Ranges of stratigraphically significant microplankton in the Jansz Sandstone reservoir sequence.

Quantitative results of species occurrences (counts) and presence of accessory species are recorded in Appendix 4. The ranges of stratigraphically useful taxa identified in this study are presented in Figure 6.3.

The Jansz Sandstone reservoir sequence was readily subdivided using microplankton biostratigraphic events. The absence of *Wanaea spectabilis* in the Jansz-Io preparations indicates that the top of the *W. spectabilis* Zone is not present in analysed samples. *W. spectabilis* is shown in Riding *et. al.* (2010) to have a restricted range of approximately the top one-third of the eponymous Zone. Therefore, these analyses approximately encompass the lower two-thirds of the *W. spectabilis* Zone sequence. Although the Jansz Sandstone is truncated by the Base Cretaceous Unconformity resulting in an anachronic upper reservoir boundary, the top of the analysed sequence is determined by the cored interval of the analysed wells. Palynological slides were prepared from conventional core samples to obtain the most biostratigraphically accurate zonation possible by minimising potential contamination. Since the cored intervals of the examined wells were close to, but did not intersect the very top of the reservoir, the uppermost section of the Jansz Sandstone and the full extent of the *W. spectabilis* Zone could not be examined in this study.

Key bioevents common to the Foster (2001) and Morgan *et al.* (2002) subzonation schemes were utilised where possible to: 1/ facilitate regional correlation; and 2/ present the most broadly applicable subzone revision possible, given that these events are confirmed to be applicable over a large geographical area. However, key bioevents from those schemes were absent or difficult to apply to the examined samples. For example:

- *Cygnusicysta taltarniana*, which has a widely recorded acme in the mid-Oxfordian, was absent from these samples;
- the *Oligosphaeridium* spp. / *Rigaudella aemula* acme at the Morgan *et al.* (2002) biii subzone was not a distinct event but rather a broad trend; and,
- the spore-pollen increase recorded at the Morgan *et al.* (2002) aii/aiii boundary was not clearly distinguishable from surrounding samples.

The absence or ambiguity of these events may be due to a marginal depositional environment influencing microplankton distributions and the spore-pollen signature.

Therefore, new bioevents have been identified for subdivision of the intersected *W. spectabilis* Zone sequence (Figure 6.4). Where possible, first and last stratigraphic or common taxon occurrences are utilised (FSO, LSO, FCO and LCO respectively). However, acme (abundance) events were used in the upper half of the intersected reservoir sequence because of: 1/ the absence of major traceable appearance or extinction events; and, 2/ the presence of intraformational reworking, as indicated by inconsistent and anomalously high occurrences of

Systematophora geminus in all wells. Acme events may be generated by local environmental or ecological conditions. Therefore, many of these events may be restricted in their extent and difficult to identify on a regional scale. Consequentially, the proposed subzonation scheme must be considered as informal until the regional extent of the bioevents can be determined.

6.3 PROPOSED *WANAEA SPECTABILIS* SUBZONATION

The following informal subzonation scheme is proposed for subdivision of the *Wanaea spectabilis* Interval Zone as recognised in the intersected Jansz Sandstone reservoir sequence (Figure 6.4). The regional applicability of these proposed subzones and zonules need to be determined if they are to be formalised. The subzonation hierarchy reflects the confidence level of the boundaries: WS1-3 are bounded by regionally recognised events, whereas the zonule boundaries are less certain, and may be bounded by minor acme events that may be of limited extent. Proposed subzones follow the guidelines for biozones presented by Salvador, 1994.

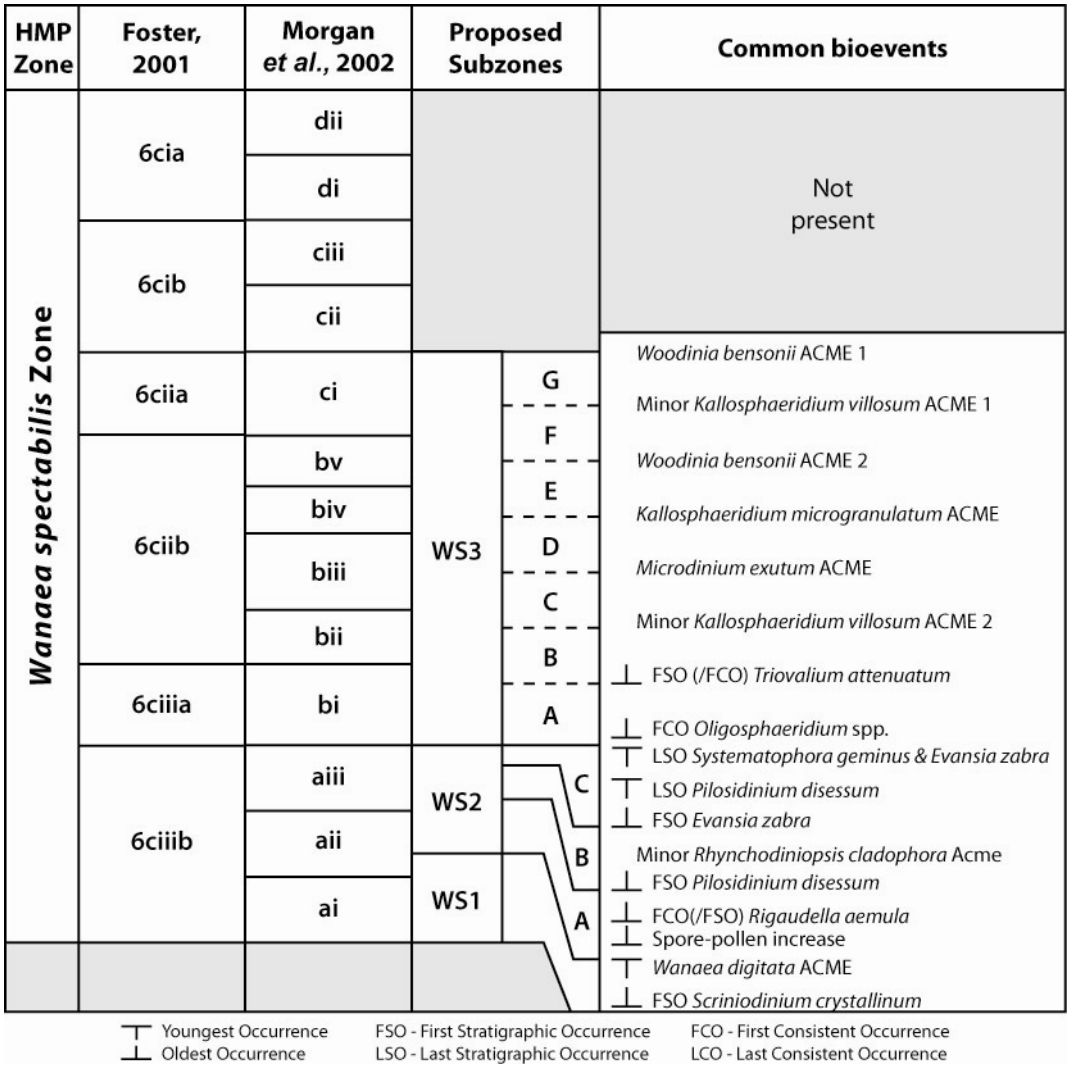

Figure 6.4: Proposed *W. spectabilis* Zone subzonation scheme for the Jansz Sandstone reservoir sequence.

WS1 Interval Subzone

Base: First Stratigraphic Occurrence (FSO) of *Scriniodinium crystallinum.*

Top: Sharp decrease in *Wanaea digitata* following acme.

Remarks: This subzone is characterised by an increase in dinoflagellate cyst diversity from the underlying sedimentary sequence. Species first appearances include *Cygnusicysta delicata, Kallosphaeridium microgranulatum, Microdinium? tantillum, Pilosidinium equispinum, Wanaea macula* and *Yalkalpodinium proteiformum,* although the actual FSO of newly described species will need to be confirmed in conformable sequences. Short acmes of *Meiourogounyaulax viriosa* (24%) and *Michrystridium* spp. (5-11%) are common at the base of this zone. The top of a *Wanaea digitata* acme (12-17%) marks the top of the subzone.

Reference section: Jansz-2, 2917-2916m, Jansz Sandstone.

WS2 Interval Subzone

Base: Sharp decrease in *Wanaea digitata* following acme.

Top: LCO of *Systematophora geminus* and LSO of *Evansia zabra.*

Remarks: The LCO of *Systematophora geminus* and LSO of *Evansia zabra* typically occur at the same level. However, the upper boundary of this subzone may sometimes be more clearly indicated by one taxon only. In the Jansz Sandstone the LSO of *Evansia zabra* is the more distinct marker, since all observed wells possess sporadic, younger occurrences of *S. geminus* that are apparently reworked. However, while it may be difficult to use the LCO of *S. geminus* alone to identify the upper WS2 boundary in the Jansz Sandstone, this taxon may prove to be the more consistent regional subzone marker.

This subzone is subdivided into three zonules, WS2A-C, in stratigraphically ascending order.

Reference section: Jansz-3, 2864-2830m, Jansz Sandstone.

WS2A Interval Zonule

Base: Sharp decrease in *Wanaea digitata* following acme.

Top: FSO of *Pilosidinium disessum.*

Remarks: In addition to the decrease in *Wanaea digitata*, the base of this zonule is indicated by a large increase of *Escharisphaeridia mantellii* and the first appearance of *Kallosphaeridium villosum* and *Leberidocysta endogranulata. Dissiliodinium volkheimeri* may dominate some sequences (up to 42% in Jansz-2, 2914m). An increase in spore-pollen may be recognised in the lower section of this zonule, and the

FCO (concurrent with the FSO in some wells) of *Rigaudella aemula* occurs in the upper section.

Reference section: Jansz-3, 2864-2855m, Jansz Sandstone.

WS2B Interval Zonule

Base: FSO of *Pilosidinium disessum.*

Top: FSO of *Evansia zabra.*

Remarks: The base of this zonule is consistently marked by the FSO of *Pilosidinium disessum.* A significant reduction in the abundance of *Dissiliodinium volkheimeri* and the LCO of *Yalkalpodinium proteiformum* may be evident during this zonule. An acme of *Rhynchodiniopsis cladophora* commences near the end of this zonule, as recorded in the Foster (2001) and Morgan *et al.* (2002) subzones; however this may be very minor to unnoticeable in some wells (1-7%). Another minor acme consist of *Sepispinula florida* (up to 6%), and an extended minor acme of *Cygnusicysta delicata* commences within this zonule.

Reference section: Jansz-3, 2854-2846m, Jansz Sandstone.

WS2C Interval Zonule

Base: FSO of *Evansia zabra.*

Top: LSO of *Systematophora geminus* and *Evansia zabra.*

Remarks: *Evansia zabra* provides an excellent marker for the base and top of WS2C. In all wells except Io-1 the LSO of *Evansia zabra* coincides with the LCO of *Systematophora geminus*, which may prove a more suitable regional marker. The upper boundary is also marked by the LCO of *Wanaea macula.* The LSO of *Pilosidinium disessum* occurs near the base, and a second minor acme of *Sepispinula florida* commences during this zonule.

Reference section: Jansz-3, 2843-2830m, Jansz Sandstone.

WS3 Interval Subzone

Base: LSO of *Systematophora geminus* and *Evansia zabra.*

Top: Sharp decrease in *Woodinia bensonii* following acme (Acme 1).

Remarks: This subzone represents a significant shift in the dinoflagellate flora, with the basal boundary marked by the LSO and FCO of multiple taxa (see below). However, although many new taxa are recorded during this interval, few of them have a consistent FSO/FCO or LSO/LCO occurrences to assist with correlation. Therefore, this extended sequence is subdivided into seven zonules, WS3A-G, mainly using acme events. Apart from the upper *Woodinia bensonii* acme which is known to be laterally extensive

(Foster, 2001 and Morgan *et al.,* 2002 subzones) these acme events are traceable and consistent across the Jansz-Io field but their regional extent is yet to be determined.

Reference section: Io-1, 2875-2841m, Jansz Sandstone. Note: the clearly defined LSO of *Evansia zabra* alone is used to identify the base of WS3 in this sequence due to the inconsistency and reworking of *Systematophora geminus* in this well.

WS3A Interval Zonule

Base: LSO (/LCO) of *Systematophora geminus* and *Evansia zabra.*

Top: FSO (/FCO) of *Triovalium attenuatum.*

Remarks: The base of WS3A is clearly indicated by the LSO or LCO of *Evansia zabra, Systematophora geminus* and *Wanaea macula*, and the FCO of *Lanterna reticulata, Microdinium jurassicum, Oligosphaeridium?* spp. / *Contracysta* Complex morphotypes and *Woodinia bensonii*. Rare individual specimens of *Triovalium attenuatum* occur below the WS3A/B boundary in some wells, but the FSO (/FCO) of *Triovalium attenuatum* is a consistent marker for the top of this zonule.

Reference section: Io-1, 2875-2866m, Jansz Sandstone. As for the WS3 Subzone, the base of WS3A is determined by the LSO of *Evansia zabra.*

WS3B Interval Zonule

Base: FCO (/FSO) of *Triovalium attenuatum.*

Top: Sharp decrease in *Kallosphaeridium villosum* following stratigraphically lower acme (Acme 2).

Remarks: The FCO (concurrent with the FSO in some wells) of *Triovalium attenuatum* marks the base of WS3B. This species is very thin and pale, so may be easily damaged or overlooked, and the base of WS3B may be difficult to recognise. This zonule is characterised by the onset of the younger of two acme phases of *Cygnusicysta delicata*. The top of this zonule is indicated by the stratigraphically lower minor acme (5-9%; Acme 2) of *Kallosphaeridium villosum* and a significant reduction in the relative abundance of *Escharisphaeridia mantellii*. WS3B questionably occurs in Jansz-1 at 2887m and appears to be missing entirely from Jansz-2, possibly indicating a short, localised depositional hiatus.

Reference section: Io-1, 2865-2862m, Jansz Sandstone.

WS3C Abundance Zonule

Base: Sharp decrease in *Kallosphaeridium villosum* following stratigraphically lower acme (Acme 2).

Top: Sharp decrease in *Microdinium exutum* following acme.

Remarks: The base of WS3C is marked by the end WS3B minor acme of *Kallosphaeridium villosum* and a significant reduction in the relative abundance of *Escharisphaeridia mantellii*. This zonule is characterised by the conclusion of the younger of two acme phases of *Cygnusicysta delicata*. The upper boundary is marked by the end of a short acme of *Microdinium exutum* (2-19%) soon after its FSO.

Reference section: Io-1, 2861-2859m, Jansz Sandstone.

WS3D Abundance Zonule

Base: Sharp decrease in *Microdinium exutum* following acme.

Top: Sharp decrease in *Kallosphaeridium microgranulatum* following minor acme.

Remarks: The base of WS3D is marked by the end WS3C *Microdinium exutum* acme while the top is indicated by a minor acme of *Kallosphaeridium microgranulatum*. Given the dominance of this taxon in the samples, the acme is relative to the local taxon occurrences in each well, ranging from 28% in Io-1 to 51% in Jansz-1. The LCO of *Cygnusicysta delicata* occurs around the WS3E/WS3F boundary.

Reference section: Io-1, 2858-2856m, Jansz Sandstone.

WS3E Abundance Zonule

Base: Decrease in *Kallosphaeridium microgranulatum* following minor acme.

Top: Sharp decrease in *Woodinia bensonii* following stratigraphically lower acme (Acme 2).

Remarks: The end of the minor *Kallosphaeridium microgranulatum* acme marks the base of WS3E. The top of this zonule is indicated by a minor relative *Woodinia bensonii* acme (up to 16% of the assemblage in Jansz-3) stratigraphically lower than the top WS3G event. The last, inconsistent occurrences of *Wanaea macula* and first, sporadic occurrences of *Dingodinium jurassicum* occur around mid-WS3E.

Reference section: Io-1, 2855-2853m, Jansz Sandstone. Also refer to Jansz-3, 2813m.

WS3F Abundance Zonule

Base: Sharp decrease in *Woodinia bensonii* following stratigraphically lower acme (Acme 2).

Top: Sharp decrease in *Kallosphaeridium villosum* following stratigraphically higher acme (Acme 1).

Remarks: Acme 2 of *Woodinia bensonii* (as discussed above) and a second minor acme of *Kallosphaeridium villosum* (2-8%; Acme 1) define the lower and upper boundaries of WS3F respectively. The LSO of (probably reworked) *Yalkalpodinium proteiformum* occurs around the WS3F/WS3G boundary.

Reference section: Io-1, 5825-2847m, Jansz Sandstone.

WS3G Abundance Zonule

Base: Sharp decrease in *Kallosphaeridium villosum* following stratigraphically higher acme (Acme 1).

Top: Sharp decrease in *Woodinia bensonii* following stratigraphically higher acme (Acme 1).

Remarks: The end of the minor *Kallosphaeridium villosum* Acme 1 represents the base of this zonule. The LCO, to LSO in some wells, of *Rigaudella filamentosa* occurs around the base of WS3G. The upper boundary Acme 1 of *Woodinia bensonii* represents up to 22% of the assemblage in Io-1.

Reference section: Io-1, 2846-2841m, Jansz Sandstone. Also refer to Jansz-3, 2811m.

6.4 CORRELATION

The biostratigraphic and chronostratigraphic correlation of the *Wanaea spectabilis* Zone was comprehensively examined in the recent review of the HMP microplankton scheme by Riding *et al.* (2010). These authors reviewed Australasian dinoflagellate cyst taxon ranges and compared them with dinoflagellate cyst ranges from other regions, including New Zealand (Wilson & Helby, 1987), Papua New Guinea (Davey, 1987, 1999), and the northern hemisphere, in particular the well studied Northern Hemisphere Dinoflagellate Cyst Zones of Poulsen & Riding (2003) from Europe and Russia. The dinoflagellate cyst zonation was correlated to the 2008 Geologic Time Scale using ammonite (Arkell, 1956; McWhae *et al.*, 1958; Helby *et al.*, 1988; Francis & Westermann, 1993; Stevens, 1997; Campbell *et al.*, 2004) and nannofossil assemblages (Bown & Cooper, 1998; Rexilius *et al.*, 1998; Howe, 2000) where available. Therefore, the upper and lower *W. spectabilis* Zone boundaries of Riding *et. al.* (2010) are applied as the framework herein.

The subzones and zonules proposed herein are correlated to the Foster (2001) and Morgan *et al.* (2002) subzonation schemes using bioevents identified in all schemes. The major boundaries of WS1-3 coincide with regionally identified bioevents, so are relatively certain. However, the zonule boundaries, especially within WS3, are less certain, since these bioevents are mostly based on newly described taxa and minor acmes with unknown regional applicability. Therefore, the WS3 zonules are spaced evenly apart to fill the available time.

Correlation with the Foster (2001) and Morgan *et al.* (2002) subzonations enables tentative correlation to the Poulsen & Riding, 2003 Northern Hemisphere Dinoflagellate Cyst Zones; Bown & Cooper, 1998 Nannofossil Zones; the Groupe Français d'Étude du Jurassique, 1997 Tethyan, Sub-Boreal and Boreal Ammonoid Zones; and the ICS 2008 Geologic Time Scale (Figure 6.5). However, correlation remains tentative until stronger chronostratigraphic ties, such as ammonites or radiometric dating of the Jansz Sandstone, can be determined.

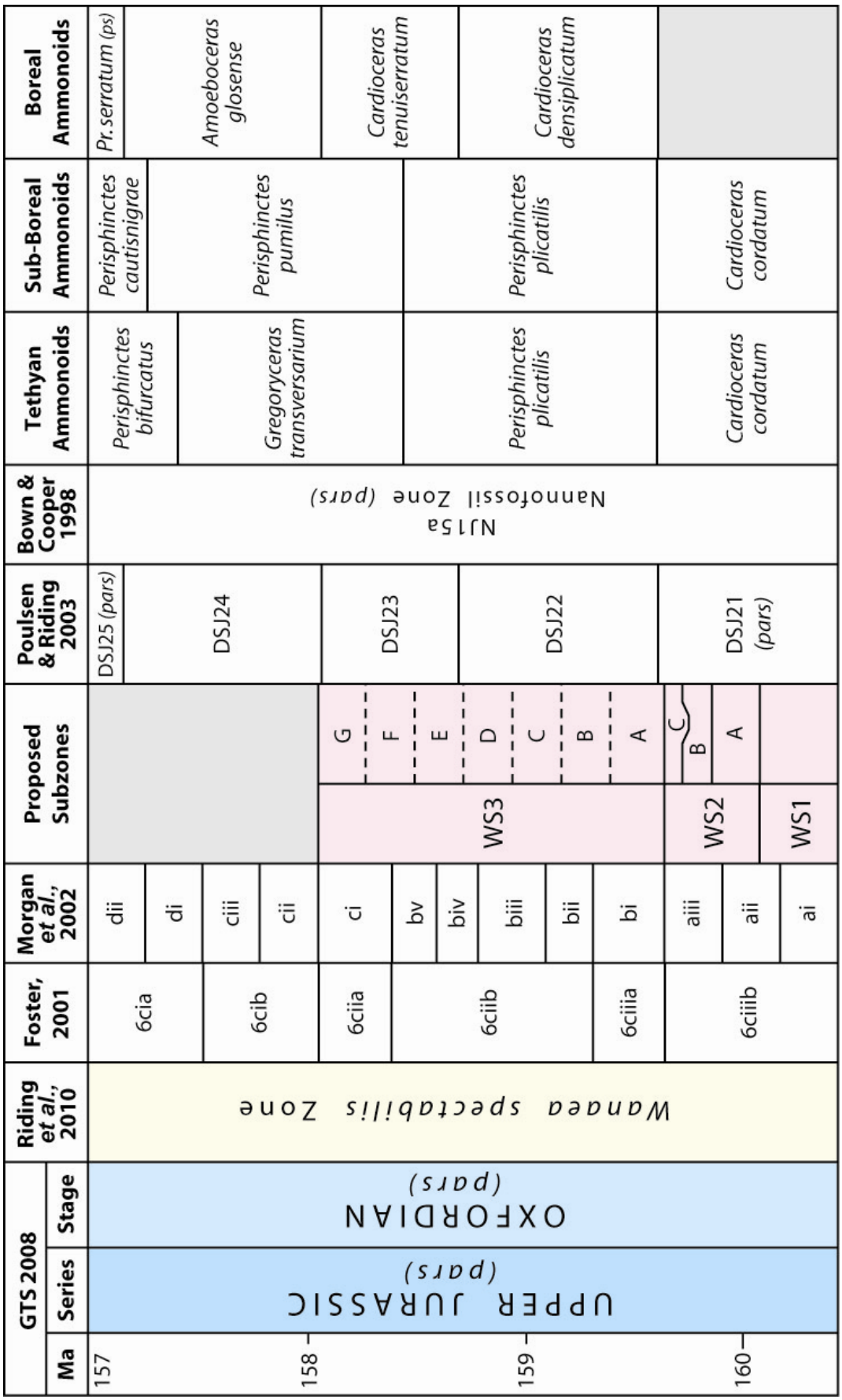

Figure 6.5: Correlation of the proposed subzones with the Poulsen & Riding, 2003 Northern Hemisphere Dinoflagellate Cyst Zones, Bown & Cooper, 1998 Nannofossil Zones and the Groupe Français d'Étude du Jurassique, 1997 Tethyan, Sub-Boreal and Boreal Ammonoid Zones.

Chapter 7
FACIES ANALYSIS AND BIOSEQUENCE STRATIGRAPHY

7.1 LITHOFACIES

Primary sedimentary structures evident in conventional core, such as grainsize, grading, bedding surfaces and bioturbation, were recorded to assist in determining the palaeodepositional environment and provide a lithostratigraphic framework of the Jansz Sandstone reservoir sequence. The lithological data were collected during palynological sampling of the archived portions of Jansz-1, -2 and -3 conventional core stored at Geoscience Australia, and compared with detailed core photographs contained in the Io-1 Well Completion Reports, as outlined in Chapter 4 and recorded in Appendix 2.

The cored intervals can be differentiated into three main lithofacies in stratigraphically ascending order:

- Lithofacies 1 – Bioturbated, glauconitic, siltstone to muddy, fine-grained sandstone;
- Lithofacies 2 – Bioturbated, glauconitic, muddy, fine- to coarse-grained sandstone;
- Lithofacies 3 – Coarse- to very coarse-grained, ferruginous, muddy sandstone.

Common glauconite and extensive bioturbation in Lithofacies 1 and 2 indicate a low sedimentation rate. The poorly sorted, unstratified Lithofacies 1 and 2 sediments with rare, coarse-grained intervals suggest pulses of high-energy, coarse-grained sedimentation interbedded with low-energy, fine-grained sedimentation. The low sedimentation rate enabled fine- and coarse-grained sediments to be fully churned by grazing fauna between high-energy events. The presence of both glauconite and pyrite indicate dysoxic to anoxic sedimentary conditions, while the presence of ichnofauna indicates normoxic to dysoxic sediments and an oxic water column; therefore, the sedimentary conditions are interpreted to be dysoxic with an overlying oxic water column.

Lithofacies 1 – 3 were observed to sequentially intergrade, producing an overall coarsening-upwards sequence. In particular, the frequency and thickness of Lithofacies 3 units increases towards the top of the Jansz-3 core. Coarsening-upwards, bioturbated, siltstones to sandstones with common belemnites, bivalves and gastropods are characteristic of a mid-shelf to upper-offshore/distal lower shoreface marine sequence of a prograding coastline or delta (Walker & James, 1992). Evidence of a low sedimentation rate in Lithofacies 1 and 2 suggests the Jansz

Sandstone was deposited below storm wave base in a wave- and storm-dominated shoreface environment rather than a wave-dominated deltaic environment.

The sediments are variably cemented by carbonate and ferruginous cements. Cemented intervals are frequently independent of the bedding surfaces and so are interpreted to be authigenic and diagenetic overprints. Therefore, cementation horizons may influence the wireline log signatures and be correlatable across the field.

The observed lithofacies correspond to 'Waste' + Unit A, Unit B and Unit C, respectively, of Jenkins *et al.*, 2003, which have been revised to Lithofacies S_{43}, Lithofacies S_{42}, and Lithofacies S_1 of Jenkins *et al.*, 2008. Personal observations concur with the recently revised and improved lithofacies conclusions of Jenkins *et al.*, 2008 as outlined in Chapter 2.2.2, hence the lithofacies names of that paper are employed herein for consistency.

7.2 PALYNOFACIES

Palynofacies refers to the assemblage proportions of the total acid-resistant organic content (kerogen) of sediments, comprised of palynomorphs (*e.g.* microplankton, acritarchs, spores, pollen) and palynodebris (*e.g.* leaf cuticle, woody tissues, organic membranes, resin, amorphous organic matter [AOM]; Wood *et al.*, 1996). Variation in the composition of palynofacies provides useful information for stratigraphic correlation and palaeoenvironmental interpretations. The usefulness of palynofacies analysis for palynostratigraphy and sequence stratigraphy is well documented (Habib & Miller, 1989; Van der Zwan, 1990; Prauss, 1993; Steffen & Gorin, 1993; Oboh-Ikuenobe *et al.*, 1997, 2005; Jaramillo & Oboh-Ikuenobe, 1999; Al-Ameri *et al.*, 2001; Schiøler *et al.*, 2002; Dybkjaer, 2004; Torricelli *et al.*, 2006; Götz *et al.*, 2008, Mantle, 2009b). Palynofacies and palynostratigraphic analyses are typically conducted on extensive sedimentary sequences where palynofacies are controlled by significant changes in the depositional environment and variation between units is often quite distinct. However, palynofacies variations have also been recognised to reflect cyclical variations of 4^{th}-6^{th} order parasequences (Huault *et al.*, 1995; Waterhouse, 1995, 1999; Rameil *et al.*, 2000; Haas *et al.*, 2010).

Palynofacies analyses are highly subjective as a result of differences in sample preparation methods, and the quantitative and qualitative assessments of the textural and compositional characteristics of the palynofacies assemblage (Batten, 1996; Wood *et al.*, 1996). Therefore, there is no standard method or technique for palynofacies analysis, and palynofacies categories included in analyses must be adapted to reflect the overall palynofacies assemblage. The Jansz-

Io kerogen and +5µm sieved fraction preparations are dominated by very fine-grained AOM obscuring all other palynofacies signatures. Therefore palynofacies analyses were conducted on slightly oxidised, +20µm sieved fraction preparations along with the quantitative microplankton counts. A total of 100 palynomorph and palynodebris grains greater than 5µm were included in the palynofacies count for each sample in all examined wells. The palynofacies count was conducted by identifying an apparently representative palynofacies assemblage on each slide and counting grains consecutively to avoid selective bias. The palynofacies assemblage was analysed independently from the lithofacies data to ensure an unbiased palynofacies interpretation.

The terminology used to classify palynofacies categories varies significantly between studies, such as Whitaker (1984), Boulter & Riddick (1986), Van Bergen *et al.*, (1990), Tyson (1995), Batten (1996), Smith (1996), Oboh-Ikuenobe *et al.* (1997, 2005). While the types of palynodebris and palynomorphs are broadly equivalent, the category classifications necessarily differ according to the assemblage proportions and the aim of the study (Rameil *et al.*, 2000). For this project, terminology and classification follows simplified categories of those outlined by Tyson (1995) and Batten (1996).

Palynomorph and palynodebris types recorded for quantitative analysis in this study include:

- Dinoflagellate cysts
    - Specimens
    - Indeterminate fragments (fragments identifiable as dinoflagellate in origin, but not large enough to be counted as an entire specimen; *e.g.* isolated opercula or broken processes.)
- Acritarchs
- Foraminiferal test linings
- Algae
    - Leiospheres
    - Tasmanites
- *Pterospermella*
- *Botryococcus* & *Pediastrum*
- Spores & pollen
    - Specimens
    - Indeterminate fragments (fragments identifiable as spore-pollen in origin, but not large enough to be counted as an entire specimen; *e.g.* broken saccae.)
- Megaspore
- Sporangium
- Fungi
- Miscellaneous palynomorphs (*e.g.* scolecodonts)
- Indeterminate Palynomorph (unidentifiable degraded or fragmented specimens)
- Fecal pellet / floc
- AOM (irregularly-shaped, diffuse-edged particles)
    - Heterogenous
    - Homogenous
- Organic sheet / membrane
- Cuticle
    - With guard cells

    - Cellular - not nodular
    - Cellular - nodular
- Cortex tissue
    - Roots
    - Bark
- Tracheid
- Brown wood (including black-brown internally opaque particles with brown edges)
    - Amorphous (irregularly-shaped, almost spongeous)
    - Polygonal
    - Fibrous
    - Biostructured
    - Degraded
- Opaque wood
    - Amorphous (irregularly-shaped)
    - Polygonal
    - Blades
    - Biostructured
- Resin

Quantitative analysis (recorded in Appendix 4 charts) revealed that the most useful categories for palynofacies analysis of the Jansz Sandstone are:

- Dinoflagellate cysts
    - Specimens
    - Indeterminate fragments
- Acritarchs
- Foraminiferal test linings
- Other Algae (combined; predominantly Botryococcus)
- Spores & pollen
    - Specimens
    - Indeterminate fragments
- Indeterminate Palynomorphs
- AOM - total
- Organic sheet / membrane
- Cuticle - total
- Brown wood - total
- Opaque wood - total
- Resin

As shown in Figure 7.1 to Figure 7.4, AOM remains the dominant palynofacies category within +20µm sieved fraction preparations. AOM constitutes up to 71% of the assemblage in Jansz-3, 2816mRT(c; = core depth), and typically comprises more than 40% of the total assemblage in Jansz-3 and Io-1 and up to 40% in Jansz-1 and -2. Brown wood and opaque wood are the next most common particles in each of the wells, frequently independently comprising 25-35% of the assemblage and brown wood reaching 44% at Jansz-1, 2880mRT(c). The dominance of these three main categories masks subtle variations in the remaining categories. Although dinoflagellate cysts are numerous and diverse in the samples, they rarely represent more than 20% of the total assemblage unless AOM or woody particles are proportionally low.

Figure 7.1 to Figure 7.4 series: Palynofacies analysis of the Jansz Sandstone from Jansz-1, -2, -3 and Io-1. Depths are core depths (mRT(c) = metres below rotary table as recorded on conventional core) which are used for palynological samples and core logging notes. Grey shading of the core depth column indicates the cored interval, with palynological sample locations collected from the core indicated by small triangles. Palynofacies categories are as outlined in Chapter 7.2. Palynofacies category values are charted as a percentage of the total palynofacies assemblage.

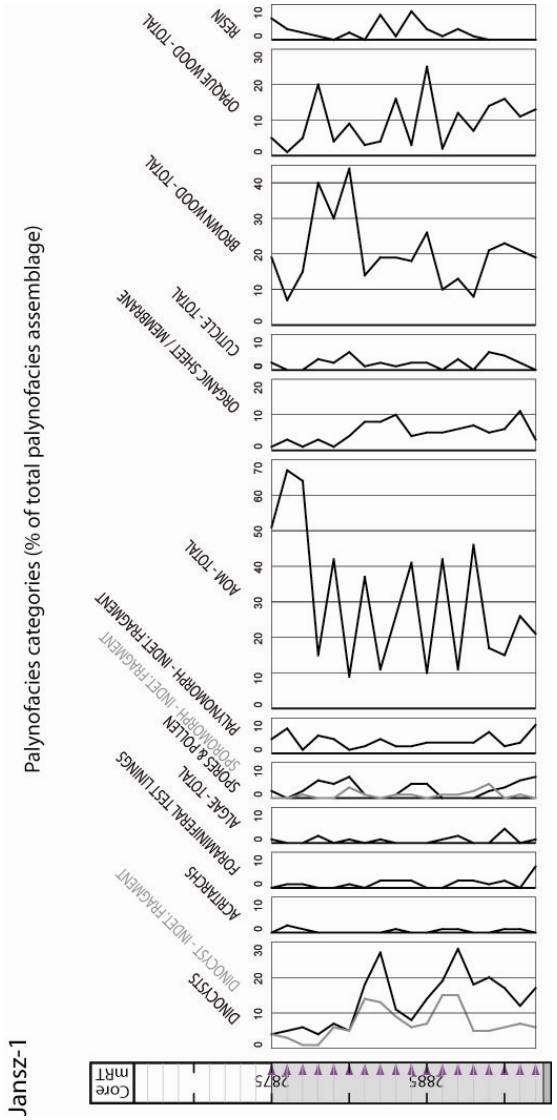

Figure 7.1: Distribution of the main palynofacies categories within Jansz-1 preparations.

Dinoflagellate cysts reach a maximum of 48% (and 5% dinoflagellate cyst fragments) in Jansz-2, 2906mRT(c), and 40% (and 27% fragments) in Io-1, 2841mRT(c), where AOM and woody debris each comprise less than 12% of the total assemblage. The cause of the relatively high proportion of fragmented dinoflagellate cysts in some samples, such as Io-1, 2854mRT(c), is uncertain. Fragmentation may be a result of mechanical breakage during high-energy depositional cycles, intraformational reworking (*e.g.* anomalous taxon occurrences such as *Systematophora geminus*), influenced by the extensive bioturbation. Mechanical breakage during sample processing is unlikely, since all samples were prepared in the same manner, and

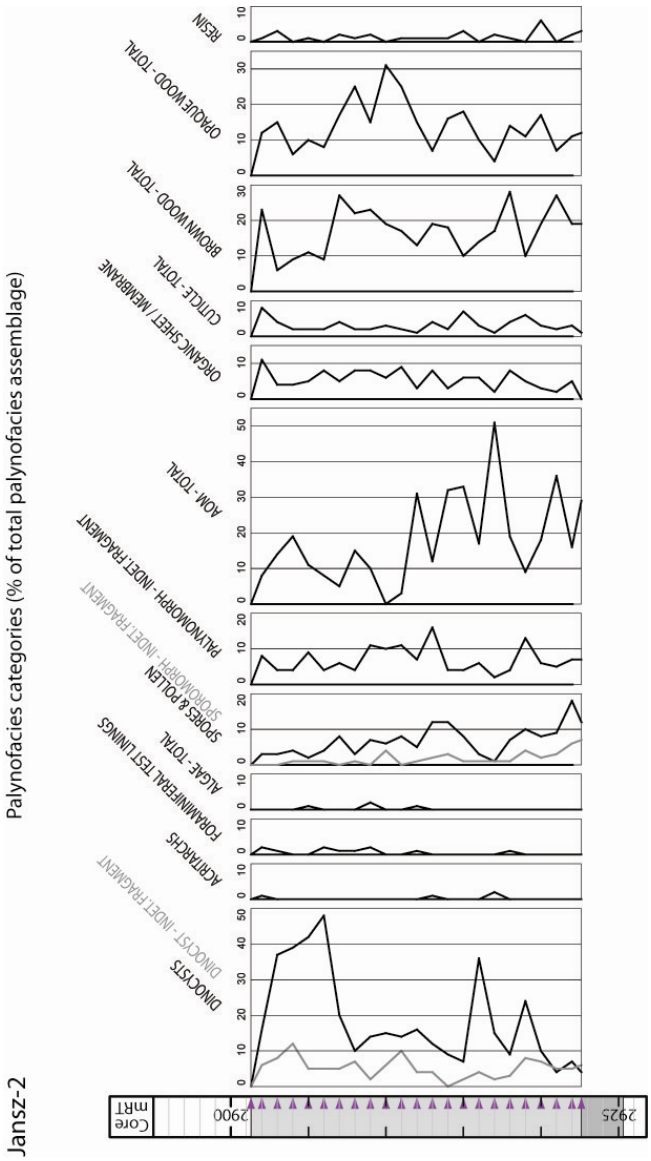

Figure 7.2: Distribution of the main palynofacies categories within Jansz-2 preparations.

not all samples display the same degree of fragmentation. Remaining palynofacies groups were poorly represented in the Jansz Sandstone. Spore-pollen typically represent less than 5% of the assemblage, but higher in Jansz-2, reaching a maximum of 12% in Jansz-2, 2913-2914mRT(c). The majority of sporomorphs are specimens and fragments of bisaccate pollen, most of which are reworked from Permo-Triassic sediments. The higher proportion of pollen in Jansz-2 may be a reflection of the low-energy depositional environment at Jansz-2 allowing buoyant bisaccate pollen grains to settle out of suspension.

AOM is generated through the biodegradation of terrestrial and aquatic organic matter and the organic precipitate products of this process (Tyson, 1995; Batten, 1996). A high proportion of AOM in marine sediments is commonly associated with maximum flooding surfaces (Huault *et al.*, 1995) which promotes AOM generation, and dysoxic to anoxic facies (Tyson, 1995) which

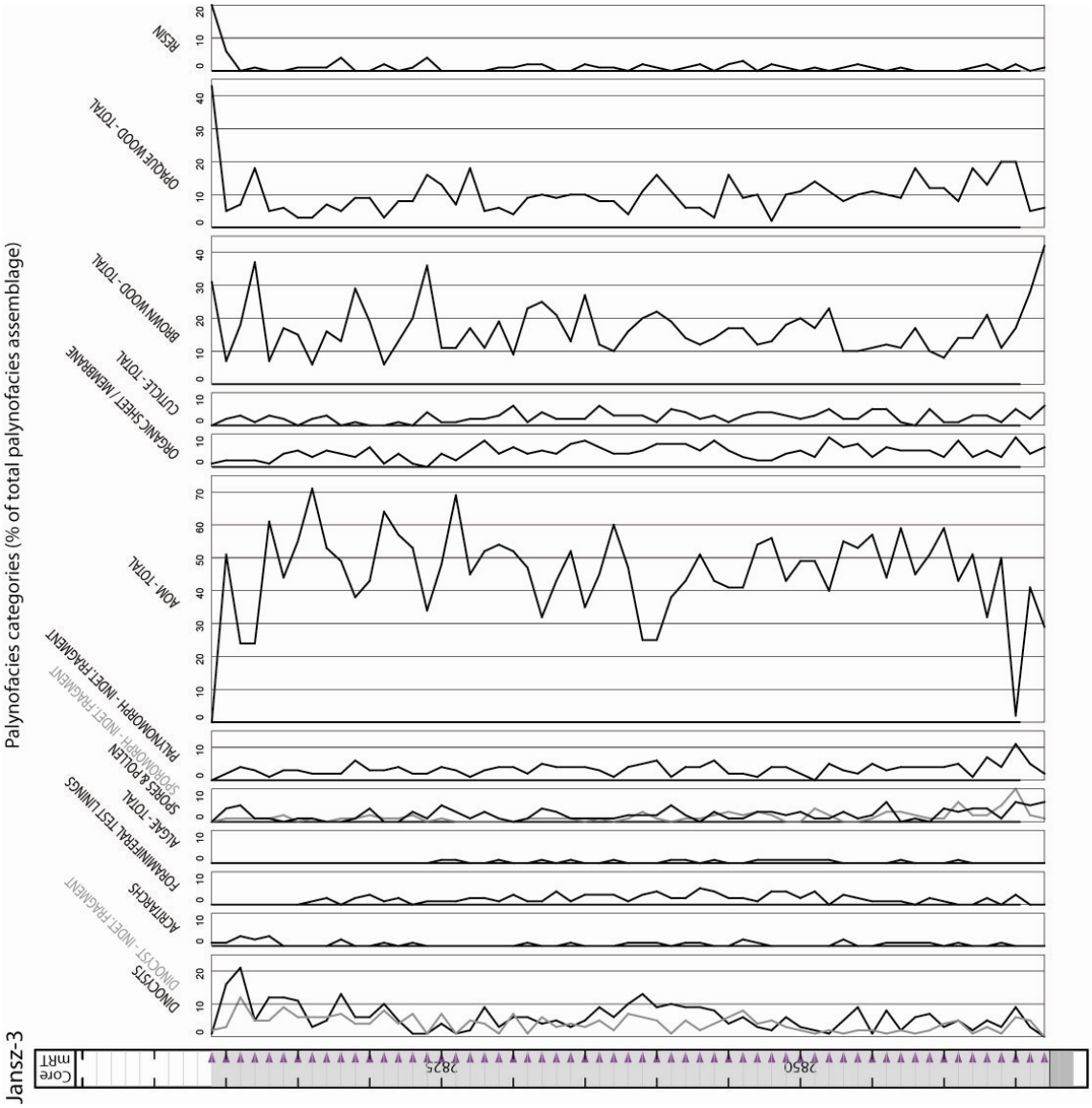

Figure 7.3: Distribution of the main palynofacies categories within Jansz-3 preparations.

promotes AOM preservation. Brown, black-brown and opaque woody particles are derived from the degraded tissues of vascular plants (Tyson, 1995; Batten, 1996). Brown and black-brown particles may be structured, reflecting original cellular structure, or highly degraded to gelified. These particles are common in intermediate- to high-energy deposits, including nearshore environments (Tyson, 1995). Opaque particles may be fragments derived from lignified wood or pyrolysed charcoal. Lathe- or blade-shaped particles (predominantly buoyant charcoal) and equidimensional polygonal particles (predominantly dense woody particles) may have different hydrodynamic properties and are often differentiated in palynofacies analyses (Van der Zwan, 1990). However, while polygonal particles dominated the opaque wood group in all wells, preferential distribution of opaque particles was not apparent within the Jansz Sandstone. This may reflect the fluctuating hydrodynamic energy levels indicated by grain-size variations in the lithofacies; hence all opaque particles are considered as a group.

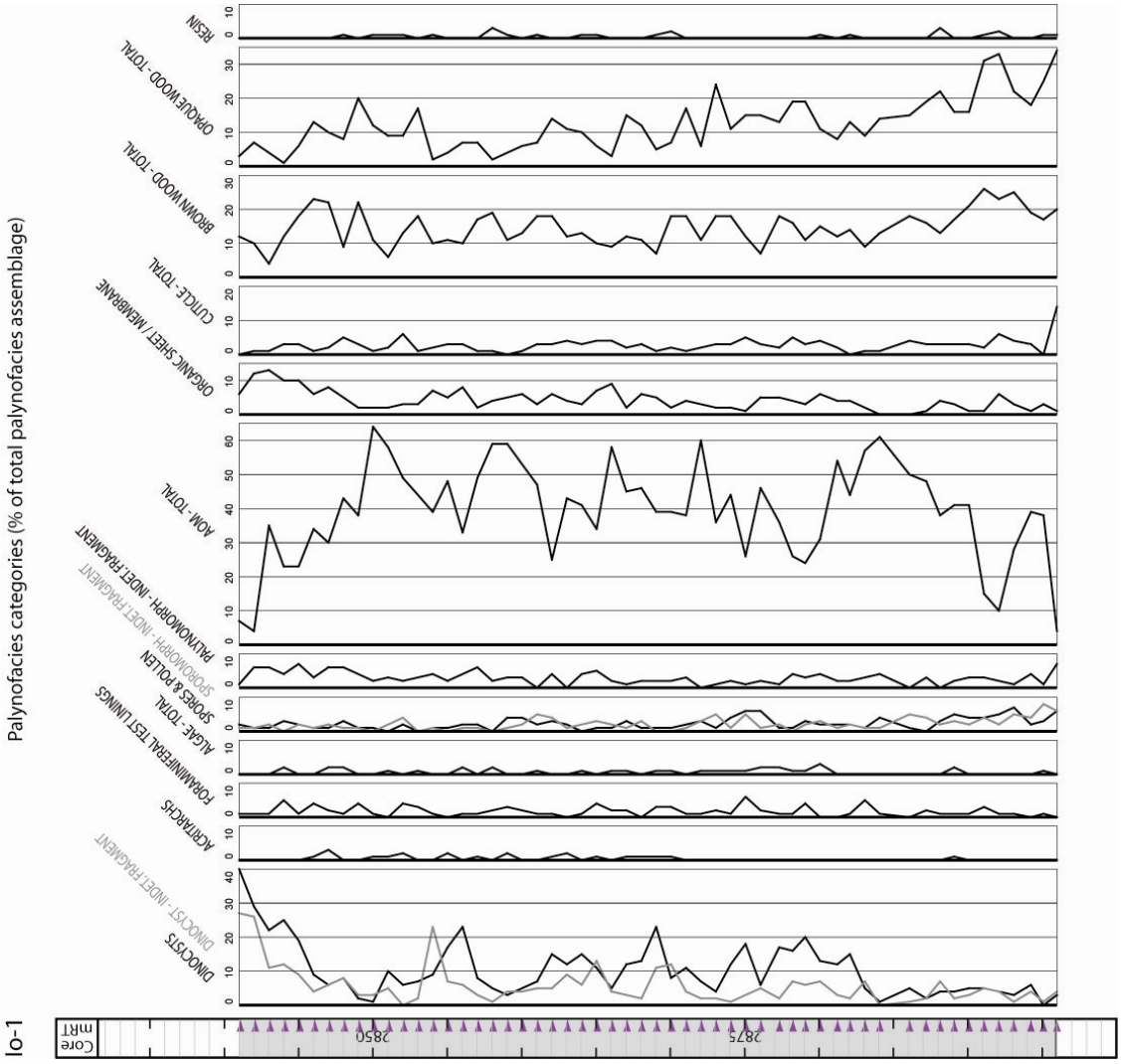

Figure 7.4: Distribution of the main palynofacies categories within Io-1 preparations.

The palynofacies signature is broadly consistent through the stratigraphic interval, with no distinct palynofacies events indicating major 3rd order depositional or environmental changes. The observed palynofacies assemblage is consistent with a nearshore marine palynofacies as outlined by Van der Zwan (1990). The presence of numerous and diverse microforaminiferal test linings is indicative of normal marine coastal environments and euryhaline conditions (Tyson, 1995). These observations further support the lithofacies palaeoenvironmental observations outlined above. Furthermore, the palynofacies signature is observed to oscillate, with increased proportions of woody particles where AOM is relatively reduced. The consistently vacillating palynofacies signature means that broad-scale correlation of the Jansz reservoir can not be independently derived from the palynofacies assemblage. However, when calibrated to the microplankton subzones the palynofacies provides important information for sequence stratigraphic interpretation, as outlined below.

7.3 INTEGRATED BIOSEQUENCE STRATIGRAPHY

Microplankton biostratigraphy, lithofacies and palynofacies interpretations were combined and calibrated to selected wireline logs to produce an integrated biosequence stratigraphic interpretation of the Jansz Sandstone reservoir. Figure 7.5 to Figure 7.8 shows the integration of analyses for each well, while the Figure 7.9 composite of all wells shows interpreted intra-reservoir correlation.

7.3.1 Biosequence Stratigraphic Interpretation

The Jansz Sandstone is a coarsening-upwards, nearshore marine sandstone sequence bounded by unconformities and enclosed within deeper marine mudstones and siltstones. This relationship is characteristic of a Lowstand Systems Tract (Walker & James, 1992). Biostratigraphic, lithofacies and palynofacies analyses indicate that the Jansz Sandstone sequence is comprised of multiple stacked progradational and aggradational parasequences in transgressive/regressive couplets (Refer to Chapter 7.3.5). These parasequences were deposited during a Lowstand Systems Tract caused by tectonically driven relative sea-level fall related to the Oxfordian Phase 3 continental break-up event.

7.3.2 Base Oxfordian Unconformity

The Base Oxfordian Unconformity (BOU) basal sequence boundary is recovered in the cored interval of the Jansz-2 and -3 wells. This boundary is clearly recognised within the Jansz-3 core as two 1-2cm thick layers of granular glauconite at 2865 & 2865.1mRT(c) overlying a bleached, glauconite-rich, bioturbated muddy-siltstone unit. Microplankton data supports this boundary, with the base *Wanaea spectabilis* Zone marker, the first stratigraphic occurrence (FSO) of *Scriniodinium crystallinum*, occurring at 2865mRT(c).

The BOU boundary is not so clearly recognised within the Jansz-2 core, where all bedding surfaces have been removed through bioturbation. An increase in glauconite and a reduction in grain-size and cementation are recorded at Jansz-2, 2916mRT(c), which is interpreted to be the base of the main Jansz Sandstone sequence. This boundary corresponds to the upper glauconite layer at Jansz-3, 2865mRT(c) as indicated by a *Wanaea digitata* acme immediately overlying the high glauconite concentration in both wells.

However, the FSO of *S. crystallinum*, a *Michrystridium* spp. acme, and a distinct switch in microplankton fauna compared to underlying samples is recorded at Jansz-2, 2917mRT(c),

which is within a continuous 2.3m unit of bioturbated muddy-siltstone located between under- and overlying silty mudstones. The occurrence of *S. crystallinum* 1m below the glauconitic horizon suggests that basal *W. spectabilis* Zone sediments are recorded at Jansz-2 that are not identified elsewhere. Hence, deposition was apparently condensed but continuous at Jansz-2 across the regionally recognised BOU sequence boundary. This Jansz-2, 2.3m thick, basal *W. spectabilis* Zone unit is interpreted to correspond to the 10cm thick muddy-siltstone layer enclosed between the two glauconite layers at Jansz-3 2865 & 2865.1mRT(c); however biostratigraphic sampling is required to confirm this interpretation.

7.3.3 'Lower Wedge' Correlation

Wireline log signatures closely reflect the Jansz Sandstone lithological sequence, showing finely fluctuating muddy-sand lithofacies coarsening-upwards into coarse-grained sandstones at the top of Jansz-3 and Io-1. Distinctive, low sonic (DTCO) log peaks in the lower-third of the sequence (*e.g.* Jansz-3, 2847mRT(c/l) and Io-1, 2878 mRT(c)/2886.5mRT(l)) are confirmed through core observations to reflect cemented intervals independent of bedding surfaces. Therefore, while lateral correlation of these horizons may be possible, they may not reflect chronostratigraphic surfaces.

These more highly cemented sediments in the lower-third of the sequence correspond to the Lower Wedge of Jenkins *et al.* (2008) bounded by the Base High Permeability (BHPerm.) marker. The BHPerm. marker is figured here at depths supplied in the WCRs. This marker produces a strong reflection in seismic and permeability models (Figure 7.10) and is mappable across much of the field, but the Lower Wedge is interpreted to pinchout prior to the Jansz-2 location (Figure 7.11). However, if cemented horizons are completely independent of bedding surfaces, as suggested by the core, then these cemented sediments may not represent a discrete progradational wedge as interpreted by Jenkins *et al.* (2008).

Figure 7.5 to Figure 7.9 series: Integrated biostratigraphic, lithofacies and palynofacies analyses for the Jansz Sandstone sequence stratigraphic interpretation. Selected wireline logs are gamma ray (broadly reflecting grainsize and lithology) and DTCO (dipole sonic, compressional wave delay time; broadly reflecting porosity). Depths are provided for both the wireline log depths (mRT(l) = metres below rotary table as recorded by wireline logs) and core depths (mRT(c) = metres below rotary table as recorded on conventional core) which are used for palynological samples and core logging notes. Core depths are calibrated to wireline logs according to the adjustments stated in the Jansz-1, -2, -3 and Io-1 Interpretive Well Completion Reports (WCRs). Grey shading of the core depth column indicates the cored interval, with palynological sample locations collected from the core indicated by small triangles. The Base Oxfordian Unconformity (BOU), Base High Permeability (BHPerm.), Top Porosity (TPor.) and Base Cretaceous Unconformity (BCU) markers are figured as supplied in the WCRs. These markers roughly differentiate intervals of dominant lithofacies, being Lithofacies S43 at the base of the sequence, Lithofacies S42 above the BHPerm. marker, and Lithofacies S1 at the TPor. marker in Jansz-3 and Io-1. The BOU position was confirmed in Jansz-2 and -3 through lithofacies analysis, as discussed herein. The subzones are as proposed in Chapter 6. These subzones are coloured to facilitate comparison, and underlain beneath the wireline logs and palynofacies graphs to identify and highlight palynofacies signatures and intra-reservoir correlation.

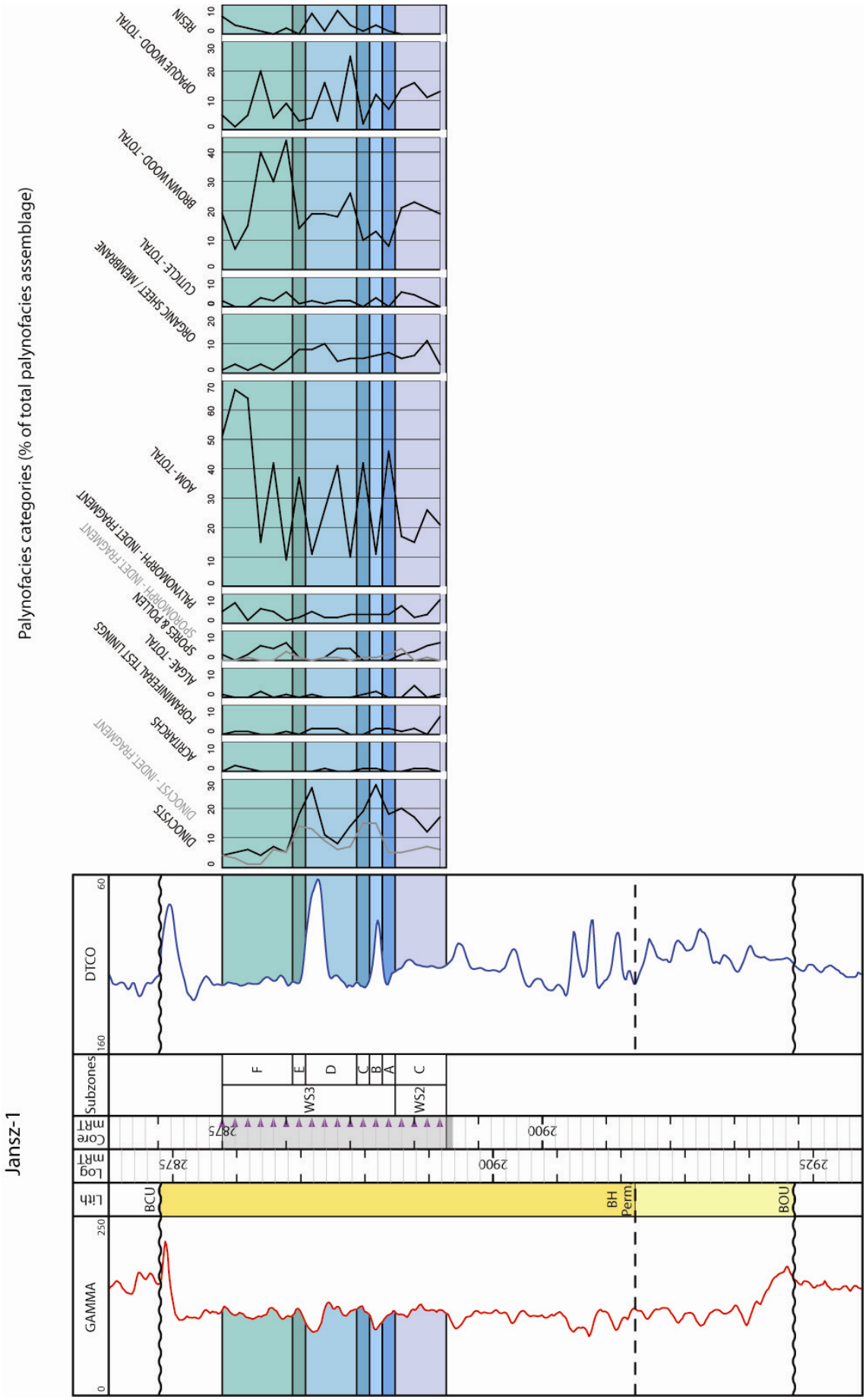

Figure 7.5: Integration of Jansz-1 biostratigraphic, lithofacies and palynofacies analyses with wireline logs for the sequence stratigraphic interpretation of the Jansz Sandstone.

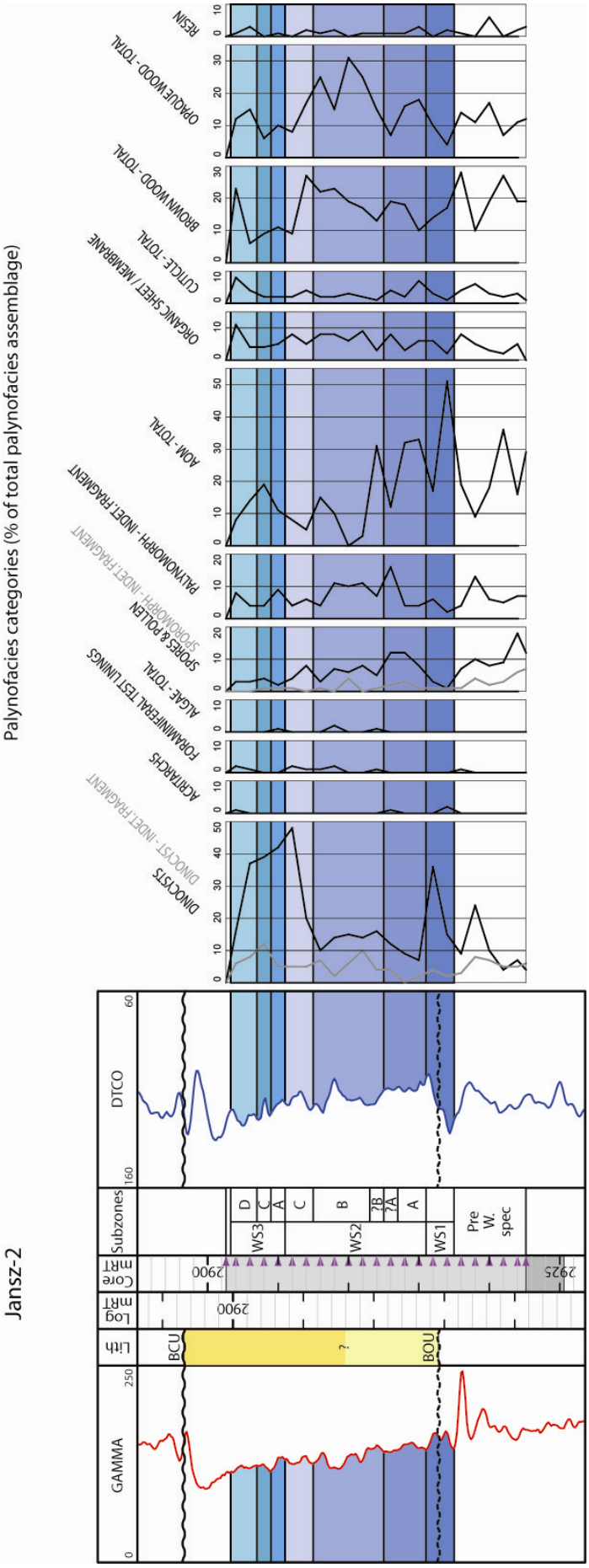

Figure 7.6: Integration of Jansz-2 biostratigraphic, lithofacies and palynofacies analyses with wireline logs for the sequence stratigraphic interpretation of the Jansz Sandstone.

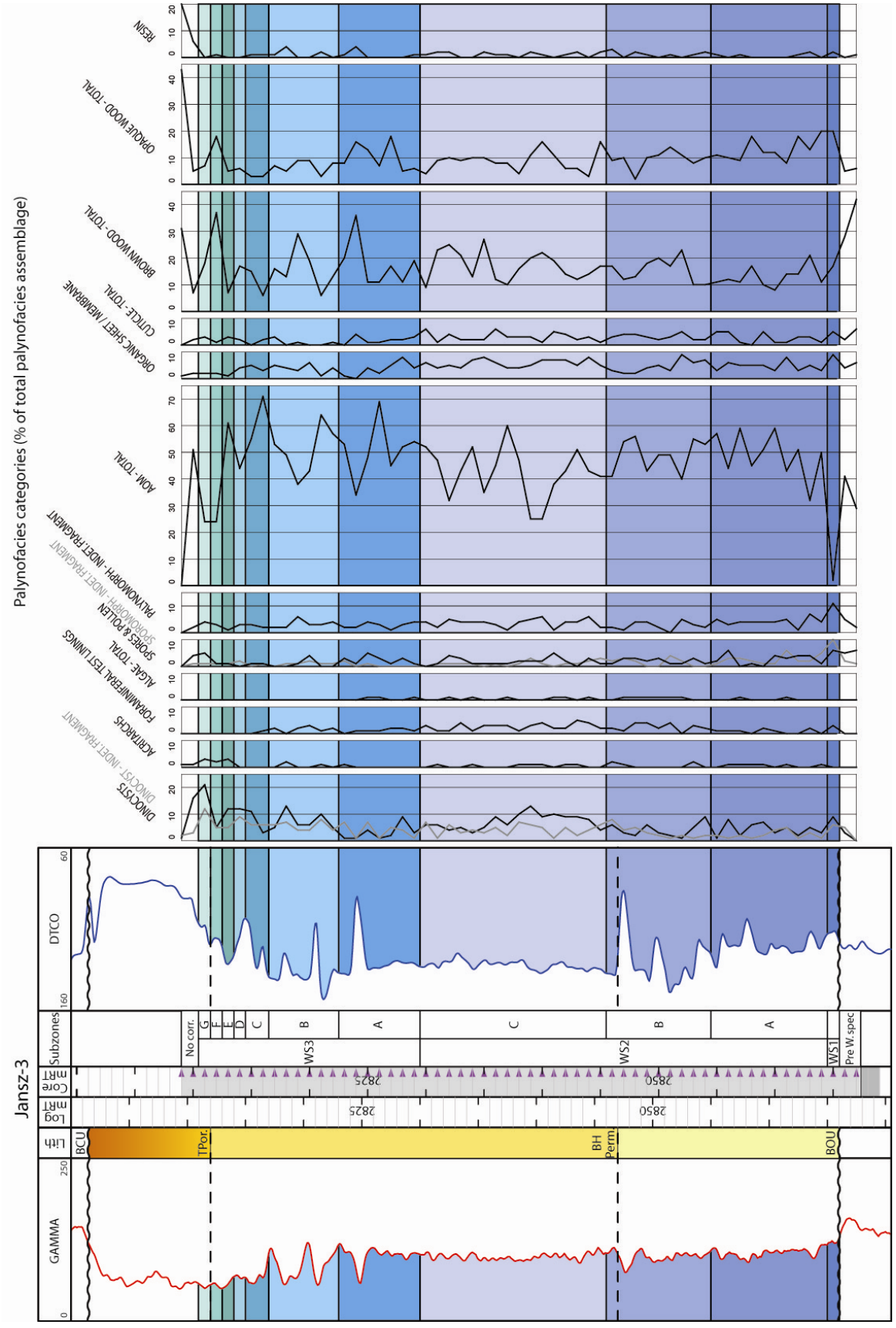

Figure 7.7: Integration of Jansz-3 biostratigraphic, lithofacies and palynofacies analyses with wireline logs for the sequence stratigraphic interpretation of the Jansz Sandstone.

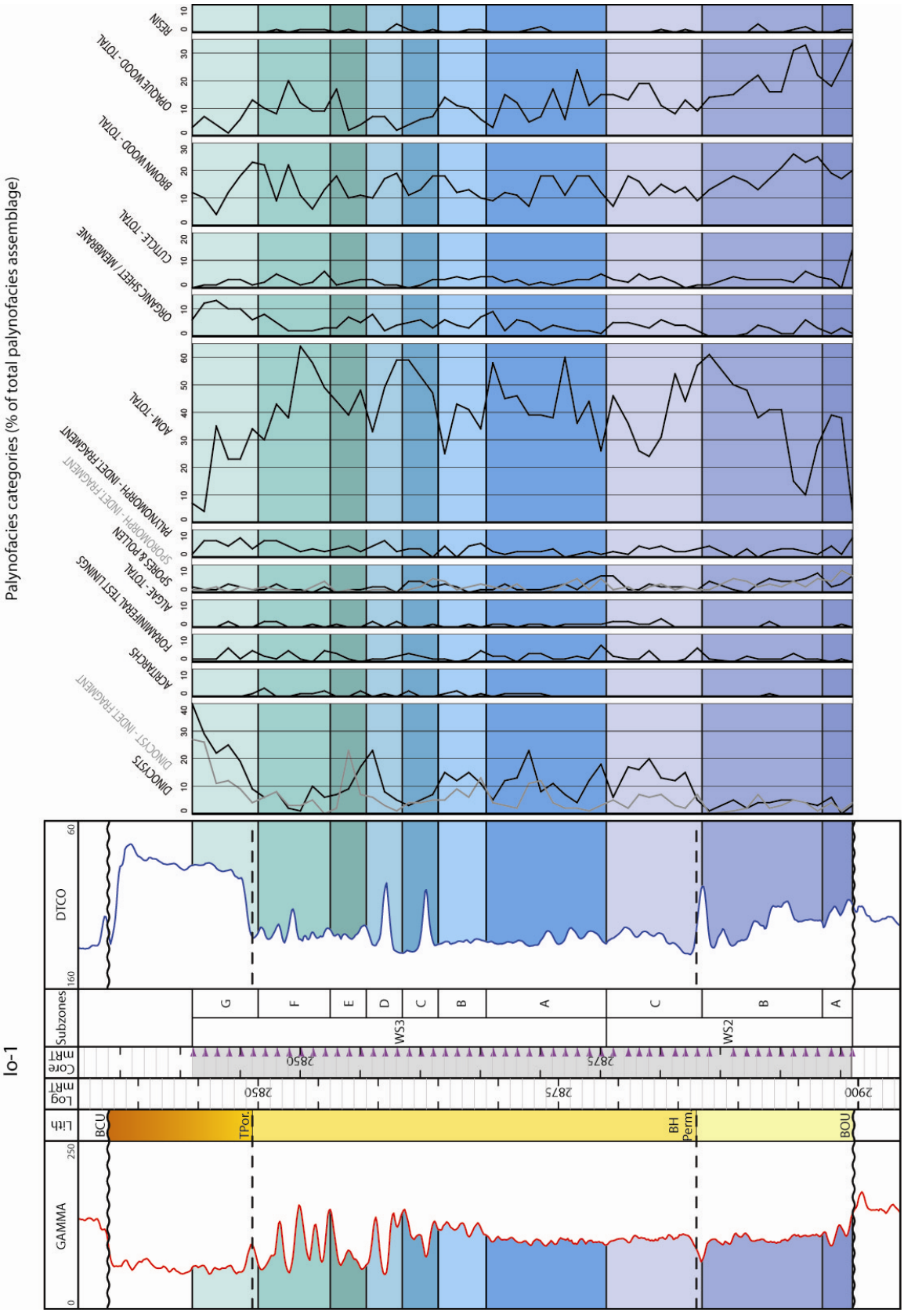

Figure 7.8: Integration of Io-1 biostratigraphic, lithofacies and palynofacies analyses with wireline logs for the sequence stratigraphic interpretation of the Jansz Sandstone.

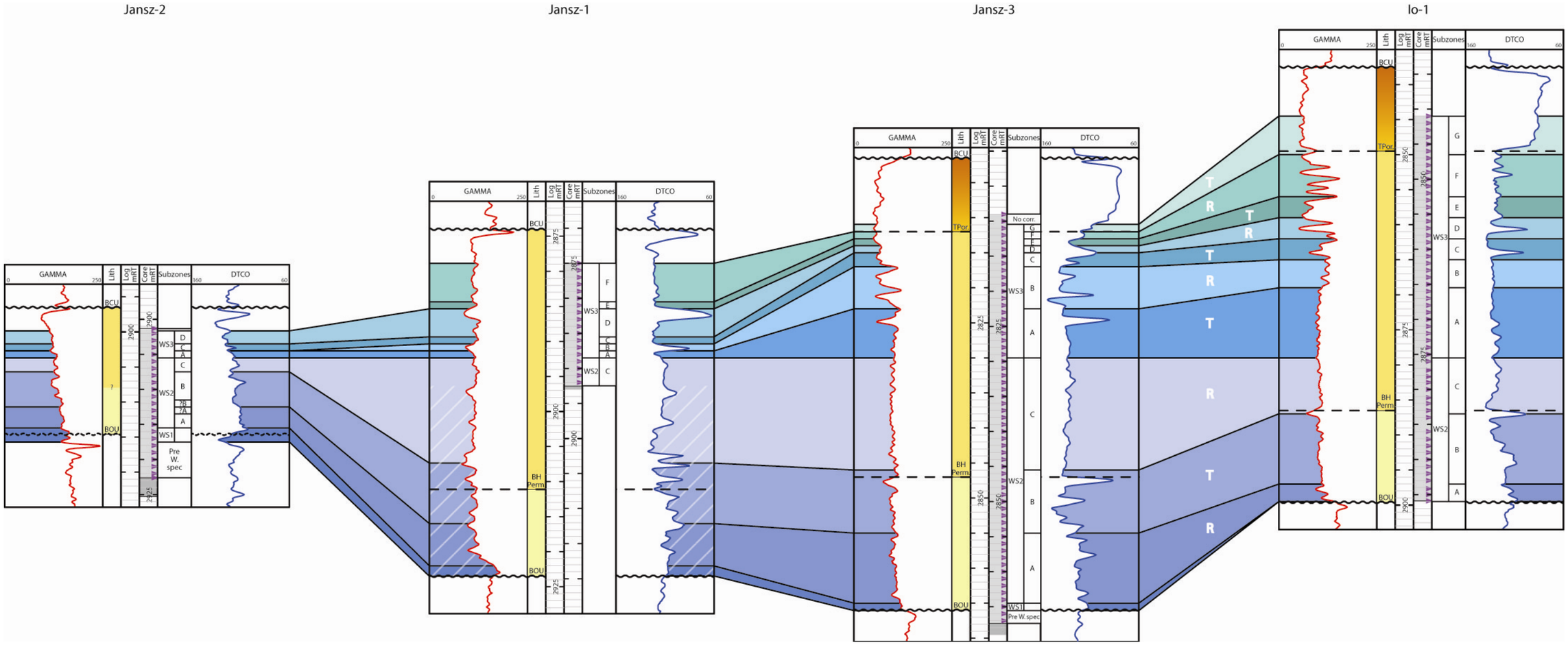

Figure 7.9: Composite summary of the integrated Jansz Sandstone sequence stratigraphic interpretation. Wells are arranged to approximately demonstrate proximal (Io-1) to distal (Jansz-2) mid-shelf to upper-offshore/distal lower shoreface depositional environment. Correlative surfaces of WS3 zonule boundaries delineate chronostratigraphic packages with boundaries that strongly resemble the sigmoidal geometries of lithostratigraphic parasequences. These 'biostratigraphic parasequences' appear to form transgressive/regressive couplets in a progradational sequence. T and R = interpreted Transgressive and Regressive biostratigraphic parasequences respectively. Note: the Jansz-1 WS1 - base WS2C correlations are projections only.

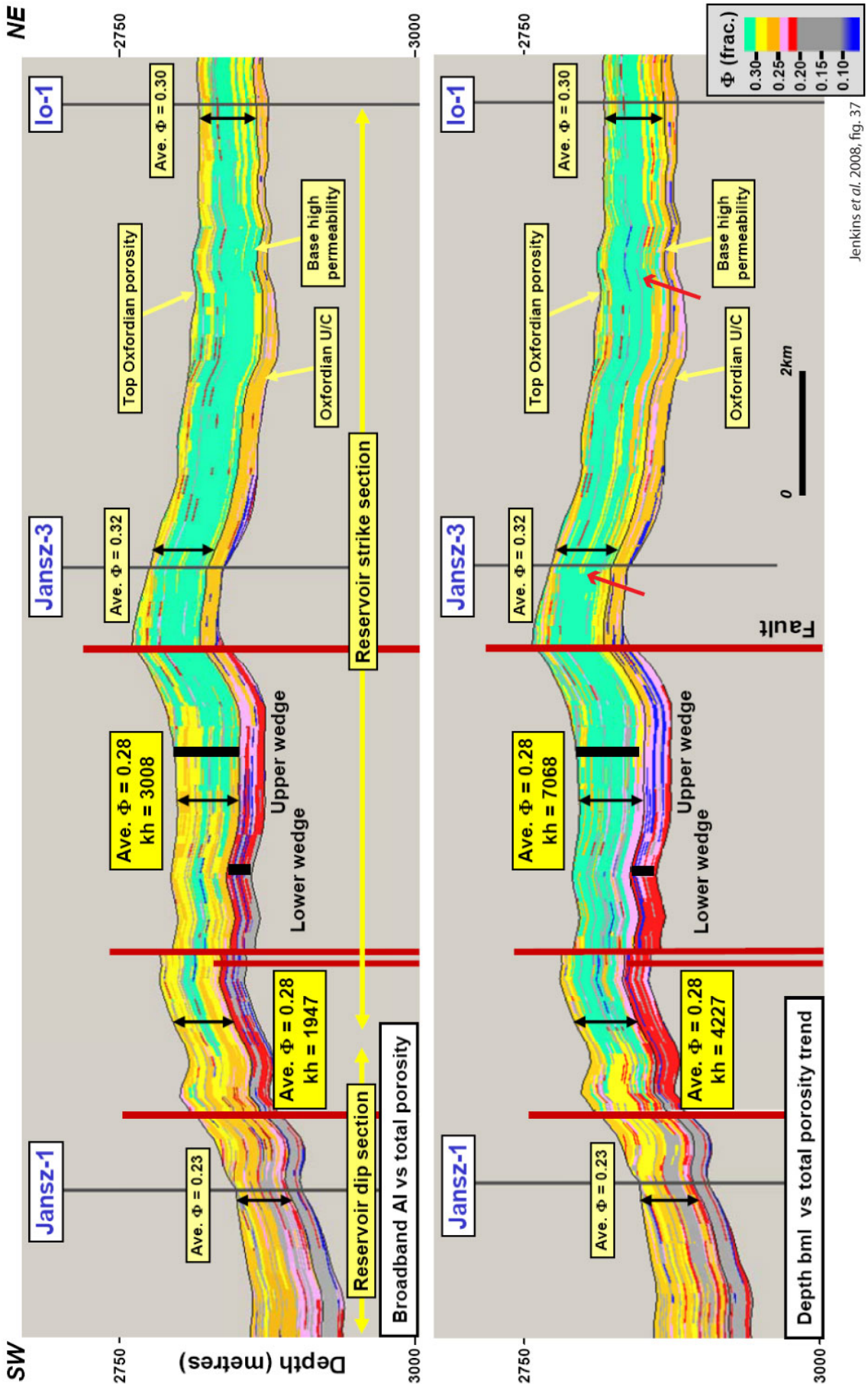

Figure 7.10: Porosity models of Jenkins *et al.* (2008, fig. 37) showing horizons within Jansz-3 which pinchout prior to the Io-1 location (red arrows), supporting the biostratigraphic subzones herein.

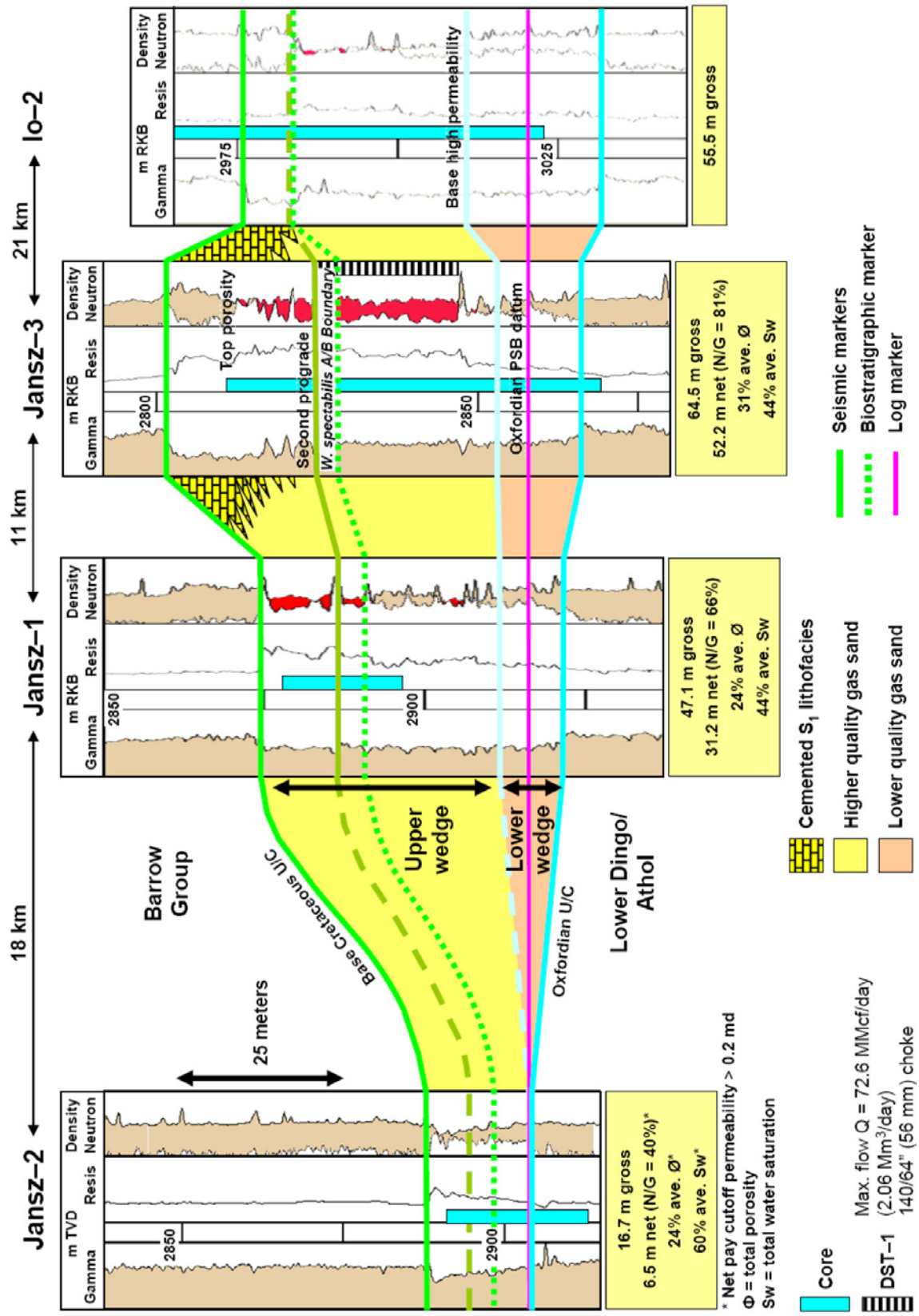

Figure 7.11: Depositional-dip stratigraphic cross section of Jenkins *et al.* (2008, fig. 4).

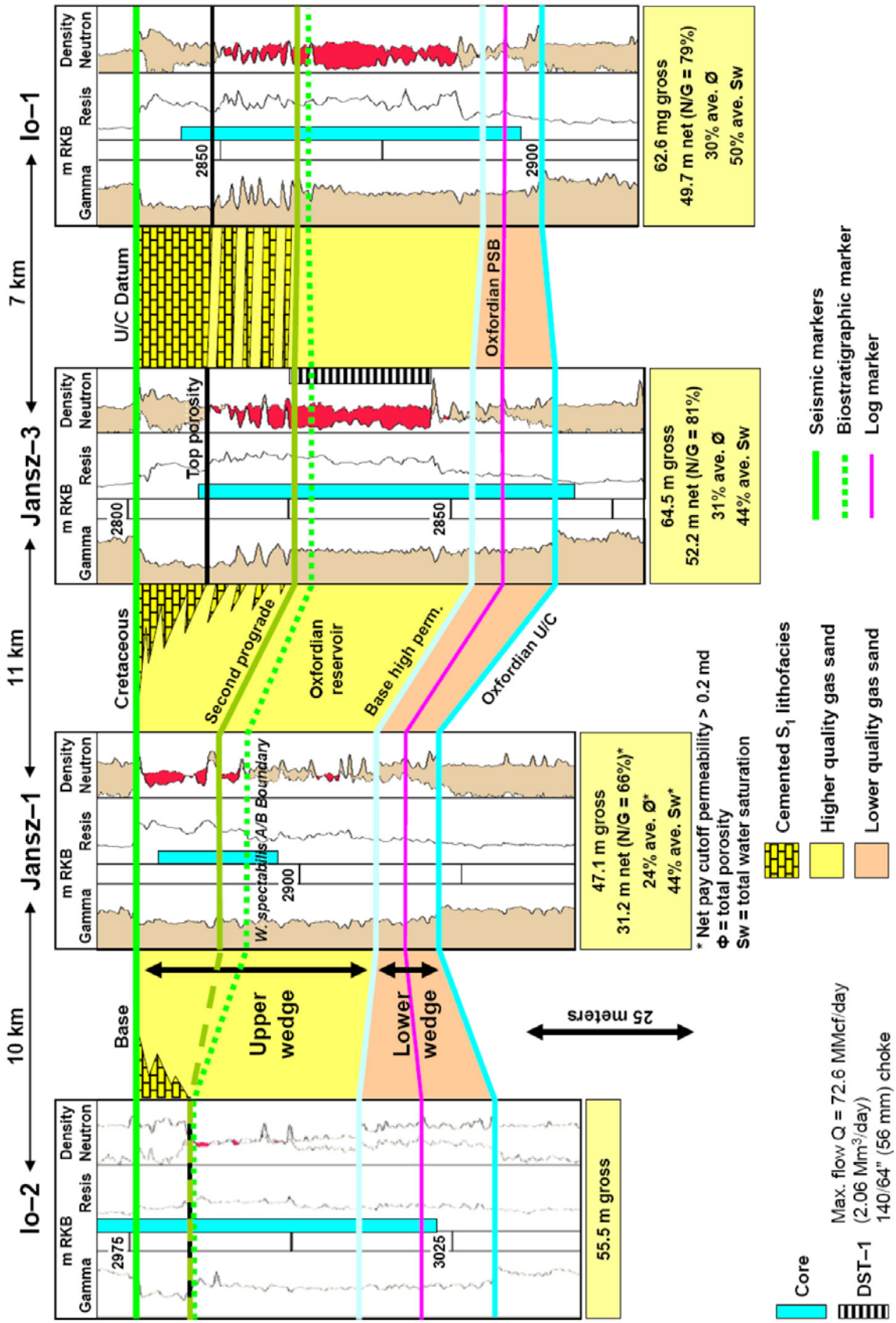

Figure 7.12: Depositional-strike stratigraphic cross section of Jenkins *et al.* (2008, fig. 4).

In contrast to Jenkins *et al.* (2008), biostratigraphic evidence indicates that 'Lower Wedge' equivalent sediments do extend to Jansz-2. Bioevents reveal that the BHPerm. marker correlates quite well to the WS2B/C subzone boundary in Jansz-3 and Io-1, and that a relatively thick succession of WS1-WS2B sediments occurs at Jansz-2. This strongly supports the interpretation that cementation does not reflect a chronostratigraphic surface.

Alternatively, the cemented sequence may reflect authigenic cementation controlled by the mineralogic composition of the primary sediments. Similar to grain-size variations, sediment mineralogy may laterally vary within chronostratigraphic units reflecting depositional environmental controls or sediment provenance. The primary minerals required to generate the authigenic cement may not occur in distal environments such as at Jansz-2; therefore, resultant cementation may not extend to the distal limits of the field. In which case, the cemented sediments may indeed represent a lithostratigraphic unit. Therefore, more analysis is recommended to determine the exact relationship of the BHPerm. marker to the lithostratigraphy and depositional parasequences.

7.3.4 'Lithofacies S_1' Correlation

Contrary to the cemented sequence, low gamma log peaks in the upper-third of the Jansz-3 and Io-1 wells (*e.g.* Jansz-3, 2824mRT(c/l)) are observed to reflect coarse-grained Lithofacies S_1 intervals. The Jansz-3 and Io-1 log signatures appear to correlate very well on first examination. The onset of these units are apparently interpreted by Jenkins *et al.* (2008, fig. 3, reproduced here as Figure 7.12) to represent the Second Prograde of the Upper Wedge, indicating a parasequence boundary. The correlation of these units is indicated to be supported by biostratigraphic evidence of the *Wanaea spectabilis* A/B Boundary closely preceding the Second Prograde surface.

Lithofacies analysis confirms that the Jansz-3, 2824mRT(c/l) lowermost Lithofacies S_1 bed does possess characteristics of a transgressive lag base when observed in core, including a sharp basal contact, large basal clasts and mollusc accumulations in a fining-upwards bed. The 2824mRT(c) palynological sample produced a low AOM/high wood palynofacies assemblage, with very low palynomorph content such that a 250 microplankton specimen count could not be conducted. This palynofacies signature is characteristic of a high-energy deposit and supports the interpretation of a transgressive parasequence boundary.

However, revised biostratigraphic correlation indicates that the lowermost Lithofacies S_1 horizons in Jansz-3 and Io-1 are not contemporaneous. The *W. spectabilis* A/B Boundary

equates to the WS2/WS3 boundary of the subzones proposed herein, which are both typically defined by the last stratigraphic occurrence (LSO) of *Systematophora geminus*. However, this taxon is frequently observed to be reworked within the Jansz Sandstone sequence, resulting in anomalously high *W spectabilis* A/B Boundary placement, particularly within Io-1. Therefore, the concurrent LSO of *Evansia zabra* is here identified as an associate key taxa for the WS2/3 boundary, providing a more consistent bioevent for correlation within the Jansz Sandstone. The LSO of *E. zabra* occurs at 2830mRT(c) in Jansz-3 and 2876mRT(c) in Io-1. Revised placement of this bioevent locates the *W. spectabilis* A/B Boundary approximately 10-15m lower in Io-1 than previously assigned, as indicated on Jenkins *et al.* (2008, fig. 3; here Figure 7.12).

According to the revised biostratigraphic correlation, the lowermost Lithofacies S_1 bed in Jansz-3 (2824mRT(c/l)) occurs within the WS3A subzone, while the lowest Lithofacies S_1 bed in Io-1 (2860mRT(c)/2864mRT(l)) occurs in the later WS3C subzone. Therefore, these units could not have been deposited synchronously. This results in a significantly different correlation between the Jansz-3 and Io-1 wells than deduced by Jenkins *et al.* (2008) in Figure 7.12. This revised correlation is supported by porosity models presented in Jenkins *et al.* (2008, fig. 37, reproduced here as Figure 7.10), where horizons in the central Jansz-3 region are observed to pinchout prior to the Io-1 location. Therefore, all available data indicates that the Jansz-3, 2824mRT(c/l) Lithofacies S_1 bed is a transgressive surface, and does represent a parasequence boundary. However, this surface is not clearly reflected in the sequences of adjacent wells and in particular does not correlate to the lowermost Lithofacies S_1 unit of Io-1.

7.3.5 Biostratigraphic Parasequences

As the Lithofacies S_1 example above illustrates, correlatable parasequence boundaries linked to sedimentary surfaces are typically indeterminate through lithofacies analysis in the Jansz Sandstone. This is a result of intense bioturbation which has removed most primary sedimentary structures, including bedding surface contacts. Therefore, individual parasequences, in the traditional sense, and their associated surfaces are not identifiable within this project. However, biostratigraphic correlation and palynofacies analyses provide valuable evidence regarding parasequence geometry and relationships.

Palynofacies data were calibrated to the microplankton subzones to identify palynofacies signatures in chronostratigraphic sediments. Calibration revealed that oscillation in the Jansz-1 AOM signature closely corresponds to zonules of the proposed subzones (Figure 7.5). This association is particularly well defined at subzones based upon acme bioevents, such as within the WS3 subzone.

As mentioned in Chapter 7.2 above, the palynofacies signature is observed to alternate between high relative proportions of AOM and woody debris. Similar oscillations in various palaeodepositional environments are recorded as "alternating sapropelic and humic palynofacies" by Huault *et al.* (1995) and "altered lignocellulosic debris / amorphous organic matter ratio" by Garcia *et al.* (2011). Such signatures are interpreted to reflect hydrodynamic variations in response to sea-level fluctuations or humid/arid climate variations in response to orbital forcing. A high proportion of AOM in marine sediments is commonly associated with maximum flooding surfaces (MFS) and highstand systems tracts (HST; Huault *et al.*, 1995; Bucefalo-Palliani *et al.*, 1998), which are typically periods of deep water and low hydrodynamic energy. Conversely, woody particles are common in intermediate- to high-energy deposits in all environments (Tyson, 1995), which in a nearshore marine environment is shallow water. Therefore, if the relative proportions of AOM and woody particles indicate deep and shallow water respectively, the ratio of these groups (AOM/wood ratio) represents a good proxy for relative sea-level.

The close correspondence of the AOM/woody particle ratio to the biostratigraphic zonules indicates that the acme events of the key zonule markers are directly influenced by sea-level changes. Therefore, the associated zonule boundaries directly reflect parasequence surfaces. As a result, depending on the biostratigraphic resolution, each zonule may directly represent an individual parasequence, with the relative sea-level indicated by the AOM/wood ratio.

Biostratigraphic correlation of the Jansz Sandstone is presented in Figure 7.9. Correlative surfaces of zonule boundaries defined by acme events, such as the WS3 zonules, delineate chronostratigraphic packages with boundaries that strongly resemble the sigmoidal geometries of lithostratigraphic parasequences. Furthermore, these 'biostratigraphic parasequences' appear to form transgressive/regressive couplets, which is supported by the broad AOM / wood particle trends for each of the WS3 zonules evident in Figure 7.5 to Figure 7.8. Transgressive biostratigraphic parasequences, being the WS3A, C, E & G zonules, have the thickest sedimentary accumulation in the proximal Io-1 well. Conversely, regressive, or progradational, biostratigraphic parasequences are typically thickest in the more distal Jansz-1 well. Where Io-1 zonules have a thick progradational sequence, these are interpreted to be coarse Lithofacies S_1 storm or mass-flow deposits which are of limited lateral extent and thickest close to the source. This is supported by the distinct decreasing trend of AOM in Io-1 (and Jansz-3) in the stratigraphically higher zonules.

The WS3 biostratigraphic parasequences also show a progradational series from proximal to distal environments, with WS3A & B thickest in Io-1 and Jansz-3 and significantly condensed in Jansz-1 and -2. While the WS3B zonule is not recovered in the Jansz-2 palynological

preparations, the core does not indicate any depositional break between the recovered WS3A and WS3C zonules. Therefore the WS3B zonule is interpreted to be present within Jansz-2, but below sampling resolution.

AOM/wood ratios appear to be highly sensitive to sea-level fluctuations. In fact, the Jansz-1 AOM signature suggests that WS3D is made up of more parasequences than currently identified by the zonules. Jansz-1 WS3D is comprised of an upper and lower regressive trend separated by a transgressive trend. However, the relatively thin accumulation of WS3D sediments in other wells has not enabled the identification of additional acme bioevents for correlation. Such minor acmes may occur, but are either to subtle to be recognised or occur below sampling resolution. This suggests that much higher-resolution correlation of the Jansz Sandstone may be possible if this would be advantageous for field production.

The biostratigraphic parasequences identified within WS3B subzone are interpreted to represent 4^{th} order cyclicity within the Jansz Sandstone. Such fine cyclicity is not observed with the WS1 and WS2 subzone correlations, which may be due to the subzone boundaries being defined by FSO/LSO events rather than acmes, which may be less influenced by hydrodynamic changes. However the palynofacies graphs do indicate that these zonules are influenced by cyclicity. Broad AOM/wood ratios show decreasing trends in WS2A & C and increasing trends in WS2B, suggesting regressive and transgressive cycles respectively.

While the identification of biostratigraphic parasequences appears very promising for correlation and resolution of bioturbated sequences, these events have not yet been lithologically tested. It must be noted that the exact occurrence of taxon acme events may be offset and not exactly correspond to actual lithological parasequence boundaries. Furthermore, it is uncertain if some important parasequence surfaces may not be identified due to palynofacies limitations. For example, the Jansz-3, 2824mRT(c/l) Lithofacies S_1 intervals is interpreted as a parasequence surface, but has not been identified in the biostratigraphic parasequences. However, this project shows that biostratigraphic parasequences can provide good evidence of sequence and reservoir architecture in the absence of lithostratigraphic controls.

Chapter 8
PALAEOENVIRONMENT

8.1 Dinoflagellate cysts as palaeoenvironmental proxies

Palynofacies and lithofacies analyses indicate that the Jansz Sandstone was deposited in a nearshore marine palaeodepositional environment, as outlined in Chapter 7.

As indicated by the quantitative and palynofacies analyses calibration, the microplankton assemblage is influenced by environmental and ecological preferences. The ranges of some dinoflagellate cysts appear to be influenced by shoreline proximity or have abundances influenced by sea-level fluctuations. The following taxa appear to have ecological preference for deeper water:

1. *Dissiliodinium volkheimeri* – abundances in each well directly proportional to relative sea-level depth, being most abundant in distal Jansz-2 and least abundant in proximal Io-1.
2. *Kallosphaeridium microgranulatum* – very highly abundant in Jansz-wells, relatively reduced at the more proximal Io-1.
3. *Rigaudella filamentosa* – abundances in each well directly proportional to relative sea-level depth, being most abundant in Jansz-2 and least abundant in Io-1. Additionally, shows a sharp decrease in above WS3E, possibly reflecting the shoaling-upwards sequence.
4. *Limbodinium absidatum* – highest (but low) abundance in distal Jansz-2 with very few occurrences in more proximal environments.

(Refer to Appendix 4 charts for quantitative values).

Conversely, the following appear to have an ecological preference for shallower water:

1. *Microdinium tantillum* – highest abundance in Jansz-3, proportionally declines at Io-1 and towards Jansz-2.
2. *Pilosidinium equispinum* – FSO varies between wells, but abundance significantly increases above WS2C in all wells.

Interestingly, reportedly common Oxfordian taxa elsewhere are not recorded within the Jansz preparations at all. These include *Gonyaulacysta ceratophora* and *Cygnusicysta taltarniana.* The conspicuous absence of these otherwise prevalent taxa may reflect an ecological preference of these taxa to deeper waters than recorded in any Jansz-Io wells. Alternatively, the absence of these taxa may be caused by subtle environmental parameters, such as nutrient levels etc, that are not identifiable.

8.2 Palaeoenvironmental anomalies

While the nearshore marine palaeodepositional environment of the Jansz Sandstone is relatively certain, the observed dinoflagellate assemblage is atypical of aspects of a nearshore environment in the following areas in particular:

1. **Skolochorate cyst abundance increases with shallower water-depth.** Skolochorate cysts are typically interpreted to be deep water, low hydrodynamic energy indicators of offshore, open marine environments (Tyson, 1995; Stover *et. al.*, 1996; Quattrocchio *et. al.*, 2006). However, the Jansz Sandstone is a shoaling-upwards sequence, indicating an inverse preference to a higher-energy regime. This anomalous signature is interpreted to result from an expansion in the diversity of skolochorate cysts, with only *Adnatosphaeridium* and *Rigaudella* occurring in the lower half of the sequence, and with *Contracysta*, *Oligosphaeridium*, *Perisseiasphaeridium* and *Stiphrosphaeridium* appearing around the WS2/3 subzone boundary. Therefore, the increasing proportion of skolochorate cysts in the Jansz sequence appears to be related to taxon evolution and range expansion rather than environmental controls.

2. **Distinctive absence of Peridinioid cysts.** The Jansz Sandstone sequence contains only one identifiable Peridinioid cyst, being the informally described but distinctive Gen. et. sp. indet. H. The Peridinioid/Gonyaulacoid (P/G) ratio is widely accepted as a reliable indicator of heterotrophic (P-cysts) and autotrophic (G-cysts) dinoflagellates reflecting upwelling related nutrient levels and productivity (Bujak, 1984; Harland, 1973, 1988; Tyson, 1995; Stover *et. al.*, 1996). The striking absence of P-cysts in the Jansz Sandstone may therefore indicate nutrient poor conditions. However, the abundant AOM content of the Jansz sequence suggests that productivity was high, therefore nutrient levels were sufficient. Therefore, two main possible explanations for the absence of P-cysts are viable for the Jansz sequence:

   A/ Bioturbation has selectively reduced the P-cyst content. This has been demonstrated in sediments from Peru by Powell *et al.* (1990). The extent of bioturbation of the Jansz Sandstone sequence may have resulted in the low P-cyst ratio; or,

   B/ Similar to skolochorate cyst diversity, P-cysts evolved during the Jurassic but did not become common until the Cretaceous (Wall & Dale, 1968; Fensome *et al.*, 1993, 1996). Therefore their absence from the Jansz sequence may simply be due to their restricted distribution in the Oxfordian.

3. **High dinoflagellate cyst abundance in some oxidised, ferruginous intervals.** Coarse-grained, oxidised, ferruginous Lithofacies S_1 sediments were identified during sampling as having poor palynological potential for two reasons:

   A/ Palynomorphs and palynodebris act as fine sedimentary particles, and therefore accumulate in fine-grained sediments. As such, coarse-grained sediments typically are palynomorph poor; and

   B/ Organic matter is destroyed through oxidisation. Oxidised sedimentary layers are typically identified by their characteristic rust-brown colour, which usually indicates subaerial exposure and oxic to suboxic sedimentary conditions (Tyson, 1995).

   Therefore, the presence of oxidised (rust-coloured), ferruginous sediments in combination with coarse grain-size suggested these samples may be palynomorph barren.

   While this was confirmed in rare samples (*e.g.* Jansz-3, 2809mRT(c)), some Lithofacies S_1 preparations were highly productive and yielded the highest quality and best preserved specimens of all preparations examined in this study (*e.g.* Io-1, 2841-2844mRT(c)). The exact mechanism for this result is uncertain. However, Lithofacies S_1 sediments are often poorly sorted, and concentration of the fine-grained matrix prior to processing may have produced an artificially high yield. However, the high species diversity (>100 dinoflagellate cyst species per sample) and excellent preservation suggests matrix concentration was not significant.

   Lithofacies S_1 sediments are interpreted to be gravity flows from lagoonal environments (Jenkins *et al.*, 2008). However, these coarse units do not contain a high proportion of organic material derived from terrestrial or brackish water environments. The very high abundance of typically open marine microplankton, such as skolochorate dinoflagellate cysts, may be a result of the high hydrodynamic energy required to transport the coarse sediment. High energy regimes do not permit palynomorphs and palynodebris to settle *in situ*, reducing the terrestrial/lagoonal palynomorph signature. The observed dinoflagellate cysts may have then accumulated in the finer grained muddy-sandstones which accumulated between the coarse-grained mass-flow units. The sediments were then homogenised through bioturbation, retaining the high dinoflagellate volumes in the fine-grained matrix.

   One postulation regarding preservation may be that the high concentration of ferruginous ooids within these sediments may have been oxidised preferentially, acting as a sacrificial oxidiser and preserving the organic matter. Dinoflagellate cysts may then have been protected from compression damage by grain-supported sediments during subsequent compaction events.

8.3 Palaeoclimate induced intraspecific variability

A significant amount of intraspecific variability was observed in the Jansz-Io preparations. Variability was not restricted to one group or lineage, but common in a range of cysts, including cavate, chorate and proximate cysts. Examples include *Broomea fusticula, Barbatacysta creberbarbata* and *Productodinium chenii.* The most prominent example of 'intraspecific' variability was observed in the proximate to skolochorate *Contracysta* Complex. This complex exhibits a complete continuum of intergrading morphotypes, including proximate, proximochorate, skolochorate and phragmochorate cysts.

Intraspecific variability within the Jansz-Io preparations is consistently observed throughout the WS3 sequence. Furthermore, all morphological variants of a single species were observed to occur within individual samples, although some morphotypes may be more dominant than the other. Therefore, the driver for intraspecific variability within this sequence must be cyclical – to occur throughout the sequence without producing a major change in the sedimentary sequence – but each event must be of very short duration, so that different morphotypes can occur concurrently in individual samples.

Recent publications on extant dinoflagellate cultures have shown that cyst morphology directly correlates with salinity and temperature (Mertens *et al.*, 2009; Rochon *et al.*, 2009). Mertens *et al.*, (2009) demonstrated a correlation between increased process length and salinity in *Lingulodinium polyedrum*, with shortest process lengths occurring in low salinities. Rochon *et al.* (2009) determined that extreme cyst variability within a single *Gonyaulax spinifera* culture was triggered by certain low salinity conditions (25-30psu at 12°C). Their research supports core evidence by Ellegaard (2000) of dinoflagellate cyst morphological variations over the last 2000 years related to assumed low salinity stress. Therefore, evidence suggests that the main driver for intraspecific variability is low salinity.

The most likely mechanism for reduced salinity within a nearshore marine sequence is increased fresh-water runoff. The cyclical driver for this increased runoff must be of shorter duration than the probable orbital forcing signature observed in the biostratigraphic parasequences, since intraspecific variability is not restricted to parasequence-scale cyclicity. Short-duration cycles producing high-volume changes in rainfall and runoff can be attributed to a seasonal monsoonal system. A monsoonal climatic regime is consistent with the identification of a wave- and storm-dominated coastline at the Jansz location. Large monsoonal events may have instigated the failure of adjacent lagoon systems, providing the sediment source for Lithofacies S_1 ferruginous ooids as interpreted by Jenkins *et al.* (2008) and hydrodynamic energy levels for coarse-grained sediment deposition.

Considerable evidence exists for Jurassic “summer wet” monsoon systems in the north-west of Australia (Parrish, 1992; Hallam *et al.*, 1994; Philippe *et al.,* 2004). Therefore, it is proposed that a stable, long-term, cyclical monsoonal regime generated rapid fluctuations in nearshore marine salinity levels (and possibly temperature). This resulted in low-salinity stress morphological responses in dinoflagellate cysts, which is recorded as the high amounts of intraspecific variability observed in the Jansz Sandstone sequence.

Chapter 9
CONCLUSIONS

This study has comprehensively examined the *Wanaea spectabilis* Zone microplankton content from the Jansz Sandstone reservoir sequence of four wells in the Jansz Gas Field.

Palynological preparations from 155 conventional core samples yielded a highly diverse assemblage of dinoflagellate cysts and acritarchs of good to excellent preservation. Taxonomic analysis identified 112 genera with 194 microplankton species and varieties. Of these, 2 new genera and 26 new species were formally described, 2 species were emended with 1 species generically reattributed. An additional 11 genera and 37 species were informally described for future comparison with other *Wanaea spectabilis* Zone sequences. Examples of each species from this well-preserved material are illustrated in a large catalogue of plates.

Examination of a complex continuum of dinoflagellate cyst morphotypes with intratabular processes, the "*Contracysta* complex", revealed new insights into the process and trabeculum development of dinoflagellate cysts. This lead to the identification of a 'reverse' wall relationship for skolochorate dinoflagellate cysts observed in Jansz-Io preparations. A new genus, *Contracysta*, was erected to include proximate, proximochorate and phragmochorate morphotypes displaying this wall relationship that may not be attributed to existing skolochorate genera. Future examination of similar skolochorate genera, such as *Oligosphaeridium* and *Rigaudella*, may reveal that a reverse wall relationship is common to many, or all, of the currently attributed species.

Qualitative and quantitative palynological analyses were conducted to refine the intersected *Wanaea spectabilis* Zone sequence. The absence of *Wanaea spectabilis* indicates that the upper one-third of the eponymous microplankton zone is not recorded in the cored interval, and therefore unfortunately could not be analysed in this study.

Biostratigraphic analysis enabled high-resolution correlation of the Jansz Sandstone. Sampling of the reservoir sequence at 1m intervals enabled the identification of minor bioevents that may not have been evident at wider sampling intervals. Therefore, greater resolution could be achieved in intra-reservoir biostratigraphic correlation than is possible through a typical petroleum exploration sampling regime. A comparison of quantitative methods revealed that a 250 specimen count is advantageous in highly diverse assemblages, since subtle abundance signatures are difficult to identify in a 100 specimen count. However, for routine palynological analyses, a 100 specimen count at high density sampling intervals will often enable more

accurate biostratigraphic correlation of reservoir sequences than 250 specimen counts at wider intervals.

Key bioevents common to the informal Foster (2001) and Morgan *et al.* (2002) *Wanaea spectabilis* Zone subzones were utilised where possible to: 1/ facilitate regional correlation; and 2/ present the most broadly applicable subzone revision possible, given that these events are confirmed to be applicable over a large geographical area. However, key bioevents from those schemes were absent or difficult to apply to the examined samples. Therefore, new bioevents, predominantly from new taxa identified during taxonomic analysis, were used for subdivision of the intersected *W. spectabilis* Zone sequence.

The first stratigraphic occurrences of multiple newly identified taxa occur concurrently with the basal zone marker, *Scriniodinium crystallinum*. The lower half of the examined *Wanaea spectabilis* Zone sequence is well defined by first and last stratigraphic and common taxon appearance or extinction events. However, the upper half of the sequence contains very few consistent FSO/FCO and LSO/LCO bioevents to utilise for biozonation refinement. Discordant taxon events may be due to the more marginal marine palaeoenvironmental setting of some Jansz-Io wells, particularly Io-1, with habitat limitations reflected in species occurrences and abundances.

Three *Wanaea spectabilis* Zone subzones, WS1-3, are proposed for the analysed sequence. WS2 and WS3 are divided into 3 (WS2A-C) and 7 (WS3A-G) zonules respectively. The subzonation hierarchy reflects the confidence level of the boundaries: WS1-3 are bounded by regionally recognised events, whereas the zonule boundaries are less certain, and may be bounded by minor acme events that may be of limited regional extent. Consequentially, the proposed subzonation scheme is considered as informal until the regional extent of the bioevents can be determined.

This proposed biozonation scheme was then combined with lithofacies and palynofacies analyses to produce integrated biostratigraphic and bio-sequence stratigraphic interpretations of the Jansz Sandstone reservoir sequence.

Lithofacies analysis supports the revised lithological interpretations of Jenkins *et al.* (2008).

The overall palynofacies signature reflects the monotypic sedimentary sequence, with no distinct palynofacies events indicating major 3rd order depositional or environmental changes. Therefore, broad-scale correlation of the Jansz reservoir can not be independently derived from the palynofacies assemblage. Detailed palynofacies analysis revealed an inversely oscillating

AOM/wood ratio reflecting cyclic hydrodynamic energy levels through sea-level change associated with 4th order (or less) cyclicity. When callibrated to the biostratigraphy, the WS3 bioevent-based zonule boundaries and AOM/wood ratio signatures revealed 'biostratigraphic parasequences' forming transgressive/regressive couplets. The identification of 'biostratigraphic parasequences' provides valuable information regarding sequence and reservoir architecture in the absence of lithostratigraphic controls.

The application of selected dinoflagellate cyst species as palaeoenvironmental proxies was examined. The ranges of some dinoflagellate cysts appear to be influenced by shoreline proximity or have abundances influenced by sea-level fluctuations and therefore reflect environmental and ecological preferences. Atypical taxon distributions observed within the Jansz Sandstone sequence, such as skolochorate genera and the absence of Peridinioid (P) cysts, are interpreted to be related to taxon evolution and range expansion rather than environmental controls. Extreme intraspecific variability of some observed dinoflagellate cyst taxa may reflect low salinity and/or temperature changes caused by a high-frequency, cyclical climatic regime, such as a seasonal monsoonal climate.

Chapter 10

REFERENCES

AGSO North West Shelf Study Group, 1994. Deep reflections on the North West Shelf: changing perceptions of basin formation. In Purcell, P. G. and Purcell, R. R., (Eds), *The Sedimentary Basins of Western Australia.* Proceedings of the Petroleum Exploration Society of Australia West Australian Basins Symposium, Perth, 63-76.

Al-Ameri, T. K., Al-Najar T. K. and Batten, D. J., 2001. Palynostratigraphy and palynofacies indications of depositional environments and source potential for hydrocarbons: the mid Cretaceous Nahr Umr and lower Mauddud formations, Iraq. *Cretaceous Research 22,* 735-742.

Albert, N. R. D., Evitt, W. R. and Stein, J. A., 1986. *Lacrymodinium*, n. gen., a gonyaulacoid dinoflagellate with intercalary archeopyle from the Jurassic and Early Cretaceous of California and Alaska. *Micropaleontology 32 (4),* 303-316.

Alberti, G., 1961. Zur Kenntnis mesozoischer und alttertiärer Dinoflagellaten und Hystrichosphaerideen von Nord- und Mitteldeutschland sowie einigen anderen europäischen Gebieten. *Palaeontographica, Abt A, Band 116,* 1-58.

Arkell, W. J., 1956. *Jurassic Geology of the World.* Oliver and Boyd, Edinburgh and London, 806p.

Ashraf, A. R., 1979. Die Räto-jurassischen Floren des Iran und Afghanistans. 6. Jurassische und unterkretazische Dinoflagellaten und Acritarchen aus Nordafghanistan. *Palaeontographica, Abt B, Band 169,* 122-158.

Backhouse, J., 1988. Late Jurassic and Early Cretaceous Palynology of the Perth Basin, Western Australia. *Bulletin Geological Survey of Western Australia 135,* 233p.

Backhouse, J., 2006. Albian (Lower Cretaceous) dinoflagellate cyst biostratigraphy of the Lower Gearle Siltstone, Southern Carnarvon Basin, Western Australia. *Palynology 30,* 43-68.

Bailey, D. A., 1987. *Durotrigia daveyi* gen. et sp. nov., an Early Bajocian dinocyst with a variable precingular archeopyle. *Journal of Micropalaeontology 6 (2),* 89-96.

Bailey, D. A. and Partington, M., 1991. Some Middle Jurassic dinocysts from the Brent Group of the northern North Sea. *Journal of Micropalaeontology 9 (2),* 245-252.

Baillie, P. W., Powell, C. M., Li, Z. X. and Ryall, A. M., 1994. The tectonic framework of Western Australia's Neoproterozoic to Recent sedimentary basins. In Purcell, P. G. and Purcell, R. R., (Eds), *The Sedimentary Basins of Western Australia.* Proceedings of the Petroleum Exploration Society of Australia West Australian Basins Symposium, Perth, 45-62.

Banfield, J. and Beattie, R. J., 2002. *Well Completion Report Interpretive Data – Io 1. Carnarvon Basin Exploration Permit WA-267-P*. Unpublished.

Barber, P. M., 1988. The Exmouth Plateau deep water frontier: a case history. In Purcell, P. G. and Purcell, R. R., (Eds), *The North West Shelf, Australia.* Proceedings of the Petroleum Exploration Society of Australia North West Shelf Symposium, Perth, 173-187.

Barber, P. M., 1994. Sequence stratigraphy and petroleum potential of Upper Jurassic-Lower Cretaceous depositional systems in the Dampier Sub-basin, North West Shelf, Australia. In Purcell, P. G. and Purcell, R. R., (Eds), *The Sedimentary Basins of Western Australia.* Proceedings of the Petroleum Exploration Society of Australia West Australian Basins Symposium, Perth, 525-42.

Batten, D. J., 1996. Chapter 26A: Palynofacies and palaeoenvironmental interpretation. In Jansonius, J. and McGregor, D. C. (Eds), Palynology: principles and applications. *American Association of Stratigraphic Palynologists Foundation 3,* 1011-1064.

Beju, D., 1971. Jurassic microplankton from the Carpathian Foreland of Roumania. *Annales Instituti Geologici Publici Hungarici 54 (2),* 275-317.

Below, R., 1981. Dinoflagellaten-Zysten aus dem oberen Hauterive bis unteren Cenoman Süd-West-Marokkos. *Palaeontographica, Abt B, Band 176,* 1-145.

Below, R., 1982a. Dinoflagellate cysts from Valanginian to Lower Hauterivian sections near Ait Hamouch, Morocco. *Revista Española de Micropaleontología 14 (1-3),* 23-52.

Below, R., 1982b. *Rigaudella*, ein neues Genus von Dinoflagellaten-Zysten. *Neues Jahrbuch für Geologie und Paläontologie, Monatshefte 3,* 137-150.

Below, R., 1982c. Scolochorate zysten der Gonyaulacaceae (Dinophyceae) aus der Unterkreide Marokkos. *Palaeontographica, Abt B, Band 182,* 1-51.

Below, R., 1987a. Evolution und Systematik von Dinoflagellaten-Zysten aus der Ordnung Peridiniales. I. Allgemeine Grudlagen und Subfamilie Rhaetogonyaulacoideae (Familie Peridiniaceae). *Palaeontographica, Abt B, Band 205,* 1-164.

Below, R., 1987b. Evolution und Systematik von Dinoflagellaten-Zysten aus der Ordnung Peridiniales. II. Cladopyxiaceae und Valvaeodiniaceae. *Palaeontographica, Abt B, Band 206,* 1-115.

Below, R., 1990. Evolution und Systematik von Dinoflagellaten-Zysten aus der Ordnung Peridiniales. III. Familie Pareodiniaceae. *Palaeontographica, Abt B, Band 220,* 1-96.

Benson, D. G., 1985. Observations and recommendations on the fossil dinocyst genera *Ctenidodinium, Dichadogonyaulax,* and *Korystocysta. Tulane Studies in Geology and Paleontology 18 (4),* 145-155.

Bint, A. N. and Marshall, N. G., 1994. High resolution palynostratigraphy of the Tithonian Angel Formation in the Wanaea and Cossack oil fields, Dampier Sub-basin. In Purcell, P. G. and Purcell, R. R., (Eds), *The Sedimentary Basins of Western Australia.* Proceedings of the Petroleum Exploration Society of Australia West Australian Basins Symposium, Perth, 543-554.

Borges, M. E. N., Riding, J. B., Fernandes, P. and Pereira, Z., 2011. The Jurassic (Pliensbachian to Kimmeridgian) palynology of the Algarve Basin and the Carrapateira outlier, southern Portugal. *Review of Palaeobotany and Palynology 163,* 190-204.

Bown, P. R., Cooper, M. K. E., 1998. Jurassic. In Bown, P. R. (Ed.). *Calcareous Nannofossil Biostratigraphy*. Chapman and Hall, London, 34-85.

Bradshaw, M. T., Yeates, A. N., Beynon, R. M., Brakel, A. T., Langford, R. P., Totterdell, J. M. and Yeung, M., 1988. Palaeogeographic Evolution of the North West Shelf Region. In Purcell, P. G. and Purcell, R. R., (Eds), *The North West Shelf, Australia.* Proceedings of the Petroleum Exploration Society of Australia North West Shelf Symposium, Perth, 29-54.

Brenner, W., 1988. Dinoflagellaten aus dem unteren Malm (oberer Jura) von Süddeutschland; Morphologie, Ökologie, Stratigraphie. *Tübinger Mikropaläontologische Mitteilungen 6,* 1-116.

Brideaux, W. W., 1971. Palynology of the Lower Colorado Group, central Alberta, Canada. I. Introductory remarks. Geology and microplankton studies. *Palaeontographica, Abt B, Band 135,* 53-114.

Brideaux, W. W., 1975. Taxonomic note: redefinition of the genus *Broomea* and its relationship to *Batioladinium* gen. nov. (Cretaceous). *Canadian Journal of Botany 53 (12),* 1239-1243.

Brideaux, W. W., 1977. Taxonomy of Upper Jurassic-Lower Cretaceous microplankton from the Richardson Mountains, District of Mackenzie, Canada. *Geological Survey of Canada, Bulletin 281,* 1-89.

Brideaux, W. W. and Fisher, M. J., 1976. Upper Jurassic-Lower Cretaceous dinoflagellate assemblages from arctic Canada. *Geological Survey of Canada, Bulletin 259,* 1-53.

Brideaux, W. W. and McIntyre, D. J., 1975. Miospores and microplankton from Aptian-Albian rocks along Horton River, District of Mackenzie. *Geological Survey of Canada, Bulletin 252,* 1-85.

Brinkhuis, H., Klinkenberg, E., Williams, G. L., and Fensome, R. A., 2000. Two unusual new dinoflagellate cyst genera from the Bunde Borehole, Maastrichtian type area, southern Netherlands. *Review of Palaeobotany and Palynology 110,* 93-110.

Bucefalo-Palliani, R., Cirilli, S. and Mattioli, E., 1998. Phytoplankton response and geochemical evidence of the lower Toarcian relative sea level rise in the Umbria-Marche Basin (Central Italy). *Palaeogeography, Palaeoclimatology, Palaeoecology 142,* 33-50.

Bucefalo Palliani, R., Riding, J. B. and Torricelli, S., March 1997. The dinoflagellate cyst *Mendicodinium* Morgenroth, 1970, emend. from the lower Toarcian (Jurassic) of central Italy. *Review of Palaeobotany and Palynology 96,* 99-111.

Bujak, J. P., 1984. Cenozoic dinoflagellate cysts and acritarchs from the Bering Sea and northern North Pacific, DSDP Leg 19. *Micropaleontology 30 (2),* 180-212.

Bujak, J. P. and Davies, E. H., 1983. Modern and Fossil Peridiniineae. *American Association of Stratigraphic Palynologists, Contributions Series 13,* 203p.

Burger, D., 1980a. Palynological studies in the Lower Cretaceous of the Surat Basin, Australia. *Bureau of Mineral Resources, Geology and Geophysics, Bulletin 189,* 106p.

Burger, D., 1980b. Early Cretaceous (Neocomian) microplankton from the Carpentaria Basin, northern Queensland. *Alcheringa 4,* 263-279.

Burger, D., 1994. Palynology of Mesozoic dredge samples from the North West Shelf. In Exon, N. F. (Ass. Ed.), Thematic issue: Geology of the outer North West Shelf, Australia. *AGSO Journal of Geology & Geophysics, 15 (1),* 89-100.

Burger, D., 1996. Mesozoic palynomorphs from the North West Shelf, offshore Western Australia. *Palynology 20,* 49-103.

Campbell, H. J., Raine, J. I., Wilson, G. J., 2004. Chapter 9, Jurassic (Herangi, Kawhia and Oteke Series). In Cooper, R. A. (Ed.), The New Zealand Geological Timescale. *Institute of Geological and Nuclear Sciences Monograph, 22,* 88-101.

Clarke, R. F. A. and Verdier, J. -P., 1967. An investigation of microplankton assemblages from the Chalk of the Isle of Wight, England. *Verhandelingen der Koninklijke Nederlandse Akademie ven Wetenschappen, Afdeeling Natuurkunde, Eerste Reeks 24 (3),* 1-96.

Conway, B. H., 1978. Microplankton from the Upper Bathonian of Zohar 5 and Yinnon 1 boreholes in Southern Israel. *Review of Palaeobotany and Palynology 26,* 337-362.

Cookson, I. C. and Eisenack, A., 1958. Microplankton from Australian and New Guinea Upper Mesozoic sediments. *Proceedings of the Royal Society of Victoria 70,* 19-79.

Cookson, I. C. and Eisenack, A., 1960a. Microplankton from Australian Cretaceous sediments. *Micropaleontology 6 (1),* 1-18.

Cookson, I. C. and Eisenack, A., 1960b. Upper Mesozoic Microplankton from Australia and New Guinea. *Palaeontology 2 (2),* 243-261.

Cookson, I. C. and Eisenack, A., 1962a. Some Cretaceous and Tertiary microfossils from Western Australia. *Proceedings of the Royal Society of Victoria 75,* 269-273.

Cookson, I. C. and Eisenack, A., 1962b. Additional microplankton from Australian Cretaceous sediments. *Micropaleontology 8 (4),* 485-507.

Cookson, I. C. and Eisenack, A., 1974. Mikroplankton aus australischen mesozoischen und tertiären Sedimenten. *Palaeontographica, Abt B, Band 148,* 44-93.

Courtinat, B., 1989. Les organoclastes des formations lithologiques du Malm dans le Jura méridional. Systématique, biostratigraphie et éléments d'interprétation paléoécologique. *Laboratoires de Géologie de la Faculté des Sciences de Lyon, Documents 105,* 361p.

Courtinat, B., 1999. Review of the dinoflagellate cyst *Stephanelytron* Sarjeant 1961 emend. *Journal of Micropalaeontology 18 (2),* 169-182.

Courtinat, B., 2006. Palynostratigraphie du Callovien-Oxfordien (Jurassique) dans les Terres noires, sud-est France. *Geobios 39 (2),* 201-213.

Courtinat, B. and Gaillard, C., 1980. Les dinoglagellés des calcaires lités de Trept (Oxfordien supérieur). Inventaire et répartition comparée à celle de la microfaune benthique. *Laboratoires de Géologie de la Faculté des Sciences de Lyon, Documents 78,* 123p.

Courtinat, B. and Méon, H., 1991. Les microforaminifères (Scytinascia) un groupe palynologique méconnu (historique). Leur analyse dans le Cénomanien-Turonien de Vergons (Bassin Vocontien, France). *Geobios 24 (5),* 559-567.

Davies, E. H., 1983. The dinoflagellate Oppel-zonation of the Jurassic-Lower Cretaceous sequences in the Sverdrup Basin, arctic Canada. *Geological Survey of Canada, Bulletin 359,* 1-59.

Davey, R. J., 1969. Non-calcareous microplankton from the Cenomanian of England, northern France and North America, Part I. *British Museum (Natural History) Geology, Bulletin 17,* 103-180.

Davey, R. J., 1979a. Two new early Cretaceous dinocyst species from the northern North Sea. *Palynology 22 (2),* 427-437.

Davey, R. J., 1979b. Marine Apto-Albian palynomorphs from holes 400A and 402A, IPOD Leg 48, Northern Bay of Biscay. In Montadert, L. and Roberts, D. G., *Initial Reports of the Deep Sea Drilling Project XLVIII (48),* 547-577.

Davey, R. J., 1979c. The stratigraphic distribution of dinocysts in the Portlandian (latest Jurassic) to Barremian (Early Cretaceous) of northwest Europe. *American Association of Stratigraphic Palynologists, Contributions Series 5B (2),* 48-81.

Davey, R. J., 1979d. A re-appraisal of the genus *Chytroeisphaeridia* Sarjeant, 1962. *Palynology 3,* 209-218.

Davey, R. J., 1982. Dinocyst stratigraphy of the latest Jurassic to Early Cretaceous of the Haldager No 1 borehole, Denmark. *Geological Survey of Denmark, Series B 6,* 57p.

Davey, R. J., 1987. Palynological Zonation of the Lower Cretaceous, Upper and Upper Most Middle Jurassic in the Northwestern Papuan Basin of Papua New Guinea. *Geological Survey of Papua New Guinea Memoir 13,* 77p.

Davey, R. J., 1999. Revised Palynological Zonation for the Late Cretaceous, Early Cretaceous and Late Jurassic of Papua New Guinea. *Department of Mineral Resources, Geological Survey of Papua New Guinea Memoir 17,* 51p.

Davey, R. J., Downie, C., Sarjeant, W. A. S. and Williams, G. L., 1966a. Studies on Mesozoic and Cainozoic dinoflagellate cysts. *British Museum (Natural History) Geology, Bulletin, Supplement 3,* 248p.

Davey, R. J., Downie, C., Sarjeant, W. A. S. and Williams, G. L., 1966b. VII. Fossil dinoflagellate cysts attributed to *Baltisphaeridium*. In Davey, R. J., Downie, C., Sarjeant, W. A. S. and Williams, G. L., Studies on Mesozoic and Cainozoic

dinoflagellate cysts. *British Museum (Natural History) Geology, Bulletin, Supplement 3,* 157-175.

Davey, R. J., Downie, C., Sarjeant, W. A. S. and Williams, G. L., 1969. Generic reallocations. In Davey, R. J., Downie, C., Sarjeant, W. A. S. and Williams, G. L., Appendix to "Studies on Mesozoic and Cainozoic dinoflagellate cysts". *British Museum (Natural History) Geology, Bulletin, Appendix to Supplement 3,* 15-17.

Davey, R. J. and Williams, G. L., 1966. V. The genus *Hystrichosphaeridium* and its allies. In Davey, R. J., Downie, C., Sarjeant, W. A. S. and Williams, G. L., Studies on Mesozoic and Cainozoic dinoflagellate cysts. *British Museum (Natural History) Geology, Bulletin, Supplement 3,* 53-106.

Deák, M. H., 1964. Les Scytinascias. *Földtani Közlöny (Bulletin of the Geological Society of Hungary) 94,* 95-106.

de Coninck, J., 1969. Dinophyceae et Acritarcha de l'Yprésien du sondage de Kallo. *Mémoires de l'Institut Royal des Sciences Naturelles de Belgique 161,* 1-67.

Deflandre, G., 1935. Considérations biologiques sur les microorganismes d'origine planctonique conservés dans les silex de la craie. *Bulletin biologique de la France et de la Belgique 69,* 213-244.

Deflandre, G., 1936. Microfossiles des silex crétacés. Première partie. Généralités. Flagellés. *Annales de paléontologie 25,* 20-191.

Deflandre, G., 1937. Microfossiles des silex crétacés. Deuxième partie. Flagellés incertae sedis. Hystrichosphaeridés. Sarcodinés. Organismes divers. *Annales de paléontologie 26,* 51-103.

Deflandre, G., 1938. Sur le microplancton des mers jurassiques, conservé à l'état de matière organique dans les marnes des Villers-sur-Mer. *Comptes rendus hebdomadaires des séances de l'Académie des sciences 206,* 687-689.

Deflandre, G., 1939. Microplancton des mers jurassiques conservé dans les marnes de Villers-sur-Mer (Calvados). Étude liminaire et considérations générales. *Station zoologique de Wimereux, Travaux 13,* 147-200.

Deflandre, G., 1941. Le microplancton kiméridgien d'Orbagnoux et l'origine des huiles sulfurées naturelles. *Mémoires de l'Académie des Sciences (France) 65 (5),* 1-32.

Deflandre, G., 1946. Remarques sur la systématique des hystrichosphaeridés. *Comptes rendus de la Société géologique de France 7,* 110-111.

Deflandre, G., 1947a. Sur une nouvelle hystrichosphére des silex crétacés et sur les affinities du genre *Cannosphaeropsis* O. Wetzel. *Comptes rendus hebdomadaires des séances de l'Académie des sciences 224,* 1574-1576.

Deflandre, G., 1947b. Sur quelques microorganismes planctoniques des silex Jurassiques. *Institut océanographique, Monaco, Bulletin 921,* 1-12.

Deflandre, G., 1964. Remarques sur la classification des dinoflagellés fossiles, à propos d'*Evittodinium*, nouveau genre crétacé de la famille des Deflandreaceae. *Comptes rendus hebdomadaires des séances de l'Académie des sciences 258,* 5027-5030.

Deflandre, G. and Cookson, I. C., 1955. Fossil microplankton from Australian Late Mesozoic and Tertiary sediments. *Australian Journal of Marine and Freshwater Research 6 (2),* 242-313.

Deflandre, G. and Courteville, H., 1939. Note préliminaire sur les microfossiles des silex crétacés du Cambrésis. *Bulletin de la société française de microscopie 8,* 95-106.

Deunff, J., 1954. *Veryhachium*, genre nouveau d'hystrichosphères du Primaire. *Compte rendu sommaire des séances de la Société géologique de France 13,* 305-306.

Dodekova, L., 1967. Les dinoflagellés et acritarches de l'Oxfordien-Kiméridgien de la Bulgarie du nord-est. *Annuaire de l'Université de Sofia, Faculté de Géologie et Géographie 60, Livre 1, Géologie, 1965-1966,* 9-30.

Dodekova, L., 1969. Dinoflagellés et acritarches du Tithonique aux environs de Pleven, Bulgarie centrale du nord. *Bulgarska Akademiya na Naulute, Izvestiya na Geologicheskiya Institut, Seriya Paleontologiya 18,* 13-24.

Dodekova, L., 1975. New Upper Bathonian dinoflagellate cysts from northeastern Bulgaria. Bulgarska Akademiya ne Naukite, Paleontologiya, *Stratigrafiya i Litologiya 2,* 17-34.

Dodekova, L., 1990. Dinoflagellate cysts from the Bathonian-Tithonian (Jurassic) of north Bulgaria. I. Taxonomy of Bathonian and Callovian dinoflagellate cysts. *Geologica Balcanica 20 (2),* 3-45.

Dodekova, L., 1992. Dinoflagellate cysts from the Bathonian-Tithonian (Jurassic) of north Bulgaria. II. Taxonomy of Oxfordian and Kimmeridgian dinoflagellate cysts. *Geologica Balcanica 22 (3),* 33-69.

Dodekova, L., 1994. Dinoflagellate cysts from the Bathonian-Tithonian (Jurassic) of north Bulgaria. III. Tithonian dinoflagellate cysts. *Geologica Balcanica 24 (5),* 11-46.

Dodge, J. D., 1989. Some revisions of the family Gonyaulacaceae (Dinophyceae) based on a scanning electron microscope study. *Botanica Marina 32,* 275-298.

Dörhöfer, G. and Davies, E. H., 1980. Evolution of archeopyle and tabulation in Rhaetogonyaulacinean dinoflagellate cysts. *Miscellaneous Publication, Royal Ontario Museum, Life Sciences Division, Toronto, Canada,* 91p.

Downie, C. and Sarjeant, W. A. S., 1965. Bibliography and index of fossil dinoflagellates and acritarchs. *Geological Society of America, Memoir 94,* 1-180.

Drugg, W. S., 1967. Palynology of the Upper Moreno Formation (Late Cretaceous – Paleocene), Escarpado Canyon, California. *Palaeontographica, Abt B, Band 120,* 1-71.

Drugg, W. S., 1970b. Some new genera, species, and combinations of phytoplankton from the lower Tertiary of the Gulf Coast, USA. *Proceedings, North American Paleontological Convention 1969,* 809-843.

Drugg, W. S., 1978. Some Jurassic Dinoflagellate Cysts from England, France and Germany. *Palaeontographica, Abt B, Band 168,* 61-79.

Dürr, G., 1988. Palynostratigraphie des Kimmeridgium und Tithonium von Süddeutschland und correlation mit borealen Floren. *Tübinger Mikropaläontologische Mitteilungen 5,* 1-159.

Duxbury, S., 1980. Barremian phytoplankton from Speeton, east Yorkshire. *Palaeontographica, Abt B, Band 173,* 107-146.

Duxbury, S., 1983. A study of dinoflagellate cysts and acritarchs from the Lower Greensand (Aptian to Lower Albian) of the Isle of Wight, southern England. *Palaeontographica, Abt B, Band 186,* 18-80.

Duxbury, S., 2001. A palynological zonation scheme for the Lower Cretaceous – United Kingdom sector, central North Sea. *Neues Jahrbuch für Geologie und Paläontologie, Abhandlungen 219 (1-2),* 97-137.

Dybkjær, K., 2004. Dinocyst stratigraphy and palynofacies studies used for refining a sequence stratigraphic model—uppermost Oligocene to lower Miocene, Jylland, Denmark. *Review of Palaeobotany and Palynology 131 (3-4),* 201-249.

Eaton, G. L., Fensome, R. A., Riding, J. B. and Williams, G. L., 2001. Re-evaluation of the status of the dinoflagellate cyst genus *Cleistosphaeridium. Neues Jahrbuch für Geologie und Paläontologie, Abhandlungen 219 (1-2),* 171-205.

Edgell, H. S., 1964. The correlative value of microplankton in the Cretaceous of the Perth Basin. *Geological Survey of Western Australia, Ann. Rep., 1963,* 50-55.

Edwards, D. and Zumberge, J., 2005. *The Oils of Western Australia II: Regional Petroleum Geochemistry and Correlation of Crude Oils and Condensates from Western Australia and Papua New Guinea*. Geoscience Australia and GeoMark Research Ltd., unpublished report.

Ehrenberg, C. G., 1838. Über das Massenverhältniss der jetzt lebenden Kiesel-Infusorien und über ein neues Infusorien-Conglomerat als Polierschiefer von Jastraba in Ungarn. *Königlich Akademie der Wissenschaften zu Berlin, Abhandlungen, 1836 1,* 109-135.

Ehrenberg, C. G., 1843a. Über die Verbreitung des jetzt wirkenden kleinsten organischen Lebens in Asien, Australien und Afrika und über die vorherrschende Bildung auch des Oolithkalkes der Juraformation aus kleinen polythalamischen Thieren. *Königlich Preussische Akademie der Wissenschaften zu Berlin, Bericht über die zur Bekanntmachung geeigneten Verhandlungen,* 100-106.

Ehrenberg, C. G., 1843b. Über einige Jura-Infusorien-Arten des Corallrags bei Krakau. *Königlich Preussische Akademie der Wissenschaften zu Berlin, Verhandlungen, Monatsberichte,* 61-63.

Eisenack, A., 1935. Mikrofossilien aus Doggergeschieben Ostpreussens. *Zeitschrift für Geschiebeforschung 11,* 167-187.

Eisenack, A., 1958. Mikroplankton aus dem norddeutschen Apt, nebst einigen Bemerkungen über fossile Dinoflagellaten. *Neues Jahrbuch für Geologie und Paläontologie, Abhandlungen 106 (3),* 383-422.

Eisenack, A., 1963. Zur *Membranilarnax*-Frage. *Neues Jahrbuch für Geologie und Paläontologie, Monatshefte (2),* 98-103.

Eisenack, A. and Cookson, I. C., 1960. Microplankton from Australian Lower Cretaceous sediments. *Proceedings of the Royal Society of Victoria 72,* 1-11.

Eisenack, A. and Klement, K. W., 1964. *Katalog der Fossilen Dinoflagellaten, Hystrichosphären und Verwandten Mikrofossilien. Band I. Dinoflagellaten*. E. Schweizerbart'sche Verlagsbuchhandlung, Stuttgart, Germany, 888p.

El Beialy, S. Y. and Ibrahim, M. I. A., 1997. Callovian-Oxfordian (Middle-Upper Jurassic) mircoplankton and miospores from the Masajid Formation, WX1 borehole, E1 Maghara area, North Sinai, Egypt. *Neues Jahrbuch für Geologie und Paläontologie, Abhandlungen 204 (3),* 379-398.

Ellegaard, M., 2000. Variations in dinoflagellate cyst morphology under conditions of changing salinity during the last 2000 years in the Limfjord, Denmark. *Review of Palaeobotany and Palynology 109,* 65–81.

Erkmen, U. and Sarjeant, W. A. S., 1980. Dinoflagellate cysts, acritarchs and tasmanitids from the uppermost Callovian of England and Scotland; with a reconsideration of the *"Xanthidium pilosum"* problem. *Geobios 13 (1), 45-99.*

Evitt, W. R., 1961. The dinoflagellate *Nannoceratopsis* Deflandre; morphology, affinities and intraspecific variability. *Micropaleontology 7,* 305-316.

Evitt, W. R., 1985. *Sporopollenin Dinoflagellate Cysts – Their Morphology and Interpretation*. American Association of Stratigraphic Palynologists Foundation, 333p.

Fauconnier, D., 1995. Jurassic palynology from a borehole in the Champagne area, France-correlation of the lower Callovian-middle Oxfordian using sequence stratigraphy. *Review of Palaeobotany and Palynology 87 (1),* 15-26.

Fauconnier, D., Courtinat, B., Gardin, S., Lachkar, G. and Rauscher, R., 1996. Biostratigraphy of Jurassic and Triassic successions in the Balazuc-1 borehole (GPF Programme). Stratigraphic setting inferred from dinoflagellate cysts, pollen, spores and calcareous nannofossils. *Marine and Petroleum Geology 13,* 707-724.

Fauconnier, D and Masure, E. (Co-ordinators), 2004. Les dinoflagellés fossile. Guide pratique de détermination. Les genres à processus et à archéopyle apical. BRGM Editions. 602p.

Feist-Burkhardt, S. and Monteil, E., 2001. Gonyaulacacean dinoflagellate cysts with multi-plate precingular archeopyle. *Neues Jahrbuch für Geologie und Paläontologie, Abhandlungen 219 (1-2),* 33-81.

Fensome, R. A., 1979. Dinoflagellate cysts and acritarchs from the Middle and Upper Jurassic of Jameson Land, east Greenland. *Grønlands Geologiske Undersøgelse, Bulletin 132,* 1-98.

Fensome, R. A., 1981. The Jurassic dinoflagellate genera *Wanaea* and *Energlynia*: their morphology and evolution. *Neues Jahrbuch für Geologie und Paläontologie, Abhandlungen 161,* 47-61.

Fensome, R. A., Goght, H., Stover, L. E. and Williams, G. L., 1993. *The Eisenack Catalog of Fossil Dinoflagellates. New Series. Volume 2.* E. Schweizerbart'sche Verlagsbuchhandlung, Stuttgart, Germany, 829-1461.

Fensome, R. A., Goght, H. and Williams, G. L., 1995. *The Eisenack Catalog of Fossil Dinoflagellates. New Series. Volume 3*. E. Schweizerbart'sche Verlagsbuchhandlung, Stuttgart, Germany, 1462-2008.

Fensome, R. A., Riding, J. B. and Taylor, F. J. R., 1996. Chapter 6: Dinoflagellates. In Jansonius, J. and McGregor, D.C. (Eds), Palynology: principles and applications. *American Association of Stratigraphic Palynologists Foundation 1,* 107-169.

Fensome, R. A., Taylor, F. J. R., Norris, G., Sarjeant, W. A. S., Wharton, D. I. and Williams, G. L., 1993. A Classification of Living and Fossil Dinoflagellates. *Micropalaeontology Special Publication 7,* 351p.

Fensome, R. A., and Williams, G. L., 2004. The Lentin and Williams Index of Fossil Dinoflagellates, 2004 Edition. *American Association of Stratigraphic Palynologists Contributions Series 42,* 909p.

Fenton, J. P. G., Neves, R. and Piel, K. M., 1980. Dinoflagellate cysts and acritarchs from Upper Bajocian strata of central and southern England. *Palaeontology 23 (1),* 151-170.

Filatoff, J., 1975. Jurassic Palynology of the Perth Basin, Western Australia. *Palaeontographica, Abt B, Band 154,* 1-113.

Firth, J. V., 1993. Dinoflagellate assemblages and sea-level fluctuations in the Maastrichtian of southwest Georgia. *Review of Palaeobotany and Palynology 79,* 179-204.

Foster, C. B., 2001. Introduction to Studies in Australian Mesozoic Palynology II. In Laurie, J. R. and Foster, C. B. (Eds), *Association of Australasian Palaeontologists Memoir 24,* i-iii.

Francis, G. and Westermann, E. G., 1993. The Kimmeridgian problem in Papua New Guinea and other parts of the Indo-southwest Pacific. In Carman, G. J. and Carman, Z. (Eds), *Petroleum Exploration and Development in Papua New Guinea: Proceedings of the Second PNG Petroleum Convention, Port Moresby, 31 May – 2 June 1993,* 75-93.

Garcia, Y. C., Martinez, J. I., Velez, M. I., Yokoyama, Y., Battarbee, R. W. and Suter, F. D., Palynofacies analysis of the late Holocene San Nicolás terrace of the Cauca paleolake and paleohydrology of northern South America. *Palaeogeography, Palaeoclimatology, Palaeoecology 299,* 298-308.

Garg, R., Khowaja-Ateequzzaman, Krishna, J. and Jain, K. P., 2003. Biostratigraphic potential of dinoflagellate cysts recovered from the Late Jurassic ammonites of the Tethys Himalaya, India. *Journal of The Palaeontological Society of India 48,* 41-58.

Gitmez, G. U., 1970. Dinoflagellate cysts and acritarchs from the basal Kimmeridgian (Upper Jurassic) of England, Scotland and France. *British Museum (Natural History) Geology, Bulletin 18 (7),* 231-331.

Gitmez, G. U. and Ertug, K., 1999. Dinoflagellate cysts and acritarchs from the Jurassic-Cretaceous boundary, Northwest Anatolia, Turkey. *Micropaleontology 45 (1),* 69-98.

Gitmez, G. U. and Sarjeant, W. A. S., 1972. Dinoflagellate cysts and acritarchs from the Kimmeridgian (Upper Jurassic) of England, Scotland and France. *British Museum (Natural History) Geology, Bulletin 21 (5),* 171-257.

Gocht, H., 1970. Dinoflagellaten-zysten aus dem Bathonium des Erdölfeldes Aldorf (NW-Deutschland). *Palaeontographica, Abt B, Band 129.* p125-161.

Gocht, H., 1975. Morphologie und Wandstruktur von *Lithodinia jurassica* Eisenack 1935 (Dinoflagellata, Oberjura). Morphology and wall structure of the Upper Jurassic dinoflagellate *Lithodinia jurassica* Eisenack. *Neues Jahrbuch für Geologie und Paläontologie, Monatshefte 6,* 343-359.

Górka, H., 1965. Les microfossiles du Jurassique supérieur de Magnuszew (Pologne). *Acta Palaeontologica Polonica 10 (3),* 391-334.

Götz, A. E., Feist-Burkhardt, S. and Ruckwied, K., 2008. Palynofacies and sea-level changes in the Upper Cretaceous of the Vocontian Basin, southeast France. *Cretaceous Research 29,* 1047-1057.

Gradstein, F. M., Ogg, J. G. and Smith, A. G. (Eds.), 2004. A Geologic Time Scale 2004. *Episodes 27 (2),* 83-100.

Groupe Français d'Étude du Jurassique (co-ord.'s Cariou, E., and Hantzpergue, P.), 1997. Biostratigraphie du Jurassique ouest-européen et méditerranéen: Zonations parallèles et distribution des invertébrés et microfossiles. *Bulletin des Centres de Recherches Exploration- Production Elf-Aquitaine, Mémoire 17,* 422p.

Haas, J., Götz, A. E. and Pálfy, J., 2010. Late Triassic to Early Jurassic palaeogeography and eustatic history in the NW Tethyan realm: New insights from sedimentary and organic facies of the Csővár Basin (Hungary). *Palaeogeography, Palaeoclimatology, Palaeoecology 291,* 456-468.

Habib, D., 1972. (Chapter) 10. Dinoflagellate stratigraphy Leg 11, Deep Sea Drilling Project. In Hollister, C. D., Ewing, J. I., *et al*. *Initial Reports of the Deep Sea Drilling Project XI,* 367-425.

Habib, D. and Miller, J. A., 1989. Dinoflagellate species and organic facies evidence of marine transgression and regression in the Atlantic Coastal Plain. *Palaeogeography, Palaeoclimatology, Palaeoecology 74,* 23-42.

Hallam, A., Crame, J. A., Mancenido, M. O., Francis, J., and Parrish, J. T., 1993. Jurassic Climates as Inferred from the Sedimentary and Fossil Record [and Discussion]. *Philosophical Transactions of the Royal Society B: Biological Sciences 341 (1297),* 287-296.

Harding, I. C., 1990. A dinocyst calibration of the European Boreal Barremian. *Palaeontographica, Abt B, Band 218,* 1-76.

Harland, R., 1973. Dinoflagellate cysts and acritarchs from the Bearpaw Formation (upper Campanian) of southern Alberta, Canada. *Palaeontology 16,* 665-706.

Harland, R., 1988. Quaternary dinoflagellate cyst biostratigraphy of the North Sea. *Palaeontology 31,* 877-903.

Harris, A. J. and Tocher, B. A., 2003. Palaeoenvironmental analysis of Late Cretaceous dinoflagellate cyst assemblages using high-resolution sample correlation from the Western Interior Basin, USA. *Marine Micropaleontology 48,* 127-148.

Hefti, J., Dewing, S., Jenkins, C., Arnold, A. and Korn, B. E., 2006. Improvements in seismic imaging, Io Jansz Gas Field North West Shelf, Australia. *APPEA Journal 46 (1),* 135-160.

Helby, R., Morgan, R. and Partridge, A., 1987. A Palynological Zonation of the Australian Mesozoic. In Jell, P. A. (Ed), *Association of Australasian Palaeontologists Memoir 4,* 1-94.

Helby, R., Morgan, R. and Partridge, A., 2004. Updated Jurassic – Early Cretaceous dinocyst zonation, NWS Australia. *Geoscience Australia Publication.* ISBN 1 920871 01 2.

Helby, R. and Partridge, A. D., 2001. *Bonbonadinium granulatum* gen. et sp. nov., a Late Jurassic (Tithonian) dinoflagellate cyst from the North-West Shelf, Australia. In Laurie, J. R. and Foster, C. B. (Eds), *Association of Australasian Palaeontologists Memoir 24,* 221-224.

Helby, R. and Stover, L. E., 1987. *Ternia balmei* gen. et sp. nov., a Jurassic dinoflagellate with possible dinophysialian affinity. In Jell, P. A. (Ed), *Association of Australasian Palaeontologists Memoir 4*, 135-141.

Helby, R., Wilson, G. J. and Grant-Mackie, J. A, 1988. A preliminary biostratigraphic study of Middle to Late Jurassic dinoflagellate assemblages from Kawhia, New Zealand. *Association of Australasian Palaeontologists Memoir 5,* 125-166.

Helenes, J. and Lucas-Clark, J., 1997. Morphological variations among species of the fossil dinoflagellate genus *Gonyaulacysta*. *Palynology 21,* 173-196.

Hocking, R. M., 1988. Regional geology of the Nothern Carnarvon Basin. In Purcell, P. G. and Purcell, R. R., (Eds), *The North West Shelf, Australia.* Proceedings of the Petroleum Exploration Society of Australia North West Shelf Symposium, Perth, 97-114.

Hocking, R. M., 1992. Jurassic deposition in the southern and central North West Shelf, Western Australia. Department of Mines Western Australia, *Geological Survey of Western Australia Record 1992/007,* 101p.

Hocking, R. M., 1994. Subdivisions of Western Australia Neoproterozoic and Phanerozoic Sedimentary Basins. *Geological Survey of Western Australia Record 1994/4,* 84p.

Hocking, R. M., Moors, H. T. and Van de Graaff, W. J. E., 1987. Geology of the Carnarvon Basin, Western Australia. *Geological Survey of Western Australia Bulletin 133,* 288p.

Hocking, R. M., Mory, A. J. and Williams, I. R., 1994. An atlas of Neoproterozoic and Phanerozoic basins of Western Australia. In Purcell, P. G. and Purcell, R. R., (Eds), *The Sedimentary Basins of Western Australia.* Proceedings of the Petroleum Exploration Society of Australia West Australian Basins Symposium, Perth, 21-43.

Hocking, R. M., Voon, J. W. K. and Collins, L. B., 1988. Stratigraphy and Sedimentology of the Basal Winning Group, Northern Carnarvon Basin. In Purcell, P. G. and Purcell, R. R., (Eds), *The North West Shelf, Australia.* Proceedings of the Petroleum Exploration Society of Australia North West Shelf Symposium, Perth, 203-224.

Hooker, N. P., 2003a. (Basic) Palynology of well Jansz-3, Carnarvon Basin, Western Australia. In Mobil Exploration & Producing Australia Pty Ltd, 2003. *Jansz-3 Well Completion Report – Basic Data. WA-18-R. Carnarvon Basin, Western Australia.* Unpublished.

Hooker, N. P., 2003b. (Interpretive) Palynology of well Jansz-3, Carnarvon Basin, Western Australia. In Mobil Exploration & Producing Australia Pty Ltd, 2003. *Jansz-3 Well Completion Report – Interpretive Data. WA-18-R. Carnarvon Basin, Western Australia.* Unpublished.

Hooker, N. P. and Morgan, R., 2000a. (Basic) Palynology of well Jansz-1, Carnarvon Basin, Western Australia. In Mobil Exploration & Producing Australia Pty Ltd, 2000. *Jansz-1 Well Completion Report – Basic Data – Drilling and Engineering. WA-268-P. Carnarvon Basin, Western Australia.* Unpublished.

Hooker, N. P. and Morgan, R., 2000b. (Interpretive) Palynology of well Jansz-1, Carnarvon Basin, Western Australia. In Mobil Exploration & Producing Australia Pty Ltd, 2001. *Jansz-1 Well Completion Report – Interpretive Data. WA-268-P. Carnarvon Basin, Western Australia.* Unpublished.

Hooker, N. P. and Morgan, R., 2003a. (Basic) Palynology of well Jansz-2, Carnarvon Basin, Western Australia. In Mobil Exploration & Producing Australia Pty Ltd, 2003. *Jansz-2 Well Completion Report – Basic Data. WA-18-R. Carnarvon Basin, Western Australia.* Unpublished.

Hooker, N. P. and Morgan, R., 2003b. (Interpretive) Palynology of well Jansz-2, Carnarvon Basin, Western Australia. In Mobil Exploration & Producing Australia Pty Ltd, 2003. *Jansz-2 Well Completion Report – Interpretive Data. WA-18-R. Carnarvon Basin, Western Australia.* Unpublished.

Howe, R. W., 2000. Jurassic calcareous nannofossil biostratigraphy of the North West Shelf and Timor Sea areas. *Minerals and Energy Research Institute of Western Australia (MERIWA) Project M319 report, University of Western Australia,* 154p. Unpublished.

Hssaïda, T. and Morzadec-Kerfourn, M.-T., 1993. Kystes de dinoflagellés et palynofaciès: indicateurs des variations bathymétriques dans le bassin de Guercif (Maroc) au Jurassique (bathonien terminal—Oxfordien basal). *Review of Palaeobotany and Palynology 77 (1-2),* 97-106.

Huault, V., 1999. Zones de kystes de dinoflagellés de l'intervalle Aalénien–Oxfordien sur la bordure méridionale du bassin de Paris: Dinoflagellate cyst zonation of the Aalenian–Oxfordian interval on the southern margin of the Paris Basin. *Review of Palaeobotany and Palynology 107 (3-4),* 145-190.

Huault, V., Merzeraud, G., Rauscher, R., and Schuler, M., 1995. Palynological variations and sedimentary cycles in the Jurassic from the Paris basin. *Review of Palaeobotany and Palynology 87,* 27-41.

Ibrahim, M. I., Aboul Ela, N. M. and Kholeif, S. E., 2002. Dinoflagellate cyst biostratigraphy of Jurassic-Lower Cretaceous formations of the North Eastern Desert, Egypt. *Neues Jahrbuch für Geologie und Paläontologie Abhandlungen, 224 (2),* 255-319.

Ibrahim, M. I. and Schrank, E., 1996. Palynological studies on the Late Jurassic-Early Cretaceous of the Kahraman-l well, northern Western Desert, Egypt. *Géologie de l'Afrique et de l'Atlantique du sud: Actes Colloques Angers 1994,* 611-629.

Ingram, B. and Hooker, N. P., 2001a. Palynology Basic Data Report, Io-1, Carnarvon Basin, Western Australia. In ChevronTexaco, 2001. *Io-1 Well Completion Report – Basic Data. WA-267-P. Carnarvon Basin, Western Australia.* Unpublished.

Ingram, B. and Hooker, N. P., 2001b. Interpretive Palynological Report, Io-1, Carnarvon Basin, Western Australia. In Banfield, J. and Beattie, R. J., 2002. *Well Completion Report Interpretive Data – Io 1. Carnarvon Basin Exploration Permit WA-267-P*. Unpublished.

Ioannides, N. S., Stavrinos, G. N. and Downie, C., 1977. Kimmeridgian microplankton from Clavell's Hard, Dorset, England. *Micropaleontology 22 (4),* 443-478.

Islam, M. A., 1993. Review of the fossil dinoflagellate *Cleistosphaeridium*. *Revista Española de Micropaleontología 25 (2),* 81-94.

Jablonski, D., 1997. Recent advances in the sequence stratigraphy of the Triassic to Lower Cretaceous succession in the northern Carnarvon Basin, Australia. *APPEA Journal 37 (1),* 429-54.

Jablonski, D. and Saitta, A. J., 2004. Permian to Lower Cretaceous plate tectonics and its impact on the tectono-stratigraphic development of the Western Australian margin. *APPEA Journal 44 (1),* 287-327.

Jain, K.P., 1977. Additional dinoflagellates and acritarchs from Grey Shale Member of Dalmiapuram Formation, south India. *The Palaeobotanist 24,* 170-194.

Jain, K.P., Garg, R., Kumar, S., Singh, I.B., 1984. Upper Jurassic dinoflagellate biostratigraphy of Spiti Shale (Formation), Malla Johar area, Tethys Himalaya, India. *Journal of the Palaeontology Society of India 29,* 67-83.

Jan du Chêne, R. and Adediran, S. A., 1985. Late Paleocene to Early Eocene dinoflagellates from Nigeria. *Cahiers de micropaléontologie, Centre nationale de la recherche scientifique 1984-3*, 5-38.

Jan du Chêne, R., Becheler, I., Helenes, J. and Masure, E., 1986. Les genres *Diacanthum, Exiguisphaera, Occisucysta* et *Tehamadinium* gen. nov. (kystes fossiles de dinoflagellés). *Cahiers de micropaléontologie, Centre national de la recherche scientifique, Nouvelle série 1 (3-4),* 5-37. (Citation in text is Jan du Chêne et al., 1986b)

Jan du Chêne, R., Fauconnier, D. and Fenton, J. P. G., 1985. Problèmes taxonomiques liés à la révision de l'espèce *"Gonyaulax" cornigera* Valensi, 1953, kyste fossile de dinoflagellé. *Revue de Micropaléontologie 28,* 109-124.

Jan du Chêne, R., Masure, E., Becheler, I., Biffi, U., de Vains, G., Fauconnier, D., Ferrario, R., Foucher, J. -C., Gaillard, M., Hochuli, P., Lachkar, G., Michoux, D., Monteil, E., Moron, J. -M., Rauscher, R., Raynaud, J. -F., Taugourdeau, J. and Turon, J. -L., 1986. Guide pratique pour la détermination de kystes de dinoflagellés fossiles. Le complexe *Gonyaulacysta*. *Bulletin des Centres de recherches exploration-production Elf-Aquitaine, Mémoire 12,* 479p. (Citation in text is Jan du Chêne et al., 1986a)

Jan du Chêne, Stover, L. E. and de Coninck, J., 1984. New observations on the dinoflagellate cyst genus *Kallosphaeridium* de Coninck, 1969. *Cahiers de micropaléontologie 4,* 1-18.

Jansonius, J., 1986. Re-examination of Mesozoic Canadian dinoflagellate cysts published by S. A. J. Pocock (1962, 1972). *Palynology 10,* 201-223.

Jansonius, J., 1989. The species of *Fromea* (fossil dinoflagellates). *Review of Palaeobotany and Palynology 61,* 63-68.

Jaramillo, C. A. and Oboh-Ikuenobe, F. E., 1999. Sequence stratigraphic interpretations from palynofacies, dinocyst and lithological data of Upper Eocene–Lower Oligocene strata in southern Mississippi and Alabama, U.S. Gulf Coast. *Palaeogeography, Palaeoclimatology, Palaeoecology 145,* 259-302.

Jell, P. A. (Ed), 1987. Studies in Australian Mesozoic Palynology. *Association of Australasian Palaeontologists Memoir 4,* 341p.

Jenkins, C. C., Maughan, D. M., Acton, J. H., Duckett, A., Korn, B. E. and Teakle, R. P., 2003. The Jansz Gas Field, Carnarvon Basin, Australia. *APPEA Journal 43,* 303-324.

Jenkins, C. C., Chiquito, R. M., Glenton, P. N., Mills, A. A., McPherson, J. G., Schapper, M. C. and Williams, M. A., ExxonMobil, 2008. Reservoir Definition at the Jansz/Io Gas Field, NW Shelf, Australia: A Case Study of an Integrated Project from Exploration to

Development. International Petroleum Technology Conference, 3-5 December 2008, Kuala Lumpur, Malaysia.

Jiang, Q., Mungai, M. W., Downie, C. and Neves, R., 1992. Late Jurassic dinoflagellate assemblages of the Mto Panga Quarry, Mombasa, Kenya. *Review of Palaeobotany and Palynology 74 (1-2),* 77-100.

Johnson, C. D. and Hills, L. V., 1973. Microplankton zones of the Savik Formation (Jurassic), Axel Heiberg and Ellesmere Islands, District of Franklin. *Bulletin of Canadian Petroleum Geology 21,* 178-218.

Keep, M., Clough, M., and Langhi, L., 2002. Neogene tectonic and structural evolution of the Timor Sea region, NW Australia. In Keep, M. and Moss, S. (Eds), *The Sedimentary Basins of Western Australia 3.* Proceedings of the Petroleum Exploration Society of Australia West Australian Basins Symposium 3, Perth, 341-353.

Kemp, E. M., 1976. Palynological observations in the Officer Basin, Western Australia. In Burger, D. and Kemp, E. M., 1976. *Palynological Papers. Department of Natural Resources, Bureau of Mineral Resources, Geology and Geophysics, Bulletin 160,* 23-39.

Kholeif, S. E., Al-Saad, H. and Ibrahim, M. I. A., 2004. Palynology of the Hanifa Formation (Oxfordian), from two onshore wells, Qatar – Arabian Gulf. *7th International Conference on the Geology of the Arab World, Cairo University, February 2004,* 285-297.

Klement, K. W., 1957. Revision der Gattungszugehörigkeit einiger in die Gattung *Gymnodinium* Stein eingestufter Arten jurassischer Dinoflagellaten. *Neues Jahrbuch für Geologie und Paläontologie, Monatshefte 9,* 408-410.

Klement, K. W., 1960. Dinoflagellaten und Hystrichosphaerideen aus dem unteren und mittleren Malm Südwestdeutschlands. *Palaeontographica, Abt A, Band 114,* 1-104.

Kokinos, J. P. and Anderson, D. M., 1995. Morphological development of resting cysts in cultures of the marine dinoflagellate *Lingulodinium polyedrum (=L. machaerophorum). Palynology 19,* 143-166.

Kumar, A., 1986. A dinocyst assemblage from the Middle Member (Lower Kimmeridgian-Tithonian) of the Jhuran Formation, Kachchh, India. *Review of Palaeobotany and Palynology 48,* 377-407.

Kunz, R., 1990. Phytoplankton und Palynofazies im Malm NW-Deutschlands (Hannoversches Bergland). Phytoplankton and palynofacies in the Malm of NW Germany (Hannoversches Bergland). *Palaeontographica, Abt B, Band 216,* 1-105.

Laurie, J. R. and Foster, C. B. (Eds), 2001. Studies in Australian Mesozoic Palynology II. *Association of Australasian Palaeontologists Memoir 24,* 235p.

Lebedeva, N. K., 2006. Dinocyst biostratigraphy of the Upper Cretaceous of northern Siberia. *Paleontological Journal 40, Supplement 5,* S604-S621.

Lebedeva, N. K. and Nikitenko, B. L., 1998. Mikrofitoplankton i mikroforaminifery opornogo razreza nizhnego mela Pripolyarnogo Zaural'ya, Zapadnaya Sibir. (Translated Title: Microphytoplankton and microforaminifers in Lower Cretaceous reference section in Polar Transurals, West Siberia). *Geologiya i Geofizika, 39,* 799-820.

Lentin, J. K. and Vozzhennikova, T. F., 1990. Fossil dinoflagellates from the Jurassic, Cretaceous and Paleogene deposits of the USSR – a re-study. *American Association of Stratigraphic Palynologists, Contributions Series 23,* 221p.

Lentin, J. K. and Williams, G. L., 1976. A monograph of Fossil Peridinioid Dinoflagellate Cysts. *Bedford Institute of Oceanography, Report Series BI-R-75-16,* 237p.

Lentin, J. K. and Williams, G. L., 1977. Fossil dinoflagellate genus *Isabelidinium* nom. nov. *Palynology 1,* 167-168.

Lentin, J. K. and Williams, G. L., 1981. Fossil dinoflagellate cysts: index to genera and species, 1981 Edition. *Bedford Institute of Oceanography, Report Series BI-R-81-12,* 345p.

Lentin, J. K. and Williams, G. L., 1989. Fossil dinoflagellates: index to genera and species, 1989 Edition. *American Association of Stratigraphic Palynologists, Contributions Series 20,* 473p.

Lentin, J. K. and Williams, G. L., 1993. Fossil dinoflagellate cysts: index to genera and species, 1993 Edition. *American Association of Stratigraphic Palynologists, Contributions Series 28,* 856p.

Lewis, J. and Hallett, R., 1997. *Lingulodinium polyedrum (Gonyaulax polyedra)* a blooming dinoflagellate. *Oceanography and Marine Biology: an Annual Review 35,* 97-161.

Loeblich, A. R. Jr. and Loeblich, A. R. III, 1968. Index to the genera, subgenera, and sections of the Pyrrhophyta, II. *Journal of Paleontology 42,* 210-213.

Longley, I. M., Buessenschuett, C., Clydsdale, L., Cubitt, C. J., Davis, R. C., Johnson, M. K., Marshall, N. M., Murray, A. P., Somerville, R., Spry, T. B. and Thompson, N. B., 2002. The North West Shelf of Australia - a Woodside Perspective. In Keep, M. and Moss, S. (Eds), *The Sedimentary Basins of Western Australia 3.* Proceedings of the Petroleum Exploration Society of Australia West Australian Basins Symposium 3, Perth, 28-88.

Lucas-Clark, J., 1987. *Wigginsiella* n. gen., *Spongodinium,* and *Apteodinium* as members if the Aptiana-Ventriosum complex (fossil Dinophyceae). *Palynology 11,* 155-184.

Lund, J. J. and Ecke, H.-H., 1988. Dinoflagellate cyst stratigraphy applied to the Middle to Late Jurassic of the Regensburg-Passau area, Bavaria. *Bulletin des Centres de recherches exploration-production Elf-Aquitaine 12 (1),* 345-359.

Mackó, S., 1963. Sporomorphs from Upper Cretaceous near Opole (Silesia) and from the London Clays. *Prace Wrocławskiego Towarzystwa Naukowego, Seria B, 106,* 1-136.

Mantle, D. J., 2005. New dinoflagellate cyst species from the upper Callovian–lower Oxfordian *Rigaudella aemula* Zone, Timor Sea, northwestern Australia. *Review of Palaeobotany and Palynology 135 (3-4),* 245-264.

Mantle, D. J., 2009a. Palynology, sequence stratigraphy, and palaeoenvironments of Middle to Upper Jurassic strata, Bayu-Undan Field, Timor Sea region. Part One. *Palaeontographica, Abt B, Band 280,* 86p.

Mantle, D. J., 2009b. Palynology, sequence stratigraphy, and palaeoenvironments of Middle to Upper Jurassic strata, Bayu-Undan Field, Timor Sea region. Part Two. *Palaeontographica, Abt B, Band 280,* 87-212.

Manum, S. B. and Cookson, I. C., 1964. Cretaceous microplankton in a sample from Graham Island, arctic Canada, collected during the second "Fram" expedition (1898-1902). With notes on microplankton from the Hassel Formation, Ellef Ringnes Island. Norske Videnskaps-Akademi i Oslo, I. *Matematisk-Naturvidenskapelig Klasse, Skrifter, Ny Serie 17,* 1-36.

Marshall, N. G., 1989. An unusual assemblage of algal cysts from the Late Cretaceous of the Gippsland Basin, southeastern Australia. *Palynology 13,* 21-56.

Marshall, N. G., 1990. The dinoflagellate *Canninginopsis* Cookson and Eisenack 1962 from the Cretaceous of the Perth and Gippsland Basins, Australia. *Alcheringa 14,* 77-87.

Masure, E., 1991. Morphology of the dinoflagellate genus *Atopodinium* Drugg emend., senior synonym of *Maghrebinia* Below and *Bejuia* Stover and Williams. *Palynology 15,* 63-80.

McIntyre, D. J. and Brideaux, W. W., 1980. Valanginian miospore and microplankton assemblages from the northern Richardson Mountains, District of Mackenzie, Canada. *Geological Survey of Canada, Bulletin 320,* 57p.

McNeill, J., Barrie, F. R., Burdet, H. M., Demoulin, V., Hawksworth, D. L., Marhold, K., Nicolson, D. H., Prado, J., Silva, P. C., Skog, J. E., Wiersema, J. H., and Turland, N. J. (Eds.), 2006. *International Code of Botanical Nomenclature (Vienna Code)*. Regnum Vegetabile 146. A.R.G. Gantner Verlag KG. ISBN 0080-0694.

McWhae, J. R. H., Playford, P. E., Lindner, A. W., Glenister, B. F., Balme, B. E., 1958. The stratigraphy of Western Australia. *Journal of the Geological Society of Australia 4,* 161p.

Mehrotra, N. C. and Sarjeant, W. A. S., 1984. *Dingodinium*, a dinoflagellate cyst genus exhibiting variation in archeopyle character. *Micropaleontology 30 (3),* 292-305.

Mertens, K. N., Ribeiro, S., Bouimetarhan, I., Caner, H., Combourieu Nebout, N., Dale, B., De Vernal, A., Ellegaard, M., Filipova, M., Godhe, A., Goubert, E., Grøsfjeld, K., Holzwarth, U., Kotthoff, U., Leroy, S. A.G., Londeix, L., Marret, F., Matsuoka, K., Mudie, P. J., Naudts, L., Peña-Manjarrez, J. L., Persson, A., Popescu, S.-M., Pospelova, V., Sangiorgi, F., van der Meer, M. T. J., Vink, A., Zonneveld, K. A. F., Vercauteren, D., Vlassenbroeck, J. and Louwye, S., 2009. Process length variation in cysts of a dinoflagellate, *Lingulodinium machaerophorum*, in surface sediments: Investigating its potential as salinity proxy. *Marine Micropaleontology 70 (1-2),* 54-69.

Mitsuru, A. and Koutsoukos, E. A. M., 1998. Palynoforaminifera (foraminiferal organic linings and allied material): a new tool for petroleum exploration. In *RIO 98 AAPG International Conference & Exhibition, Rio de Janeiro, 1998. Extended Abstracts Volume,* 584-585.

Mobil Exploration & Producing Australia Pty Ltd, 2001. *Jansz-1 Well Completion Report – Interpretive Data. WA-268-P. Carnarvon Basin, Western Australia.* Unpublished.

Mobil Exploration & Producing Australia Pty Ltd, 2003a. *Jansz-2 Well Completion Report – Interpretive Data. WA-18-R. Carnarvon Basin, Western Australia.* Unpublished.

Mobil Exploration & Producing Australia Pty Ltd, 2003b. *Jansz-3 Well Completion Report – Interpretive Data. WA-18-R. Carnarvon Basin, Western Australia.* Unpublished.

Morgan, R., 1975. Some Early Cretaceous organic-walled microplankton from the Great Australian Basin, Australia. *Journal and Proceedings of the Royal Society of New South Wales 108,* 157-167.

Morgan, R., 1980. Palynostratigraphy of the Australian Early and Middle Cretaceous. *Geological Survey of New South Wales, Palaeontology Memoir 18,* 1-153.

Morgan, R., Hooker, N. and Ingram, B., 2002. *Towards Higher Palynological Resolution in the Australian Mesozoic.* Morgan Palaeo & Associates Report, 10p. Unpublished.

Morgenroth, P., 1966. Mikrofossilien und konkretionen des Nordwesteuropäischen Untereozäns. *Palaeontographica, Abt B, Band 119,* 1-53.

Morgenroth, P., 1970. Dinoflagellate cysts from the Lias Delta of Lühnde/Germany. *Neues Jahrbuch für Geologie und Paläontologie, Abhandlungen 136 (3),* 345-359.

Msaky, E. S., 2007. Occurrence of dinoflagellate cyst genera *Wanaea* and *Komewuia* in Upper Jurassic strata, coastal Tanzania. *Paleontological Research 11 (1),* 41-58.

Neale, J. W. and Sarjeant, W. A. S., 1962. Microplankton from the Speeton Clay of Yorkshire. *Geological Magazine 99,* 439-458.

Nøhr-Hansen, H. 1986. Dinocyst stratigraphy of the Lower Kimmeridge Clay, Westbury, England. *Geological Society of Denmark, Bulletin 35,* 31-51.

Norris, G., 1965. Archeopyle structures in Upper Jurassic dinoflagellates from southern England. *New Zealand Journal of Geology and Geophysics 8,* 792-806.

Norris, G. and Sarjeant, W. A. S., 1965. A descriptive index of genera of fossil Dinophyceae and Acritarcha. *New Zealand Geological Survey, Paleontological Bulletin 40,* 72p.

Norvick, M. S., 2002. *Palaeogeographic maps of the northern margins of the Australian Plate – Final Report*. Report for Geoscience Australia. Unpublished.

Norvick, M. S. and Burger, D., 1976. Palynology of the Cenomanian of Bathurst Island, Northern Territory, Australia. *Department of Natural Resources, Bureau of Mineral Resources, Geology and Geophysics, Bulletin 151,* 169p.

Oboh-Ikuenobe, F. E., Benson, D. G., Scott, R. W., Holbrook, J. M., Evetts, M. J. and Erbacher, J., 2007. Re-evaluation of the Albian–Cenomanian boundary in the U.S. Western

Interior based on dinoflagellate cysts. *Review of Palaeobotany and Palynology 144 (1-2),* 77-97.

Oboh-Ikuenobe, F. E., Obi, C. G. and Jaramillo, C. A., 2005. Lithofacies, palynofacies, and sequence stratigraphy of Palaeogene strata in Southeastern Nigeria. *Journal of African Earth Sciences 41,* 79-101.

Oboh-Ikuenobe, F. E., Yepes, O. and ODP Leg 159 Scientific Party, 1997. Palynofacies analysis of sediments from the Côte d'Ivoire-Ghana transform margin: Preliminary correlation with some regional events in the Equatorial Atlantic. *Palaeogeography, Palaeoclimatology, Palaeoecology 129,* 291-314.

Ogg, J. G., Ogg, G. and Gradstein, F. M., 2008. *The Concise Geologic Time Scale*. Cambridge University Press, 184p.

Olmstead, G. A., Cornell, W. C. and Waanders, G. L., 1996. Oxfordian-Kimmeridgian (Jurassic) dinoflagellate cysts from the Chiricahua Mountains, Arizona. *Palynology 20,* 221-230.

Pantic, N. and Bajraktarevic, Z., 1988. 'Nannoforaminifera' in palynological preparations and smear-slides from Mesozoic and Tertiary deposits in Central and Southeast Europe. *Benthos '86, Revue de Paléobiologie Special Volume 2,* 953-959.

Parker, F. M., 1988. *Carnarvonodinium*, a new dinocyst genus from the Late Jurassic of northwestern Australia. In Jell, P.A. and Playford, G. (eds). Palynological and palaeobotanical studies in honour of Basil E. Balme. *Association of Australasian Palaeontologists Memoir 5,* 167-171.

Parrish, J. T., 1992. Chapter 27: Jurassic climate and oceanography of the Pacific region. In Westermann, G. E. G. (Ed). The Jurassic of the Circum-Pacific. *International Geological Correlation Programme Project 171: Jurassic of the Circum-Pacific,* 365-379.

Parry, J. C. and Smith, D. N., 1988. The Barrow and Exmouth Sub-basins. In Purcell, P. G. and Purcell, R. R., (Eds), *The North West Shelf, Australia.* Proceedings of the Petroleum Exploration Society of Australia North West Shelf Symposium, Perth, 129-145.

Partridge, A., 2006a. Jurassic – Early Cretaceous dinocyst zonation, NWS Australia: 1st update of HMP 2004. In Monteil, E. (Co-ord.), Australian Mesozoic and Cenozoic Palynology Zonations – updated to the 2004 Geologic Time Scale. *Geoscience Australia Record 2006/23*.

Partridge, A., 2006b. Jurassic – Early Cretaceous spore-pollen and dinocyst zonations for Australia. In Monteil, E. (Co-ord.), Australian Mesozoic and Cenozoic Palynology Zonations – updated to the 2004 Geologic Time Scale. *Geoscience Australia Record 2006/23*.

Partridge, A., 2006c. Late Cretaceous palynology zonations for Australia. In Monteil, E. (Co-ord.), Australian Mesozoic and Cenozoic Palynology Zonations – updated to the 2004 Geologic Time Scale. *Geoscience Australia Record 2006/23*.

Partridge, A., 2006d. Late Cretaceous – Cainozoic palynology zonations Gippsland Basin. In Monteil, E. (Co-ord.), Australian Mesozoic and Cenozoic Palynology Zonations – updated to the 2004 Geologic Time Scale. *Geoscience Australia Record 2006/23*.

Philippe, M., Bamford, M., McLoughlin, S., Alves, L. S. R., Falcon-Lang, H. J., Gnaedinger, S., Ottone, E. G., Pole, M., Rajanikanth, A., Shoemaker, R. E., Torres, T. and Zamuner, A., 2004. Biogeographic analysis of Jurassic–Early Cretaceous wood assemblages from Gondwana. *Review of Palaeobotany and Palynology 129,* 141-173.

Piel, K. M., 1985. *Lagenadinium*, a new dinocyst from British middle–late Callovian rocks, a possible evolutionary intermediate between *Stephanelytron* and *Gardodinium. Review of Palaeobotany and Palynology 45 (1-2),* 107-119.

Piel, K. M. and Evitt, W. R., 1980. Paratabulation in the Jurassic dinoflagellate genus *Nannoceratopsis* and a comparison with modern taxa. *Palynology 4,* 79-104.

Playford, G. and Dettmann, M. E., 1965. Rhaeto-Liassic Plant microfossils from the Leigh Creek Coal Measures, South Australia. *Senckenbergiana Lethaea 46* (*2-3),* 127-169.

Pocock, S. A. J., 1972. Palynology of the Jurassic sediments of western Canada. Part 2. Marine species. *Palaeontographica, Abt B, Band 137,* 85-153.

Pocock, S. A. J. and Sarjeant, W. A. S., 1972. Partitomorphitae, a new subgroup of Triassic and Jurassic acritarchs. *Geological Society of Denmark, Bulletin 21,* 346-357.

Porter, R., 1988. Palynological evidence for Jurassic microplankton provinces in Great Britain. *Review of Palaeobotany and Palynology 56 (1-2),* 21-39.

Poulsen, N. E., 1986. Callovian-Volgian dinocyst stratigraphy of the Central Trough in the Danish North Sea Area. *Geological Society of Denmark, Bulletin 35,* 1-10.

Poulsen, N. E., 1992. Jurassic dinoflagellate cyst biostratigraphy of the Danish Subbasin in relation to sequences in England and Poland: a preliminary view. *Review of Palaeobotany and Palynology 75,* 33-52.

Poulsen, N. E., 1993. Dinoflagellate cyst biostratigraphy of the Oxfordian and Kimmeridgian of Poland. *Acta Geologica Polonica 43 (3-4),* 251-272.

Poulsen, N. E., 1994a. Dinoflagellate cyst biostratigraphy of the Late Jurassic of Poland. In 3eme Symposium international de stratigraphie du Jurassique (Translated Title: Third international symposium on Jurassic stratigraphy.) Université Claude Bernard, Département de Géologie, Lyon, France. *Geobios Mémoire Spécial 17 1,* 401-407.

Poulsen, N. E., 1994b. Dinoflagellate cyst biostratigraphy of Rhaetian-Ryazanian (Uppermost Triassic-Lowermost Cretaceous) deposits from the Danish Subbasin. In 3eme Symposium international de stratigraphie du Jurassique (Translated Title: Third

international symposium on Jurassic stratigraphy.) Université Claude Bernard, Département de Géologie, Lyon, France. *Geobios Mémoire Spécial 17 1,* 409-414.

Poulsen, N. E., 1996. Dinoflagellate cysts from marine Jurassic deposits of Denmark and Poland. *American Association of Stratigraphic Palynologists, Contributions Series 31,* 227p.

Poulsen, N. E. and Riding, J. B., 1992. A revision of the Late Jurassic dinoflagellate cysts *Ambonosphaera? staffinensis* (Gitmez 1970) comb. nov., and *Senoniasphaera jurassica* (Gitmez & Sarjeant 1972) Lentin & Williams 1976. *Palynology, 16,* 25-34.

Poulsen, N. E. and Riding, J. B., 2003. The Jurassic dinoflagellate cyst zonation of Subboreal north-west Europe. With a supplement by Buchardt, B. Oxygene isotope palaeotemperatures from the Jurassic in Northwest Europe. In Ineson, J., *et al.,* (Eds), *The Jurassic of Denmark and Greenland. Geological Survey of Denmark and Greenland Bulletin 1,* 115-144.

Powell, A. J., Lewis, J. and Dodge, J. D., 1990. Late Neogene to Pleistocene palynological facies of the Peruvian continental margin upwelling, Leg 112. *Proceedings of the Ocean Drilling Program, Scientific Results 112,* 397-321.

Prauss, M., 1989. Dinozysten-Stratigraphie und Palynofazies im oberen Lias und Dogger von NW-Deutschland. *Palaeontographica, Abt B, Band 214,* 1-124.

Prauss, M, 1993. Sequence palynology - evidence from Mesozoic sections and conceptual framework. *Neues Jahrbuch für Geologie und Paläontologie, Abhandlungen 190,* 143-163.

Quattrocchio, M. E., Martínez, M. A., Pavisich, A. C. and Volkheimer, W., 2006. Early Cretaceous palynostratigraphy, palynofacies and palaeoenvironments of well sections in northeastern Tierra del Fuego, Argentina. *Cretaceous Research 27,* 584-602.

Quattrocchio, M.E. and Sarjeant, W.A.S. 1992. Dinoflagellate cysts and acritarchs from the Middle and Upper Jurassic of the Neuquén Basin, Argentina. *Revista Española de Micropaleontología 24 (2),* 67-118.

Quattrocchio, M. E. and Volkheimer, W., 1990. Jurassic and lower cretaceous dinocysts from Argentina: their biostratigraphic significance. *Review of Palaeobotany and Palynology 65 (1-4),* 319-330.

Rameil, N., Götz, A. E., and Feist-Burkhardt, S., 2000. High resolution sequence interpretation of epeiric shelf carbonates by means of palynofacies analysis: an example from the Germanic Triassic (Lower Muschelkalk, Anisian) of East Thuringa, Germany. *Facies, 43,* 123-144.

Raynaud, J. F., 1978. Principaux dinoflagellés caractéristiques du Jurassique supérieur d'Europe du nord. *Palinología, numero extraordinario, no.1,* 387-405.

Rexilius, J. P., Powell, S. L., Howe, R., 1998. Micropalaeontological analysis Alaria-1, Permit AC-L5, Bonaparte Basin for Woodside Offshore Petroleum PTY LTD. *Alaria-1 Well Completion Report, Interpretive Data*. 28p. Unpublished.

Riding, J. B., 1983. *Gonyaulacysta centriconnata* sp. nov. and a dinoflagellate cyst from Late Callovian and Early Oxfordian of eastern England. *Palynology 7,* 197-204.

Riding, J. B., 1987a. Dinoflagellate cyst stratigraphy of the Nettleton Bottom Borehole (Jurassic: Hettangian to Kimmeridgian), Lincolnshire, England. *Proceedings of the Yorkshire Geological Society 46 (3),* 231-266.

Riding, J. B., 1987b. *Limbodinium,* a new dinoflagellate genus from the Jurassic of western Europe. *Palynology 11,* 55-65.

Riding, J. B., 1994. A taxonomic study of the Mesozoic dinoflagellate cyst *Phallocysta elongata* (Beju 1971) comb. nov., emend. nov. and *Wallodinium cylindricum* (Habib 1970) Duxbury 1983 emend. nov. *Palynology 18,* 11-22.

Riding, J. B., 2005a. The Late Jurassic Dinoflagellate Cyst *Gonyaulacysta ceratophora* (Cookson & Eisenack 1960) comb. nov., emend. nov. *Palynology 29,* 13-22.

Riding, J. B., 2005b. Middle and Upper Jurassic (Callovian to Kimmeridgian) Palynology of the Onshore Moray Firth Basin, Northeast Scotland. *Palynology 29,* 87-142.

Riding, J. B., 2005c. *Fostericysta* Riding nom. nov. (Division *Dinoflagellata*). *Taxon 54 (4),* 1091.

Riding, J. B., Fedorova, V. A. and Ilyina, V. I., 1999. Jurassic and lowermost Cretaceous dinoflagellate cyst biostratigraphy of the Russian Platform and Northern Siberia, Russia. *American Association of Stratigraphic Palynologists, Contributions Series 36,* 179p.

Riding, J. B. and Fensome, R. A., 2003. A review of *Scriniodinium* Klement 1957, *Endoscrinium* (Klement 1960) Vozzhennikova 1967 and related dinoflagellate cyst taxa. *Palynology 26,* 5-33.

Riding, J. B. and Helby, R., 2001a. Early Jurassic (Toarcian) dinoflagellate cysts from the Timor Sea, Australia. In Laurie, J. R. and Foster, C. B. (Eds), *Association of Australasian Palaeontologists Memoir 24,* 1-32.

Riding, J. B. and Helby, R., 2001b. A selective reappraisal of *Wanaea* Cookson & Eisenack 1958 (Dinophyceae). In Laurie, J. R. and Foster, C. B. (Eds), *Association of Australasian Palaeontologists Memoir 24,* 33-58.

Riding, J. B. and Helby, R., 2001c. *Phallocysta granosa* sp. nov., a Mid Jurassic (Bathonian) dinoflagellate cyst from the Timor Sea, Australia. In Laurie, J. R. and Foster, C. B. (Eds), *Association of Australasian Palaeontologists Memoir 24,* 59-63.

Riding, J. B. and Helby, R., 2001d. Microplankton from the Mid Jurassic (Late Callovian) *Rigaudella aemula* Zone in the Timor Sea, north-western Australia. In Laurie, J. R. and Foster, C. B. (Eds), *Association of Australasian Palaeontologists Memoir 24,* 65-109.

Riding, J. B. and Helby, R., 2001e. Dinoflagellate cysts from the Late Jurassic (Oxfordian) *Wanaea spectabilis* Zone in the Timor Sea region. In Laurie, J. R. and Foster, C. B. (Eds), *Association of Australasian Palaeontologists Memoir 24,* 111-140.

Riding, J. B. and Helby, R., 2001f. Dinoflagellate cysts from the Late Jurassic (Kimmeridgian) *Dingodinium swanense* Zone in the North-West Shelf and Timor Sea, Australia.. In Laurie, J. R. and Foster, C. B. (Eds), *Association of Australasian Palaeontologists Memoir 24,* 141-176.

Riding, J. B. and Helby, R., 2001g. Marine microplankton from the Late Jurassic (Tithonian) of the north-west Australian region. In Laurie, J. R. and Foster, C. B. (Eds), *Association of Australasian Palaeontologists Memoir 24,* 177-220.

Riding, J. B. and Helby, R., 2001h. Some stratigraphically significant dinoflagellate cysts from the Early Cretaceous (Aptian and Albian) of Australia. In Laurie, J. R. and Foster, C. B. (Eds), *Association of Australasian Palaeontologists Memoir 24,* 225-235.

Riding, J. B., Mantle, D. J. and Backhouse, J., 2010. A review of the chronostratigraphical ages of Middle Triassic to Late Jurassic dinoflagellate cyst biozones of the North West Shelf of Australia. *Review of Palaeobotany and Palynology 162,* 543-575.

Riding, J. B., Penn, I. E. and Woollam, R., 1985. Dinoflagellate cysts from the type area of the Bathonian Stage (Middle Jurassic; Southwest England). *Review of Palaeobotany and Palynology 45 (1-2),* 149-151.

Riding, J. B., Quattrocchio, M. E. and Martínez, M. A., 2011. Mid Jurassic (Late Callovian) dinoflagellate cysts from the Lotena Formation of the Neuquén Basin, Argentina and their palaeogeographical significance. *Review of Palaeobotany and Palynology 163,* 227-236.

Riding, J. B. and Sarjeant, W. A. S., 1984. The role of dinoflagellate cysts in the biostratigraphical subdivision of the Jurassic system. In Michelsen, O. and Zeiss, A. (Eds), *International Symposium on Jurassic Stratigraphy, Symposium Volume III,* 812-835.

Riding, J. B. and Thomas, J. E., 1988. Dinoflagellate cyst stratigraphy of the Kimmeridgian Clay (Upper Jurassic) from the Dorset coast, southern England. *Palynology 12,* 65-88.

Riding, J. B. and Thomas, J. E., 1992. Chapter 2: Dinoflagellate cysts of the Jurassic System. In Powell, A. J., (Ed.), *A Stratigraphic Index of Dinoflagellate Cysts*. British Micropalaeontological Society publication series, London, 7-99.

Riley, L. A. and Fenton, J. P. G., 1982. A dinocyst zonation for the Callovian to Middle Oxfordian succession (Jurassic) of northwest Europe. *Palynology 6,* 193-202.

Riley, L. A. and Sarjeant, W. A. S., 1972. Survey of the stratigraphic distribution of dinoflagellates, acritarchs and tasmanitids in the Jurassic. *Geophytology 2 (1),* 1-40.

Rochon, A., Lewis, J., Ellegaard, M. And Harding, I. C., 2009. The *Gonyaulax spinifera* (Dinophyceae) "complex": Perpetuating the paradox? *Review of Palaeobotany and Palynology 155,* 52-60.

Salvador, A. (ed.) 1994. *International Stratigraphic Guide: a guide to stratigraphic classification, terminology, and procedure. 2nd edition*. I.U.G.S. & Geol. Soc. Amer., Boulder. 214p.

Sarjeant, W. A. S., 1960a. New hystrichospheres from the Upper Jurassic of Dorset. *Geological Magazine 97 (2),* 137-144.

Sarjeant, W. A. S., 1960b. Microplankton from the Corallian Rocks of Yorkshire. *Proceedings of the Yorkshire Geological Society 32 (4),* 389-408.

Sarjeant, W. A. S., 1961a. Microplankton from the Kellaways Rock and Oxford Clay of Yorkshire. *Palaeontology 4 (1),* 90-118.

Sarjeant, W. A. S., 1961b. *Systematophora* Klement and *Polystephanosphaera* Sarjeant. *Journal of Paleontology 35,* 1094-1096.

Sarjeant, W. A. S., 1962a. Microplankton from the Ampthill Clay of Melton, south Yorkshire. *Palaeontology 5 (3),* 478-497.

Sarjeant, W. A. S., 1962b. Upper Jurassic microplankton from Dorset, England. *Micropaleontology 8 (2),* 255-268.

Sarjeant, W.A.S., 1963a. *Favilarnax*, new genus of Mesozoic hystrichospheres. *Journal of Paleontology 37 (3),* 719-721.

Sarjeant, W. A. S., 1963b. Two new Jurassic species of *Gonyaulax* (Dinophyceae). *Revue de Micropaléontologie 6,* 85-88.

Sarjeant, W. A. S., 1966a. Dinoflagellate cysts with *Gonyaulax*-type tabulation. In Davey, R. J., Downie, C., Sarjeant, W. A. S. and Williams, G. L., Studies on Mesozoic and Cainozoic dinoflagellate cysts; *British Museum (Natural History) Geology, Bulletin, Supplement 3,* 107-156.

Sarjeant, W. A. S., 1966b. Further dinoflagellate cysts from the Speeton Clay. In Davey, R. J., Downie, C., Sarjeant, W. A. S. and Williams, G. L., Studies on Mesozoic and Cainozoic dinoflagellate cysts; *British Museum (Natural History) Geology, Bulletin, Supplement 3,* 199-214.

Sarjeant, W. A. S., 1968. Microplankton from the Upper Callovian and Lower Oxfordian of Normandy. *Revue de Micropaléontologie 10 (4),* 221-242.

Sarjeant, W. A. S., 1969. Taxonomic changes. In Davey, R. J., Downie, C., Sarjeant, W. A. S. and Williams, G. L., Appendix to "Studies on Mesozoic and Cainozoic dinoflagellate cysts". *British Museum (Natural History) Geology, Bulletin, Appendix to Supplement 3,* 7-15.

Sarjeant, W. A. S., 1972. Dinoflagellate cysts and acritarchs from the Upper Vardekløft Formation (Jurassic) of Jameson Land, East Greenland. *Meddelelser om Grønland 195,* 1-69.

Sarjeant, W. A. S., 1974. Jurassic dinoflagellate cysts with epitractal archaeopyles – A reconsideration. *Grana 14 (2-3),* 49-56.

Sarjeant, W. A. S., 1976a. *Energlynia,* a new genus of dinoflagellate cysts from the Great Oolite Limestone (Middle Jurassic: Bathonian) of Lincolnshire, England. *Neues Jahrbuch für Geologie und Paläontologie, Monatshefte 3,* 163-173.

Sarjeant, W. A. S., 1976b. English Jurassic dinoflagellate cysts and acritarchs: a re-examination of some type and figured specimens. *Geoscience and Man 15,* 1-24.

Sarjeant, W. A. S., 1978. A guide to the identification of Jurassic dinoflagellate cysts. *School of Geoscience, Louisiana State University, Miscellaneous Publication 78-1,* 107p.

Sarjeant, W. A. S., 1979. Middle and Upper Jurassic dinoflagellate cysts: the world excluding North America. *American Association of Stratigraphic Palynologists Contributions Series 5B (2),* 133-157.

Sarjeant, W. A. S., 1980. A restudy of some dinoflagellate cyst holotypes in the University of Kiel collections. I. The Jurassic holotypes of Walter Wetzel (1966a,b). *Meyniana 32,* 113-128.

Sarjeant, W. A. S., 1982. The dinoflagellate cysts of the *Gonyaulacysta* group: a morphological and taxonomic restudy. *American Association of Stratigraphic Palynologists, Contributions Series 9,* 1-81.

Sarjeant, W. A. S., 1984. A restudy of some dinoflagellate cysts and an acritarch from the Malm (Upper Jurassic) of southwest Germany. *Palaeontographica, Abt B, Band 191,* 154-177.

Sarjeant, W. A. S., 1985. The German Aptian dinoflagellate cysts of Eisenack (1958): a restudy. *Review of Palaeobotany and Palynology 45,* 47-106.

Sarjeant, W. A. S. and Stancliffe, R. P. W., 1994. The *Micrhystridium* and *Veryhachium* complexes (Acritarcha: Acanthomorphitae and Polygonomorphitae); a taxonomic reconsideration. *Micropaleontology 40 (1),* 1-77.

Sarjeant, W. A. S. and Stover, L. E., 1978. *Cyclonephelium* and *Tenua:* a problem in dinoflagellate cyst taxonomy. *Grana 17 (1),* 47-54.

Sarjeant, W. A. S., Volkheimer, W and Zhang, W.-P., 1992. Chapter 13: Jurassic palynomorphs of the circum-Pacific region. In Westermann, G. E. G. (Ed). The Jurassic of the Circum-Pacific. *International Geological Correlation Programme Project 171: Jurassic of the Circum-Pacific,* 273-292.

Schiøler, P., 1993. New species of dinoflagellate cysts from Maastrichtian-Danian chalks of the Danish North Sea. *Journal of Micropalaeontology 12 (1),* 99-112.

Schiøler, P., Brinkhuis, H., Roncaglia, L. and Wilson, G. J., 1997. Dinoflagellate biostratigraphy and sequence stratigraphy of the Type Maastrichtian (Upper Cretaceous), ENCI Quarry, The Netherlands. *Marine Micropaleontology 31,* 65-95.

Schiøler, P., Crampton, J. S., and Laird, M. G., 2002. Palynofacies and sea-level changes in the Middle Coniacian–Late Campanian (Late Cretaceous) of the East Coast Basin, New Zealand. *Palaeogeography, Palaeoclimatology, Palaeoecology 188,* 101-125.

Schrank, E., 2005. Dinoflagellate cysts and associated aquatic palynomorphs from the Tendaguru Beds (Upper Jurassic–Lower Cretaceous) of southeast Tanzania. *Palynology 29,* 49-85.

Singh, C., 1971. Lower Cretaceous Microfloras of the Peace River Area, Northwestern Alberta – Volume 2 (Microplankton). *Research Council of Alberta, Bulletin 28,* 301-542.

Slimani, H., 1994. Les dinokystes des craies du Campanien au Danien à Beutenaken (Pays-Bas). *Mémoires pour server à l'explication des cartes géologiques et miniéres de la Belgique 37,* 1-173.

Smelror, M., 1988a. Bathonian to Early Oxfordian dinoflagellate cysts and acritarchs from Kong Karls Land, Svalbard. *Review of Palaeobotany and Palynology 56,* 275-304.

Smelror, M., 1988b. Late Bathonian to Early Oxfordian dinoflagellate cyst stratigraphy of Jameson Land and Milne Land, East Greenland. *Grønlands Geologiske Undersøgelse, Rapport 137,* 135-159.

Smelror, M., 1989. *Chlamydophorella ectotabulata* sp. nov. and a gonyaulacoid dinoflagellate cyst from the Late Bathonian to the Oxfordian of the Arctic. *Review of Palaeobotany and Palynology 61,* 139-145.

Stancliffe, R. P. W., 1989. Microforaminiferal linings; their classification, biostratigraphy and paleoecology, with special reference to specimens from British Oxfordian sediments. *Micropaleontology 35 (4),* 337-352.

Stancliff, R. P. W., 1991. Dinoflagellate cysts from the Oxfordian (Upper Jurassic) of Skye, Scotland and southern Dorset, England. *Journal of Micropalaeontology 10 (2),* 185-201.

Stancliffe, R. P. W., 1996. Chapter 13D: Microforaminiferal Linings. In Jansonius, J. and McGregor, D.C. (Eds), Palynology: principles and applications. *American Association of Stratigraphic Palynologists Foundation 1,* 373-379.

Stancliffe, R. W. P. and Sarjeant, W. A. S., 1988. Oxfordian dinoflagellate cysts and provincialism. In Rocha, R. B. and Soares, A. F., (Eds). Second International Symposium on Jurassic Stratigraphy, Lisbon, 1987. *Centro de Estratigraphia e Paleobiologia da Universidade Nova de Lisboa e Centro de Geociências da Universidade de Coimbra, Lisboa, 2 (4),* 763-798.

Stancliff, R. P. W. and Sarjeant W. A. S., 1990. The complex chorate dinoflagellate cysts of the Bathonian to Oxfordian (Jurassic): their taxonomy and stratigraphic significance. *Micropaleontology 36 (3),* 197-228.

Stancliffe, R. P. W. and Sarjeant, W. A. S., 1996. The acritarch genus *Dorsennidium* Wicander 1974, emend; Sarjeant and Stancliffe 1994; a reassessment of its constituent species. *Micropaleontology 42 (2),* 151-166.

Steffen, D. and Gorin, G., 1993. Palynofacies of the Upper Tithonian-Berrisasian deep sea carbonates in the Vocontian Trough (SE France). *Bulletin des Centres de Recherches Exploration- Production Elf-Aquitaine, Mémoire, 17,* 235-247.

Stevens, J., 1987. Some Early Cretaceous dinoflagellates from the *Cassiculosphaeridia delicata* Zone on the Exmouth Plateau, Western Australia. In Jell, P. A. (Ed), *Association of Australasian Palaeontologists Memoir 4,* 185-197.

Stevens, G. R., 1997. The Late Jurassic ammonite fauna of New Zealand. *Institute of Geological and Nuclear Sciences Monograph 18,* 216p.

Stevens, J. and Helby, R., 1987. Some Early Cretaceous dinoflagellates encountered in the Australian *Kalyptea wisemaniae* Zone. In Jell, P. A. (Ed), 1987. *Association of Australasian Palaeontologists Memoir 4,* 165-184.

Stover, L. E., 1975. Observations on some Australian Eocene dinoflagellates. *Geoscience and Man 11,* 35-45.

Stover, L. E., 1977. Oligocene and Early Miocene dinoflagellates from Atlantic Corehole 5/5B, Blake Plateau. *American Association of Stratigraphic Palynologists, Contributions Series 5A,* 66-89.

Stover, L. E., Brinkhuis, H., Damassa, S. P., De Verteuil, L., Helby, R. J., Monteil, E., Partridge A. D., Powell, A. J., Riding, J. B., Smelror, M. and Williams, G. L., 1996. Chapter 19: Mesozoic-Tertiary dinoflagellates, acritarchs and prasinophytes. In Jansonius, J. and McGregor, D.C. (Eds), Palynology: principles and applications. *American Association of Stratigraphic Palynologists Foundation 2,* 641-750.

Stover, L. E. and Evitt, W. R., 1978. *Analyses of Pre-Pleistocene Organic-walled Dinoflagellates*. Stanford University Publications, Geological Sciences XV. Stanford, USA, 300p.

Stover, L. E. and Helby, R., 1987a. Some Australian Mesozoic microplankton index species. In Jell, P. A. (Ed), *Association of Australasian Palaeontologists Memoir 4,* 101-134.

Stover, L. E. and Helby, R., 1987b. The Jurassic dinoflagellate *Omatia* and allied genera. In Jell, P. A. (Ed), *Association of Australasian Palaeontologists Memoir 4,* 143-157.

Stover, L. E. and Helby, R., 1987c. Early Cretaceous dinoflagellates from the Vinck-1 well, offshore Western Australia. In Jell, P. A. (Ed), *Association of Australasian Palaeontologists Memoir 4,* 227-260.

Stover, L. E. and Helby, R., 1987d. Some Early Cretaceous dinoflagellates from the Houtman-1 well, Western Australia. In Jell, P. A. (Ed), *Association of Australasian Palaeontologists Memoir 4,* 261-295.

Stover, L. E., Sarjeant, W. A. S. and Drugg, W. S., 1977. The Jurassic dinoflagellate genus *Stephanelytron*: emendation and discussion. *Micropaleontology 23 (3),* 330-338.

Stover, L. E. and Williams, G. L., 1987. Analyses of Mesozoic and Cenozoic organic-walled dinoflagellates 1977-1985. *American Association of Stratigraphic Palynologists, Contributions Series 18,* 243p.

Strother, P. K., 1996. Chapter 5: Acritarchs. In Jansonius, J. and McGregor, D.C. (Eds), Palynology: principles and applications. *American Association of Stratigraphic Palynologists Foundation 1,* 81-106.

Szaniawski, H., 1996. Chapter 12: Scolecodonts. In Jansonius, J. and McGregor, D.C. (Eds), Palynology: principles and applications. *American Association of Stratigraphic Palynologists Foundation 1,* 337-354.

Tappan, H. and Leoblich, A. R., 1965. Foraminiferal remains in palynological preparations. *Revue de Micropaléontologie 8,* 61-63.

Thomas, J. E. and Cox, B. M., 1988. The Oxfordian-Kimmeridgian Stage boundary (Upper Jurassic): Dinoflagellate cyst assemblages from the Harome Borehole, north Yorkshire, England. *Review of Palaeobotany and Palynology 56,* 313-326.

Thusu, B. and Vigran, J. O., 1985. Middle-Late Jurassic (Late Bathonian - Tithonian) palynomorphs. In Thusu, B., and Owens, B. (Eds), Palynostratigraphy of north-east Libya. *Journal of Micropalaeontology 4,* 113-130.

Torricelli, S., Knezaurek, G. and Ulderico, B., 2006. Sequence biostratigraphy and palaeoenvironmental reconstruction in the Early Eocene Figols Group of the Tremp-Graus Basin (south-central Pyrenees, Spain). *Palaeogeography, Palaeoclimatology, Palaeoecology 232,* 1-35.

Tykoezinski, H. R. G., Smith, S. W., Hogg, N. M. and Bailey, D. A., 2000. Three new dinoflagellate cyst species from the Bathonian and Callovian of England. *Palynology 24,* 79-93.

Tyson, R. V., 1995. *Sedimentary Organic Matter: Organic facies and palynofacies.* Chapman and Hall, London, 615p.

Valensi, L., 1953. Microfossiles des silex du Jurassique moyen. *Remarques pétrographiques. Mémoires de la Société géologique de France, Nouvelle série 32 (4/68),* 1-100.

Van der Zwan, C. J., 1990. Palynostratigraphy and palynofacies reconstruction of the Upper Jurassic to Lowermost Cretaceous of the Draugen Field, offshore Mid Norway. *Review of Palaeobotany and Palynology 62, 157-186.*

Van Simaeys, S., Brinkhuis, H., Pross, J., Williams, G. L. and Zachos, J. C., 2005. Arctic dinoflagellate migrations mark the strongest Oligocene glaciations. *Geology 33 (9),* 709-712.

Veevers, J. J., 1988. Morphotectonics of Australia's Northwestern Margin – A review. In Purcell, P. G. and Purcell, R. R., (Eds), *The North West Shelf, Australia.* Proceedings of the Petroleum Exploration Society of Australia North West Shelf Symposium, Perth, 19-29.

Volkheimer, W. and Sarjeant, W. A. S., 1993. *Systematophora rosenfeldii* n. sp., a Lower Cretaceous dinoflagellate from the Neuquén Basin, central western Argentina. *Neues Jahrbuch für Geologie und Paläontologie, Monatshefte 4,* 246-256.

Vozzhennikova, T. F., 1967. *Iskopaemye peridinei Yurskikh, Melovykh i Paleogenovykh otlozheniy SSSR.* Izdatelstvo Nauka, Moscow, U.S.S.R., 347p.
(Translation: Lees and Sarjeant, 1971. Fossil peridinians of the Jurassic, Cretaceous and Paleogene deposits of the U.S.S.R.)

Walker, R. G. and James, N. P. (Eds), 1992. *Facies Models: Response to sea level change.* Geological Association of Canada, St Johns, Newfoundland, 409p.

Wall, D., 1965. Microplankton, pollen, and spores from the lower Jurassic in Britain. *Micropaleontology 11 (2),* 151-190.

Wall, D., 1967. Fossil microplankton in deep-sea cores from the Caribbean Sea. *Palaeontology 10 (1),* 95-123.

Waterhouse, H. K., 1995. High-resolution palynofacies investigation of Kimmeridgian sedimentary cycles. In House, M. R., Gale, A. S. (Eds.), Orbital forcing timescales and cyclostratigraphy. *Geological Society London Special Publication 85,* 75-114.

Waterhouse, H. K., 1999. Orbital forcing of palynofacies in the Jurassic of France and the United Kingdom. *Geology 27,* 511-514.

Wheeler, J. W. and Sarjeant, W. A. S., 1990. Jurassic and Cretaceous palynomorphs from the central Alborz Mountains, Iran: their significance in biostratigraphy and palaeogeography. *Modern Geology 14 (4),* 267-374.

Wiggins, V. D., 1969. Two Lower Cretaceous dinoflagellate species from Alaska. *Micropaleontology 15 (2),* 145-150.

Wiggins, V. D., 1972. Two new Lower Cretaceous dinoflagellate genera from southern Alaska (U.S.A.) *Review of Palaeobotany and Palynology 14,* 297-308.

Wiggins, V. D., 1975. The dinoflagellate family Pareodiniaceae: a discussion. *Geoscience and Man 11,* 95-115.

Williams, G. L., 1975. Dinoflagellate and spore stratigraphy of the Mesozoic-Cenozoic, offshore eastern Canada. *Geological Survey of Canada, Paper 74-30 2,* 107-161.

Williams, G. L. and Downie, C., 1966. Further dinoflagellate cysts from the London Clay. In Davey, R. J., Downie, C., Sarjeant, W. A. S. and Williams, G. L., Studies on Mesozoic

and Cainozoic dinoflagellate cysts; *British Museum (Natural History) Geology, Bulletin, Supplement 3,* 215-236.

Williams, G. L. and Downie, C., 1969. Section V: Generic reallocations proposed by G. L. Williams & C. Downie. In Davey, R. J., Downie, C., Sarjeant, W. A. S. and Williams, G. L., Appendix to "Studies on Mesozoic and Cainozoic dinoflagellate cysts". *British Museum (Natural History) Geology, Bulletin, Appendix to Supplement 3,* 17.

Williams, G. L., Fensome, R. A., Miller, M. A., and Sargent, W. A. S., 2000. A glossary of the terminology applied to dinoflagellates, acritarchs and prasinophytes, with emphasis on fossils: Third edition. *American Association of Stratigraphic Palynologists, Contributions Series 37,* 370p.

Williams, G. L., Lentin, J. K. and Fensome, R. A., 1998. The Lentin and Williams Index of Fossil Dinoflagellates, 1998 Edition. *American Association of Stratigraphic Palynologists Contributions Series 34,* 817p.

Williams, G. L., Stover, L. E. and Kidson, E. J., 1993. Morphology and stratigraphic ranges of selected Mesozoic-Cenozoic dinoflagellate taxa in the Northern Hemisphere. *Geological Survey of Canada, Paper 92-10,* 137p.

Wilson, G. J. and Helby, R., 1987. A probable Oxfordian dinoflagellate assemblage from North Canterbury, New Zealand. In Begg, J. (Ed), Research notes 1987. *New Zealand Geological Survey, Record 20,* 119-125.

Wiseman, J. F., 1980. Palynostratigraphy near the 'Jurassic-Cretaceous Boundary' in the Carnarvon Basin, Western Australia. *Proceedings of the IV International Palynological Conference, Lucknow 2,* 330-349.

Wiseman, J. F. and Williams, A. J., 1974. (Chapter 41) Palynological investigation of samples from Sites 259, 261 and 263, Leg 27, Deep Sea Drilling Project. In Veevers, J. J., Heirtzler, J. R., *et al.*, *Initial Reports of the Deep Sea Drilling Project XXVII, Washington,* 915-924.

Wood, G. D., Gabriel, A. M. and Lawson, J. C., 1996. Chapter 3. Palynological techniques – processing and microscopy. In Jansonius, J. and McGregor, D.C. (Eds), Palynology: principles and applications. *American Association of Stratigraphic Palynologists Foundation 1,* 29-50.

Woollam, R., 1980. Jurassic dinocysts from shallow marine deposits of the East Midlands, England. *Journal, University of Sheffield Geological Society 7,* 243-261.

Woollam, R., 1982. Observations on the Jurassic dinocyst genera *Energlynia* and *Wanaea*. In *Journal of Micropalaeontology 1,* 45-52.

Woollam, R., 1983. A review of the Jurassic dinocyst genera *Ctenidodinium* Deflandre 1983 and *Dichadogonyaulax* Sarjeant 1966. *Palynology 7,* 183-196.

Woollam, R and Riding, J. B., 1983. Dinoflagellate cyst zonation of the English Jurassic. *Report of the Institute of Geological Sciences 83/2*, 1-42.

Yun Hyesu, 1981. Dinoflagellaten aus der Oberkreide (Santon) von Westfalen. *Palaeontographica, Abt B, Band 177,* 1-89.

Zhu Youhua and He Chengquan, 2007. Middle Jurassic to Early Cretaceous dinoflagellate assemblage zones in eastern Heilongjiang Province, northeast China. *Cretaceous Research 28,* 327-332.

Zonneveld, K. A. F. and Susek, E., 2007. Effects of temperature, light and salinity on cyst production and morphology of *Tuberculodinium vancampoae* (the resting cyst of *Pyrophacus steinii*). *Review of Palaeobotany and Palynology 145 (1-2),* 77-88.

Zotto, M., Drugg, W. S. and Habib, D., 1987. Kimmeridgian dinoflagellate stratigraphy in the southwestern North Atlantic. *Micropaleontology 33,* 193-213.

ADDENDUM

Following completion of Chapter 5 Palynology: Systematics and Inventory, evidence surfaced to support the reattribution of the new genus, *Triovalium,* as a dinoflagellate cyst. Although the correction of this genus and the resultant data and charts was not possible before submission of this thesis, the following systematic adjustment is presented, and will be corrected for any potential future publications.

Genus ***Triovalium*** gen. nov.

Type species: *Triovalium attenuatum* gen. et sp. nov.

Derivation of name: From *trēs* (Latin): "three", and *ova* (Latin): "eggs", in reference to the three, ovoidal membranes arranged concentrically.

Diagnosis: Intermediate to large, proximate, cavate (probably circumcavate), strongly lenticular cysts composed of three, concentrically arranged, ovoidal to ellipsoidal membranes. Endophragm, mesophragm and periphragm smooth to faintly ornamented, devoid of spines, processes or projections. One or more dark, amorphous accumulation bodies common. Archeopyle not observed. Faint latitudinal and longitudinal folds common; interpreted to indicate paracingulum and parasulcus. Paratabulation indeterminate; possibly gonyaulacacean.

Comments: Although an archeopyle and clear paratabulation are not observed, the combination of the cyst size, shape, presence of accumulation bodies and faint, probably paratabular folds on this genus strongly indicate a dinoflagellate cyst affinity. In particular, the presence of accumulation bodies within unruptured fossil specimens is considered by Evitt, 1985 (p. 18) to be "reasonable presumptive evidence for identifying an otherwise appropriately constituted specimen as a dinoflagellate".

Comparison: Very few dinoflagellate cysts possess three or more distinct wall layers: the majority being Peridinioid genera or attributed species of *Cepadinium* Duxbury, 1983, *Chatangiella* Vozzhennikova, 1967, *Isabelidinium* Lentin & Williams, 1977, *Lasagniella* Brinkhuis *et al.*, 2000, *Luxadinium* Brideaux & McIntyre, 1975, *Manumiella* Bujak & Davies, 1983 and *Trithyrodinium* Drugg, 1967; and a single Gonyaulacoid dinoflagellate cyst genus, *Triphragmadinium* Van Simaeys *et al.*, 2005. Each of these examples differ from *Triovalium* gen. nov. in ambital shape, sphericity, the presence of a clear archeopyle, horns, ornamentation, or more than three wall layers. The size, shape and circumcavation of this genus is vaguely reminiscent of *Endoscrinium* (Klement, 1960) Vozzhennikova, 1967 and *Scriniodinium*

Klement, 1957, which differ in having two walls only, faint to distinct paratabulation and a precingular Type P archeopyle.

Triovalium attenuatum sp. nov.

Pl. 114, figs. D-E

Holotype and type locality: Pl. 114, fig. D, Jansz-3, Core, 2810m, GA sample no. 1631224, slide no. 5, England Finder co-ordinates: W23, CPC no. 41056.

Derivation of name: From *attenuatus* (Latin): "simply, without ornament" in reference to the thin, simple, unornamented membranes.

Synopsis: Intermediate-sized, proximate, cavate (probably circumcavate), strongly lenticular cysts composed of three, concentrically arranged, ovoidal to ellipsoidal membranes. Endophragm, mesophragm and periphragm smooth to scabrate; extremely pale, thin and easily folded or broken. Faint latitudinal and longitudinal folds common; interpreted to indicate paracingulum and parasulcus. One or more dark, amorphous accumulation bodies common; one typically centrally located at the junction of latitudinal and longitudinal folds. Archeopyle not observed. Paratabulation indeterminate; possibly gonyaulacacean.

Diagnosis:

Shape: Ovoidal; very strongly lenticular.

Wall Relationships: Endophragm, mesophragm and periphragm; concentrically arranged; extremely pale, thin and easily folded or broken; mesocoel (<6µm) typically slightly narrower than pericoel (<8µm).

Wall Features: All walls smooth to scabrate. One or more dark, amorphous accumulation bodies common; one typically centrally located at the junction of latitudinal and longitudinal folds.

Archeopyle: Not observed.

Paratabulation: Faint latitudinal and longitudinal folds common; interpreted to vaguely indicate the paracingulum and parasulcus. Frequent occurrence of a radial fold extending mid way between the paracingulum and parasulcus in one quarter is interpreted to indicate the 1-

2’’’/1p parasuture, which suggests a probable gonyaulacacean affinity. Probable paratabular folds easily obscured by poor preservation.

Paracingulum: Possibly vaguely indicated by widely-spaced latitudinal folds; frequently slightly offset suggesting a slight laevorotatory spiral.

Parasulcus: Possibly vaguely indicated by one or more longitudinal folds.

Size: Intermediate.

Dimensions: (µm; 12 specimens measured)
Total length: 72 (85) 94
Total width: 49 (61) 76

Comments: The consistent presence of one or more amorphous accumulation bodies identifies this species as a dinoflagellate cyst. This is supported by additional circumstantial evidence, including the cyst size, shape and common, vaguely paratabular folds.

Comparison: All dinoflagellate cysts with three or more wall layers are clearly differentiated from *Triovalium attenuatum* by their ambital shape, sphericity, paratabulation, ornamentation or archeopyle (refer to generic comparison above). Within the Jansz-Io preparations *Triovalium attenuatum* is most similar to *Leberidocysta? strigosa* Mantle, 2009b in being strongly lenticular, pale, thin and unornamented. However, *L.? strigosa* differs in having a smaller size, subcircular ambitus, only two wall layers and a definite apical archeopyle.

APPENDICES

The following supplementary information is appended on the attached disk:

Appendix 1 - List of samples examined

Appendix 2 - Core logs

Appendix 3 - Register of illustrated specimens

Appendix 4 - Quantitative analysis charts – palynofacies and microplankton specimen counts in Excel spreadsheet format and various Stratabugs formats

SPECIES INDEX

DINOFLAGELLATE CYSTS

ACRITARCHS

MICROFORAMINIFERAL TEST LININGS